
DISSERTATION ZUR ERLANGUNG DES DOKTORGRADES
AN DER FAKULTÄT FÜR CHEMIE UND PHARMAZIE DER
LUDWIG-MAXIMILIANS-UNIVERSITÄT MÜNCHEN

**Investigation of Oxygen- and Nitrogen-rich Heterocyclic
Compounds as Potential High-Energy Dense Oxidizers or
Secondary Explosives**

Tobias Sebastian Hermann

aus München, Deutschland

2018

Erklärung

Diese Dissertation wurde im Sinne von §7 der Promotionsordnung vom 07. Januar 2015 von Herrn Prof. Dr. T. M. Klapötke betreut.

EIDESSTATTLICHE VERSICHERUNG

Diese Dissertation wurde eigenständig und ohne unerlaubte Hilfe erarbeitet.
München, den 09.02. 2018

Tobias S. Hermann

Dissertation eingereicht am:	15.02.2018
1. Gutachter:	Prof. Dr. T. M. Klapötke
2. Gutachter:	Prof. Dr. K. Karaghiosoff
Mündliche Prüfung:	06.04.2018

*“Just remember, you can't climb the ladder of success with your
hands in your pockets.”*

Arnold Schwarzenegger

Danksagung

Mein Dank gilt an vorderster Stelle meinem Doktorvater Prof. Dr. Thomas M. Klapötke für die Aufnahme in den Arbeitskreis, die interessante Themenstellung, die stetige finanzielle und fachliche Unterstützung meiner Forschungsvorhaben sowie seine Begeisterung für die Wissenschaft.

Herrn Prof. Dr. Konstantin Karaghiosoff danke ich nicht nur für die freundliche Übernahme des Zweitgutachtens dieser Dissertation, sondern auch für die Einarbeitung in die Kristallographie und deren Faszination dafür, die ich nun mehr als nur nachvollziehen kann.

Der Prüfungskommission, bestehend aus Prof. Dr. T. M. Klapötke, Prof. Dr. K. Karaghiosoff, Prof. Dr. W. Beck, Prof. Dr. H. Böttcher, Prof. Dr. A. Kornath und Prof. Dr. M. Heuschmann, danke ich für Ihre Zeit und die Bereitschaft zur Bildung der selbigen.

Herrn Dr. Burkhard Krumm danke ich für die gute Betreuung, die zahllosen Anregungen, Diskussionen und Hilfestellungen sowie für die Aufnahme zahlreicher NMR Spektren. Des Weiteren möchte ich Ihm für die immer sehr akribische Korrektur jeglicher Schriftstücke danken.

Dr. Jörg Stierstorfer danke ich für Hilfestellungen, Korrekturen und Anregungen aller Art, sowie seine teambildenden Maßnahmen im Arbeitskreis.

Frau Irene Scheckenbach danke ich für Ihr organisatorisches Multitalent und Ihre Unterstützung in verschiedensten und alltäglichen bürokratischen Aufgaben.

Allen während meiner Promotion anwesenden Laborkollegen im Arbeitskreis danke ich für die stets sehr gute freundschaftliche Arbeitsatmosphäre. Besonderer Dank geht hier an alle Doktoranden des Labors D.3.103. Besonders möchte ich dabei Alicia Dufter, Dr. Andreas Preimeßer, Thomas Reich, Norbert Szimhardt und Stefan Huber für eine großartige Zeit im Labor danken.

Besonderer Dank geht auch an alle meinen Praktikanten, die alle mit viel Engagement einen erheblichen Beitrag zum Gelingen dieser Arbeit beigetragen haben.

Meinen besten Freunden Daniele Adesso, Iris und Jasmin Rosenberger danke ich für Ihre Unterstützung in der nicht immer sehr einfachen Zeit. Danke auch für all die großartigen Ablenkungen!

Nicht zuletzt geht mein Dank an meine Familie, im Besonderen meinen Eltern Liane und Hans und meine Schwester Laura-Marie, die mir durch Ihre unaufhörliche Unterstützung und Liebe dies alles erst ermöglicht haben. Nicht zu vergessen meine Großeltern Sieglinde und Anton Molthäufel, sowie Annemarie Kraus, Manfred Danner, Nina Jäger und Gerhard Osterrieder, die mir ein einzigartiger Rückhalt sind.

Table of Contents

I General Introduction	1
1. Definition and Classification of Energetic Material	1
2. Primary Explosives	2
3. Secondary Explosives	2
3.1 Motivation and requirements for new secondary explosives	6
4. Propellants	8
4.1 High Energy Dense Oxidizers	9
4.2 Oxygen Balance	11
4.3 Specific impulse	11
4.4 Motivation and requirements for new High Energy Dense Oxidizers	12
5. Pyrotechnics	14
6. Publications	14
7. General Methods and Characterization:	14
5.1 Analytical Methods	15
II Results and Discussion	23
The Reagent-depending Nitration of 1,3-Dihydroxyacetone Dimer	24
1. Introduction	25
2. Results and Discussion	26
3. Conclusions	29
4. Experimental Section	30
5. Supporting Information	32
5.1 NMR spectroscopy	32
5.2 Vibrational spectroscopy	32
5.3 X-ray diffraction	33
5.4 Thermal and energetic properties	35
5.5 Experimental	36
5.6 Heat of formation calculations	37
6. References	39

The Energetic 3-Trinitromethyl-5-nitramino-1*H*-1,2,4-triazole and Nitrogen-rich Salts. 42

1. Introduction	43
2. Results and Discussion	44
3. Conclusion	49
4. Experimental Part	50
5. Supporting Information	52
5.1 General Methods	52
5.2 X-ray Diffraction	52
5.3 Heat of formation calculations	55
6. References	57

Formation and Characterization of Heavy Alkali and Silver Salts of the 4-Nitro-pyrazolo-(3,4-*c*)-furazan-5-*N*-oxide Anion61

1. Introduction	62
2. Results and Discussion	63
3. Conclusions	71
4. Experimental Section	72
5. References	74

High Temperature Stable Picrylamino Substituted Furazanes and Triazoles 78

1. Introduction	79
2. Results and Discussion	80
3. Conclusions	88
4. Experimental Section	88
5. References	90

Synthesis, Characterization and Properties of Ureido-Furazan Derivatives..... 94

1. Introduction	95
2. Results and Discussion	96

3. Conclusion.....	105
4. Experimental Section.....	106
5. Reverences	112

Energetic Compounds Based on 3,4-Bis(4-nitramino-1,2,5-oxadiazol-3-yl)-1,2,5-furoxan (BNAFF) 116

1. Introduction	117
2. Results and Discussion.....	118
3. Conclusion.....	127
4. Experimental Section.....	128
5. Reference	135
6. Supporting Information	138
6.1 X-ray Diffraction.....	138
6.2 Computations.....	141
6.3 Differential Thermal Analysis (DTA)	144
6.4 NMR Spectra.....	146
6.5 References.....	147

Synthesis, Characterization and Properties of Di- and Trinitromethyl-1,2,4-Oxadiazoles and Salts150

1. Introduction	151
2. Results and Discussion.....	154
3. Conclusions	170
4. Experimental Section.....	170
5. References.....	185

Synthesis and Characterization of 2,2'-Dinitramino-5,5'-bi(1-oxa-3,4-diazole) and Derivatives as Economic and Highly Dense Energetic Materials..... 188

1. Introduction	189
2. Results and Discussion.....	190
3. Conclusion.....	194
4. Supporting Information	195

Table of Contents

4.1 X-ray Diffraction	195
4.2 Analytical Data	203
4.3 Heat of formation calculation.....	205
4.4 Experimental	207
5 References.....	211
III Summary and Conclusion.....	214
IV Appendix	224
Curriculum Vitae.....	227

I General Introduction

1. Definition and Classification of Energetic Material

Since the reinvestigation of black powder as energetic material for barrel charges in Europe in the 13th century, the demand for new materials with different specific properties has been of increasing importance in the development of energetic materials.^[1] During the last decades the investigation of this class of materials has become a major interest in chemical research all over the world. In literature there are different definitions for energetic materials, for example by the American Society for Testing and Materials: “...a compound or mixture of substances which contains both the fuel and the oxidizer ...”.^[2] A more precise description is given by Agrawal: “energetic materials are substances or mixtures, which release a large amount of energy in the form of heat and pressure during a fast exothermic decomposition, when they are exposed to thermal or mechanical stress. During decomposition, the temperatures can reach 3000–5000 °C, and the gaseous volume increased by a factor of up to 12000–15000 than that of the original volume”.^[3] Meyer and Köhler also take the environment impact of energetic materials into account by giving the definition: “An explosion is a sudden increase in volume and release of energy in a violent manner, usually with generation of high temperatures and release of gases. An explosion causes pressure waves in the local medium in which it occurs. Explosions are categorized as deflagration, where these waves are subsonic or detonation, where they are supersonic.”^[4]

All of the three definitions mentioned before divided energetic materials into classes. However, the classification by functional groups does not hold any information about applications or the energetic properties of the respective compounds. Therefore; energetic materials are commonly classified into primary explosives, secondary explosives, propellants and pyrotechnics (Figure 1).

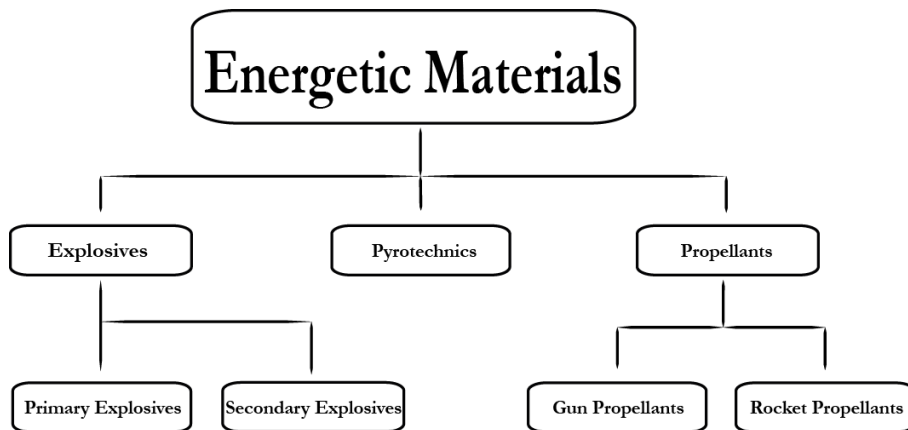


Figure 1: Classification of energetic materials.

2. Primary Explosives

Among energetic materials, primary explosives are the most sensitive compounds. Their main application, as initiators for main charges can be explained by the fact that they can be initiated by a simple initiation impulse (SII). This means they can easily be initiated mechanically, by impact, friction, electrostatic discharge, but also by thermal stimuli.^[1] The impact sensitivity of primaries is usually less than 4 J and their friction sensitivity below 10 N.^[1] The detonation after thermal initiation, that even occurs in an unconfined state is just one of the main characteristics of primary explosives. Former primary explosives significantly differed from secondary explosives by its lower detonation properties. The detonation velocity of an usual primary explosive is in the range of 3500–5500 m s⁻¹ compared to 5500–9500 m s⁻¹ for a typical secondary explosive. Nowadays, the detonation properties of primary explosives are near or even equal to those of secondary explosives. Here, a fast deflagration-to-detonation transition (DDT) takes place, whereby the subsonic heat transfer of the decomposition converts into a supersonic shock wave.^[5] The initiation potential of primary explosives is used to initiate main charges, for example in torpedos or other missiles. Common representatives of primary explosives are mercury fulminate (MF), lead azide (LA), lead styphnate (LS) and Diazodinitrophenol (DDNP) (Figure 2).

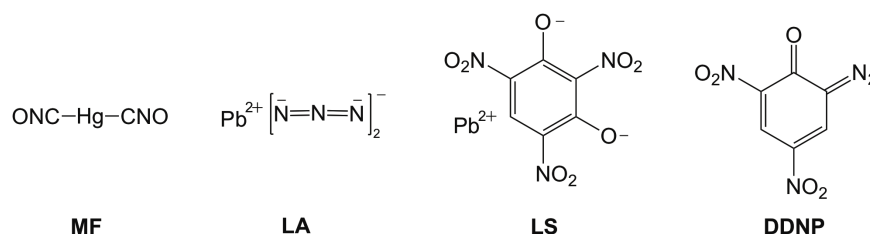


Figure 2: Molecular structure of MF, LA, LS and DDNP.

The presence of highly toxic metal cations in such compounds gives reason for further research in this field. The search for more environmentally friendly compounds is based on synthesis of metal free primaries or salts with copper, potassium or iron cations.

3. Secondary Explosives

In contrary to primary explosives, secondary explosives are much less sensitive towards shock, friction, electrostatic discharge as well as to heat and thus typically kinetic stable compounds.^[1] In numbers this means they should have impact sensitivities above 5 J and friction sensitivities higher than 60 N.

Consequently, the initiation of this class of energetic materials desires much more violent stimuli. This part is normally taken over by the powerful shock wave of a primary explosive. Nevertheless, the low sensitivity of secondary explosives is advantageous with respect to safe synthesis, transport and storage as well as their area of application. For today's synthetic research, this important feature of secondary explosives is one of the most difficult challenges.

There are different models and theories that correlate the sensitivity and the initiation potential with respect to special molecular and crystal properties.^{[6], [7]} These theories and models are based on different fields of science, for example continuum mechanics, chemistry and quantum chemistry.^[8] Anyways, one has to note that a correlation does not indispensably indicate a relationship and a specific behavior can emerge symptomatically.^[9]

Some examples of the most commonly used secondary explosives are given in Figure 3.

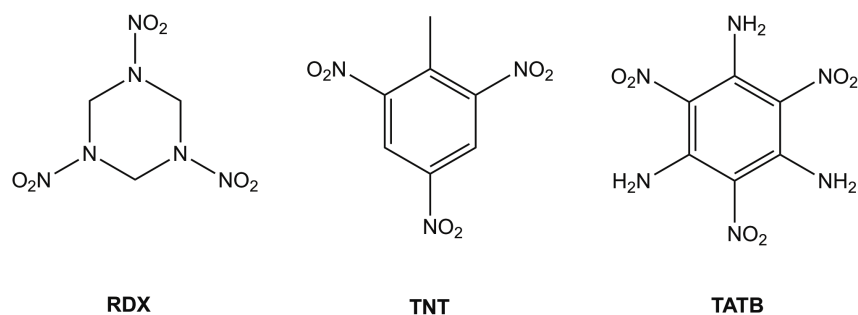


Figure 3: Molecular structure of 1,3,5-trinitro-1,3,5-triazine (**RDX**), 2-methyl-1,3,5-trinitrobenzene (**TNT**) and 1,3,5-triamino-2,4,6-trinitrobenzene (**TATB**).

After initiation by some form of energy input, generally by a primary, a series of steps leads to a self-sustaining, exothermal chemical decomposition. The latter is due to the detonation shock wave with supersonic spreading, whereby the shock wave front moves through the unreacted system.^{[4] [10]}

As the shock wave moves through the secondary explosive, the pressure behind the shock wave front rises up to 330 kbar and compacts the secondary explosive so that its density increases by a factor of 1.3–1.5. As a consequence, the material is adiabatically heated up to 3000 °C, which exceeds its decomposition temperature. The subsequent high exothermic decomposition further accelerates the shock wave.

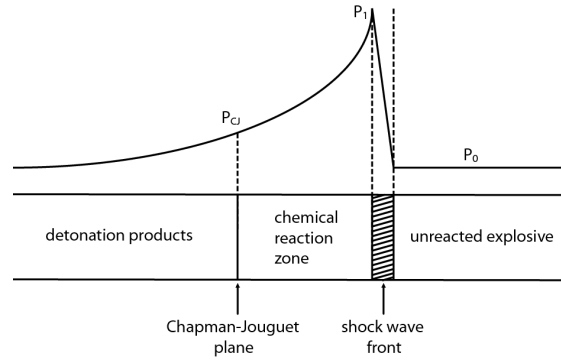


Figure 4: Schematic representation of the detonation process with shock wave structure and according changes in pressure.

In contrast to primary explosives, secondaries usually produce a larger volume of gaseous products upon initiation.^[1] The release of more energy and gaseous products is reflected by the much higher detonation properties. During the decomposition of many energetic materials, solid carbon and stable gaseous decomposition products, like dinitrogen, carbon monoxide, carbon dioxide and water are generated.^{[11], [12], [13]} The higher volume of gaseous decomposition products and energy content compared to primaries is reflected by the superior detonation properties. The volume of gases is generally calculated for standard conditions (273 K and 1 bar) using equations following the ideal gas law.^[1] In the case of a secondary explosive, the high amount of gaseous products and their high stability results in a high amount of energy, which is mainly released as heat. However, the most important detonation properties of secondary explosives are detonation velocity (D), detonation pressure (P_{CJ}) by Chapman-Jouguet and heat of explosion (Q_v). The detonation velocity and detonation pressure has been empirically associated by the Kamlet-Jacobs equations (1 and 2):

$$P_{C-J} = K\rho_0^2\phi \quad [\text{kbar}] \quad (1)$$

$$D = A\phi^2(1 + B\rho_0) \quad [\text{mm}/\mu\text{s}] \quad (2)$$

Where K , A and B are absolute terms. The heat of explosion at determined volume can be calculated with the Hess's law or measurements with a bomb calorimeter. In this case, the heat of explosion correlates with the released energy under adiabatic conditions. The oxygen balance (Ω) also has an important influence and increases the heat of explosion if it is positive or at least balanced.^[14]

Based on the value of the heat of explosion and the volumes of the gaseous products, the explosive power can be calculated. The explosive power is the product of heat of explosion and the volume of the gaseous products and can be describe by equation 3. The values of the explosive power of RDX, TNT and NQ are given in Table 1.

$$P = Q_V \times V \quad [\text{kJ}/\text{kg}^2] \quad (3)$$

Table 1: Heat of explosion, volume of gaseous products and explosive power of RDX, TNT and NQ.

	RDX	TNT	NQ
$Q_V [\text{kJ}/\text{kg}]$	5036	4247	2471
$V [1/\text{kg}]$	908	740	1077
$P [\text{kJ}/\text{kg}^2]$	457	314	266

The detonation velocity is the rate of propagation of a detonation in an explosion. It is characteristic for each explosion and not influenced by external factors. This is due to a maximum of density of an energetic material when it is placed in columns, which are bigger than the critical diameter. Generally, with increasing density the detonation velocity increases. Kamlet and Jacobsen established an empirical correlation between the detonation velocity and the detonation pressure. They state that at loading density ρ_0 the detonation velocity is linear, while the pressure even increases exponentially. In order to increase the detonation velocity or the detonation pressure of an energetic material, the initial density can be increased or the crystal density, which is the limiting theoretical maximum density (TMD), is high.

Another less important characteristic is the explosion temperature (T_{ex}), which is the calculated temperature of the fumes generated during an explosion. The explosion temperature refers to the temperature of the shock wave front of a detonation.

The brisance (B) is another important value to define the performance of an energetic material. It is defined as the destructive fragmentation on the immediate environment of an explosive. It is derived from the loading density, specific energy (F) and mainly influenced by the detonation velocity. Also, for the performance of a brisant explosive, the loading density plays a key role and refers to the ratio between the weight of an explosive material and the space in which it will detonate. According to Kast the brisance of an explosive can be calculated with respect to equation 4.

$$B = \rho \times F \times D \quad [\text{kg}/\text{s}^3] \quad (4)$$

Table 2: Brisance values of RDX, TNT and PETN.

	RDX	TNT	PETN
$B [\text{kg}/\text{s}^3]$	1.25-1.45	1.00	1.27-1.41

According to this equation, an energetic material is more brisant if the density or/and the detonation velocity is higher.

3.1 Motivation and requirements for new secondary explosives

Development of new secondary explosives should be based on the improvement of three main demands: 1) performance, 2) safety and 3) practicability.^{[1], [15]} In developing new secondary explosives the main challenge is the combination of higher performance and low sensitivity because these properties often are contradictory.^[16] According to performance the detonation velocity should be greater than 8500 m s^{-1} , detonation pressure greater than 340 kbar and the heat of formation greater than 6000 kJ kg^{-1} . To follow the stability aspects, the thermal stability should be higher than 180°C , impact sensitivity $>7 \text{ J}$, friction sensitivity $>120 \text{ N}$ and electrostatic discharge $>0.2 \text{ J}$. However, there are also chemical properties that should be taken into account, like low water solubility, hydrolytically stable or compatibility with binder and common metals and other explosives.

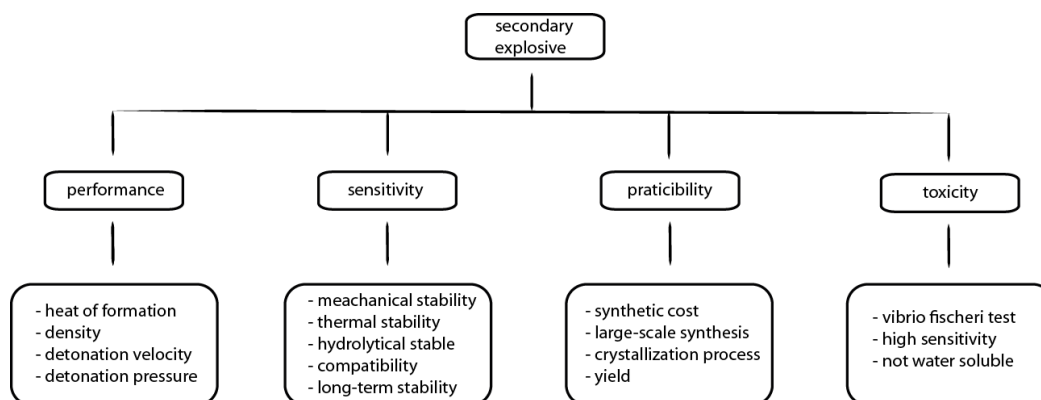


Figure 5: Requirements for the development of new secondary explosives.

Furthermore, environmental and toxicological aspects are becoming more important with the use of high amounts of explosives. The disadvantages of currently used energetic materials are manifold. High sensitivity, high toxicity or missing applicability for special uses are just some examples. The commonly used secondary explosive RDX was found to be a carcinogen, according to the US Environmental Protection Agency (EPA).^[17] Also, RDX, aside from its decomposition products, is highly toxic towards microorganisms, plants, microbes and smaller organisms.^{[18], [19], [20]} Similar results were found for another widely used explosive, TNT, which is also carcinogenic and its degradation products are toxic and can cause damage to the liver and blood system.^[21] With these negative impacts, the environmental and toxicological suitability is an increasing objective for the synthesis of new secondary explosives.^{[1], [22], [23]}

A very promising strategy in developing new secondary explosives, which satisfy the requirements, is the synthesis of nitrogen-rich materials. The advantage of nitrogen-rich compounds with high positive enthalpies of formation is enhanced detonation performance and lower environmental impact.

Furthermore, the formation of high amounts of non-toxic nitrogen (N_2) upon decomposition leads to high enthalpies of formation due to the high stability of N_2 . This becomes clear by comparison of the enthalpy of formation of the triple bond (946 kJ mol^{-1}) to the double bond (418 kJ mol^{-1}) and single bond (159 kJ mol^{-1}).^[24] Appropriate molecule backbones are nitrogen-rich heterocycles, like tetrazoles triazoles or oxadiazoles (Figure 6). The combination of heterocycles with specific energetic functional groups, like nitro-, nitramine or polynitro groups, turns out to form valuable energetic materials.

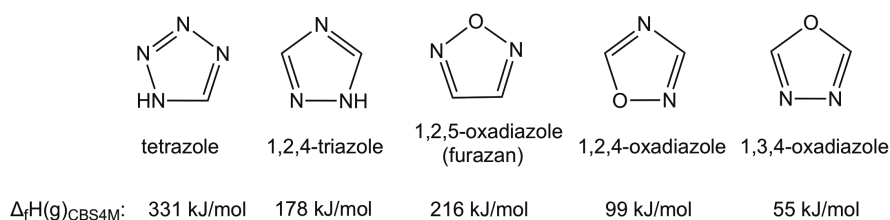


Figure 6: Nitrogen-rich heterocycles for the synthesis of secondary explosives.

Further improvement of the thermochemical, physical properties and detonation parameters can be achieved by the formation of energetic salts with nitrogen-rich cations. Their formation and properties have been extensively studied and put in relation with common used secondary explosives. The physical advantages of nitrogen-rich salts are manifold, for example due to lower vapor pressure, reduced sensitivities and often improved performances.^{[23], [25], [26]} Thereby the better performance, through nitrogen-rich cations, is archived by higher enthalpies of formations. Furthermore, the compatibility of the energetic material can be improved by salt formation, in order to the lessen the acidity, which can cause reaction with the binder or other materials.^[27]

The first major scope of this study was the development of potential new energetic materials with high enthalpies of formation, high density and high performance in order to replace RDX. Due to their energetic and physiochemical properties their application may differ from explosives to propellant charges. Beside the synthesis of novel energetic materials their chemical characterization and physiochemical properties were measured and calculated. This also includes the analysis and measurement of literature known compounds with promising properties.

In general, this research is of academic interest with the focus on gaining a deeper understanding of enhancing performance and decreasing sensitivity. This research should better the understanding in designing new high-energy dense materials with specific properties for specialized application.

4. Propellants

The class of propellants can be divided into two very similar groups; propellant charges and rocket propellants (Figure 7). The major difference between them, and the previously illustrated explosives, is the fact that they are combustible materials, which do not detonate but burn or deflagrate. Propellant charges show a higher burning rate, lower temperatures of combustion and a higher chamber pressure (4000 bar) formed in the combustion chamber compared to rocket propellants (70 bar).^[1]

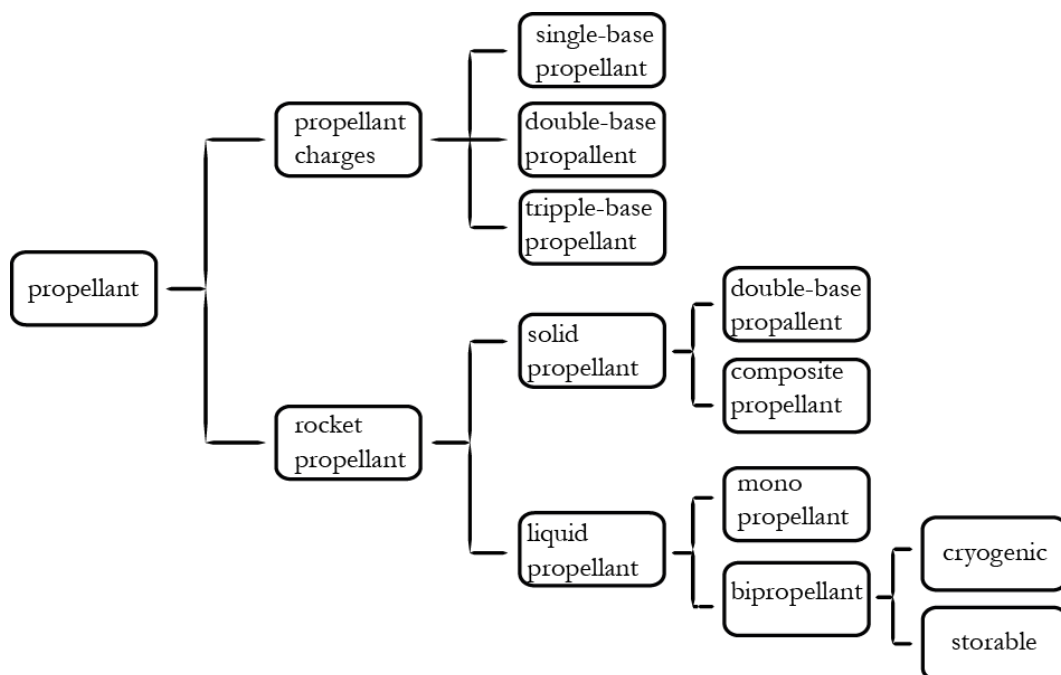


Figure 7: Classification of propellants.

Propellant charges are used in several kinds of weapons from pistols to artillery guns. The first known propellant charge was black powder (75 % KNO_3 , 10 % sulfur and 15 % charcoal dust). Black powder was extensively replaced because of its low efficiency. The most commonly used alternative is nitrocellulose (NC), which shows a lower burning rate and a lower amount of corrosive gases evolved during decomposition. Propellant charges consisting only of NC are classified as single-base propellants. Adding nitroglycerine (NG) to NC results in double-base propellant charges. The disadvantage of double-base propellant charges is strong erosion due to higher combustion temperatures. This problem can be overcome by adding nitroguanidine (NQ) to the double-base propellant charge. The obtained mixtures are called triple-base propellant charges. Both the double base and the triple-base propellant charges show higher performances compared to single-base propellant charges. Modern research on propellant charges

focuses on the development of mixtures which burn with low temperatures to prevent erosion but still show good performances.^[1]

Rocket propellants are used in combustion chambers of rocket motors or missiles and not to accelerate an object. In this case, the hot gases produced during deflagration are purposefully ejected into the direction of the nozzle and the rocket moves in the opposite direction. Therefore, the fuel and the oxidizer have to be inside the combustion chamber. The class of rocket propellants is divided into solid propellants and liquid propellants. Solid propellants are based on NC (double-base propellants, homogeneous) or ammonium perchlorate (AP, composite propellant, heterogeneous).^{[1], [28]} Normally, composite propellants consist of AP as oxidizer, aluminium as fuel and a polymeric binder (e.g. hydroxyl-terminated polybutadiene, HTPB) as matrix.^[1] Liquid rocket propellants can be divided into monopropellants and bipropellants. Monopropellants are endothermic liquids (e.g. hydrazine), which react exothermically with the help of catalysts in the absence of oxygen and release only a small amount of energy. Although the performance is low, they are long-term storable and therefore used in small missiles or satellites. In systems with bipropellants, the oxidizer and the fuel are transported in different tanks and injected into the combustion chamber. The class of bipropellants can be further divided into cryogenic and storable propellants. Cryogenic propellants, for example liquid nitrogen and liquid oxygen, can only be handled at very low temperatures and therefore are not useful for military applications. Examples for storable bipropellants are monomethylhydrazine (MMH) or red fuming nitric acid (RFNA).^{[1], [3]}

4.1 High Energy Dense Oxidizers

Solid rocket propellants mostly consist of an oxidizer in addition to components like fuels and binders. The oxidizer makes up thereby almost 70 % of the propellant from. New high energy dense oxidizers (HEDO) should be based on CHNO due to environmental aspects and safety. During combustion, such oxidizers are converted into H₂O, N₂ and CO₂. An excess of oxygen is released during combustion and reacts with the fuel and produces a large amount of hot gases, which are used to get a rocket motor running.^[22, 29] The most commonly used oxidizer in propellants is ammonium perchlorate (AP). There are some advantages of AP like full conversion into gaseous combustion products during decomposition, high oxygen balance ($\Omega_{\text{CO}} = +34 \%$) and low sensitivity towards mechanical stimuli. Also the low-cost production but the compound should be replaced due to several disadvantages. AP shows insufficient properties in the slow cook-off test.^[30] Therefore, it is assumed that AP slowly decomposes during storage and acidic side products are formed. These side products can react with the binder system to form cracks and cavities, which has a direct influence on the sensitivity, performance and burning rate. Nevertheless, the main disadvantage of ammonium perchlorate is its toxicity. During combustion AP releases a large amount of hydrogen chloride

(HCl).^{[31], [32]} This leads to serious environmental issues in an economic view. Also, from a military perspective, the separation of HCl is a disadvantage, because a lot of smoke is formed, which is easily detectable. The main toxic and environmental problems arises from the perchlorate anion. The perchlorate anion, which is well soluble in water has a high, chemical stability and chemical resistance, has negative effects on the hormone balance of humans and amphibians.^{[29], [33]} AP mainly serves as an oxidizing agent in fireworks and ,especially, in solid propellants. In the USA, up to 90 % of the solid rocket propellants use AP.^[34] The highest pollution originates from incomplete consumption of the propellants, frequent use of weapons, which use AP and synthesis of other energetic materials.^{[34], [35]} Consequently, due to its wide use in composite common propellants, the groundwater is increasingly contaminated in training and testing ranges.^[35] Therefore, new halogene-free oxidizers with a high excess of oxygen for propellants are desirable. So far some alternatives (Figure 8), such as ammonium nitrate (AN), ammonium dinitramide (ADN), hydrazinium nitroformate (HNF) and triaminoguanidine nitroformate (TAGNF) have been found.

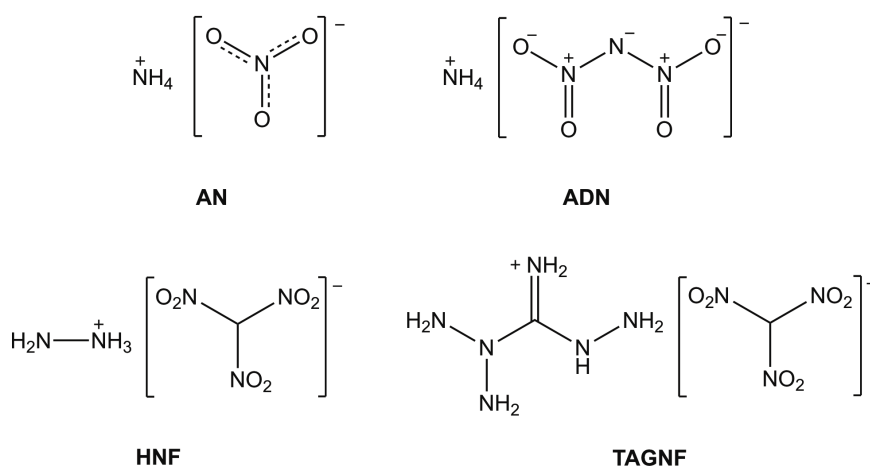


Figure 8: Molecular structure of the alternative oxidizers ammonium nitrate (**AN**), ammonium dinitramine (**ADN**), hydrazinium nitroformate (**HNF**) and triaminoguanidinium nitroformate (**TAGNF**).

These compounds involve other chemical and physical problems. The main challenges to be dealt with are low thermal stability, phase transitions, hygroscopicity and binder compatibility problems.^{[1], [36], [37], [38]} All of these problems demonstrate that further research is needed to find other suitable oxidizers for solid propellants.

4.2 Oxygen Balance

The relative amount of oxygen excess or deficit can be described by the oxygen balance (Ω). For calculating the oxygen balance, it is assumed that no external oxygen is added and the CHNO based compounds are completely oxidized to H_2O , N_2 and CO_2 during combustion. Due to high temperatures CO is formed instead of CO_2 , according to the *Boudouard* equilibrium. The oxygen balance of a compound with the general formula $C_aH_bN_cO_d$ can be calculated according to equation 5 for CO_2 and equation 6 for CO as product. M is the molecular mass of the compound.^[1, 33]

$$\Omega_{CO_2} = \frac{(d - 2a - \frac{b}{2}) \cdot 1600}{M} \quad [\%] \quad (5)$$

$$\Omega_{CO} = \frac{(d - a - \frac{b}{2}) \cdot 1600}{M} \quad [\%] \quad (6)$$

A high oxygen balance is obtained for a large amount of released oxygen atoms per molecule and for a low molecular weight of the compound. For new high energy dense oxidizers, the oxygen balance should be positive and at least in the range of AP ($\Omega_{CO_2} = +34 \%$).^[33]

4.3 Specific impulse

For high-energy dense oxidizers, the specific impulse is an important parameter. It is defined according to equation 7 as the integral of the thrust per mass unit of the propellant over the period of combustion. The thrust is a force oriented into the opposite direction of the gases, which are released during the combustion. The specific impulse expresses the effective velocity of the released gases and can be used to measure the effectiveness of the propellant.^[1]

$$I_{sp} = \frac{F \cdot t_b}{m} = \frac{1}{m} \int_0^{t_b} F(t) dt \quad [m/s] \quad (7)$$

The specific impulse can also be determined based on the gravitation of the earth according to equation 8 with force of gravity g , the ideal gas constant R , the temperature in the combustion chamber T_c , the average molecular weight of the formed gases M and the ratio of the specific heat capacities γ .^[1]

$$I_{sp}^* = \frac{1}{g} \sqrt{\frac{2\gamma RT_c}{(\gamma-1)M}} \quad [s] \quad (8)$$

The specific impulse is proportional to the square root of the temperature in the combustion chamber and the reciprocal of the average molecular weight of the gases (equation 9).

$$I_{sp}^* \propto \sqrt{\frac{T_c}{M}} \text{ [s]} \quad (9)$$

A higher specific impulse can be obtained by increasing the temperature in the combustion chamber and by lowering the average molecular weight of the formed gases.^[39] An increase of the specific impulse by 20 s empirically leads to a doubling of the payload of the carrier system.^[1]

4.4 Motivation and requirements for new High Energy Dense Oxidizers

The modern research toward new high energy dense oxidizers is aimed at developing environmentally friendly and non-toxic compounds and replacing AP. This widely used compound has civil and military applications like use as oxidizer in rocket propellants or as an air-bag inflator in the automobile industry. Due to the high solubility in water and the chemical stability, the employment of AP has led to the pollution of the surface and the ground water. There are also negative effects of the perchlorate anion to the human and amphibian health. The perchlorate anion interferes with normal thyroid function affecting the growth and development of vertebrates. It also affects the normal pigmentation of amphibian embryos.^[33]

The performance of new high-energy dense oxidizers should be in the range of AP. Therefore; the oxygen balance and the specific impulse should be as high as possible. The compounds should have a low molecular weight and, more important, the molecular weight of the formed products should be as low as possible. To increase the specific impulse, the heat of reaction should be high in order to increase the temperature in the reaction chamber. Also, the compounds should be halogen-free and highly nitrated so almost environmentally benign gaseous products are produced.^{[1], [31], [40]}

The second major scope of this thesis was to synthesize and investigate new molecules, which qualifies them as oxidizer through high oxygen content. In order to reach this goal, perchlorate free compounds based on CHNO were the main focus to potentially replace AP and overcome its environmental and health concerns. Of course the new high-energy dense oxidizers should combine good performance, good physical and chemical properties, and fulfill the requirements for new oxidizers. The density should also be close to 2 g cm⁻³, thermal stability >150 °C, sensitivity not higher than PETN and oxygen balance (Ω_{Co}) as high as possible.

To pursue the goal of increasing the oxygen content, polynitro units like dinitromethyl-, trinitromethyl-groups or nitramine and nitrate ester functional groups were used. The advantage of trinitromethyl

functional group in contrast to dinitromethyl functional group becomes clear by comparing the oxygen balances (Figure 9).

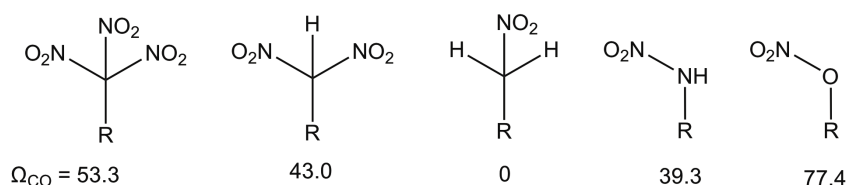


Figure 9: Overview over the oxygen balances (Ω_{CO}) of the trinitro-, dinitro-, mononitromethyl, nitramine and nitrate ester functional group.

For the synthesis of the trinitromethyl moiety, different literature known routes can be followed. In this research, nitrating acetic acid groups followed the synthesis. This synthesis of trinitromethyl moieties is generally easy, cheap and quick, which is another advantage. Furthermore, the carbon backbone can be built in the first step and the energetic part is established by a nitration in the last synthesis step, which makes handling significantly safer.

The formation of the dinitromethyl functional group for example can be achieved by nitration of an acetic acid ethyl ester group followed by acidification. The oxygen content is high but the proton is very acidic due to the adjacent nitrogen groups, which leads to higher sensitivities and short storability. These two disadvantages of the dinitromethyl functional group can be overcome by stabilization using salt formation, which on the other hand leads to a decrease of the oxygen content.

Visible in Figure 9, the use of nitrate ester functional groups brings the highest excess of oxygen in order to increase the oxygen content of a compound. Also, the synthesis of this functional group is very easy and cheap, by the nitration of alcoholic groups. Another advantage of nitrate ester compounds is their good detonation properties. A disadvantage in general is the low sensitivity and thermal stability of this moiety. Anyway, compounds with nitrate ester functional groups like PETN are commonly used explosives.

Next to the functional groups, the molecule backbone can contribute to increase the oxygen content. Heterocyclic compounds that have oxygen atoms included can achieve this. The perhaps most promising heterocycles are oxadiazoles. Different types of oxadiazoles can be synthesized according to the position of the oxygen atom with respect to the two nitrogen atoms. Oxadiazoles are known for their stability, high density and good detonation properties, which make them perfect backbones in sense of creating compounds with a positive oxygen content.

5. Pyrotechnics

Pyrotechnics mostly differ from primary and secondary explosives in that they decompose under non-detonative self-sustaining exothermic chemical reactions.^[1] Another difference to primary and secondary explosives is that pyrotechnics do not contain the oxidizer and the fuel in one molecule, but are physical mixtures of different substances consisting of an oxidizer and a reducing agent.^[1] Archetypal oxidizers are potassium perchlorate or nitrate, while the fuel consists of a carbon backbone, boron or metal. Furthermore, pyrotechnic formulations often contain a binder or a propellant charge. Depending on the field of use, a colorant, a noise- or smoke-generating additive is supplied. The most important application is the use of light-emitting pyrotechnics for fireworks in the civil section but also for visible or infrared illumination in the military section. Albeit, light-generating pyrotechnics are used as decoy flares for aerial infrared countermeasure to defend airplanes from infrared homing surface-to-air or air-to-air missiles. Further specimens are smoke-generating pyrotechnics that are used for signaling and camouflage operations, while heat-generating pyrotechnics are employed in detonators, first fire propellant charges and priming charges.

6. Publications

The following chapters have been published as articles, or parts thereof, in peer-reviewed scientific journals (Zeitschrift für Anorganische und Allgemeine Chemie; New Journal of Chemistry, Chemistry – A European Journal; Propellants, Explosives and Pyrotechnics; Journal of Heterocyclic Chemistry) and as poster contributions at the annual international seminar *New Trends in Research of Energetic Materials* (2016 and 2018). In order to create a consistent thesis the published articles were slightly modified including additional minor improvements.

7. General Methods and Characterization:

Caution! The herein synthesized energetic compounds are sensitive to impact, friction and electrostatic discharge. Notwithstanding there were rarely problems in handling the compounds, appropriate protective measures (ear protection, Kevlar® gloves, face shield, body armor and earthed equipment) and a plastic spatula should be used.

5.1 Analytical Methods

NMR

Nuclear Magnetic Resonance measurements were operated using the spectrometers JEOL Eclipse 270, JEOL Eclipse 400, JEOL ECX 400, Bruker Avance III 400, Bruker 400 TR. The samples were prepared in regular glass NMR tubes (\varnothing 5mm) and the measurements were conducted under standard conditions. For interpretation tetramethylsilane (^1H , ^{13}C) and nitromethane ($^{14/15}\text{N}$) were used as external standards. Further evaluation with internal standard the reference values of the partially deuterated solvent impurity (^1H) and the deuterated solvent (^{13}C) were used.^[41]

Vibrational Spectroscopy

For infrared (IR) measurements a PerkinElmer BX FT IR spectrometer equipped with a Smiths DuraSamplIR II diamond ATR unit recorded spectra. Construed values are qualitatively labeled as “strong” (s), “medium” (m) and “weak” (w).

Raman analysis were accomplished on a Bruker RAM II spectrometer equipped with a Nd:YAG laser running at 1064 nm and a reflection angle of 180°. Sample tubes were prepared in glass tubes (\varnothing 5mm). The measured intensities are described as percentage with the most intense peak given as 100 in parentheses.

As bulk analysis of compounds the carbon, hydrogen and nitrogen contents were measured by combustion analysis using an Elementar Vario EL Analyser. A little disadvantage of this method is that the nitrogen content often is determined lower than calculated, which is common for nitrogen-rich compounds. Also measurements of very energetic materials, mainly in the primary range, the values used to be not corresponding. This is due to their explosive behavior.

The decomposition temperatures were measured using either a differential scanning calorimetry (DSC) or a differential thermal analysis (DTA). The DSC measurements were conducted with a Linseis DSC-PT10 in closed aluminum pans, equipped with a hole for gas release and a heating rate of 5 °C min⁻¹. The DTA measurements were conducted with an OZM Research DTA 552-Ex in open glass tubes at a heating rate of 5 °C min⁻¹. The reported temperatures are not at the climax of the measured peaks but the onsets.

X-ray diffraction was used for measurements of crystal structures by single-crystals. The X-ray device an Oxford Diffraction Xcalibur 3 diffractometer was equipped with a Sapphire CCD detector, four circle kappa platform operating with molybdenum K_α radiation source ($\lambda = 0.71073 \text{ \AA}$) and Oxford Cryosystems Cryostream cooling unit. Responsible for data collection and reduction was the program CrysAlisPro.^[42] If the crystals were too small for the Xcalibur device single-crystals were measured on a Bruker D8 Venture diffractometer with a fixed-chi three-circle platform using enhanced molybdenum K_α radiation ($\lambda = 0.71073 \text{ \AA}$). Therefore the program Bruker SAINT was used for data collection.^[43] All structures were

solved with SIR97,^[44] or SHELXS-97,^[45] refined with SHELXL-97,^[45] or SHELXL-2013,^[46] and finally checked with PLATON,^[47] all integrated into the WinGX software.^[48] The final version was checked with checkCIF^[49] and deposited at the Cambridge Crystallographic Data Centre (CCDC).^[50] For the analysis of the intra- and intermolecular contacts MERCURY was used.^[51] The final figure of the crystal structure was drawn with DIAMOND.^[52]

Sensitivities

In accordance to BAM standards^[53] the sensitivities to impact (IS), friction (FS) were determined, using a BAM drop hammer and a BAM friction apparatus.^{[54], [55], [56], [57], [58], [59]} According to the tests, the compounds were classified in accordance with UN guidelines. Impact: insensitive >40 J, less sensitive ≥ 35 J, sensitive ≥ 4 J, very sensitive ≤ 3 J. Friction: insensitive >360 N, less sensitive =360 N, sensitive <360 N and >80 N, very sensitive ≤ 80 N, extremely sensitive ≤ 10 N. For the measurement of the sensitivity to electrostatic discharge (ESD) served an OZM Research ESD 2010 EN.

Calculated Heats of Formation

In order to get more precise values for the enthalpies of combustion ($\Delta_c H$) and consequently enthalpies of formation ($\Delta_f H^\circ$), they were calculated at the CBS-4M level of theory, applied in GAUSSIAN 09.^{[60], [61], [62]} For this calculation experiment the atomization energy method and utilizing experimental data were used.^{[63], [64], [65], [66], [67]}

If possible, the initial geometries of the structures were taken from the corresponding X-ray crystal structure. Becke's B3 three parameter hybrid functions carried out the structure optimization and frequency analyses, using the LYP correlation functional (B3LYP). For the calculation of the C, H, N and O a correlation consistent polarized double- ζ basis set was used (cc-pVDZ). Optimization of the structures was done with symmetry constrains, while the energy was corrected applying the zero point vibrational energy. For precise vales of the enthalpies (H) and free energy (G) the calculations were performed using the complete basis set (CBS) method. Thereby for extrapolation the CBS model uses a finite basis set in order to estimate the complete basis set limit from the known asymptotic convergence of pair natural orbital expressions. The first step, a HF/3-21G(d) geometry optimization, an initial guess for the following SCF calculation a base energy. Secondly, a MP2/6-31+G calculation with CBS extrapolation for energy correction was done. Additionally to approximate higher order contributions the CBS-4M method enforce MP4(SDQ)/631+(d,p) calculations, but also involves some additional empirical corrections. Utilizing the atomization energy method the enthalpies of the gas-phase species were estimated.

For neutral compounds, the Trouton's rule was used and therefore the gas-phase enthalpies were transformed to solid state enthalpies.^{[68], [69]} For ionic compounds the Jenkin's method was used.^{[70], [71], [72]}

Calculated Performance

Calculations for determining the detonation or combustion parameters were performed using the program package EXPLOS5 V.6.03 (EOS BKWG-S).^{[73], [74]} Using a modified Becker-Kistiakowski-Wilson equation of state for modeling the system the detonation parameters were calculated at the Chapman-Jouguet (CJ) point, based on the steady-state detonation model. The CJ point is found from the Hugoniot curve of the first derivative.

- [1] T. M. Klapötke, *Chemistry of High-Energy Materials, 4th Edition*, Walter de Gruyter GmbH & Co KG, Berlin, **2017**.
- [2] ASTM International, <http://www.astm.org>, **2017**.
- [3] J. P. Agrawal, *High Energy Materials Propellants, Explosives and Pyrotechnics, 1st Ed.*, Weinheim, **2010**.
- [4] J. Köhler, R. Meyer, A. Homburg, *Explosives, 7th Edition*, Wiley-VCH, **2016**.
- [5] P. M. Dickson, J. E. Field, *Proc. R. Soc. London, Ser. A*, **1993**, *441*, 359–375.
- [6] S. Zeeman, *Sensitivities of High Energy Compounds, in Structure and Bonding - High Energy Density Materials, 125th*, Ed. T.M. Klapötke, Springer, Berlin, Germany, **2007**.
- [7] R. W. Shaw, T. B. Brill, D. L. Thompson, Editors, *Overviews of Recent Research on Energetic Materials. [In: Adv. Ser. Phys. Chem.; 2005, 16]*, World Scientific Publishing Co. Pte. Ltd., **2005**.
- [8] D. D. Dlott, *Adv. Ser. Phys. Chem.*, **2005**, *16*, 303–333.
- [9] T. B. Brill, K. J. James, *Chem. Rev. (Washington, D. C.)*, **1993**, *93*, 2667–2692.
- [10] D. D. Dlott, *Theor. Comput. Chem.*, **2003**, *13*, 125–191.
- [11] P. Politzer, J. S. Murray, *Cent. Eur. J. Energ. Mater.*, **2011**, *8*, 209–220.
- [12] M. J. Kamlet, S. J. Jacobs, *J. Chem. Phys.*, **1968**, *48*, 23–35.
- [13] C. L. Mader, *Numerical Modeling of Explosives and Propellants, 3th ed.*, CRC, **1997**.
- [14] T. Urbanski, *Chemistry and Technology of Explosives, Vol. 4*, Pergamon Press, **1984**.
- [15] D. Fischer, T. M. Klapötke, M. Reymann, J. Stierstorfer, *Chem. Eur. J.*, **2014**, *20*, 6401–6411.
- [16] H.-H. Licht, *Propellants, Explos., Pyrotech.*, **2000**, *25*, 126–132.
- [17] United States Environmental Protection Agency (EPA), *Technical Fact Sheet - Hexahydro-1,3,5-trinitro-1,3,5-triazine (RDX)*, **2014**.
- [18] Agency for Toxic Substances and Disease Registry (ATSDR), *Toxicological Profile for RDX*, **2012**.
- [19] P. Y. Robidoux, J. Hawari, G. Bardai, L. Paquet, G. Ampleman, S. Thiboutot, G. I. Sunahara, *Arch. Environ. Contam. Toxicol.*, **2002**, *43*, 379–388.
- [20] E. L. Etner, *Regul. Toxicol. Pharmacol.*, **1989**, *9*, 147–157.
- [21] United States Environmental Protection Agency (EPA), *Technical Fact Sheet - 2,4,6-Trinitrotoluene (TNT)*, **2012**.
- [22] J. Akhavan, *The chemistry of Explosives, Vol. 2*, Royal Society of Chemistry, **2004**.
- [23] H. Gao, J. M. Shreeve, *Chem. Rev.*, **2011**, *111*, 7377–7436.
- [24] A. F. Holleman, E. Wiberg, N. Wiberg, *Lehrbuch der Anorganischen Chemie*, 102nd ed., de Gruyter, Berlin, **2007**.
- [25] Q. Yu, P. Yin, J. Zhang, C. He, G. H. Imler, D. A. Parrish, J. M. Shreeve, *J. Am. Chem. Soc.*, **2017**, in press.

- [26] R. P. Singh, R. D. Verma, D. T. Meshri, J. n. M. Shreeve, *Angew. Chem., Int. Ed.*, **2006**, *45*, 3584–3601.
- [27] P. F. Pagoria, G. S. Lee, A. R. Mitchell, R. D. Schmidt, *Thermochim. Acta*, **2002**, *384*, 187–204.
- [28] T. Altenburg, T. M. Klapötke, A. Penger, J. Stierstorfer, *Z. Anorg. Allg. Chem.*, **2010**, *636*, 463–471.
- [29] Q. J. Axthammer, B. Krumm, T. M. Klapötke, R. Scharf, *Chem. - Eur. J.*, **2015**, *21*, 16229–16239.
- [30] a) W. H. Beck, *Combust. Flame*, **1987**, *70*, 171–190; b) S. Chaturvedi, P. N. Dave, *Arabian J. Chem.*, **2015**, DOI: 10.1016/j.arabjc.2014.1012.1033.
- [31] T. M. Klapötke, B. Krumm, R. Moll, S. F. Rest, W. Schnick, M. Seibald, *J. Fluorine Chem.*, **2013**, *156*, 253–261.
- [32] A. M. Mebel, M. C. Lin, K. Morokuma, C. F. Melius, *J. Phys. Chem.*, **1995**, *99*, 6842–6848.
- [33] T. M. Klapötke, B. Krumm, R. Moll, S. F. Rest, M. Suceśka, *Z. Naturforsch., B: J. Chem. Sci.*, **2014**, *69*, 8–16.
- [34] C. W. Trumpolt, J. Crain, G. D. Cullison, S. J. P. Flanagan, L. Siegel, S. Lathrop, *Remediation*, **2005**, *16*, 65–89.
- [35] B. Gu, J. D. Coates, *Perchlorates: Environmental Occurrence, Interactions and Treatment*, Springer Science, New York, **2006**.
- [36] J. Cui, J. Han, J. Wang, R. Huang, *J. Chem. Eng. Data*, **2010**, *55*, 3229–3234.
- [37] a) M. Göbel, T. M. Klapötke, *Z. Anorg. Allg. Chem.*, **2007**, *633*, 1006–1017; b) H. F. R. Schoyer, A. J. Schnorhk, P. A. O. G. Korting, P. J. Van Lit, J. M. Mul, G. M. H. J. L. Gadiot, J. J. Meulenbrugge, *J. Propul. Power*, **1995**, *11*, 856–869.
- [38] K. Menke, J. Bohnlein-Mauss, H. Schmid, K. M. Bucerius, W. Engel, in *US 5596168A*, **1997**.
- [39] T. M. Klapötke, B. Krumm, S. F. Rest, M. Suceśka, *Z. Anorg. Allg. Chem.*, **2014**, *640*, 84–92.
- [40] A. Baumann, A. Erbacher, C. Evangelisti, T. M. Klapötke, B. Krumm, S. F. Rest, M. Reynders, V. Sproll, *Chem. - Eur. J.*, **2013**, *19*, 15627–15638.
- [41] G. R. Fulmer, A. J. M. Miller, N. H. Sherden, H. E. Gottlieb, A. Nudelman, B. M. Stoltz, J. E. Bercaw, K. I. Goldberg, *Organometallics*, **2010**, *29*, 2176–2179.
- [42] *CrysAlisPro 1.171.37.33*, **2014**, Agilent Technologies, Santa Clara, Ca (USA).
- [43] Saint, V.818C, Bruker AXS GmbH, Karlsruhe, Germany, **2011**.
- [44] A. Altomare, M. C. Burla, M. Camalli, G. L. Cascarano, C. Giacovazzo, A. Guagliardi, A. G. G. Moliterni, G. Polidori, R. Spagna, *J. Appl. Crystallogr.*, **1999**, *32*, 115–119.
- [45] G. M. Sheldrick, *Acta Crystallogr., Sect. A: Found. Crystallogr.*, **2008**, *64*, 112–122.
- [46] G. M. Sheldrick, *Acta Crystallogr., Sect. C: Struct. Chem.*, **2015**, *71*, 3–8.
- [47] L. Spek, *PLATON*, **2015**, *Utrecht University, Utrecht, Netherlands*.
- [48] L. J. Farrugia, *J. Appl. Crystallogr.*, **1999**, *32*, 837–838.

- [49] (IUCr)checkCIF/PLATON, <http://www.journals.iucr.org/services/cif/checkcif.html>, **2017**.
- [50] The Cambridge Crystallographic Data Centre, <http://www.ccdc.cam.ac.uk>, **2017**.
- [51] C. F. Macrae, P. R. Edgington, P. McCabe, E. Pidcock, G. P. Shields, R. Taylor, M. Towler, J. van de Streek, *J. Appl. Crystallogr.*, **2006**, *39*, 453–457.
- [52] Klaus Brandenburg, DIAMOND, 3.2k ed., C. I. GbR, Berlin, Germany, **2017**.
- [53] Bundesanstalt für Materialforschung und -prüfung, **2012**, <http://www.bam.de>.
- [54] M. Sućeska, *Test Methods for Explosives, Vol. New York, Berlin, Heidelberg*, **1995**.
- [55] NATO , Standardization A. S. 4489) on explosives, *Impact sensitivity tests*, **1999**, No. 4489, 1st ed., Sept. 17.
- [56] NATO, Standardization Agreement (STANAG), *Chemical compatibility of ammunition components with explosives (non-nuclear application)*, **2006**, No. 4147, 2.ed.
- [57] *WIWEB-Standardarbeitsanweisung 4-5.1.02, Ermittlung der Explosionsgefährlichkeit, Schlagempfindlichkeit mit dem Fallhammer*, **2002**.
- [58] *WIWEB-Standardarbeitsanweisung 4-5.1.03, Ermittlung der Explosionsgefährlichkeit, Reibeempfindlichkeit mit dem Reibeapparat*, **2002**.
- [59] Reichel & Partner GmbH, **2012**, <http://www.reichelt-partner.de>.
- [60] M. J. Frisch, G. W. Trucks, H. B. Schlegel, G. E. Scuseria, M. A. Robb, J. R. Cheeseman, G. Scalmani, V. Barone, B. Mennucci, G. A. Petersson, H. Nakatsuji, M. Caricato, X. Li, H. P. Hratchian, A. F. Izmaylov, J. Bloino, G. Zheng, J. L. Sonnenberg, M. Hada, M. Ehara, K. Toyota, J. H. R. Fukuda, M. Ishida, T. Nakajima, Y. Honda, O. Kitao, H. Nakai, M. T. Vreven, J. E. Peralta, F. Ogliaro, M. Bearpark, J. J. Heyd, E. Brothers, K. N. Kudin, V. N. Staroverov, R. Kobayashi, J. Normand, K. Raghavachari, A. Rendell, J. C. Burant, S. S. Iyengar, J. Tomasi, M. Cossi, N. Rega, J. M. Millam, M. Klene, J. E. Knox, J. B. Cross, V. Bakken, C. Adamo, J. Jaramillo, R. Gomperts, R. E. Stratmann, O. Yazyev, A. J. Austin, R. Cammi and C. Pomelli, J. W. Ochterski, R. L. Martin, K. Morokuma, V. G. Zakrzewski, G. A. Voth, P. Salvador, J. J. Dannenberg, S. Dapprich, A. D. Daniels, Ö. Farkas, J. B. Foresman, J. C. J. V. Ortiz, D. J. Fox, *Gaussian 09; Rev. C.01 ed., Gaussian, Inc., Wallingford CT (USA)*, **2010**.
- [61] J. W. Ochterski, G. A. Petersson, J. A. Montgomery, Jr., *J. Chem. Phys.*, **1996**, *104*, 2598–2619.
- [62] J. A. Montgomery, Jr., M. J. Frisch, J. W. Ochterski, G. A. Petersson, *J. Chem. Phys.*, **2000**, *112*, 6532–6542.
- [63] B. M. Rice, J. J. Hare, *J. Phys. Chem. A*, **2002**, *106*, 1770–1783.
- [64] B. M. Rice, S. V. Pai, J. Hare, *Combust. Flame*, **1999**, *118*, 445–458.
- [65] P. J. Linstrom, W. G. M. (Eds.), *NIST Standard Reference Database Number 69*, **2017**, <http://www.webbook.nist.gov/chemistry/>.

- [66] E. F. C. Byrd, B. M. Rice, *J. Phys. Chem. A*, **2006**, *110*, 1005–1013.
- [67] J. D. Cox, D. D. Wagman, V. A. Medvedev, *CODATA Key Values for Thermodynamics*, **1984**, Hemisphere Publishing Corp., New York, USA.
- [68] F. Trouton, *Philos. Mag.*, **1884**, *18*, 54–57.
- [69] M. S. Westwell, M. S. Searle, D. J. Wales, D. H. Williams, *J. Am. Chem. Soc.*, **1995**, *117*, 5013–5015.
- [70] H. D. B. Jenkins, D. Tudela, L. Glasser, *Inorg. Chem.*, **2002**, *41*, 2364–2367.
- [71] H. D. B. Jenkins, J. F. Liebman, *Inorg. Chem.*, **2005**, *44*, 6359–6372.
- [72] H. D. B. Jenkins, H. K. Roobottom, J. Passmore, L. Glasser, *Inorg. Chem.*, **1999**, *38*, 3609–3620.
- [73] M. Sućeska, *Propellants, Explos., Pyrotech.*, **1991**, *16*, 197–202.
- [74] M. Sućeska, *EXPLO5 V.6.03*, **2014**, Zagreb (Croatia).

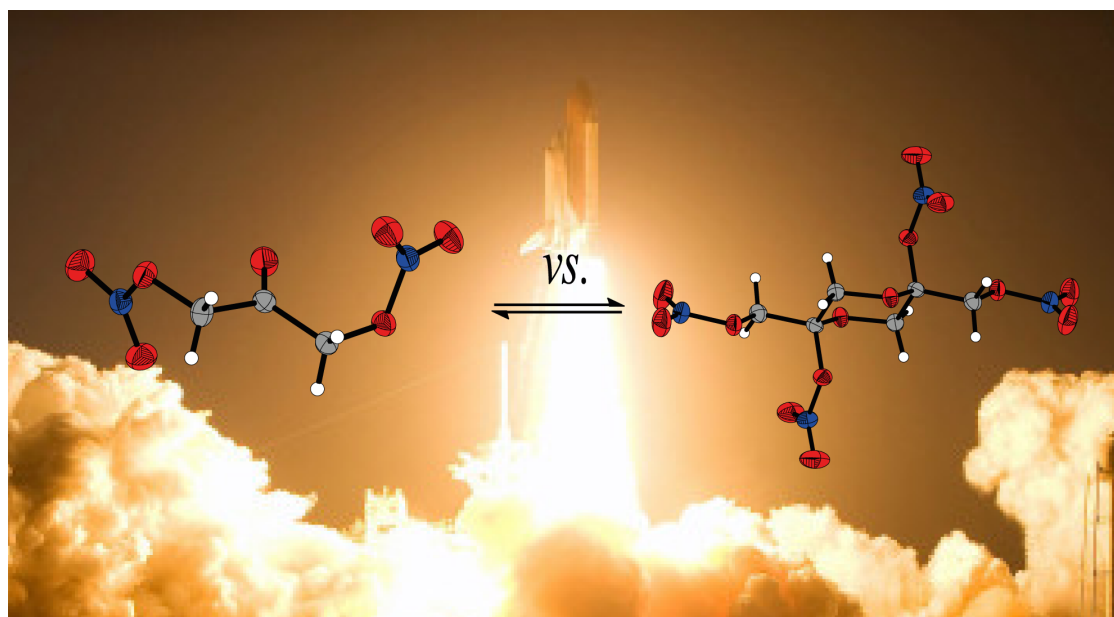
II Results and Discussion

- 1 Nitration of Dihydroxyacetone Monomer and Dimer
- 2 Trinitromethyl-1,2,4-Triazoles
- 3 Pyrazole Fused Furazanes
- 4 Picrylamine-1,2,5-Oxadiazoles and 1,2,4-Triazoles
- 5 Nitroureido-1,2,5-Oxadiazoles
- 6 Bis-(Nitramino-1,2,5-oxadiazol)-furoxanes
- 7 Trinitomethyl-1,2,4-Oxadiazoles
- 8 Bis-Nitramino-1,3,4-Oxadiazole

The Reagent-depending Nitration of 1,3-Dihydroxyacetone Dimer

Tobias S. Hermann, Thomas M. Klapötke,* Burkhard Krumm and Jörg Stierstorfer

Zeitschrift für anorganische und allgemeine Chemie, **2017**, 643, 149–151.



The Reagent-depending Nitration of 1,3-Dihydroxyacetone Dimer

Tobias S. Hermann, Thomas M. Klapötke,* Burkhard Krumm and Jörg Stierstorfer

Zeitschrift für anorganische und allgemeine Chemie, **2017**, *643*, 149–151.

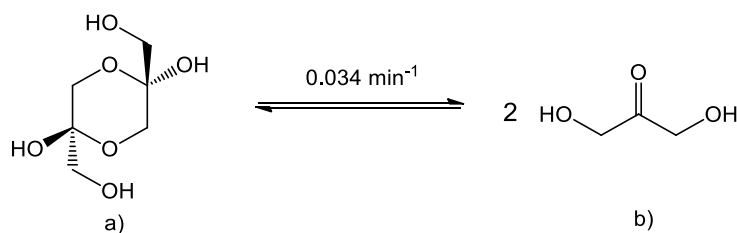
Abstract:

Two highly energetic nitric acid esters were synthesized from the dimer of dihydroxyacetone. 1,3-Dinitratoacetone (**1**) and its dimer 2,5-bis(nitratomethyl-2,5-nitrato)-1,4-dioxane (**2**) were characterized by single-crystal X-ray diffraction, vibrational spectroscopy (IR and Raman), multinuclear NMR spectroscopy, and elemental analysis. The thermal behavior was investigated with DTA measurements. Although showing the same atomic stoichiometry, dimer **2** shows significantly higher sensitivities measured by BAM methods (drophammer and friction tester). Due to the high oxygen content of 62.2%, **1** and **2** were evaluated as potential high energy dense oxidizers.

1. Introduction

In the past few decades the synthesis of halogen-free, high performance high energy dense oxidizers (HEDOs) has become increasingly important. One of our goals is to replace ammonium perchlorate (AP) with compounds showing a higher performance. While AP is widely used as an oxidizer in solid propellant rockets formulations, up to 70%,^{[1] [2]} it faces drawbacks due to the negative health effects and environment concerns. Perchlorate anions are toxic to humans and also the formation of HCl during the combustion is harmful.^[3] Consequently, CHNO-based oxidizers with a large excesses of oxygen have the potential to overcome these effects.^{[4] [5] [6] [7]} One of the most commonly used CHNO-based explosives are pentaerythritol tetranitrate (PETN) and nitroglycerine (NG),^[7] due to their low costs, easy synthesis and good performance. PETN and NG are easily synthesized by nitration in mixed acid from pentaerythritol or glycerol, respectively. Mixed acid nitration has been commonly used but non-acidic nitration is also possible. For example, dinitrogen pentoxide or nitronium salts like nitronium tetrafluoroborate have been used in the

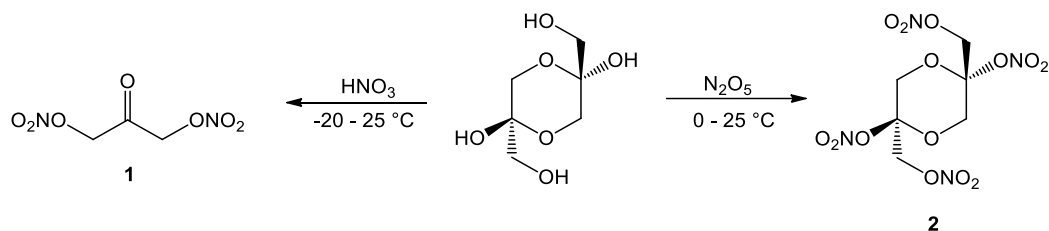
search of new energetic materials with similar or better oxygen balances and sensitivities.^[8] In this report, acidic and non-acidic nitration of the dimer of 1,3-dihydroxyacetone led to the formation of two nitrate esters, 1,3-dinitratoacetone (**1**) and 2,5-bis(nitratomethyl-2,5-nitrato)-1,4-dioxane (**2**), with better oxygen balances and sensitivities. Dihydroxyacetone (DHA) can be present as a dimer or monomer. The monomer only exists in solution and is obtained by dissolving the dimer in aqueous solutions, e.g. water or acids. The equilibrium dimer-to-monomer in water takes place with an apparent first-order rate constant of 0.034 min^{-1} (Scheme 1).^[9] DHA is a natural product in human, bacteria, and plants metabolism and plays an important role in the research of new biomaterials, biological polymers and drug designs. The low toxicity of DHA ($\text{LD}_{50} = 160000 \text{ mg/kg}$)^{[10] [11] [12]} proposes hopefully comparable properties for nitrated derivatives. Based on the fact, that sugars can react with primary amines to form brown pigments,^[13] DHA, a three-carbon sugar, can also react with amino acids.^[14] DHA is the browning ingredient in commercial sunless tanning lotions since the late 1950s.^{[14] [15]}



Scheme 1: Equilibrium between dihydroxyacetone dimer (a) and dihydroxyacetone monomer (b).

2. Results and Discussion

The commercially available starting material 1,3-dihydroxyacetone dimer was nitrated using two different methods. Compound **1** was obtained from fuming nitric acid after extraction, whereas mixed acid nitrations resulted only in poor yields. Compound **2** was synthesized in non-acidic conditions using dinitrogen pentoxide (Scheme 2). Recrystallization from chloroform yielded colorless crystals of **1** and **2**, which were suitable for single crystal X-ray diffraction. Compound **2** is hygroscopic and deliquescent.



Scheme 2: Nitration of 1,3-Dihydroxyacetone Dimer

Compounds **1** and **2** were investigated by low-temperature single-crystal X-ray diffraction (Figure 1 and Figure 2). Compound **1** crystallizes in the orthorhombic space group $Fdd2$ with eight formula units per unit cell and a density of 1.785 g cm^{-3} at 173 K. The dimer **2** crystallizes in the triclinic space group $P-1$ with two formula units per unit cell and a density of 1.839 g cm^{-3} at 173 K. The bond lengths of **1** and **2** are in a similar range to literature known CHNO based nitrate compounds.^{[8] [16]} Selected bond lengths and angles are reported in Figures 1 and 2. Measurement and refinement values are listed in Supporting Information. Compound **2** shows typical chair conformation with the nitrate groups at C1/C6 in the axial position and the nitratomethyl groups in the equatorial position.

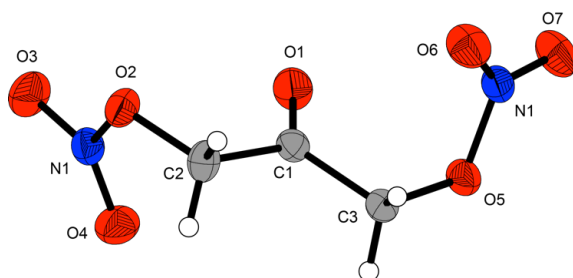


Figure 1: Molecular structure of 1,3-dinitratoacetone (**1**). Selected bond lengths (Å): C1–O1 1.203 (2), C2–O2 1.4334 (15), O2–N1 1.4021 (14), N1–O3 1.2028 (15). N1–O2–C2 112.28 (9). C2–O2–N1–O4 11.67 (16), O1–C1–C2–O2 5.52 (12).

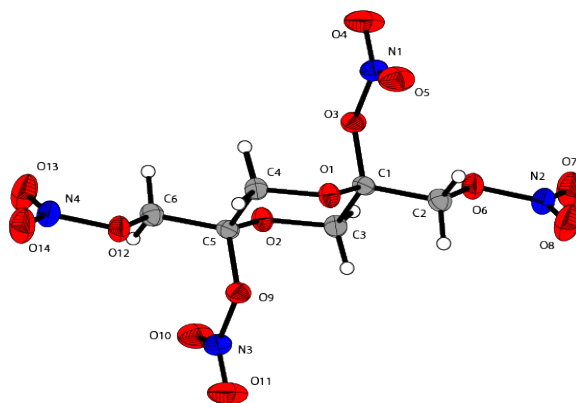


Figure 2: Molecular structure of 2,5-bis(nitratomethyl-2,5-nitrato)-1,4-dioxane (**2**). Selected bond lengths (Å): O1–C1 1.394(4), C1–O3 1.460(4), O3–N1 1.418(3), N1–O5 1.196(4). O1–C1–C2 106.1(2), O1–C1–O3 112.5(2), C2–O6–N2 113.1(2), C1–O3–N1 118.8(2). O1–C4–C5–O9 68.5(3), O1–C4–C5–C6 170.3(3), C3–C1–C2–O6 64.5(3), C3–C1–O3–N1 179.9(2).

The physicochemical properties and selected calculated values of **1** and **2** are summarized in Table 1. Thermal stabilities were investigated by DTA measurements (heating rate 5 K min^{−1}) with both compounds showing low thermal stability. Compounds **1** and **2** burn smokeless and are free of residues, which can be attributed to their high Ω_{CO} oxygen balance of +17.8%, which is in the range of PETN (+15.2 %). **1** shows a slightly lower calculated (see ESI) mass dependent heat of formation (**1**: −1987.9 kJ kg^{−1}, **2**: −1973.2 kJ kg^{−1}). The specific impulse of an oxidizer/aluminum/HTPB matrix was optimized due to the fact that the compounds already contain carbon and hydrogen atoms as fuel, which is accomplished by using lower amounts of the organic binder (HTPB). The specific impulse of both compounds was calculated to be 271 s and 277 s, compared to 264 s for AP. The sensitivities were experimentally determined with compound **1** (*IS*: 8 J, *FS*: 360 N) less sensitive and **2** equally sensitive to PETN (*IS*: 3 J, *FS*: 60 N).

Table 2: Physical and chemical properties of **1**, **2**, ammonium perchlorate (AP), nitroglycerine (NG) and pentaerythritol tetranitrate (PETN).

	1	2	AP	NG	PETN
$T_{\text{melt}} / ^\circ\text{C}^{\text{a)}$	65	-	-	13	141
$T_{\text{dec}} / ^\circ\text{C}^{\text{b)}$	115	45	240	185	202
$\rho / \text{g cm}^{-3 \text{ c)}$	1.75	1.79	1.95	1.59	1.75
$IS / \text{J}^{\text{d)}$	8	3	20	0.2	3
$FS / \text{N}^{\text{e)}$	360	60	360	350	60

$ESD / J^{f)}$	0.6	- ^{p)}	0.5	- ^{q)}	0.19
$N / \%^{g)}$	15.6	15.6	11.9	18.5	17.7
$O / \%^{h)}$	62.2	62.2	54.5	63.4	60.7
$N+O / \%^{i)}$	77.8	77.8	66.4	81.9	78.4
$\Delta H_f^\circ / kJ \text{ mol}^{-1}{}^{j)}$	-358.0	-710.7	-296	-334	-515
$\Omega_{CO} / \%^{k)}$	+17.8	+17.8	+34.0	+24.7	+15.2
$\Omega_{CO_2} / \%^{l)}$	-8.8	-8.8	+34.0	+3.5	-10.1
$I_s / s^{m)}$	258	259	157	259	264
$I_s / s^{n)}$	250	250	264	264	257
$I_s / s^{o)}$	271	277	259	270	277

a) Onset melting point T_{melt} from DTA measurement carried out at a heating rate of 5 K min⁻¹. b) Onset decomposition point T_{dec} from DTA measurement carried out at a heating rate of 5 K min⁻¹. c) Density at room temperature from X-ray measurement. d) Impact sensitivity. e) Friction sensitivity. f) Sensitivity towards electrostatic discharge. g) Nitrogen content. h) Oxygen content. i) Sum of nitrogen and oxygen content. j) Heat of formation. k) Oxygen balance Ω assuming the formation of CO at the combustion. l) Oxygen balance Ω assuming the formation of CO₂ at the combustion. m) Specific Impulse (100% compound). n) Specific impulse (15% Al, 15% Hydroxyl-terminated polybutadiene) (EXPLO V6.03: 70 bar chamber pressure, isobaric combustion conditions (1 bar), equilibrium expansion). o) Optimized specific impulse (19% Al, 5% Hydroxyl-terminated polybutadiene) (EXPLO V6.03: 70 bar chamber pressure, isobaric combustion conditions (1 bar), equilibrium expansion). p) Not determined, decomposition point too low. q) Liquid.

3. Conclusions

The reaction of dihydroxyacetone dimer with two different nitrating agents resulted in the formation and isolation of 1,3-dinitratoacetone (**1**) and 2,5-bis(nitratomethyl-2,5-nitrato)-1,4-dioxane (**2**) with crystal densities of 1.75 and 1.79 g cm⁻³, respectively. The thermal stability ($T_{\text{dec}} = 115$ °C (**1**), 45 °C (**2**)) was investigated by DTA measurements. The sensitivities measurements, according to BAM standards, show equal or lower values than PETN. The sensitivities of dimer **2** are significantly higher than those observed for **1**. Selected energetic propulsion parameters were calculated due to the positive oxygen balance of $\Omega_{CO} = +17.8\%$. The optimized specific impulse of 271/277 s of a rocket propulsion mixture (19% Al, 5% HTPB, 76% **1** or **2**) is slightly higher than that calculated for ammonium perchlorate (264 s).

4. Experimental Section

General experimental procedures are described in the Supporting Information.

Reaction of 1,3-dihydroxyacetone dimer with HNO₃

Fuming nitric acid was cooled to $-20\text{ }^{\circ}\text{C}$ and dihydroxyacetone dimer (0.5 g, 2.7 mmol) was added slowly. The reaction mixture was allowed to warm up to room temperature and stirred for an hour and then poured on ice. The solution was extracted with tert-butyl methyl ether (3 x 20 ml) and then dried with MgSO₄. The solvent was removed in vacuum and the obtained colorless oil was purified by treatment with chloroform. After removal of the solvent colorless crystals of **1** were obtained (0.40 g, 40 %).

DTA ($5\text{ }^{\circ}\text{C min}^{-1}$): $65\text{ }^{\circ}\text{C}$ (m.p.), $115\text{ }^{\circ}\text{C}$ (dec.); **IR** (ATR, cm^{-1}): $\tilde{\nu} = 3388$ (w, b), 1623 (s), 1467 (w), 1429 (w), 1376 (w), 1279 (m), 1267 (s), 1263 (m), 1009 (m), 991 (m), 957 (w), 861 (s), 830 (m), 753 (m), 715 (w), 704 (m), 666 (m), 622 (w); **Raman** (1064 nm, 500 mW, $25\text{ }^{\circ}\text{C}$, cm^{-1}): $\tilde{\nu} = 3032$ (14), 3009 (5), 2981 (62), 2907 (7), 2848 (2), 1630 (12), 1510 (2), 1464 (10), 1431 (21), 1388 (6), 1297 (6), 1283 (35), 1255 (5), 1205 (16), 1159 (2), 1096 (5), 1048 (2), 1013 (5), 995 (3), 960 (11), 873 (22), 815 (3), 707 (6), 670 (90), 625 (14), 597 (33), 516 (13), 435 (2), 398 (5), 308 (5), 262 (3), 230 (32), 173 (12), 157 (30), 94 (100), 84 (7); **¹H NMR** (CDCl₃, $25\text{ }^{\circ}\text{C}$, ppm) δ : 5.06 (s, CH₂), **¹³C NMR** (CDCl₃, $25\text{ }^{\circ}\text{C}$, ppm) δ : 193.7 (CO), 72.1 (CH₂), **¹⁴N NMR** (CDCl₃, $25\text{ }^{\circ}\text{C}$, ppm) δ : -50 ; **EA** (C₃H₄N₂O₇, 180.07): calc.: C 20.01, H 2.24, N 15.56 %; found: C 20.34, H 2.37, N 15.11 %; Sensitivities ($100\text{ }\mu\text{m} \geq \text{g.s.} \geq 50\text{ }\mu\text{m}$): **IS**: 8 J; **FS**: 360 N (neg.); **ESD**: 0.6 J.

Reaction of 1,3-dihydroxyacetone dimer with N₂O₅

Dinitrogen pentoxide (1.0 g; 9.25 mmol) was dissolved in 10 ml of dry acetonitrile and then cooled to $-20\text{ }^{\circ}\text{C}$. Commercially available dihydroxyacetone dimer (0.27 g; 1.54 mmol) was added and stirred for 30 min at this temperature. Afterwards the mixture was stirred for 30 min at ambient temperature and then poured on 20 ml ice/water. A colorless precipitate was obtained and filtered off. After recrystallization from chloroform colorless crystals of **2** (0.48 g, 88 %) were obtained.

DTA ($5\text{ }^{\circ}\text{C min}^{-1}$): $45\text{ }^{\circ}\text{C}$ (m.p. + dec.); **IR** (ATR, cm^{-1}): $\tilde{\nu} = 3033$ (w), 2960 (w), 2915 (w), 2713 (w), 2340 (w), 2272 (w), 1670 (m), 1651 (m), 1633 (s), 1467 (m), 1446 (w), 1405 (w), 1370 (m), 1289 (s), 1278 (s), 1257 (s), 1192 (m), 1180 (s), 1089 (m), 1071 (s), 1021 (m), 960 (m), 922 (w), 877 (m), 859 (m), 838 (m), 808 (s), 766 (s), 752 (s), 695 (s), 665 (m); **Raman** (1064 nm, 500 mW, $25\text{ }^{\circ}\text{C}$, cm^{-1}): $\tilde{\nu} = 3033$ (35), 2976 (65), 2947 (85), 2912 (27), 2300 (23), 1775 (22), 1678 (24), 1646 (29), 1448 (27), 1373 (24), 1294 (100),

936 (24), 873 (55), 802 (25), 629 (34), 598 (27), 561 (89), 448 (23), 433 (33), 390 (49), 364 (29), 347 (27), 326 (32), 263 (38), 234 (51), 209 (64), 188 (80); **¹H NMR** (CDCl₃, 25 °C, ppm) δ: 5.09 (d, 2H, CHHONO₂, ²J_{H,H} = 13.5 Hz), 4.73 (d, 2H, CHHONO₂), 4.06 (d, 2H, CHHOC, ²J_{H,H} = 13.1 Hz), 3.94 (d, 2H, CHHOC); **¹³C NMR** (CDCl₃, 25 °C, ppm) δ: 101.0 (CONO₂), 69.0 (CH₂ONO₂), 62.5 (CH₂-cycle); **¹⁴N NMR** (CDCl₃, 25 °C, ppm) δ: -51 (CH₂ONO₂), -56 (ONO₂); **EA** (C₆H₈N₄O₁₄, 360.14): calc.: C, 20.01, H, 2.24, N, 15.56; found: C, 20.64, H, 2.39, N, 14.79; Sensitivities (100 μm ≥ g.s. ≥ 50 μm): **IS**: 3 J; **FS**: 60 N.

5. Supporting Information

5.1 NMR spectroscopy

The compounds were characterized by ^1H , ^{13}C and ^{14}N NMR spectroscopy. The multinuclear NMR spectra were recorded in CDCl_3 .

As expected, the ^1H NMR spectrum of **1** shows one singlet for the CH_2 group that is observed at 5.06 ppm. In comparison, the ^1H NMR spectrum of **2** shows two doublets of doublets at 5.09/4.73 ppm ($^2J(\text{H},\text{H})=13.5\text{ Hz}$) and 4.06/3.94 ppm ($^2J(\text{H},\text{H})=13.1\text{ Hz}$). This is due to the coupling of each proton at the CH_2 moiety in the AB system.

The ^{13}C NMR spectrum of **1** shows two peaks. The resonance for the carbonyl group is visible at 193.7 ppm and that of the CH_2 group at 72.1 ppm. In the ^{13}C NMR spectra of **2**, three resonances are observed. The resonance of the CONO_2 moiety is observed at 101.0 ppm. The CH_2ONO_2 group is observed at 69.0 ppm and the $\text{CH}_{2\text{-cyclic}}$ at 62.5 ppm, respectively. The resonance of the nitrate groups for compounds **1** and **2** in the ^{14}N NMR spectrum are observed at -50 ppm (**1**) and -51 ppm and -56 (**2**), respectively.

5.2 Vibrational spectroscopy

The vibrational spectra of **1** and **2** show characteristic asymmetric NO_2 stretching vibrations in the range of 1615–1588 cm^{-1} and the symmetric stretching vibrations at 1304 to 1271 cm^{-1} (Table S1). The nitrate group vibrations of **1** and **2** are in a similar range, explained by the similarity of the functional groups. The carbonyl stretch vibration of **1** is observed between 1780 to 1720 cm^{-1} and the C-C vibrations are observed in the typical ranges for CHNO based compounds. [17] [18]

Table S1: IR and Raman bands of carbonyl and nitrate groups of **1** and **2**.

	1		2	
	IR	Raman	IR	Raman
$\nu(\text{C}=\text{O})$	1743	1762		
$\nu_{\text{as}}(\text{ONO}_2)$	1623	1629	1633	1646
$\nu_{\text{s}}(\text{ONO}_2)$	1267	1296	1278	1293

5.3 X-ray diffraction

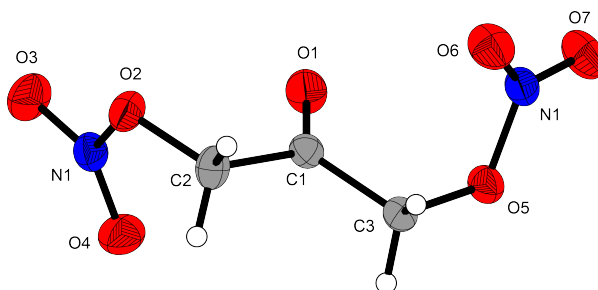


Figure S1: Molecular structure of 1,3-dinitratoacetone (**1**).

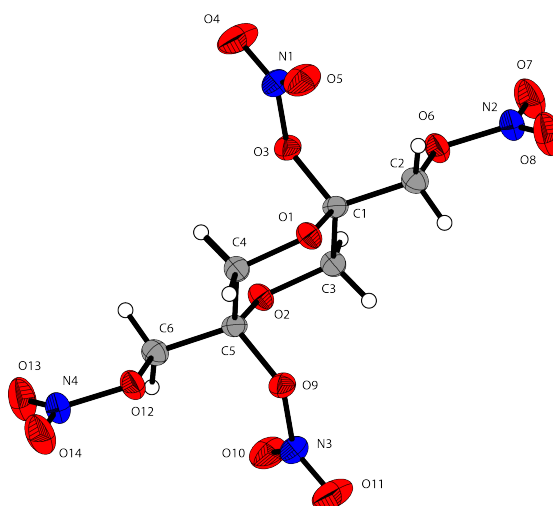


Figure S2: Molecular structure of 2,5-bis(nitratomethyl-2,5-nitrato)-1,4-dioxane (**2**).

Compounds **1** and **2** were investigated by low-temperature, single crystal X-ray diffraction. Crystallographic data for both compounds are summarized in Table S2. Measurable single crystals for the X-ray diffraction were obtained by slow evaporation in chloroform.

The molecular structure of 1,3-dinitratoacetone (**1**) is shown in Figure 1. Compound **1** crystallizes in the orthorhombic space group *Fdd2* with eight formula units per unit cell and a density of 1.785 g cm⁻³ at 173 K. The bond lengths of **1** are similar to literature known CHNO based nitrate compounds.^{[8] [16]} The average N-O bond lengths of the nitrate moieties in **1** and **2** are 1.20 Å. Compound **1** shows a planar like geometry with a C1-C2-C3-O5 torsion angle of -174.48(12)°. The O4-C2-C3-O5 torsion angle shows a slight deviation of 5.52(12)°. The nitrates twist out of the plane with a C3-O5-N2 angle of 112.28(9)°.

The crystal structure of 2,5-bis(nitratomethyl-2,5-nitrato)-1,4-dioxane (**2**) is shown in Figure 2. It crystallizes in the triclinic space group $P\bar{1}$ with two formula units per unit cell and a density of 1.839 g cm^{-3} at 173 K. The average N-O bond lengths and the $\text{O}_2\text{NO-C}$ bond lengths are comparable to **1** in the range of 1.20 Å and 1.44 Å, respectively. These values are similar to literature reported compounds ^[16]. The C-O bonds (1.43 Å) in the heterocycle are slightly shorter than the C-C bonds (1.52 Å). The geometry of **2** shows a typical chair conformation.

Table S2: Crystal and structure refinement data for **1** and **2**.

	1	2
Empirical formula	$\text{C}_3\text{H}_4\text{N}_2\text{O}_7$	$\text{C}_6\text{H}_8\text{N}_4\text{O}_{14}$
Formula mass (g mol^{-1})	180.07	360.14
Temperature (K)	173(2)	173(2)
Crystal size (mm^3)	0.40 x 0.35 x 0.35	0.38 x 0.46 x 0.70
Crystal description	Colorless block	Colorless block
Crystal system	Orthorhombic	Triclinic
Space group	$Fdd2$	$P\bar{1}$
a (Å)	13.2800(11)	5.1866(6)
b (Å)	20.4970(4)	6.4475(7)
c (Å)	4.9240(18)	20.157(2)
β (°)	90.00	87.640(9)
V (Å ³)	1340.3(5)	653.57(12)
Z	8	2
ρ_{calc} (g cm^{-3})	1.785	1.839
μ (mm^{-1})	0.181	0.186
$F(000)$	736	368
θ range (°)	4.53–28.28	4.14–26.49
Index range	$-17 \leq h \leq 17$ $-27 \leq k \leq 27$ $-6 \leq l \leq 6$	$-6 \leq h \leq 5$ $-8 \leq k \leq 8$ $-21 \leq l \leq 25$
Reflection collected	5398	3547
Reflection observed	839	2676
Reflection unique	783	1924
R1, wR2 (2σ data)	0.0276/	0.0925/0.1623

R1, wR2 (all data)	0.0311/	0.0648/0.1417
Data/restraints/parameter	839/1/57	1824/0/249
GOOF an F ²	1.097	1.110
Larg. diff. peak/hole (e Å ⁻³)	0.191/-0.149	0.484/-0.285
CCDC entry	1500574	1500575

5.4 Thermal and energetic properties

The thermal stabilities were investigated by DTA measurements with a heating rate of 5 °C min⁻¹. The values are shown in Table S3. 1,3-Dinitratoacetone (**1**) melts at 65 °C (onset) and is thermally stable up to 115 °C (onset). It burns residue-free with a smokeless flame due to its oxygen balance. The sensitivities toward impact, friction and electrostatic discharge of **1** and **2** were determined experimentally according to standards of the Federal Institute for Materials Research and Testing (BAM). 1,3-Dinitratoacetone (**1**) is not sensitive towards friction (360 N) but is sensitive to impact (8 J). 2,5-Bis(nitratomethyl-2,5-nitrato)-1,4-dioxane (**2**) decomposes at 45 °C without melting. Compared to **1**, compound **2** is more sensitive towards friction (60 N) and to impact (3 J). Compound **2** also burns residue-free with a smokeless flame.

Table S3: Physical and chemical properties of **1**, **2**, ammonium perchlorate (AP), nitroglycerine (NG) and pentaerythritol tetranitrate (PETN).

	1	2	AP	NG	PETN
$T_{\text{melt}} / ^\circ\text{C}^{\text{a)}$	65	-	-	13	141
$T_{\text{dec}} / ^\circ\text{C}^{\text{b)}$	115	45	240	185	202
$\rho / \text{g cm}^{-3}^{\text{c)}$	1.75	1.79	1.95	1.59	1.75
$IS / \text{J}^{\text{d)}$	8	3	20	0.2	3
$FS / \text{N}^{\text{e)}$	360	60	360	360	60
$ESD / \text{J}^{\text{f)}$	0.6	nd	0.5	nd	0.19
$N / \%$ ^{g)}	15.6	15.6	11.9	18.5	17.7
$O / \%$ ^{h)}	62.2	62.2	54.5	63.4	60.7
$N+O / \%$ ⁱ⁾	77.8	77.8	66.4	81.9	78.4
$\Omega_{\text{CO}} / \%$ ^{j)}	+17.8	+17.8	+34.0	+24.7	+15.2
$\Omega_{\text{CO}_2} / \%$ ^{k)}	-8.8	-8.8	+34.0	+3.5	-10.1

a) Onset melting point T_{melt} from DTA measurement carried out at a heating rate of 5 K min⁻¹. b) Onset decomposition point T_{dec} from DTA measurement carried out at a heating rate of 5 K min⁻¹. c) Density at room temperature from X-ray measurement. d) Impact sensitivity. e) Friction sensitivity. f) Sensitivity towards electrostatic discharge. g) Nitrogen content. h) Oxygen content. i) Sum of nitrogen and oxygen content. j) Oxygen balance Ω assuming the formation of CO at the combustion. k) Oxygen balance Ω assuming the formation of CO₂ at the combustion.

Table S4: Calculated heats of formation, predicted detonation and combustion parameters (using the EXPLO5 V6.03 code) for **1**, **2** and **AP**.

	1	2	AP
$\Delta_f H^\circ / \text{kJ mol}^{-1 \text{ a)}$	358.0	650.9	296
$\Delta_f U^\circ / \text{kJ kg}^{-1 \text{ b)}$	1898.5	1883.8	2433
$Q_v^{\text{ c)}$	-5845	-5872	1422
$T_{\text{ex}}^{\text{ d)}$	3999	3923	1725
$V_0^{\text{ e)}$	430	415	408
$P_{\text{CJ}}^{\text{ f)}$	297	324	158
$V_{\text{Det}}^{\text{ g)}$	8282	8582	6368
$I_s / \text{s}^{\text{ h)}$	258	259	157
$I_s / \text{s}^{\text{ i)}$ (5% Al, 15% binder)	233	234	251
$I_s / \text{s}^{\text{ i)}$ (10% Al, 15% binder)	244	244	257
$I_s / \text{s}^{\text{ i)}$ (15% Al, 15% binder)	250	250	264
$I_s / \text{s}^{\text{ i)}$ (20% Al, 15% binder)	247	247	264
$I_s / \text{s}^{\text{ i)}$ (19% Al, 15% binder)	251	251	264

a) Enthalpy calculated by the CBS-4 M method using Gaussian 09 [19] [20]. b) Energy of formation calculated by the CBS-4 M method using Gaussian 09 [19] [20]. c) Heat of explosion. d) Detonation temperature. e) Volume of gaseous products. f) Detonation pressure. g) Detonation velocity calculated by using the EXPLO5 (Version 6.03) program package.[21] h) Specific impulse of the neat compound using the EXPLO5 (Version 6.03) program package at 70.0 bar chamber pressure and with equilibrium expansion.[21] i) Specific impulse for compositions with different percentage of aluminum binder 15 % HTPB.

5.5 Experimental

General procedures:

The low-temperature single-crystal X-ray diffraction measurements were performed on an Oxford XCalibur3 diffractometer equipped with a Spellman generator (voltage 50 kV, current 40 mA) and a KappaCCD detector operating with $\text{Mo}_{\text{K}\alpha}$ radiation ($\lambda = 0.7107 \text{ \AA}$). Data collection was performed using the CRYSTALIS CCD software.[22] The data reduction was carried out using the CRYSTALIS RED software.[23] The solution of the structure was performed by direct methods (SIR97)[24] and refined by full-matrix least-squares on F2 (SHELXL)[25] implemented in the WINGX software package[26] and finally checked with the PLATON software.[27] All non-hydrogen atoms were refined anisotropically. The

hydrogen atom positions were located in a difference Fourier map. ORTEP plots are shown with thermal ellipsoids at the 50 % probability level. These data can be obtained free of charge from The Cambridge Crystallographic Data Centre.

All chemicals were used as supplied. Raman spectra were recorded in a glass tube with a Bruker MultiRAM FT-Raman spectrometer with Nd:YAG laser excitation up to 1000 mW (at 1064 nm). Infrared spectra were measured with a PerkinElmer Spectrum BX-FTIR spectrometer equipped with a Smiths Dura/SamplIR II ATRdevice. All spectra were recorded at ambient (25 °C) temperature. NMR spectra were recorded with a JEOL/Bruker instrument and chemical shifts were determined with respect to external Me₄Si (¹H, 399.8 MHz; ¹³C, 100.5 MHz) and MeNO₂ (¹⁴N, 28.9 MHz). Analyses of C/H/N were performed with an Elemental Vario EL Analyzer. Melting and decomposition points were measured using differential thermal analysis (DTA) at a heating rate of 5 °C min⁻¹ with an OZM Research DTA 552-Ex instrument. The sensitivity data were explored using a BAM drop hammer and a BAM friction tester.^[7] The heats of formations were calculated by the atomization method based on CBS-4M electronic enthalpies. All calculations affecting the detonation parameters were carried out using the program package EXPLO5 6.03.^{[21],[28]}

Caution! All high nitrogen and oxygen containing compounds are potentially explosive energetic materials, although no hazards were observed during preparation and handling these compounds. Nevertheless, this necessitates additional meticulous safety precautions (earthed equipment, Kevlar gloves, Kevlar sleeves, face shield, leather coat and ear plugs). Particular care should be exercised in handling of those materials and derivatives.

5.6 Heat of formation calculations

All calculations were carried out using the Gaussian G09W (revision A.02) program package. The enthalpies (H) and free energies (G) were calculated using the complete basis set (CBS) method of Petersson and coworkers in order to obtain very accurate energies. The CBS models use the known asymptotic convergence of pair natural orbital expressions to extrapolate from calculations using a finite basis set to the estimated complete basis set limit. CBS-4 begins with a HF/3-21G(d) geometry optimization; the zero point energy is computed at the same level. It then uses a large basis set SCF calculation as a base energy, and a MP2/6-31+G calculation with a CBS extrapolation to correct the energy through second order. A MP4(SDQ)/6-31+(d,p) calculation is used to approximate higher order contributions. In this study we applied the modified CBS-4M method (M referring to the use of Minimal Population localization) which is a re-parametrized version of the original CBS-4 method and also includes some additional empirical

corrections.^{[29] [30]} The enthalpies of the gas-phase species M were computed according to the atomization energy method (eq.1).

$$\Delta_f H^\circ_{(g, M, 298)} = H_{(Molecule, 298)} - \sum H^\circ_{(Atoms, 298)} + \sum \Delta_f H^\circ_{(Atoms, 298)} \quad (1)$$

Table S5: CBS-4M results and calculated gas-phase enthalpies.

	M	$-H^{298} / \text{a.u.}$	$\Delta_f H^\circ(g, M) / \text{kcal mol}^{-1}$
1	180.07	751.640744	-74.6
2	360.15	1503.291411	-155.5

Table S6: CBS-4M values and literature values for atomic $\Delta_f H^\circ_{298} / \text{kcal mol}^{-1}$.

	$-H^{298} / \text{a.u.}$	NIST ^[8]
H	0.500991	52.1
C	37.786156	171.3
N	54.522462	113.0
O	74.991202	59.6

In the case of the ionic compounds, the lattice energy (U_L) and lattice enthalpy (ΔH_L) were calculated from the corresponding X-ray molecular volumes according to the equations provided by Jenkins and Glasser. With the calculated lattice enthalpy (Table S6) the gas-phase enthalpy of formation (Table S5) was converted into the solid state (standard conditions) enthalpy of formation (Table S6). These molar standard enthalpies of formation (ΔH_m) were used to calculate the molar solid state energies of formation (ΔU_m) according to equation 2.

$$\Delta U_m = \Delta H_m - \Delta n RT \quad (2)$$

(Δn being the change of moles of gaseous components)

Table S7: Solid state energies of formation ($\Delta_f U^\circ$).

	$\Delta_f H^\circ(s) /$ kcal mol^{-1}	$\Delta_f H^\circ(s) /$ kJ mol^{-1}	Δn	$\Delta_f U^\circ(s) /$ kJ mol^{-1}	M / g mol^{-1}	$\Delta_f U^\circ(s) /$ kJ kg^{-1}
1	-85.5	-358.0	6.5	-341.9	180.09	-1898.5
2	-169.7	-710.7	13	-678.5	360.18	-1883.8

Notes: Δn being the change of moles of gaseous components when formed.

6. References

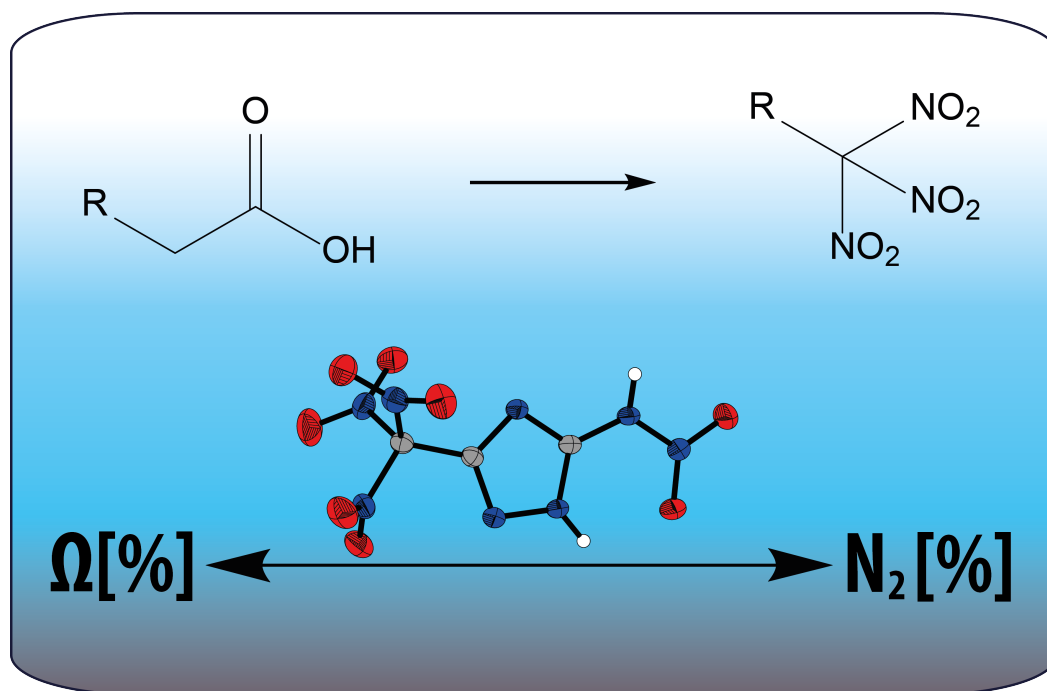
- [1] T. M. Klapötke, *New Trends Res. Energ. Mater. Proc. Semin. 13th*, **2010**, 2, 642-651.
- [2] J. P. Agrawal, *High Energy Materials Propellants, Explosives and Pyrotechnics*, 1st ed, **2010**, Weinheim.
- [3] C. Hogue, *Chem. Eng. News*, **2011**, 89, 43-44.
- [4] Q. J. Axthammer, T. M. Klapötke, B. Krumm, *Chem. Asian J.*, **2016**, 11, 568-575.
- [5] T. M. Klapötke, B. Krumm, R. Moll, S. F. Rest, *Z. Anorg. Allg. Chem.*, **2011**, 637, 2103-2110.
- [6] J. Köhler, R. Meyer, A. Homburg, *Explosives*, 7th Edition, Wiley-VCH, **2016**.
- [7] T. M. Klapötke, *Chemistry of High-Energy Materials*, 3rd Edition, Walter de Gruyter GmbH & Co KG, Berlin, **2015**.
- [8] D. Fischer, T. M. Klapötke, J. Stierstorfer, *Chem. Commun.*, **2016**, 52, 916-918.
- [9] L. Davis, *Bioorg. Chem.*, **1973**, 2, 197-201.
- [10] N. G. Ricapito, J. Mares, D. Petralia, D. Putnam, *Macromol. Chem. Phys.*, **2016**, 217, 1917-1925.
- [11] N. G. Ricapito, D. Putnam, C. Ghobril, H. Zhang, M. W. Grinstaff, D. Putnam, *Chem Rev*, **2016**, 116, 2664-2704.
- [12] R. P. Quintana, L. R. Garson, A. Lasslo, S. I. Sanders, J. H. Buckner, H. K. Gouck, I. H. Gilbert, D. E. Weidhaas, C. E. Schreck, *J. Econ. Entomol.*, **1970**, 63, 1128-1131.
- [13] L. C. Maillard, *Compt. rend.*, **1912**, 154, 66-68.
- [14] C. Fox, *Cosmet. Toiletries*, **2003**, 118, 30, 32-35.
- [15] S. B. Levy, *Dermatol. Clin.*, **2000**, 18, 591-596.
- [16] B. S. Fedorov, M. A. Fadeev, L. T. Eremenko, *Mendeleev Commun.*, **1997**, 40-41.
- [17] G. Socrates, *Infrared and Raman Characteristic Group Frequencies: Tables and Charts*, **2004**, 3rd ed.; John Wiley & Sons, Chichester.
- [18] Y. Oyumi, T. B. Brill, A. L. Rheingold, *J. Phys. Chem.*, **1985**, 89, 4824-4828.
- [19] M. J. Frisch, G. W. Trucks, H. B. Schlegel, G. E. Scuseria, M. A. Robb, J. R. Cheeseman, G. Scalmani, V. Barone, B. Mennucci, G. A. Petersson, H. Nakatsuji, M. Caricato, X. Li, H. P. Hratchian, A. F. Izmaylov, J. Bloino, G. Zheng, J. L. Sonnenberg, M. Hada, M. Ehara, K. Toyota, J. H. R. Fukuda, M. Ishida, T. Nakajima, Y. Honda, O. Kitao, H. Nakai, M. T. Vreven, J. E. Peralta, F. Ogliaro, M. Bearpark, J. J. Heyd, E. Brothers, K. N. Kudin, V. N. Staroverov, R. Kobayashi, J. Normand, K. Raghavachari, A. Rendell, J. C. Burant, S. S. Iyengar, J. Tomasi, M. Cossi, N. Rega, J. M. Millam, M. Klene, J. E. Knox, J. B. Cross, V. Bakken, C. Adamo, J. Jaramillo, R. Gomperts, R. E. Stratmann, O. Yazyev, A. J. Austin, R. Cammi and C. Pomelli, J. W. Ochterski, R. L. Martin, K. Morokuma, V. G. Zakrzewski, G. A. Voth, P. Salvador, J. J. Dannenberg, S. Dapprich, A. D.

- Daniels, Ö. Farkas, J. B. Foresman, J. C. J. V. Ortiz, D. J. Fox, *Gaussian 09; Rev. A.02 ed., Gaussian, Inc., Wallingford CT(USA),, 2009.*
- [20] R. D. Dennington II, T. A. Keith, J. M. Millam, *GaussView, Ver.5.08 ed., Semichem, Inc., Wallingford CT (USA), 2009.*
- [21] M. Sućeska, *Propellants, Explos., Pyrotech., 1991, 16*, 197-202.
- [22] O. D. Ltd, *CrysAlisRED, 2011*, Version 1.171.135. (release116-105-2011CrysAlis 2171.Net), Abingdon, Oxford (U.K.).
- [23] O. D. Ltd., *CrysAlis RED, 2011*, Version 1.171.135.111(release 116-105-2011CrysAlis 2171.NET), Abingdon, Oxford (U.K.), 2011.
- [24] A. Altomare, M. C. Burla, M. Camalli, G. L. Cascarano, C. Giacovazzo, A. Guagliardi, A. G. G. Moliterni, G. Polidori, R. Spagna, *J. Appl. Crystallogr., 1999, 32*, 115-119.
- [25] G. M. Sheldrick, *SHELX-97, 1997*, Programs for Crystal Structure Determination.
- [26] L. J. Farrugia, *J. Appl. Crystallogr., 1999, 32*, 837-838.
- [27] A. L. Spek, *Acta Crystallogr., 2009, 65 D*, 148-155.
- [28] M. Sućeska, *EXPLO5 V.6.03, 2014*, Zagreb (Croatia).
- [29] J. W. Ochterski, G. A. Petersson, J. A. Montgomery, Jr., *J. Chem. Phys., 1996, 104*, 2598-2619.
- [30] J. A. Montgomery, Jr., M. J. Frisch, J. W. Ochterski, G. A. Petersson, *J. Chem. Phys., 2000, 112*, 6532-6542.

The Energetic 3-Trinitromethyl-5-nitramino-1*H*-1,2,4-triazole and Nitrogen-rich Salts

Tobias S. Hermann, Thomas M. Klapötke*, Burkhard Krumm and Jörg Stierstorfer

New Journal of Chemistry, **2017**, *41*, 3068–3072.



The Energetic 3-Trinitromethyl-5-nitramino-1*H*-1,2,4-triazole and Nitrogen-rich Salts

Tobias S. Hermann, Thomas M. Klapötke*, Burkhard Krumm and Jörg Stierstorfer

New Journal of Chemistry, **2017**, *41*, 3068–3072.

Abstract:

The synthesis of 3-trinitromethyl-5-nitramino-1*H*-1,2,4-triazole (**1**) is described. This triazole is a powerful energetic compound due to its high nitrogen- and oxygen-content. Selected nitrogen-rich salts were also prepared in order to tune the performance and sensitivity values. The compounds are characterised by vibrational and NMR spectroscopy, and elemental analysis. The structure of **1** was determined by X-ray diffraction. The sensitivities were measured according to BAM standards and energetic performances calculated by EXPLO5 6.03.

1. Introduction

The research and investigation of new energetic materials still is one of the most interesting fields in synthetic inorganic and organic chemistry, as observed in the steadily increasing number of publications in recent years.^[1] The chemistry of nitrogen-rich heterocyclic energetic materials such as triazoles and tetrazoles is of particular interest. The reason for the great interest in the first is because of (i) their facile synthesis and (ii) the ability of substitution on two carbon atoms, in contrast to tetrazoles with only one carbon atom. Therefore, a lot of research has been performed in this field and several trinitromethyl-triazoles and tetrazoles have been synthesized (**Figure 1**).^{[2] [3] [4]}

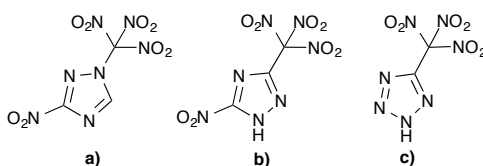


Figure 1: Examples of trinitromethyltriazoles and tetrazoles. a) 3-trinitromethyl-5-nitro-1*H*-[1,2,4]triazole. b) 1-trinitromethyl-5-nitro-1,2,4-triazole. c) 5-(trinitromethyl)-2*H*-tetrazole.

These high energy heterocycles combine several aspects which are important for good explosive materials, such as high heats of formation and high crystal densities.^[5] Because of the low amount of carbon and hydrogen, certain compounds already have a quite good oxygen balance.^[6] In terms of synthesizing high-energy dense oxidizers (HEDOs), which are needed for propellant applications, nitrogen/oxygen-rich heterocycles are promising compounds. Next to a high density, low sensitivity and high thermal stability, the oxygen balance (Ω) is one of the most important properties of HEDOs. It can be described as the oxygen excess that a compound needs to convert all carbon into carbon monoxide, all hydrogen into water and nitrogen into dinitrogen. Ω of $C_aH_bN_cO_d$ based compounds can be calculated by using the simple equation (1).^[7] The oxygen balance value should be greater than zero to produce free oxygen during combustion, therefore fuel can be completely oxidized.^[8]

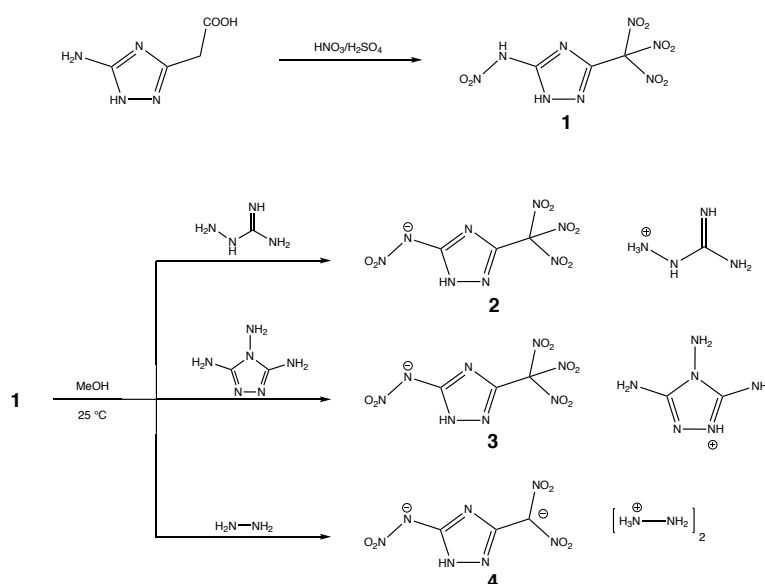
$$\Omega_{CO} = \frac{(d - a - \frac{b}{2})}{M} \cdot 1600 \quad (1)$$

In order to synthesize more powerful energetic materials with high nitrogen/oxygen contents, different functional groups can be attached to the molecule's backbone. The most interesting functional groups with respect to increasing the oxygen content are nitro, nitrate and nitramine groups. The functional groups with the highest oxygen content are trinitromethyl groups, which can be achieved for example by nitration of acetic acid functional groups, as demonstrated in this contribution. Here the combination of the benefits of nitrogen-rich heterocycles and the high oxygen contents of trinitromethyl- and nitramino moieties was attempted to explore. A new trinitromethyl triazole and nitrogen-rich salts were synthesized and characterized, and their energetic parameters calculated.

2. Results and Discussion

The synthesis of 3-trinitromethyl-5-nitramino-1H-1,2,4-triazole (**1**) was performed in mixed acid with 5-amino-1H-1,2,4-triazol-3-acetic acid as the starting material. This precursor is easily available via condensation of the economic materials aminoguanidinium bicarbonate and malonic acid.^{[9], [10]} The most acidic hydrogen atom of this triazole **1** is located at the nitramine position, and the reactivity towards selected bases was examined (Scheme 1). The deprotonation of **1** with aminoguanidine and triaminotriazole occurred at the nitramine group to result in anionic nitramides

2 and **3**. However, the reaction with hydrazine resulted in the unexpected formation of a di-anion with the proposed structure outlined in Scheme 1. Here, a dihydrazinium salt (**4**) and the loss of one nitro group of the trinitromethyl moiety by conversion into a dinitromethyl group, was obtained. There is no structural proof of these anions because of the lack of crystallization in all cases. All three salts were obtained as yellow–orange powders. Nevertheless, this type of dianion in **4** is confirmed by elemental analysis and also in comparison with other hydrazinium salts of related compounds.^[2] It was observed, that the salt **4** is unstable towards prolonged periods in the only available solvent DMSO, and therefore NMR spectroscopy is only suitable with limitations. The mechanism of the conversion of the trinitromethyl to the dinitromethyl moiety has also been discussed.^{[11], [12]} Furthermore, also other bases, such as ammonia, hydroxylamine, triamino-guanidine and triamino-triazolotriazole were reacted with **1**, but shown to be not successful. According to NMR spectroscopy and elemental analysis, evidence of compound mixtures and decomposition was observed. In addition, attempts to prepare the mono- or di-potassium salt by treatment with potassium hydroxide or potassium bicarbonate failed as well. NMR and vibrational spectroscopy (IR) and differential thermal analysis (DTA) were used to comprehensively characterize all compounds. The sensitivities of **1–4** were measured by BAM standards and theoretical parameters calculated using the EXPLO5 6.03 code (Table 1). Furthermore, the crystal structure was determined (Figure 2) and additionally the ¹⁵N NMR spectrum of **1** is displayed in Figure 3.



Scheme 1: Synthesis of 3-trinitromethyl-5-nitramino-1H-1,2,4-triazole (**1**) and nitrogen-rich salts (**2–4**).

The structure of **1** in the solid state was determined by low temperature X-ray diffraction, crystallizing in the monoclinic space group $P2_1/n$ with 4 formula units per unit cell and a calculated density of 1.95 g cm^{-3} at 173 K. The single X-ray diffraction experiment of compound **1** showed a perfect planarity of the heterocycle as well as a propeller-type orientation of the trinitromethyl moiety. The bond lengths and angles are in the typical range of aromatic azole derivatives containing a trinitromethyl moiety. Both hydrogen atoms interact in H-bonds forming layers along the x-axis. Selected bond lengths and angles are shown in Fig. 2. Details on the measurements and refinement values are listed in the Supporting Information.

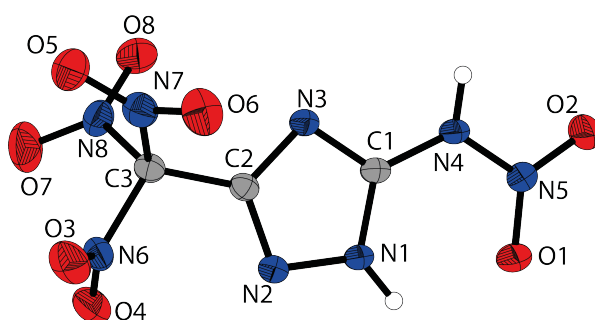


Figure 2: Molecular structure of 3-trinitromethyl-5-nitramino-1*H*-1,2,4-triazole (**1**). Selected bond lengths (Å) and angles (deg.): C3–C4 1.489 (19), N1–N2 1.355 (16) C1–N4 1.372 (18). C2–C3–N7 112.9 (11), C1–N4–N5 123.2 (12). N3–C2–C3–N7 -60.75 (17), C1–N1–N2–C2 0.28 (14), N5–N5–C1–N1 16.6 (2).

The infrared vibrational spectra of **1–4** show the typical antisymmetric $\nu_{\text{as}}(\text{NO}_2)$ and symmetric $\nu_{\text{sy}}(\text{NO}_2)$ stretching vibrations in the range of $1620\text{--}1506 \text{ cm}^{-1}$ and $1385\text{--}1251 \text{ cm}^{-1}$, respectively. The C–N, C–O and C–C vibrations observed are in the characteristic ranges for CHNO compounds.

Table 1: ^1H , ^{13}C , ^{14}N (2–4) and ^{15}N (1) NMR resonances.						
	NHNO_2	NH	C	$\text{C}(\text{NO}_2)_3$	NHNO_2	$\text{C}(\text{NO}_2)_3$
		(ring)	(ring)			
1	5.6	14.74	149.1	124.3	–42.9	–33.6
			146.8			
2	8.4		157.2	128.3	–22	–38
			148.9			
3	9.1		159.0	124.8	–16	–32
			145.8			
4	11.0		151.0	124.7	–22	–31
			145.8			

The NMR resonances of **1** and the anions of **2–4** are listed in Table 1. All resonances of the cations are in the range of literature known compounds.^{[13], [14]} The ^{15}N NMR spectrum of **1** is shown in Fig. 3 with assignments regarding the triazole heterocycle based on related compounds.^{[2], [5]}

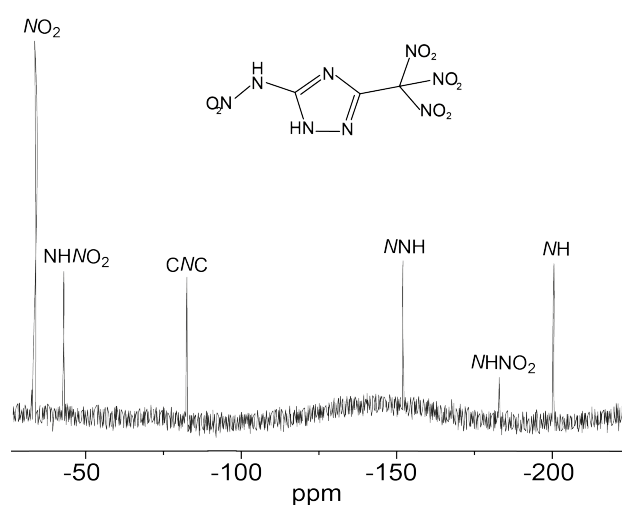


Figure 3: ^{15}N NMR spectrum of **1** in $\text{DMSO-}D_6$ at 25 °C.

The physical and chemical properties of **1–4** are shown in Table 2. The specific impulses and detonation parameters of the compounds were calculated using EXPLO5 6.03. Comparing the oxygen balances of **1–4**, **1** shows the highest value of 23 %, which is in the range of nitroglycerine (24.7 %). The optimized specific impulse of **1**, in a mixture with aluminum and binder is 264 s (neat 263 s) and therefore is as high as for ammonium perchlorate (Table 2). This would be a promising

value as replacement for commonly used oxidizers. The nitrogen-rich salts are less suitable as oxidizers due to lower oxygen contents. This is especially the case in **2** because of the loss of a nitro group. However for the same reason, this make the salts **2–4** promising as secondary explosives. They show interesting theoretical detonation values e.g. detonation pressure (**2**: 285 kbar, **3**: 288 kbar, **4**: 259 kbar) and detonation velocity (**2**: 8635 m s⁻¹, **3**: 8439 m s⁻¹, **4**: 8124 m s⁻¹).

All compounds are air stable. For **1–4** the thermal stability was determined using DTA experiments (heating rate: 5° C min⁻¹) listed in Table 2. The dihydrazinium salt **2** exhibits the highest decomposition temperature of 175 °C, while those of the neutral compound **1** (125 °C) and the other salts **3** (105 °C) and **4** (125 °C) are significantly lower.

Table 2: Physical properties and calculated detonation parameters of **1–4**, AP, NG and PETN

	1	2	3	4	AP	NG	PETN
ρ [g cm ⁻³]	1.91 ⁿ⁾	1.65 ^{q)}	1.67 ^{q)}	1.61 ^{q)}	1.95	1.59	1.75
formula	C ₃ H ₂ H ₈ O ₈	C ₃ H ₁₁ N ₁₁ O ₆	C ₄ H ₈ N ₁₂ O ₈	C ₅ H ₈ N ₁₄ O ₈	NH ₄ ClO ₄	C ₃ H ₅ N ₃ O ₉	C ₃ H ₈ N ₄ O ₁₂
$\Delta_f H^\circ$ [kJ mol ⁻¹] ^{a)}	269	209	166	890	296	311	480
$\Delta_f U^\circ$ [kJ kg ⁻¹] ^{b)}	777	819	791	1244	2623	1278	1423
$T_{\text{dec onset}}$ ^{c)}	125	175	105	125	240	185	202
IS [J] ^{d)}	2	40	2	1	20	0.2	3
FS [N] ^{e)}	40	360	36	120	360	360	60
ESD [m] ^{f)}	150	250	90	60	0.5	nd ^{p)}	0.19
N [%] ^{g)}	40.3	51.8	47.7	50.0	11.9	18.5	17.7
Ω_{CO} [%] ^{h)}	+23.0	-13.5	0.0	-4.1	+34.0	+24.7	+15.2
I_s [s] ⁱ⁾	263	253	254	278	157	264	257
I_s [s] ^{j)}	258	241	239	249	261	265	257
I_s [s] ^{k)}	264	244	240	251	257	259	251
$\Delta_{\text{ex}} U^\circ$ [kJ kg ⁻¹] ^{l)}	-5792	-5159	-5219	-5088	-1421	-6099	-5995
T_{ex} [K] ^{m)}	4270	3387	3731	3765	1725	4317	3959
P_{CJ} [kbar] ⁿ⁾	369	285	288	259	183	237	316
V_{det} [m s ⁻¹] ^{o)}	9250	8635	8439	8124	1373	7850	8525

a) Standard of formation enthalpy calculated by the atomization method and CBS-4M electronic enthalpies from Gaussian 09 [15], [16]. b) Energy of formation. c) Decomposition temperature. d) Impact sensitivity. e) Friction sensitivity. f) Sensitivity toward electrostatic discharge. g) Nitrogen content. h) Oxygen balance Ω assuming the formation of CO at the combustion i) Specific impulse (EXPLO5 6.03: 70 bar chamber pressure, 1 bar expansion conditions equilibrium expansion). j) Specific impulse (15 % Al, 6 % polybutadiene acrylic acid, 6 % polybutadiene acrylonitrile and 2 % bisphenyl A ether; EXPLO5 6.03: 70 bar chamber pressure, 1 bar expansion conditions equilibrium expansion). k) Optimized specific impulse (10 % Al, 6 % polybutadiene acrylic acid, 6 % polybutadiene acrylonitrile and 2 % bisphenyl A ether; EXPLO5 6.03: 70 bar chamber pressure, 1 bar expansion conditions equilibrium expansion). l) Detonation energy. m) Detonation temperature. n) Detonation pressure. o) Detonation velocity.^[17] p) Liquid q) measured by pycnometry r) measured by X Ray

The low decomposition points can be explained by the well-known instability of the trinitromethyl moiety at higher temperatures.

The sensitivities toward external stimuli for **1–4** were determined according to standards of the Federal Institute for Materials Research and Testing (BAM) and the results are also displayed in Table 2. The observed values for their impact sensitivity of compounds **1** (2 J), **3** (2 J) and **4** (1 J) correspond to sensitive materials. The lower sensitivity of **2** may be explained by the loss of one nitro group and by the formation of a double salt.

Comparing the detonation velocity of **1–4** with PETN, it appears that **2–4** are slightly higher but in the same range, furthermore **1** is significantly higher. Also the detonation pressures of **2–4** are close to PETN, whereas **1** is slightly better.

3. Conclusion

The nitration of 5-amino-1*H*-1,2,4-triazol-3-acetic acid with mixed acid resulted in the nitrogen/oxygen-rich energetic heterocycle 3-trinitromethyl-5-nitramino-1*H*-1,2,4-triazole (**1**). The reaction with various nitrogen-rich bases was proven to be difficult, however the dihydrazinium (**2**), aminoguanidinium (**3**) and 3,4,5-triaminotriazolium (**4**) salts were obtained. All compounds were analytically characterized and the corresponding detonation properties calculated. The salt **2** shows low sensitivity values (IS 20 J, FS 360 N). The sensitivity values for compounds **1**, **3** and **4** are in the range of primary explosives. With respect to the oxygen balance, **1** could be a potential candidate as a new high-energy dense oxidizer with a oxygen balance of $\Omega_{\text{CO}} = +23\%$.

4. Experimental Part

3-Trinitromethyl-5-nitramino-1*H*-1,2,4-triazole (1):

To 1 mL of fuming nitric acid was added slowly 2-(5-amino-1*H*-1,2,4-triazol-3-yl)acetic acid (0.25 g; 1.76 mmol) at 0 °C. After stirring for 5 min at 0 °C, sulfuric acid (1.5 ml) was slowly added. The reaction was stirred at 0 °C for one hour and at ambient temperature for 12 hours. Then the mixture was poured on 10 g ice and extracted 12 times with 20 mL dichloromethane. After drying with magnesium sulfate the solvent was reduced to 20 mL with a rotary evaporator. The remaining residue was chilled to yield 0.19 g (40 %) of pure **1** as colorless crystals.

DSC (5 °C min⁻¹): 125 °C (dec.); **IR** (ATR, cm⁻¹): $\tilde{\nu}$ = 3317 (w), 2750 (w), 1643 (m), 1619 (m), 1591 (s), 1514 (m), 1482 (w), 1414 (w), 1328 (m), 1280 (m), 1251 (s), 1176 (m), 1093 (m), 1070 (m), 1006 (m), 974 (m), 860 (w), 841 (m), 799 (s), 730 (m), 716 (m), 685 (w), 660 (w); **¹H NMR** (DMSO-*D*₆, 25 °C, ppm) δ : 14.7 (br, *NHNO*₂), 5.62 (*CNHN*); **¹³C NMR** (DMSO-*D*₆, 25 °C, ppm) δ : 149.1 (*C*(*C*(*NO*₂)₃), 146.8 (*C*(*NHNO*₂)), 124.3 (*C*(*NO*₂)₃); **¹⁵N NMR** (DMSO-*D*₆, 25 °C, ppm) δ : -33.6 (*C*(*NO*₂)₃), -42.9 (*NHNO*₂), -82.6 (*CNC*), -152.0 (*NHNC*), -182.9 (*NHNO*₂), -200.6 (*CNHN*); **EA** (C₃H₂N₈O₈, 278,10 g mol⁻¹) calc.: C, 12.96, H, 0.72, N, 40.29; found: C, 13.37, H, 1.07, N, 39.68; **pKs**: 11.1; **Sensitivities** (100 μ m \geq g.s. \geq 50 μ m): **IS**: 2 J; **FS**: 40 N; **ESD**: 150 mJ.

Hydrazinium 3-Dinitromethyl-5-nitramino -1,2,4-triazolate (2):

To a solution of **1** (0.28 g; 1 mmol) in methanol (5 ml), hydrazine hydrate (0.16 g, 5 mmol) was added slowly. The mixture was stirred for 1 hour at ambient temperature during which a precipitate was formed. The yellow precipitate was filtered off, washed with cold ether and dried to yield 0.24 g; 80 % of the hydrazinium salt **2**.

DSC (5 °C min⁻¹): 175 °C (dec.); **IR** (ATR, cm⁻¹): $\tilde{\nu}$ = 3360 (w), 3278 (w), 3246 (w), 3116 (m), 2620 (m), 2365 (w), 2250 (w), 2159 (m), 1681 (w), 1622 (w), 1584 (w), 1540 (m), 1506 (m), 1483 (m), 1434 (m), 1385 (s), 1337 (m), 1290 (m), 1235 (m), 1200 (s), 1121 (s), 1096 (s), 1019 (m), 983 (s), 969 (s), 856 (w), 826 (m), 773 (w), 740 (m), 725 (m), 669 (w); **¹H NMR** (DMSO-*D*₆, 25 °C, ppm) δ : 8.41 (s, *NH*), 6.3 (br, 10 H, *NH*₃ and *NH*₂); **¹³C NMR** (DMSO-*D*₆, 25 °C, ppm) δ : 157.2 (*C*(*NHNO*₂)), 148.9 (*C*(*C*(*NO*₂)₂)), 128.3 (*C*(*NO*₂)₂); **¹⁴N NMR** (DMSO-*D*₆, 25 °C, ppm) δ : -22 (*NHNO*₂), -38 (*C*(*NO*₂)₂), -359 (*NH*₃); **EA** (C₃H₁₁N₁₁O₆, 264.14 g mol⁻¹) C, 12.12, H, 3.73, N, 51.84; Found: C, 12.90, H, 3.94, N, 51.46; **Sensitivities** (100 μ m \geq g.s. \geq 50 μ m): **IS**: 40 J; **FS**: 360 N; **ESD**: 250 mJ.

Aminoguanidinium 3-Trinitromethyl-5-nitramino-1,2,4-triazolate (3):

Aminoguanidine bicarbonate (0.14 g, 1 mmol) was added slowly to a solution of **1** (0.28 g, 1 mmol) in 5 mL methanol. The mixture was stirred for one hour at 25 °C. The solvent was removed under reduced pressure, the formed precipitate washed with ether and dried to yield 0.31 g (87 %) of the aminoguanidinium salt **3**.

DSC (5 °C min⁻¹): 105 °C (dec.); **IR** (ATR, cm⁻¹): $\tilde{\nu}$ = 3428 (w), 3394 (w), 3257 (w), 3164 (w), 2359 (w), 2230 (w), 2180 (w), 1684 (m), 1662 (m), 1608 (m), 1587 (s), 1523 (m), 1463 (m), 1430 (m), 1397 (m), 1362 (w), 1304 (s), 1282 (s), 1222 (m), 1165 (m), 1106 (w), 1075 (m), 967 (m), 907 (w), 862 (w), 844 (m), 800 (s), 772 (w), 741 (w), 668 (w); **¹H NMR** (DMSO-*D*₆, 25 °C, ppm) δ : 9.1 (br, NHNO₂), 8.69 (C(NH)), 7.8 (br, NHHN₂), 6.9 (br, C(NH₂)), 5.0 (br, NH); **¹³C NMR** (DMSO-*D*₆, 25 °C, ppm) δ : 159.3 (CNH₂), 159.0 (CNHNO₂), 145.8 (C(C(NO₂)₃)), 124.8 (C(NO₂)₃); **¹⁴N NMR** (DMSO-*D*₆, 25 °C, ppm) δ : -16 (NHNO₂), -31 (C(NO₂)₃); **EA** (C₄H₈N₁₂O₈, 352.18 g mol⁻¹) C, 13.64, H, 2.29, N, 47.73; Found: C, 14.15, H, 2.33, N, 46.66; **Sensitivities** (100 μ m \geq g.s. \geq 50 μ m): **IS**: 2 J; **FS**: 36 N; **ESD**: 90 mJ.

3,4,5-Triamino-4H-1,2,4-triazolium 3-Trinitromethyl-5-nitramino-1,2,4-triazolate (4):

3,4,5-Triamino-1,2,4-triazole (0.11 g, 1 mmol) was added slowly to a solution of **1** (0.28 g, 1 mmol) in 5 mL methanol. The mixture was stirred for one hour at 25 °C. The solvent was removed under reduced pressure, the formed precipitate washed with ether and dried to yield 0.31 g (79 %) of the triaminotriazole salt **4**.

DSC (5 °C min⁻¹): 125 °C (dec.); **IR** (ATR, cm⁻¹): $\tilde{\nu}$ = 3466 (w), 3432 (w), 3267 (w), 2738 (w), 2360 (w), 2340 (w), 1706 (w), 1673 (m), 1601 (s), 1533 (m), 1523 (m), 1474 (m), 1429 (m), 1394 (w), 1327 (s), 1300 (m), 1280 (m), 1173 (m), 1104 (m), 1091 (m), 1015 (w), 962 (w), 909 (w), 866 (w), 843 (m), 798 (s), 777 (w), 759 (w), 713 (w), 667 (w); **¹H NMR** (DMSO-*D*₆, 25 °C, ppm) δ : 14.2 (br, NHNO₂), 11.0 (br, NNHC), 7.1 (br, N(NH₂)), 5.6 (br, 4H, C(NH₂)); **¹³C NMR** (DMSO-*D*₆, 25 °C, ppm) δ : 148.1 (C(NHNO₂)), 145.8 (C(C(NO₂)₃)), 124.7 (C(NO₂)₃), 49.2 (C(NH₂)); **¹⁴N NMR** (DMSO-*D*₆, 25 °C, ppm) δ : -22 (NHNO₂), -31 (C(NO₂)₃), -386 (N(NH₂)); **EA** (C₅H₈N₁₄O₈, 392.21 g mol⁻¹): C, 15.31, H, 2.06, N, 50.00; Found: C, 15.78, H, 2.25, N, 49.15; **Sensitivities** (100 μ m \geq g.s. \geq 50 μ m): **IS**: 1 J; **FS**: 120 N; **ESD**: 60 mJ

5. Supporting Information

5.1 General Methods

All chemicals were used as supplied. Raman spectra were recorded in a glass tube with a Bruker MultiRAM FT-Raman spectrometer with Nd:YAG laser excitation up to 1000 mW (at 1064 nm). Infrared spectra were measured with a PerkinElmer Spectrum BX-FTIR spectrometer equipped with a Smiths Dura/SamplIR II ATR device. All spectra were recorded at ambient (25 °C) temperature. NMR spectra were recorded with JEOL/Bruker instruments and chemical shifts were determined with respect to external Me₄Si (¹H, 399.8 MHz; ¹³C, 100.5 MHz) and MeNO₂ (¹⁴N, 28.9 MHz; ¹⁵N, 40.6 MHz). Analyses of C/H/N were performed with an Elemental Vario EL Analyzer. Melting and decomposition points were measured using differential thermal analysis (DTA) at a heating rate of 5° C min⁻¹ with an OZM Research DTA 552-Ex instrument. The sensitivity data were explored using a BAM drop hammer and a BAM friction tester.^[7] The heats of formations were calculated by the atomization method based on CBS-4M electronic enthalpies. All calculations affecting the detonation parameters were carried out using the program package EXPLO5 6.03.

[17], [18]

5.2 X-ray Diffraction

For the measurement, an Oxford Xcalibur3 diffractometer with a CCD area detector was employed for data collection using Mo-*K*α radiation ($\lambda = 0.71073$ Å). By using the CRYSTALISPRO software^[19] the data collection and reduction was performed. The structure was solved by direct methods (SIR92,^{[20] [21]}) and refined by full-matrix least-squares on *F*² (SHELXL^{[22] [23]}) and finally checked using the PLATON software^[24] integrated in the WinGX software suite. The non-hydrogen atoms were refined anisotropically and the hydrogen atoms were located and freely refined. The absorptions were corrected by a SCALE3 ABSPACK multiscan method.

^[25] All DIAMOND2 plots are shown with thermal ellipsoids at the 50% probability level and hydrogen atoms are shown as small spheres of arbitrary radius.

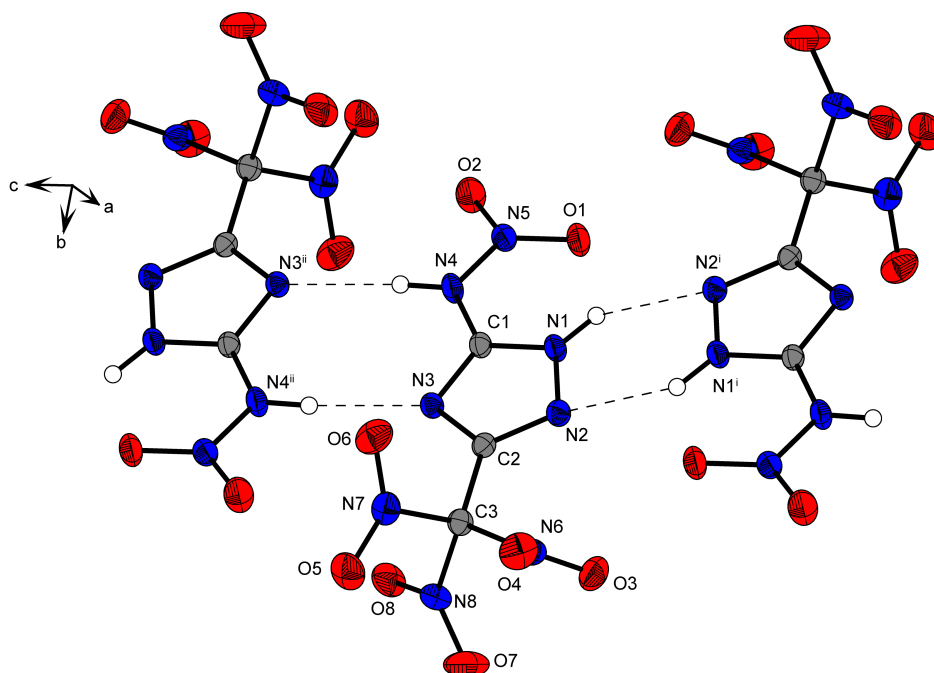
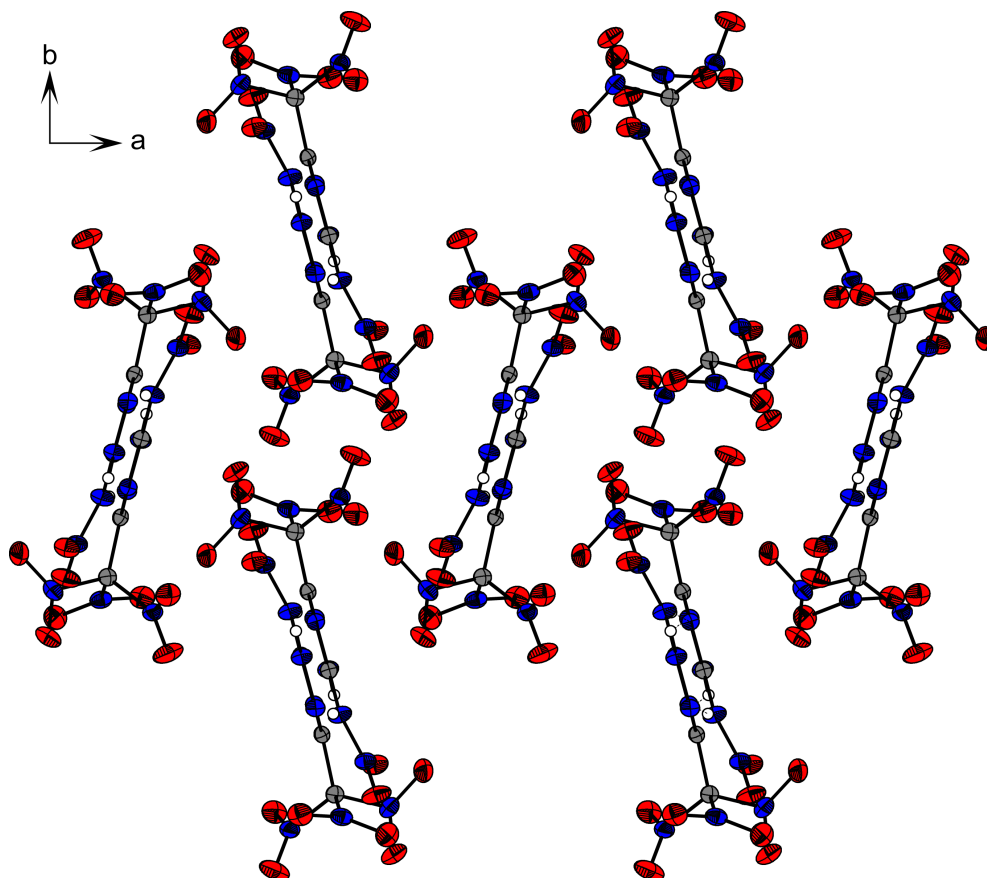


Figure S1: Crystal structure of **1** with intermolecular hydrogen bonds.

A suitable single crystal for X-ray diffraction experiments of compound **1** was obtained during the nitration work up. The crystal structure is shown in Figure 1 in the main manuscript and structure refinement data of the structure determinations are given in Table S1.

3-Nitramino-5-trinitromethyl-1*H*-1,2,4-triazole (**1**) crystallizes in the monoclinic space group $P2_1/n$ with 4 formula units per unit cell and a calculated density of 1.95 g cm^{-3} at 173 K. The bond length and angles are in the typical range of CHNO based compounds containing a trinitromethyl moiety.^{[26] [27] [28]} Due to the typical shape of triazoles the heterocycle shows a large planar arrangement area. This area consists of a heterocycle with three nitrogen atoms arranged in 1,2,4 position and two carbon atoms. This planarity is displayed by the torsions angles of $\text{C1-N1-N2-C2} = 0.28^\circ$, $\text{C2-N3-C1-N1} = -0.69^\circ$, $\text{N2-N1-C1-N3} = 0.28^\circ$ of almost 180° . The C–N bonds in compound **1** are slightly different to typical C–N bonds. Compared to regular C=N bonds, all C=N bonds in the heterocycle are a slightly longer with lengths of around 1.36 \AA . This can be explained by the adjacent trinitromethyl moiety.^{[29] [30]} Another very typical characteristic of trinitromethyl moiety is the propeller shaped arrangement of the three nitro groups. All C–N–O torsion angles are in the range of 20° – 62° of the trinitromethyl moiety, which implements a real propeller-type orientation. The N–O bonds are 1.21 \AA in average. The C2–N2 and C1–N3 bond lengths are around 1.31 \AA and therefore in the double bond range. The bond lengths of C2–N3, C1–N1 and C1–N4 are in the range of single bonds. Figure 2 shows the view along the c-axis. The rings are connected slightly shifted over hydrogen bonds. Furthermore, the trinitromethyl moiety builds oxygen-oxygen contacts in the

c-axis.

Figure S2: View on the crystal structure of **1** along the *c*-axis.Table S1. Crystal and structure refinement data of **1**.

	1
Empirical formula	C ₃ H ₂ N ₈ O ₈
Formula mass (g mol ⁻¹)	278.10
Temperature (K)	173
Crystal size (mm ³)	0.4x0.4x0.11
Crystal description	Colorless block
Crystal system	monoclinic
Space group	<i>P</i> 2 ₁ / <i>n</i>
<i>a</i> (Å)	9.1597(7)
<i>b</i> (Å)	10.5684(7)
<i>c</i> (Å)	9.9433(7)

β (°)	101.110(7)
V (Å ³)	944.51(12)
Z	4
ρ_{calc} (g cm ⁻³)	1.95
μ (mm ⁻¹)	0.192
$F(000)$	560
θ range (°)	4.39-26.50
Index range	-11 < h < 10 -13 < k < 13 -11 < l < 12
Reflection collected	7214
Reflection observed	1958
Reflection unique	1746
R1, wR2 (2 σ data)	0.0327, 0.0795
R1, wR2 (all data)	0.0373, 0.0838
Data/restraints/parameters	1958/0/180
GOOF an F ²	1.066
Larg. diff. peak/hole (e Å ⁻³)	0.344, -0.334
CCDC entry	1701785

The highest density is observed for the neutral compound **1** with $\Omega_{CO} = 23\%$ and $\rho_{K=173} = 1.95\text{ g cm}^{-3}$. For the corresponding salts, density measurements were carried out using gas pycnometry. The densities for the salts are significantly lower than the neutral compound **1**.

5.3 Heat of formation calculations

All calculations were carried out using the Gaussian G09W (revision A.02) program package. The enthalpies (H) and free energies (G) were calculated using the complete basis set (CBS) method of Petersson and coworkers in order to obtain very accurate energies. The CBS models use the known asymptotic convergence of pair natural orbital expressions to extrapolate from calculations using a finite basis set to the estimated complete basis set limit. CBS-4 begins with a HF/3-21G(d) geometry optimization; the zero point energy is computed at the same level. It then uses a large basis set SCF calculation as a base energy, and a MP2/6-31+G calculation with a CBS extrapolation to correct the energy through second order. A

MP4(SDQ)/6-31+(d,p) calculation is used to approximate higher order contributions. In this study we applied the modified CBS-4M method (M referring to the use of Minimal Population localization) which is a re-parametrized version of the original CBS-4 method and also includes some additional empirical corrections.^{[31] [32]} The enthalpies of the gas-phase species M were computed according to the atomization energy method (eq.1).

$$\Delta_f H^\circ_{(g, M, 298)} = H_{(Molecule, 298)} - \sum H^\circ_{(Atoms, 298)} + \sum \Delta_f H^\circ_{(Atoms, 298)} \quad (1)$$

Table S2. CBS-4M results and calculated gas-phase enthalpies

	M	$-H^{298} / \text{a.u.}$	$\Delta_f H^\circ(g, M) / \text{kcal mol}^{-1}$
1	278.1	1153.552952	64.2
monoanion	277.1	1153.062215	5.6
dianion	231.1	948.178386	11.2
AG⁺	75.1	260.701802	160.4
TAT⁺	115.1	408.091922	206.9
N₂H₅⁺	66.1	112.030523	184.9

Table S3 . CBS-4M values and literature values for atomic $\Delta_f H^\circ_{298} / \text{kcal mol}^{-1}$

	$-H^{298} / \text{a.u.}$	NIST ^[33]
H	0.500991	52.1
C	37.786156	171.3
N	54.522462	113.0
O	74.991202	59.6

In the case of the ionic compounds, the lattice energy (U_l) and lattice enthalpy (ΔH_l) were calculated from the corresponding X-ray molecular volumes according to the equations provided by Jenkins and Glasser. With the calculated lattice enthalpy (Table S5) the gas-phase enthalpy of formation (Table S4) was converted into the solid state (standard conditions) enthalpy of formation (Table S5). These molar standard enthalpies of formation (ΔH_m) were used to calculate the molar solid state energies of formation (ΔU_m) according to equation 2.

$$\Delta U_m = \Delta H_m - \Delta n RT \quad (2)$$

(Δn being the change of moles of gaseous components)

Table S4. Calculated gas phase heat of formation, molecular volumes, lattice energies and lattice enthalpies of **1-4**.

	$\Delta_f H^\circ(\text{g,M}) /$ kcal mol ⁻¹	V_M / nm^3	$U_L / \text{kJ mol}^{-1}$	$\Delta H_L / \text{kJ mol}^{-1}$
1	64.2			
2	11.2	0.258	1379.1	1386.6
3	166.0	0.317	447.9	451.3
4	212.5	0.354	435.6	439.0

The standard molar enthalpy of formation of solid **1** was calculated using $D_f H(\text{g})$ subtracting the enthalpy of sublimation estimated by applying Trouton's rule.^{[34] [35]} ($\Delta H_{\text{sub}} = 188 \cdot T_m$). (**1**: T_m 125°C, $\Delta H_{\text{sub}} = 74.9 \text{ kJ mol}^{-1}$).

Table S5. Solid state energies of formation ($\Delta_f U^\circ$)

	$\Delta_f H^\circ(\text{s}) /$ kcal mol ⁻¹	$\Delta_f H^\circ(\text{s}) /$ kJ mol ⁻¹	Δn	$\Delta_f U^\circ(\text{s}) /$ kJ mol ⁻¹	$M /$ g mol ⁻¹	$\Delta_f U^\circ(\text{s}) /$ kJ kg ⁻¹
1	46.3	193.8	9	216.1	278.1	777.1
2	48.9	208.8	14	243.5	297.2	819.2
3	58.2	243.9	14	278.6	352.2	790.8
4	107.	450.8	15	488.0	392.3	1244.1

Notes: Δn being the change of moles of gaseous components when formed.

6. References

- [1] a) T. T. Vo, D. A. Parrish, J. M. Shreeve, *J. Am. Chem. Soc.*, **2014**, *136*, 11934–11937; b) M. Rahm, G. Belanger-Chabot, R. Haiges, K. O. Christe, *Angew. Chem., Int. Ed.*, **2014**, *53*, 6893–6897; c) H. Gao, J. M. Shreeve, *Chem. Rev.*, **2011**, *111*, 7377–7436; d) R. P. Singh, R. D. Verma, D. T. Meshri, J. M. Shreeve, *Angew. Chem., Int. Ed.*, **2006**, *45*, 3584–3601; e) G.-H. Tao, Y. Guo, Y.-H. Joo, B. Twamley, J. M. Shreeve, *J. Mater. Chem.*, **2008**, *18*, 5524–5530.
- [2] V. Thottampudi, H. Gao, J. M. Shreeve, *J. Am. Chem. Soc.*, **2011**, *133*, 6464–6471.
- [3] T. P. Kofman, G. Y. Kartseva, E. Y. Glazkova, K. N. Krasnov, *Russ. J. Org. Chem.*, **2005**, *41*, 753–757.
- [4] R. Haiges, K. O. Christe, *Inorg. Chem.*, **2013**, *52*, 7249–7260.
- [5] V. Thottampudi, J. M. Shreeve, *J. Am. Chem. Soc.*, **2011**, *133*, 19982–19992.
- [6] D. E. Chavez, M. A. Hiskey, R. D. Gilardi, *Angew. Chem., Int. Ed.*, **2000**, *39*, 1791–1793.

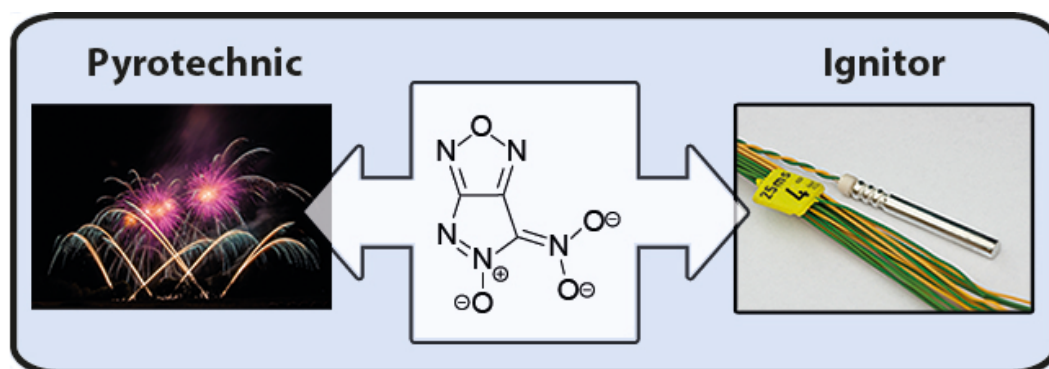
- [7] T. M. Klapötke, *Chemistry of High-Energy Materials, 4th Edition*, Walter de Gruyter GmbH & Co KG, Berlin, **2017**.
- [8] T. M. Klapötke, B. Krumm, S. F. Rest, M. Sućeska, *Z. Anorg. Allg. Chem.*, **2014**, *640*, 84–92.
- [9] A. M. Abdel-Megeed, H. M. Abdel-Rahman, G.-E. S. Alkaramany, M. A. El-Gendy, *Eur. J. Med. Chem.*, **2009**, *44*, 117–123.
- [10] V. M. Chernyshev, A. V. Chernysheva, V. A. Taranushich, *Russ. J. Appl. Chem.*, **2009**, *82*, 276–281.
- [11] V. Thottempudi, T. K. Kim, K.-H. Chung, J. S. Kim, *Bull. Korean Chem. Soc.*, **2009**, *30*, 2152–2154.
- [12] A. N. Terpigorev, I. V. Tselinskii, A. V. Makarevich, G. M. Frolova, A. A. Mel'nikov, *Zh. Org. Khim.*, **1987**, *23*, 244–254.
- [13] D. Fischer, T. M. Klapötke, M. Reymann, J. Stierstorfer, *Chem. Eur. J.*, **2014**, *20*, 6401–6411.
- [14] T. M. Klapötke, C. M. Sabate, *Eur. J. Inorg. Chem.*, **2008**, 5350–5366.
- [15] M. J. Frisch, G. W. Trucks, H. B. Schlegel, G. E. Scuseria, M. A. Robb, J. R. Cheeseman, G. Scalmani, V. Barone, B. Mennucci, G. A. Petersson, H. Nakatsuji, M. Caricato, X. Li, H. P. Hratchian, A. F. Izmaylov, J. Bloino, G. Zheng, J. L. Sonnenberg, M. Hada, M. Ehara, K. Toyota, J. H. R. Fukuda, M. Ishida, T. Nakajima, Y. Honda, O. Kitao, H. Nakai, M. T. Vreven, J. E. Peralta, F. Ogliaro, M. Bearpark, J. J. Heyd, E. Brothers, K. N. Kudin, V. N. Staroverov, R. Kobayashi, J. Normand, K. Raghavachari, A. Rendell, J. C. Burant, S. S. Iyengar, J. Tomasi, M. Cossi, N. Rega, J. M. Millam, M. Klene, J. E. Knox, J. B. Cross, V. Bakken, C. Adamo, J. Jaramillo, R. Gomperts, R. E. Stratmann, O. Yazyev, A. J. Austin, R. Cammi and C. Pomelli, J. W. Ochterski, R. L. Martin, K. Morokuma, V. G. Zakrzewski, G. A. Voth, P. Salvador, J. J. Dannenberg, S. Dapprich, A. D. Daniels, Ö. Farkas, J. B. Foresman, J. C. J. V. Ortiz, D. J. Fox, *Gaussian 09; Rev. A.02 ed.*, Gaussian, Inc., Wallingford CT(USA), **2009**.
- [16] R. D. Dennington II, T. A. Keith, J. M. Millam, *GaussView, Ver.5.08 ed.*, Semichem, Inc., Wallingford CT (USA), **2009**.
- [17] M. Sućeska, *Propellants, Explos., Pyrotech.*, **1991**, *16*, 197–202.
- [18] M. Sućeska, *EXPLO5 V.6.03*, **2014**, Zagreb (Croatia).
- [19] CrysAlisPro, Oxford Diffraction Ltd. version 171.33.41, **2009**.
- [20] SIR-92 A Program for Crystal Structure Solution: A. Altomare, G. Cascarano, C. Giacovazzo, A. Guagliardi, *J. Appl. Crystallogr.*, **1993**, *26*, 343–350.
- [21] A. Altomare, G. Cascarano, C. Giacovazzo, A. Guagliardi, A. G. G. Moliterni, M. C. Burla, G. Polidori, M. Camalli, R. Spagna, *SIR97*, **1997**.
- [22] G. M. Sheldrick, *SHELX-97*, **1997**, University of Göttingen, Göttingen, Germany.
- [23] G. M. Sheldrick, *Acta Crystallogr., Sect. A: Found. Crystallogr.*, **2008**, *64*, 112–122.

- [24] A. L. Spek, *PLATON*, **1999**, A Multipurpose Crystallographic Tool, Utrecht University, The Diffraction Ltd.
- [25] *SCALE3 - An Oxford Diffraction Program (1.0.4, gui: 1.0.3)*, **2005**, Oxford Ltd.
- [26] T. M. Klapötke, B. Krumm, R. Moll, S. F. Rest, *Z. Anorg. Allg. Chem.*, **2011**, *637*, 2103–2110.
- [27] T. M. Klapötke, B. Krumm, R. Moll, *Chem. Eur. J.*, **2013**, *19*, 12113–12123.
- [28] T. M. Klapötke, B. Krumm, S. F. Rest, M. Reynders, R. Scharf, *Eur. J. Inorg. Chem.*, **2013**, 5871–5878.
- [29] P. Taranekekar, C. Huang, T. M. Fulghum, A. Baba, G. Jiang, J. Y. Park, R. C. Advincula, *Adv. Funct. Mater.*, **2008**, *18*, 347–354.
- [30] Y. Oyumi, T. B. Brill, A. L. Rheingold, *J. Phys. Chem.*, **1985**, *89*, 4824–4828.
- [31] J. W. Ochterski, G. A. Petersson, J. A. Montgomery, Jr., *J. Chem. Phys.*, **1996**, *104*, 2598–2619.
- [32] J. A. Montgomery, Jr., M. J. Frisch, J. W. Ochterski, G. A. Petersson, *J. Chem. Phys.*, **2000**, *112*, 6532–6542.
- [33] P. J. Lindstrom, W. G. Mallard, **2011**, Nist Standard Reference Database Number 69.
- [34] F. Trouton, *Philos. Mag.*, **1884**, *18*, 54–57.
- [35] M. S. Westwell, M. S. Searle, D. J. Wales, D. H. Williams, *J. Am. Chem. Soc.*, **1995**, *117*, 5013–5015.

Formation and Characterization of Heavy Alkali and Silver Salts of the 4-Nitro-pyrazolo-(3,4-c)-furazan-5-*N*-oxide Anion

Tobias S. Hermann, Thomas M. Klapötke* and Burkhard Krumm

Propellants, Explosives, Pyrotechnics, **2017**, 42, 1–9.



Formation and Characterization of Heavy Alkali and Silver Salts of the 4-Nitro-pyrazolo-(3,4-c)-furazan-*N*-oxide Anion

Tobias S. Hermann, Thomas M. Klapötke* and Burkhard Krumm

Propellants, Explosives, Pyrotechnics, **2017**, 42, 1–9.

Abstract:

The nitration of 3-amino-4-chloro-oximidofurazan resulted in the formation of the unexpected anionic heterocycle 4-nitro-pyrazolo-(3,4,c)-furazan-5-*N*-oxide. Various experiments such as changing the reactants, oxidation or methylation were attempted to elucidate the reaction conditions and mechanism. The heavier alkali and silver salts of the above-mentioned heterocycle were isolated. The salts were characterized and investigated by means of NMR, vibrational spectroscopy, X-ray diffraction and energetic properties.

1. Introduction

The development of new green, safe and more powerful high explosives for military as well as civilian applications has become of major research interest during the last years.^[1] In order to meet environmental requirements, lower sensitivities towards friction, impact and electrical discharge, the research of high explosives (HEs) is indispensable.^[2] Nitrogen-rich heterocyclic compounds such as tetrazoles, triazoles, pyrazoles and oxadiazoles are very promising candidates due to their energetic properties: high heat of formation, density, thermal stability and promising detonation performance.^[3] Those properties and parameters can still be improved. For example, the density can be increased by adding nitramine groups, the detonation performance can be enhanced by preparing *N*-oxides.^{[4], [5]} *N*-oxides with heterocyclic parent structures have been studied for decades.^{[6], [7]} Some representative examples of an energetic *N*-oxide and two related *N*-O containing salts are given in Figure 1. Due to their versatility, heterocyclic *N*oxides have attracted lot of attention during the last years.^[8] Here especially pyrazole *N*-oxides have gained interest, not only in energetic chemistry, but also in pharmaceutical, medical and polymer chemistry.^{[6], [9], [10]}

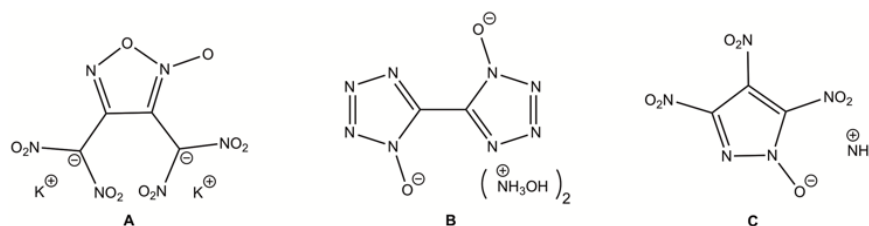
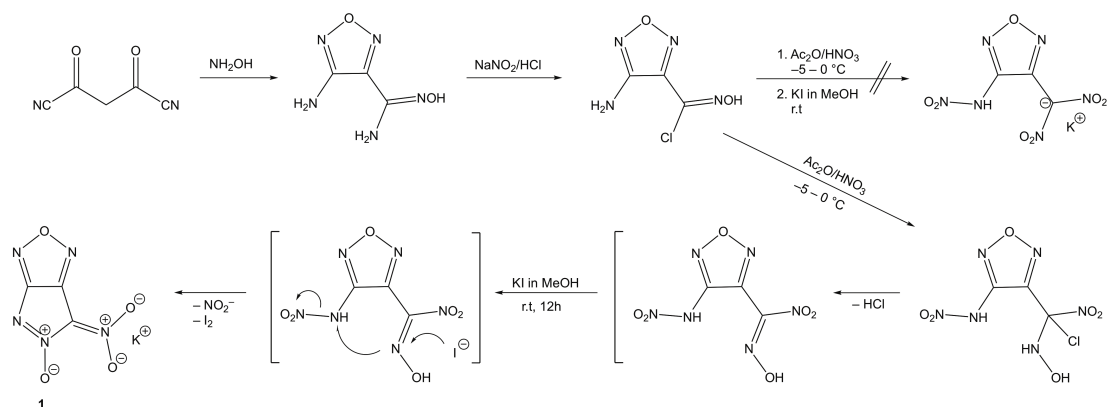


Figure 1: Examples of an heterocyclic N-oxide and two related salts: A) potassium 4,5- bis(dinitromethyl)furoxanate,^[11] B) dihydroxylammonium 5,5'- bistetrazole-1,1'-diolate (TKX-50),^[12] C) ammonium 3,4,5-trinitropyrazole-1-olate.^[4]

Further research has shown that fused heterocycles often show improved thermochemical stability, density and detonation performance. This effect can mostly be attributed to the ring strain energy.^[13] Relating to these facts energetic fused rings were synthesized in the last years.^{[13a], [14], [15]} Generally, the combination of different energetic moieties seems to be a very promising strategy for developing new energetic compounds. According to the application the properties can be tuned. The properties of a fused ring compound can be changed to meet the requirements for various applications: in case energetic compounds are desired to serve as primary or secondary explosives, they are synthesized in the form of nitrogen-rich salts; for different pyrotechnic applications only the metal of an energetic compound has to be exchanged. Based on this knowledge, in this article we present a new energetic anion containing two different heterocycles and energetic functional groups. While this work was in preparation, *Shreeve et al.* found a similar route to the anionic heterocycle 5-nitro-pyrazolo-(3,4-c)-furazan-5-*N*-oxide.^[16]

2. Results and Discussion

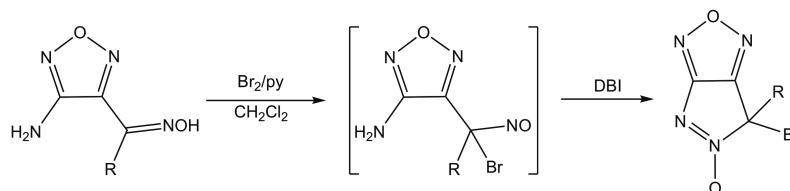
For the initial purpose to prepare an energetic furazan, 3- amino-4-chloro-oximidofurazan was treated with a mixture of acetic anhydride and HNO_3 (Scheme1).



Scheme 1: Preparation and nitration of 3-amino-4-chloro-oximidofurazan and proposed mechanism to form the potassium salt of 4-nitro-pyrazolo-(3,4-c)-furazan-5-*N*-oxide(**1**).

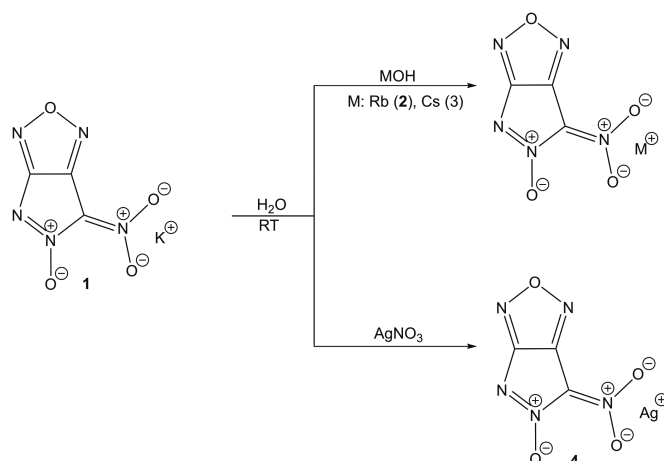
In the first step it was attempted to nitrate the amine and the oxime functional group of the starting material (3-chloro-4-amino-oximidofurazan) to yield 3-chlorodinitromethyl-4-nitraminofurazan as an intermediate. In a second step the potassium salt should be formed by treatment with potassium iodide (Figure 1). The desired nitrated furazanate anion (3-dinitromethyl-4-nitraminofurazan anion), in analogy to a procedure in the literature,^[11] was not obtained. The results of the analytical data however, especially X-ray diffraction, showed, that an unexpected heterocycle was formed which is 4-nitro-pyrazolo-(3,4-c)-furazan-5-N-oxide (**1**). However, very recently, the 3-dinitromethyl-4-nitraminofurazan anion was prepared by a different route.^{[17], [18]}

Subsequent research on this result revealed, that a related heterocycle had been reported. In this particular case, the formation of the neutral pyrazolo-(3,4-c)-furazan-5-N-oxide heterocycle was observed by bromination of the same furazan starting material (Scheme 2).^[19]



Scheme 2: Earliest formation of neutral derivatives of pyrazolo-(3,4-c)-furazan-5-N-oxide (R = Me, Cl).

With our procedure, it is possible to synthesize the anionic heterocycle **1** by nitration. In a second step, after the proposed intermediate,^[20] further reaction with potassium iodide resulted in a re-arrangement, as outlined in Scheme 1, to precipitate **1** as a yellow powder in reproducible yields around 20%. Attempts to exchange the potassium cation were successful only with the higher alkali metals. The rubidium and cesium salts (**2** and **3**) were obtained by reaction with the corresponding hydroxides in aqueous solution, respectively. The lower alkali salts were not accessible neither by Li/Nahydroxides, nor by exchange of the silver salt **4** with Li/Nachlorides/- iodides and the starting material was obtained. The silver salt **4** however, was obtained conveniently by treatment of **1** with silver nitrate in aqueous solution (Scheme 3).



Scheme 3: Preparation of Rb-, Cs- and Ag-salts **2**, **3** and **4**.

As indicated in the Introduction, others report the preparation of **1** via the identical route, as well as with nitrogenrich cations. However, we report a more economic route by using acetic anhydride, instead the rather expensive trifluoroacetic anhydride.^[16] Furthermore, we were able to isolate the rather sensitive silver salt and to characterize this compound by NMR, DTA, IR and sensitivities according to BAM. In the latter article the Ag-salt was generated in situ only, in order to exchange with nitrogen-rich cations (which we, therefore, omitted then in this study).

Since there was no indication or explanation given of a possible reaction mechanism of Scheme 2,^[19] we have undertaken further research for attempting to understand the result of our nitration outlined in Scheme 1. Therefore, it was checked if potassium iodide played a key role. Consequently, the reaction was performed as well with sodium/ barium- and ammonium iodide to see if other salts of this anion are accessible using different iodides. However, all salts failed, and no formation of the 4-nitro-pyrazolo-(3,4-c)-furazan-5-N-oxide anion was observed. In another experiment, KCl was used instead of KI, in order to check if iodide anion, possibly as a weak reducing agent, would be crucial. Indeed, iodide seems to be important, because no formation of the anionic heterocycle was observed with chloride. In summary, the presence of both potassium and iodide is important for the formation of **1**. The iodide as a strong nucleophile could be responsible for the elimination of either NO_2 or nitrite from an intermediately formed nitramine unit. Subsequently the pyrazole ring system is formed by cyclization, as indicated in Scheme 1. However, there is no evidence of such intermediates during these studies.

Efforts to obtain a protonation or methylation of **1** by using various acids (hydrochloric-, sulfuric- and perchloric acid), respectively resulted in all cases in decomposition, according to NMR spectroscopy. Efforts to methylate **1** with dimethyl sulfate or methyl iodide also failed and **1** was recovered. Further attempts of **1** to react with reducing agents Zn or $NaBH_4$, or with the chloromethyl groups of substituted nitramines, such as $(ClCH_2)N(NO_2)CH_3$ or $(ClCH_2)_2 NNO_2$, were also not successful. A possible

explanation for the restricted reactivity might be the strong coordination of the potassium cation to the oxygen atoms of the *N*-oxide and nitro groups.

All salts were comprehensively characterized by NMR, vibrational spectroscopy (IR, Raman) and differential thermal analysis (DTA). Moreover, the crystal structures of **1–3** were determined by X-ray diffraction measurements (Figures 3, 5 and 6), as well as a ^{15}N NMR spectrum of **1** was recorded, which is displayed with assignments in Figure 2.

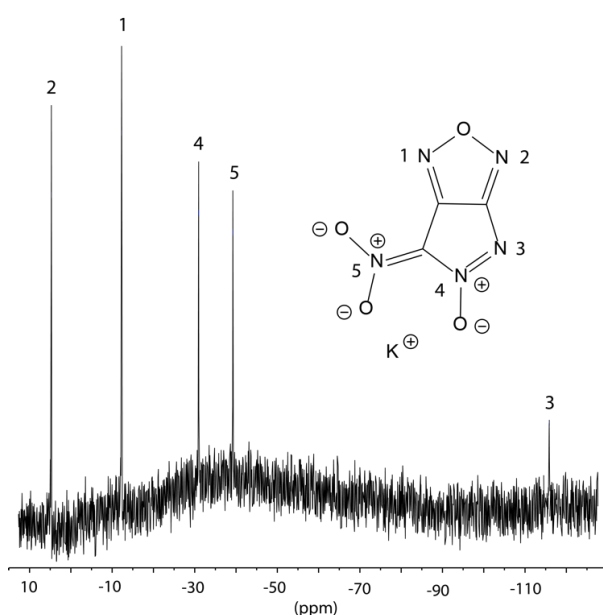


Figure 2: ^{15}N NMR spectrum of **1** in $\text{DMSO-}D_6$ at 25 °C.

All salts **1–4** show three ^{13}C NMR resonances, at 157.3 ppm for the nitro-carbon of the pyrazole, and 140.3 and 124.2 ppm for the furazan moiety, respectively. In the ^{15}N NMR spectrum of the potassium salt **1** the furazan resonances are typically found in the low-field region around 0 ppm (4.7/–12.3 ppm), those of the pyrazole nitrogen atoms at –30.9 (*N*-oxide) and –115.9. The exocyclic nitro group is found at –39.3 ppm. The resonances assignments regarding the heterocycles are based on the related compound of *Sheremetev*.^[19] The silver salt **4** is soluble in aqueous ammonia by formation of the silver diammine cation, which enabled the detection of the ^{109}Ag NMR resonance at 478 ppm. Compared to other silver solvate resonances,^[21] this resonance is found in the typical low-field region of ^{109}Ag .

The vibrational spectra of **1–4** show the typical antisymmetric $\nu_{\text{as}}(\text{NO}_2)$ and symmetric $\nu_{\text{s}}(\text{NO}_2)$ stretching vibrations in the range of 1620–1506 cm^{-1} and 1385–1251 cm^{-1} , respectively. The C–N, C–O and C–C vibrations observed are in the characteristic ranges for organic compounds.

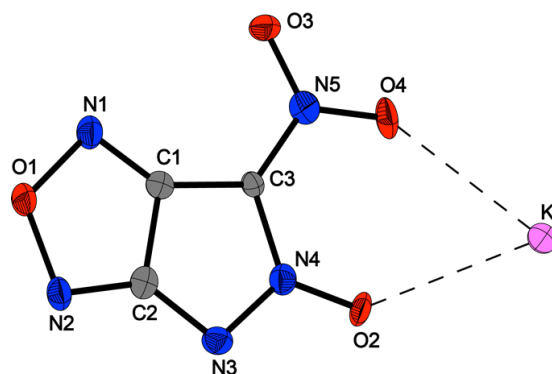


Figure 3: Molecular structure of potassium 4-nitro-pyrazolo-(3,4-c)-furan-5-*N*-oxide (**1**). Selected bond lengths (Å) and angles (deg): N3–N4 1.360(4), N4–O2 1.243(4), C3–N5 1.373(4), N5–O3 1.258(4), N5–O4 1.225(4). C1–C3–N5 128.4(3), C3–N4–O2 125.8(3), C2–N3–N4 103.1(3), N1–C1–C3–N5 1.5(9), N5–C3–N4–O2 2.7(6).

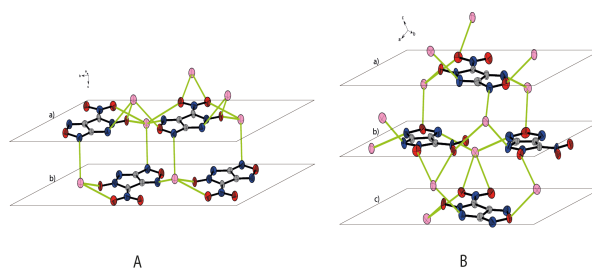


Figure 4: Layer packing of the two polymorphs of potassium salt **1**. A) polymorph in *P*–1 structure; B) polymorph in *P*_c structure.

The structures of the K/Rb/Cs-salts in the solid state were determined by low temperature X-ray diffraction. Interestingly, during recrystallization experiments from different solvents, the crystal structure of the potassium salt **1** was obtained in two different space groups. Recrystallization from water resulted in the *P*–1 space group, whereas from acetone the *P*_c space group was obtained, which also was confirmed by the powder pattern. Moreover, both differ from the recently published crystal structure of **1** (*P*21/*c*).^[16] Details on the measurement and refinement values are listed in Table 1. This phenomenon can be explained by different coordination of the metal atom to either different oxygen atoms of the functional groups. In Figure 4 the packing of the anions of both polymorphs are compared. It becomes visible that in the *P*–1 structure, the anions in layers a) and b) are oriented antiparallel, while in the *P*_c structure the anions in layers a) and c) are the same, but the anions in layer b) are rectangular oriented.

As expected, the potassium salt **1** has the lowest density (2.13 g cm^{–3}, *P*–1), compared to the rubidium salt **2** (2.50 g cm^{–3}, *P*21) and the cesium salt **3** with the highest density (2.82 g cm^{–3}, *P*21/*n*). The C–N bond distances between the pyrazole heterocycle and the nitro group (1.373–1.394 Å) are significantly shorter than a regular C–N bond (1.470 Å), which confirm the structures displayed in Schemes 1/3 and Figure 2 with C=N double bonds. In addition, the N–N(O)–C angle of the pyrazole heterocycle (103.1°) is slightly

smaller than expected for a five-membered ring (104.1°).^[22] All metals coordinate to oxygen and nitrogen atoms of the ring system. This is also obvious upon comparison of the crystal structures with the different cations in **1–3**. As visible from the Figures S1–S3 (Supporting Information), the packing of the salts consists of layered structures. The layers of **1** are connected via a disordered octahedron of the potassium cation to three different oxygen atoms of the nitro and *N*-oxide groups. The distances of the oxygen/nitrogen and potassium atoms are in the range of 2.74–2.92 Å. Each metal cation coordinates to oxygen and nitrogen atoms of different anions as visible in Figure 4; but in Figures 3, 5 and 6 contacts to oxygen only are shown for clarity. The rubidium salt **2** as well as the cesium salt **3** shows no anomalies in the structure of the anions. The coordination distances are comparable to other heterocyclic alkali salts.^[23] Both salts crystallize in staggered layers, where the cation is formally coordinated tenfold in distances of 3.00–3.40 Å and 3.13–3.67 Å to oxygen/nitrogen, respectively.

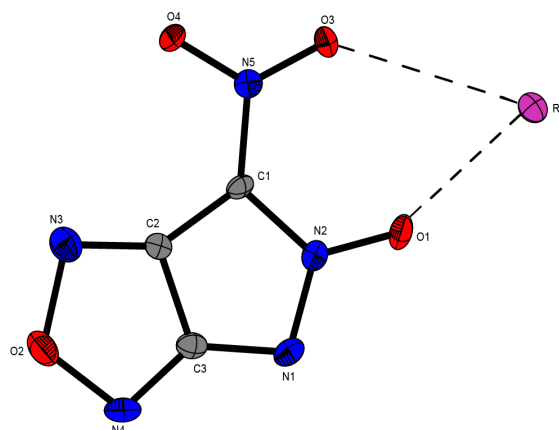


Figure 5: Molecular structure of rubidium 4-nitro-pyrazolo-(3,4-c)- furazan-5-*N*-oxide (**2**). Selected bond lengths (Å) and angles (deg): C1–N5 1.382 (9), N2–O1 1.260(6), N1–N2 1.339(9). C2–C1–N5 129.0(6), C1–N2–O1 115.0 (5), N2–N1–C3 102.2(5). N3–C2–C1–N5 178.4(10), N5–C1–N2–O1 2.2(12), C3–N1–N2–O1 179.1(7).

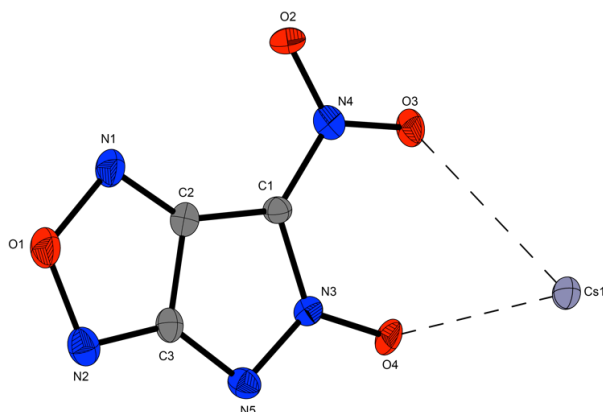


Figure 6: Molecular structure of cesium 4-nitro-pyrazolo-(3,4-c)- furazan-5-N-oxide (**3**). Selected bond lengths (Å) and angles (deg): C1–N4 1.394 (6), N3–O4 1.259 (5), N3–N5 1.346 (5). C2–C1–N4 129.8(4), C1–N3–O4 125.5(4), N3–N5–C3 101.9(3). N1–C2–C1–N4 3.3(10), N4–C1–N3–O4 2.7(7), C3–N5–N3–O4 179.5(4).

Table 1. Crystal and structure refinement data of **1–3**.

	1	1	2	3
Formula	209.16	209.16	255.53	302.97
FW (g mol ^{−1})	C ₃ KN ₅ O ₄	C ₃ KN ₅ O ₄	C ₃ N ₅ O ₄ Rb	C ₃ Cs N ₅ O ₄
Temp (K)	173	173	173	173
Crystal size (mm ³)	0.18x0.15x0.04	0.13x0.16x0.10	0.350.08x0.02	0.10x0.08x0.03
Crystal description	Colorless block	Colorless block	Yellowish Rod	Yellowish Rod
Crystal system	triclinic	monoclinic	monoclinic	monoclinic
Space group	<i>P</i> −1	<i>Pc</i>	<i>P</i> 2 ₁	<i>P</i> 2 ₁ / <i>n</i>
<i>a</i> (nm)	0.52404(4)	1.04600(3)	0.7517(7)	0.81699(5)
<i>b</i> (nm)	0.78040(8)	0.89151(3)	0.5160(5)	0.50381(3)
<i>c</i> (nm)	0.81880(7)	0.70227(3)	0.9047(10)	1.73931(11)
α (°)	86.249(8)	90	90	90
β (°)	81.455(7)	90.832(6)	105.501(11)	94.388(6)
γ (°)	78.957(9)	90	90	90
<i>V</i> (nm ³)	32.477(5)	65.481(3)	33.827(5)	71.381(8)
<i>Z</i>	2	4	2	4
ρ_{calc} (g cm ^{−3})	2.14	2.12	2.50	2.81
μ (mm ^{−1})	0.808	0.802	7.309	5.179
<i>F</i> (000)	208	416	244	560
Θ range (°)	4.379–25.487	4.157–28.278	4.5500–18.2090	4.212–25.993

Index range	$-6 \leq h \leq 6$	$-13 \leq h \leq 13$	$-9 \leq h \leq 9$	$-7 \leq h \leq 10$
	$-9 \leq k \leq 9$	$-11 \leq k \leq 11$	$-5 \leq k \leq 6$	$-6 \leq k \leq 6$
	$-9 \leq l \leq 9$	$-9 \leq l \leq 9$	$-11 \leq l \leq 11$	$-21 \leq l \leq 21$
Reflection collected	2044	3228	2345	5009
Reflection observed	2044	3228	1083	1395
Reflection unique	1408	2136	1002	1240
R1, wR2 (2 σ data)	0.0404, 0.0847	0.0531, 0.1219	0.0318, 0.0713	0.0268, 0.0576
R1, wR2 (all data)	0.0660, 0.0902	0.795, 0.1385	0.0361, 0.0742	0.0331, 0.0608
Parameters	119	236	119	118
GOOF and F^2	0.887	1.143	1.066	1.053
Larg. diff. peak/hole (e nm ⁻³)	0.0504, -0.0331	0.0757, -0.0610	0.0668, -0.0563	0.1202, -0.0704
CCDC entry	133976	133977	133974	133975

All salts are air stable. All measurements of **1** were performed with the polymorph that crystallized in the *P*-1 space group. The thermal stabilities of **1–4** were determined using DTA experiments (heating rate: 5 °C min⁻¹) listed in Table 2. As expected, when comparing the decomposition temperatures, a trend becomes visible. With increasing size of the cation, the decomposition temperature slightly decreases from 203 °C to 197 °C. The sensitivities toward impact, friction and electrical discharge were determined according to standards of the Federal Institute for Materials Research and Testing (BAM). All compounds are very sensitive towards impact (1–2 J) and therefore in the range of primary explosives. Towards friction (30–72 N) and electrical discharge (60–150 mJ), the salts **1–4** are moderate sensitive, respectively.

The detonation parameters of **1** were calculated with EXPLO5 6.03. The detonation velocity (8563 m s⁻¹), heat of detonation (-5617 KJ kg⁻¹), detonation temperature (3786 K) and detonation pressure (32.7 GPa) was calculated.

Table 2. Physical properties and calculated detonation parameters of **1–4**.

	1	2	3	4
ρ [g cm ⁻³] ^{a)}	2.10 ^{h)}	2.46 ^{h)}	2.77 ^{h)}	2.01 ⁱ⁾
formula ^{b)}	C ₃ KN ₅ O ₄	C ₃ N ₅ O ₄ Rb	C ₃ CsN ₅ O ₄	AgC ₃ N ₅ O ₄
T_{dec} [°C] ^{c)}	203	200	197	197
IS [J] ^{d)}	2	1.5	1	1
FS [N] ^{e)}	72	72	72	30
ESD [mJ] ^{f)}	150	120	60	60
N [%] ^{g)}	33.5	27.4	23.1	25.2

a) Density at room temperature. b) Compound formula. c) Decomposition temperature. d) Impact sensitivity. e) Friction sensitivity. f) Sensitivity toward electrostatic discharge. g) Nitrogen content. h) X-ray i) pycnometric measurement.

3. Conclusions

The attempt to synthesize the 3-nitramino-4-dinitromethyl furazan anion by nitration of 3-amino-4-chlorooximidofurazan yielded an unexpected product. Analytical results showed that the energetic nitrogen-rich heterobicyclic anion 4-nitro- pyrazolo-(3,4-c)-furazan-5-N-oxide as the potassium salt (**1**) was formed. Experiments with other reagents gave some insight about the reaction conditions and mechanisms. It was shown that the presence of potassium and iodide are crucial for the formation of **1**. Further experiments proved that the neutral compound (protonated form) was not feasible. In this study the higher alkali metal salts **2** and **3**, as well as silver salt **4**, were presented. The physical properties of **1–4** showed, the compounds have good thermal stabilities around 200°C, high sensitivities towards impact (1–2 J) and moderate sensitivities toward friction (30–72 N) and electrical discharge (60–150 mJ). Depending on the cation, the new salts can be classified as primary, secondary or pyrotechnical compound. According to the detonation properties, compounds **1–4** could be useful as primary explosives.

4. Experimental Section

General methods:

The low-temperature single-crystal X-ray diffraction measurements were performed on an Oxford XCalibur3 diffractometer equipped with a Spellman generator (voltage 50 kV, current 40 mA) and a KappaCCD detector operating with MoK α radiation ($\lambda = 0.7107 \text{ \AA}$). Data collection was performed using the CRYSLIS CCD software.^[24] The data reduction was carried out using the CRYSLIS RED software.^[25] The solution of the structure was performed by direct methods (SIR97)^[26] and refined by full-matrix least-squares on F2 (SHELXL)^[27] implemented in the WINGX software package^[28] and finally checked with the PLATON software.^[29] All non-hydrogen atoms were refined anisotropically. The hydrogen atom positions were located in a difference Fourier map. DIAMOND plots are shown with thermal ellipsoids at the 50 % probability level. These data can be obtained free of charge from The Cambridge Crystallographic Data Centre (133974–133977). All chemicals were used as supplied. Raman spectra were recorded in a glass tube with a Bruker MultiRAM FT-Raman spectrometer with Nd:YAG laser excitation up to 1000 mW (at 1064 nm). Infrared spectra were measured with a PerkinElmer Spectrum BX-FTIR spectrometer equipped with a Smiths Dura/SamplIR II ATRdevice. All spectra were recorded at ambient (25 °C) temperature. NMR spectra were recorded with a JEOL/Bruker instrument and chemical shifts were determined with respect to external Me₄Si (¹H, 399.8 MHz; ¹³C, 100.5 MHz) and MeNO₂ (¹⁵N, 40.6 MHz; ¹⁴N, 28.9 MHz). Analyses of C/H/N were performed with an Elemental Vario EL Analyzer. Melting and decomposition points were measured using differential thermal analysis (DTA) at a heating rate of 5° C min⁻¹ with an OZM Research DTA 552-Ex instrument. The sensitivity data were explored using a BAM drop hammer and a BAM friction tester.^{[30], [31]} The heats of formations were calculated by the atomization method based on CBS-4M electronic enthalpies. All calculations affecting the detonation parameters (see Supporting Information) were carried out using the program package Explo5 6.03.^{[32], [33]}

Potassium 4-nitro-pyrazolo-(3,4-c)-furazan-5-N-oxide (1):

Into a cold mixture consisting of acetic anhydride (14 mL) and fuming nitric acid (8 mL), 3-amino-4-chloro-oximidofurazan (2.50 g, 15.4 mmol) was slowly added maintaining the temperature at -5–0 °C. The reaction mixture was stirred for 1 h at 0 °C and 3 h at ambient temperature. After pouring onto ice, extracting with diethyl ether (3x50 mL), the combined organic phases were washed with two times with water and once with brine. Consequently dried over magnesium sulfate, the solvent was removed under reduced pressure to yield the intermediate as light yellowish oil. The oil was dissolved in methanol (40 mL).

With ice cooling potassium iodide (2.00 g, 12.0 mmol), also dissolved in methanol (40 mL), was slowly added to the reaction mixture. Stirring over night at ambient temperature resulted in precipitation of **1**. The precipitate was filtered off and washed with cold water (10mL), methanol (10mL) and diethyl ether (10 mL) to yield 0.62 g (19%) of **1** as yellow powder. **DTA** (5 °C min⁻¹): 203 °C (dec.); **IR** (ATR, cm⁻¹): $\tilde{\nu}$ = 2462 (w), 1659 (w), 1539 (w), 1494 (s), 1483 (s), 1423 (w), 1391 (s), 1372 (s), 1296 (s), 1179 (w), 1153 (s), 1102 (s), 1073 (s), 1051 (s), 982 (m), 970 (m), 839 (w), 817 (m), 800 (m), 773 (m), 747 (w), 731 (m), 694 (w), 671 (m); **Raman** (1064 nm, 500 mV, 25 °C, cm⁻¹) $\tilde{\nu}$ = 1659 (13), 1537 (50), 1493 (4), 1408 (7), 1364 (23), 1286 (100), 1157 (7), 1102 (13), 980 (9), 819 (38), 776 (4), 674 (3), 595 (19), 459 (20), 38 (6), 119 (94); **¹³C{¹H} NMR** (DMSO-D₆, 25 °C, ppm), δ = 157.3 (CNO₂), 140.3 (CCNO₂), 124.2 (NCN); **¹⁵N NMR** (DMSO-D₆, 25 °C, ppm) δ : 4.7 (N-Furazan), -12.3 (N-Furazan), -30.9 (NO), -39.3 (NO₂), -115.9 (NN). **EA** (C₃KN₅O₄, 209.16 g mol⁻¹): Calc. C 17.23, N 33.48. Found: C 17.28, N 33.44; **Sensitivities** (100 μ m \geq g. s. \geq 50 μ m): **IS**: 2 J; **FS**: 72 N; **ESD**: 150 mJ.

Conversion into the rubidium/cesium salts **2** and **3**:

The potassium salt **1** (0.10 g, 0.5 mmol) was dissolved in 5 mL water and a 50 w% rubidium/cesium hydroxide solution (0.5 mmol, Rb 0.10 g; Cs 0.14 g) was added in one portion. The reaction mixture was stirred for 1 h at room temperature, during which a precipitate was obtained. The precipitate was filtered off and washed with ice water. Recrystallization from acetone/water yielded yellowish crystals of **2** (0.10 g, 81%), respectively **3** (0.13 g, 89 %).

Rubidium 4-nitro-pyrazolo-(3,4-c)-furazan-5-N-oxide (**2**):

DTA (5 °C min⁻¹): 200 °C (dec.); **IR** (ATR, 25 °C, cm⁻¹): $\tilde{\nu}$ = 1652 (w), 1523 (w), 1483 (m), 1423 (m), 1389 (s), 1349 (s), 1291 (s), 1156 (m), 1154 (s), 1103 (s), 1070 (s), 1050 (s), 982 (m), 967 (s), 837 (m), 819 (s), 801 (m), 769 (m), 748 (m), 732 (s), 692 (m); **Raman** (1064 nm, 400 mV, 25 °C, cm⁻¹) $\tilde{\nu}$ = 3982 (10), 3976 (5), 3498 (13), 2859 (60), 1532 (16), 1429 (19), 1355 (25), 1295 (100), 823 (46), 594 (23), 157 (17), 129 (15); **¹³C{¹H} NMR** (DMSO-D₆, 25 °C, ppm), δ = 157.3 (CNO₂), 140.3 (CNO), 124.2 (CNO); **¹⁴N NMR** (DMSO-D₆, 25 °C, ppm), δ = -31 (NO), -40 (NO₂); **EA** (C₃RbN₅O₄, 255.53 g mol⁻¹): Calc. C 14.10, N 27.41. Found: C 14.38, N 27.70; **Sensitivities** (100 μ m \geq g. s. \geq 50 μ m): **IS** 1.5 J; **FS**: 72 N; **ESD**: 120 mJ.

Cesium 4-nitro-pyrazolo-(3,4-c)-furazan-5-N-oxide (3):

DTA (5 °C min⁻¹): 197 °C (dec.); **IR** (ATR, 25 °C, cm⁻¹): $\tilde{\nu}$ = 1646 (m), 1499 (s), 1480 (m), 1427 (s), 1388 (s), 1372 (m), 1349 (s), 1290 (s), 1186 (m), 1153 (s), 1100 (s), 1048 (s), 979 (s), 966 (s), 836 (m), 821 (s), 798 (s), 765 (m), 750 (m), 730 (s), 693 (m), 665 (s). **Raman** (1064 nm, 400 mV, 25 °C, cm⁻¹) $\tilde{\nu}$ = 3982 (10) 3976 (5), 3498 (13), 2859 (60), 1532 (16), 1429 (19), 1355 (25), 1295 (100), 823 (46), 594 (23), 157 (17), 129 (15); ¹³C{¹H} **NMR** (DMSO-D₆, 25 °C, ppm), δ = 157.3 (CNO₂), 140.3 (CNO), 124.2 (CNO); ¹⁴N **NMR** (DMSO-D₆, 25 °C, ppm), δ = -31 (NO₂), -40 (NO); **EA** (C₃CsN₅O₄, 302.97 g mol⁻¹): Calc.: C 11.89, N 23.12. Found: C 12.08, N 22.97. **Sensitivities** (100 μ m \geq g. s. \geq 50 μ m): **IS**: 1 J; **FS**: 72 N; **ESD**: 60 mJ.

Silver 4-nitro-pyrazolo-(3,4-c)-furazan-5-N-oxide (4)

Into a solution of **1** (0.50 g, 2.40 mmol) in 40 ml water, 15 mL of a silver nitrate (0.41 g, 2.41 mmol) was added in one portion. The mixture was stirred for 2 h at ambient temperature. The precipitate was collected by filtration and washed with water. After drying in vacuum 0.61 g (93 %) of yellowish **4** was obtained. **DTA** (5 °C min⁻¹): 197 °C (dec.); **IR** (ATR, cm⁻¹): $\tilde{\nu}$ = 3437 (w), 3074 (w), 1614 (w), 1502 (s), 1487 (s), 1360 (s), 1176 (m), 1155 (m), 1124 (w), 1103 (w), 1037 (m), 979 (m), 837 (w), 796 (m), 744 (w), 730 (w), 679 (m); ¹³C{¹H} **NMR** (conc. aq. NH₃, 25 °C, ppm), δ = 157.3 (CNO₂), 140.3 (CNO), 124.2 (CNO); ¹⁴N **NMR** (conc. aq. NH₃, 25 °C, ppm), δ = -31 (NO), -40 (NO₂); ¹⁰⁹Ag **NMR** (conc. aq. NH₃, 25 °C), δ = 478; **EA** (AgC₃N₅O₄, 277.93 g mol⁻¹): Calc.: C 12.96, N 25.20. Found: C 12.54, N 24.77; **Sensitivities** (100 μ m \geq g. s. \geq 50 μ m): **IS** 1 J; **FS**: 30 N; **ESD**: 60 mJ.

5. References

- [1] D. Fischer, J. L. Gottfried, T. M. Klapötke, K. Karaghiosoff, J. Stierstorfer, T. G. Witkowski, *Angew. Chem., Int. Ed.*, **2016**, *55*, 16132–16135.
- [2] T. M. Klapötke, *Chemistry of High-Energy Materials, 4th Edition*, Walter de Gruyter GmbH & Co KG, Berlin, **2017**.
- [3] D. G. Piercey, D. E. Chavez, B. L. Scott, G. H. Imler, D. A. Parrish, *Angew. Chem., Int. Ed.*, **2016**, *55*, 15315–15318.
- [4] Y. Zhang, D. A. Parrish, J. M. Shreeve, *J. Mater. Chem.*, **2012**, *22*, 12659–12665.

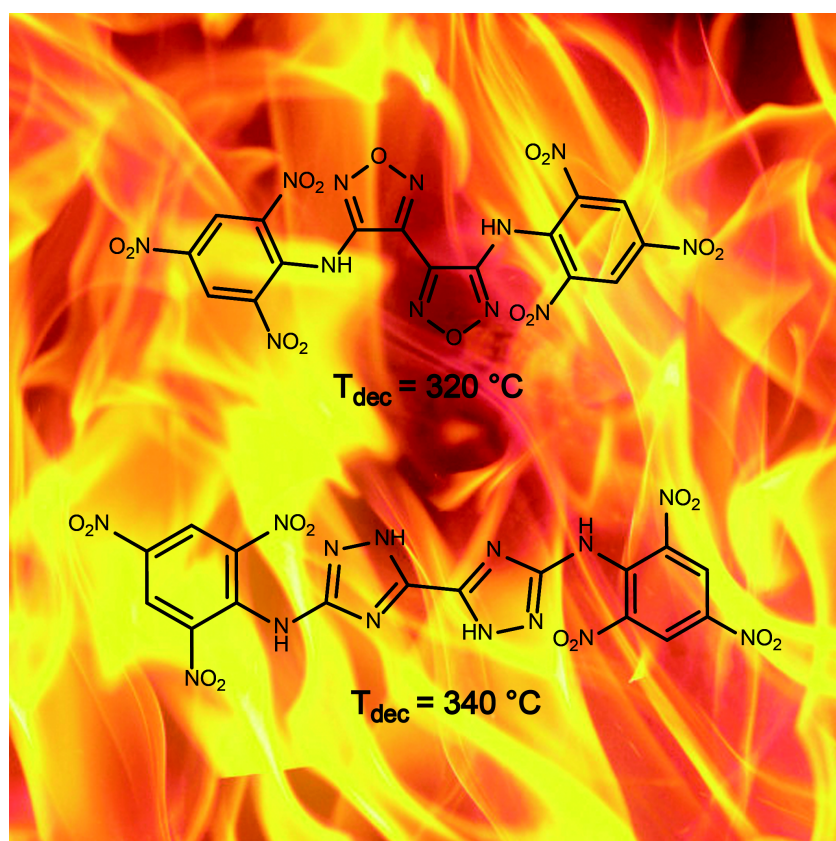
- [5] M. Göbel, K. Karaghiosoff, T. M. Klapötke, D. G. Piercey, J. Stierstorfer, *J. Am. Chem. Soc.*, **2010**, *132*, 17216–17226.
- [6] T. M. Klapötke, J. Stierstorfer, *Green Energetic Materials*, John Wiley & Sons Ltd.; Energetic tetrazole N-oxides, **2014**, p. 133–177.
- [7] I. B. Starchenkov, V. G. Andrianov, A. F. Mishnev, *Chem. Heterocycl. Compd. (N. Y.)*, **1998**, *33*, 1355–1359.
- [8] T. Wang, C. Zheng, X. Gong, M. Xia, *J. Mol. Model.*, **2015**, *21*, 1–9.
- [9] Z. Yu, E. R. Bernstein, *J. Phys. Chem. A*, **2013**, *117*, 10889–10902.
- [10] D. G. Piercey, D. E. Chavez, S. Heimsch, C. Kirst, T. M. Klapötke, J. Stierstorfer, *Propellants, Explos., Pyrotech.*, **2015**, *40*, 491–497.
- [11] C. He, J. M. Shreeve, *Angew. Chem., Int. Ed.*, **2016**, *55*, 772–775.
- [12] N. Fischer, D. Fischer, T. M. Klapötke, D. G. Piercey, J. Stierstorfer, *J. Mater. Chem.*, **2012**, *22*, 20418–20422.
- [13] a) J. Zhang, P. Yin, L. A. Mitchell, D. A. Parrish, J. M. Shreeve, *J. Mater. Chem. A*, **2016**, *4*, 7430–7436; b) D. Kumar, G. H. Imler, D. A. Parrish, J. M. Shreeve, *Chem. Eur. J.*, **2017**, *23*, 1743–1747.
- [14] M. C. Schulze, B. L. Scott, D. E. Chavez, *J. Mater. Chem. A*, **2015**, *3*, 17963–17965.
- [15] V. Thottempudi, P. Yin, J. Zhang, D. A. Parrish, J. M. Shreeve, *Chem. Eur. J.*, **2014**, *20*, 542–548.
- [16] Y. Tang, C. He, J. M. Shreeve, *J. Mater. Chem. A*, **2017**, *5*, 4314–4319.
- [17] Y. Li, H. Huang, Y. Shi, J. Yang, R. Pan, X. Lin, *Chem. - Eur. J.*, **2017**, *23*, 7353–7360.
- [18] H. Huang, Y. Li, J. Yang, R. Pan, X. Lin, *New J. Chem.*, **2017**, *41*, 7697–7704.
- [19] A. B. Sheremetev, Y. A. Strelenko, *Mendeleev Commun.*, **1993**, *3*, 120.
- [20] Y. Tang, C. He, L. A. Mitchell, D. A. Parrish, J. M. Shreeve, *Angew. Chem., Int. Ed.*, **2016**, *55*, 5565–5567.
- [21] T. M. Klapötke, B. Krumm, R. Moll, A. Penger, S. M. Sproll, R. J. F. Berger, S. A. Hayes, N. W. Mitzel, *Z. Naturforsch.*, **2013**, *68B*, 719–731.
- [22] P. J. Wheatley, *Physical Methods in Heterocyclic Chemistry, Vol. 5: Handbook of Molecular Dimensions. X-Ray Bond Angles and Lengths*, Academic, **1972**.
- [23] V. Ernst, T. M. Klapötke, J. Stierstorfer, *Z. Anorg. Allg. Chem.*, **2007**, *633*, 879–887.
- [24] CrysAlisPro, Oxford Diffraction Ltd. version 171.33.41, **2009**.
- [25] CrysAlis RED, Version 1.171.35.11 (release 16-05-2011 CrysAlis 171.Net), Oxford Diffraction Ltd., Abingdon, Oxford (U.K.), **2011**.

- [26] A. Altomare, M. C. Burla, M. Camalli, G. L. Cascarano, C. Giacovazzo, A. Guagliardi, A. G. G. Moliterni, G. Polidori, R. Spagna, *J. Appl. Crystallogr.*, **1999**, *32*, 115–119.
- [27] G. M. Sheldrick, *Acta Crystallogr., Sect. A: Found. Crystallogr.*, **2008**, *64*, 112–122.
- [28] L. J. Farrugia, *J. Appl. Crystallogr.*, **1999**, *32*, 837–838.
- [29] A. L. Spek, *PLATON*, **1999**, A Multipurpose Crystallographic Tool, Utrecht University, The Diffraction Ltd.
- [30] Reichel & Partner GmbH, <http://www.reichelt-partner.de>.
- [31] *Test Methods According to the UN Recommendations on the Transport of Dangerous Goods, Manual of Test and Criteria, Fourth Revised Edition, United Nations Publication, New York and Geneva*, **2003**, ISBN 92–1–139087–7, Sales No. E.03.VIII. 2; 13.4.2 Test 3a (ii) BAM Fallhammer.
- [32] M. Sućeska, *Propellants, Explos., Pyrotech.*, **1991**, *16*, 197–202.
- [33] M. Sućeska, *EXPLO5 V.6.03*, **2014**, Zagreb (Croatia).

High Temperature Stable Picrylamino Substituted Furazanes and Triazoles

Tobias S. Hermann, Thomas M. Klapötke^{*}, Burkhard Krumm, Jörg Stierstorfer and Ivan Gospodinov

Propellants, Explosives, Pyrotechnics, **2018**, in press.



High Temperature Stable Picrylamino Substituted Furazanes and Triazoles

Tobias S. Hermann, Thomas M. Klapötke^{*}, Burkhard Krumm, Jörg Stierstorfer and Ivan Gospodinov

Propellants, Explosives, Pyrotechnics, **2018**, in press.

Abstract:

The field of high thermally stable explosives has been extended with the synthesis of 3,4-bis(picrylamino)furazan, 4,4'-bis(picrylamino)-3,3'-bisfurazanyl, 3,5-bis(picrylamino)-1,2,4-triazole and 5,5'-bis(picrylamino)-3,3' bi-1,2,4-triazole according to literature. Full characterization of these compounds, vacuum stability tests and calculations of their energetic properties were carried out. 4,4'-Bis(picrylamino)-3,3'-bifurazane and 5,5'-bis(picrylamino)-3,3' bi-1,2,4-triazolyl have the highest decomposition temperature and therefore were tested for their compatibility with the most commonly used metals and explosive ingredients.

1. Introduction

The chemistry of high temperature explosives is mainly dominated by bis(aminopicryl)dinitropyridine (PYX)^[1] and 2,2',4,4',6,6'-hexanitro stilbene (HNS)^[2] (Figure 1). Their high thermal stability (340/320 °C) and the properties of PXY under pressure (up to 150 MPa) make them good explosives under extreme environmental conditions.^[3] Therefore, their main applications are in the oil- and space exploration. Another recently described heat-resistant explosive is 5,5'-bis(2,4,6-trinitro-phenyl)-2,2'-bi(1,3,4-oxadiazole) (TKX-55, Figure 1).^[4]

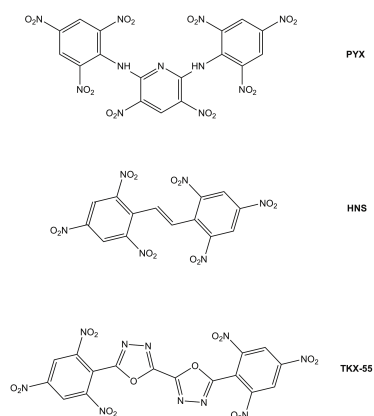


Figure 1: Examples of high thermal stable explosives.

The high thermal stability of these three compounds is mainly derived from a conjugated system with attached explosophore nitro groups. All of these compounds follow the same strategy. In order to make them heat-resistant different moieties are located between two picryl functional groups. In the case of HNS, an ethylene group and in the cases of PYX and TKX-55, aromatic heterocycles are positioned between the picryl moieties.

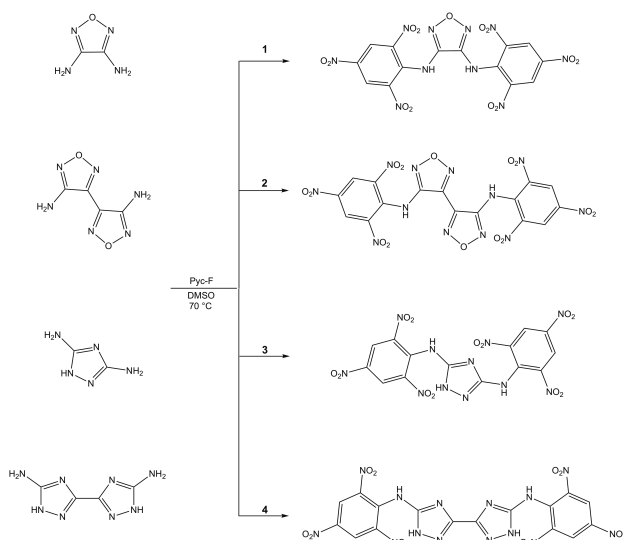
Nitrogen- and oxygen-rich heterocyclic compounds have proven to have good energetic properties. This is mostly due to a high density and high positive heat of formation.^[5] Particularly, oxadiazoles and triazoles have been intensively investigated so far because of their good properties, like high density, high heat of formation and high thermal stability, in terms of molecular backbones of explosives.^{[6], [7], [8], [9], [10], [11]} In order to follow the strategy of TKX-55, making high thermal resistant compounds, the combination of the benefits and properties of furazan and 1,2,4-triazole heterocycles with picryl functional groups were investigated in this work. The compounds 3,4-bis(picrylamino)furazan, 4,4'-bis(picrylamino)-3,3'-bisfurazanyl, 3,5-bis(picrylamino)-1,2,4-triazole and 5,5'-bis(picrylamino)-3,3' bi-1,2,4-triazole were of particular interest because of their promising structure and therefore were investigated with different measurements and calculations.

2. Results and Discussion

Synthesis and Characterization

Compound **1–4** were synthesized according to literature proceedings published by *Coburn et al.*^{[21] [22]} For the synthesis of the investigated high thermal explosives 3,4-diamino-furazan, 4,4'-diamino-3,3'-bifurazan^[23], 3,5-diamino-1*H*-1,2,4-triazole and 5,5'-diamino-1*H*-bi-1,2,4-triazole served as starting material. According to literature, the starting materials were mixed with equivalent amounts of picryl fluoride and

heated in basic conditions (Figure 2). Upon pouring on ice-water, the products precipitated. After recrystallization from a mixture of ethanol/acetone the products were obtained in analytical purity.^{[21] [22]} Picryl fluoride was used because of the *element effect*. *Sugiyama et. al.* maintained that the substitution reaction of aliphatic and aromatic systems are different.^[24] While in aliphatic systems the S_N -reaction increase like: $F \ll Cl < Br < I$, it is opposite for aromatic systems. *Sugiyama et. al.* verified the faster reaction of picryl fluoride by the reaction of picryl fluoride and picryl chloride with dimethylaniline.



Scheme 1. Reaction of picryl fluoride with selected furazanes and triazoles.

In this research, all compounds were comprehensively characterized by NMR, vibrational spectroscopy (IR, Raman), X-ray or gas pycnometry, differential thermal analysis (DTA) and vacuum stability test (VST). The sensitivities were measured according to BAM standards and the theoretical performance calculated by EXPLO5 6.03.

Spectroscopy

The vibrational analysis of **1–4** showed the characteristic antisymmetric $\nu_{as}(\text{NO}_2)$ and the symmetric $\nu_s(\text{NO}_2)$ stretching vibrations in the range of $1620\text{--}1506\text{ cm}^{-1}$ and $1385\text{--}1251\text{ cm}^{-1}$, respectively. The NH stretch vibration is detected in the range of $3250\text{--}3400\text{ cm}^{-1}$. The C–N, C–O and C–C vibrations of **1–4** are observed in the typical ranges for heterocycles and CHNO based aliphatic compounds.

In the ^1H NMR spectra of **1** and **2** the CH resonance of the picryl moiety is detected at around $9.10\text{--}9.20$ ppm and the NH moiety at around $10.50\text{--}10.53$ ppm (Figure 2). For compound **3** and **4** the picryl moiety is detected at around 8.80 and 8.90 ppm and the NH moieties broadened at $10.1\text{--}10.3$ and $11.9\text{--}12.2$ ppm (Figure 2).

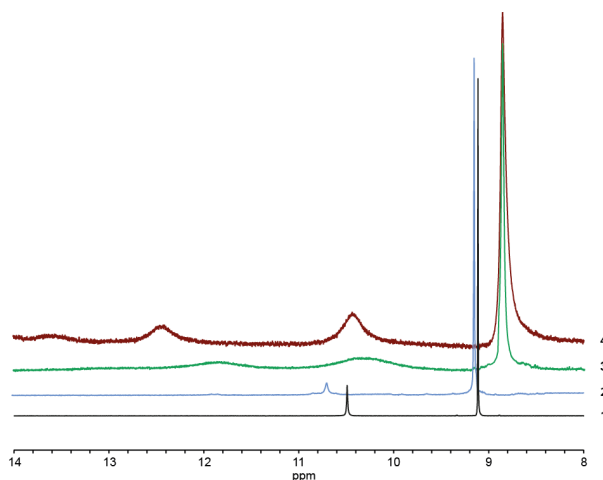


Figure 2: ^1H NMR resonances of compounds 1–4.

In the ^{13}C NMR spectra all ring carbons are visible and also the nitro resonances of the picryl moieties are detected in the range of -17 ppm to -19 ppm in the ^{14}N NMR spectra.

Crystal Structures

The structures of **1** and **2** in the solid state were determined by low temperature X-ray diffraction. The density of **3** and **4** was measured by gas-pycnometry, because of a lack of crystallization in common solvents. The density of the triazoles (**3**: 1.84 , **4**: 1.83 g cm^{-3}) are higher than the ones of the furazanes. The highest density at 173 K was measured for compound **1** with 1.81 g cm^{-3} (Figure 3) in the orthorhombic space group $P2_12_12_1$, compared to compound **2** in the monoclinic space group $P2/c$ with a density of 1.78 g cm^{-3} (Figure 4). In Figure 5 the unit cell of both compounds are illustrated. Details on the X-ray measurements are listed in Table 1.

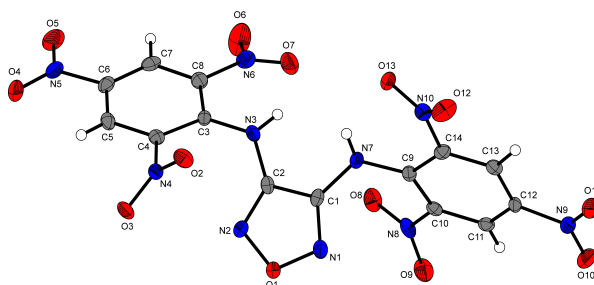


Figure 3: Molecular structure of 3,4-bis(Picrylamino)furanan (**1**). Selected bond lengths (\AA) and angles ($^\circ$): C1–N3 1.398 (**4**), C1–C2 1.428 (**4**), N3–C3 1.378 (**3**); C1–N3–C3 123.0 (**2**), N1–O1–N2 110.9 (**2**), N3–C3–C8 120.7 (**3**); C1–N3–C3–C4 40.1 (**4**).

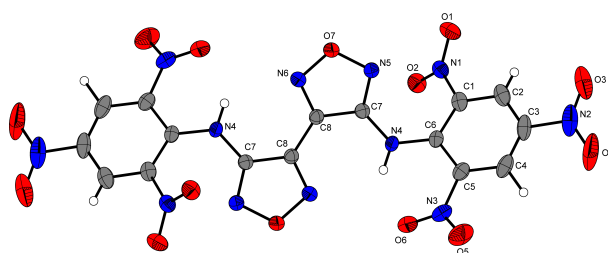


Figure 4: Molecular structure of 4,4'-bis(Picrylamino)-3,3'-bisfuryzanyl (**2**). Selected bond lengths (Å) and angles (deg.): C1–C2 1.431 (3), N3–C3 1.387 (3), C1–N3 1.373 (3), C1–N3–C3 124.63 (19), N1–O1–N2 111.12 (15), N3–C3–C4 123.3 (2); C1–N3–C3–C4 41.5 (3), C6–C5–C4–N4 168.6 (2).

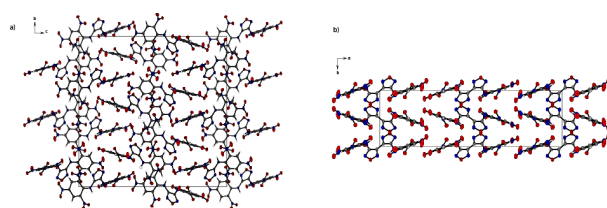


Figure 5: View on the unit cell of compound **1** and **2**. a) compound **1** along the *a*-axis, b) compound **2** along the *c*-axis.

Table 1. X-ray parameters of compounds **1–4**.

	1	2
Empirical formula	C ₁₄ H ₆ N ₁₀ O ₁₃	C ₁₆ H ₆ N ₁₂ O ₁₄
Formula mass (g mol ^{−1})	522.29	590.33
Temperature (K)	173	173
Crystal size (mm ³)	0.100x0.060x0.030	0.341x0.283x0.171
Crystal description	yellow block	yellow plate
Crystal system	orthorhombic	monoclinic
Space group	<i>P</i> 2 ₁ 2 ₁ 2 ₁	<i>P</i> 2 ₁ / <i>c</i>
<i>a</i> (Å)	8.4516(2)	31.7742(8)
<i>b</i> (Å)	23.9494(6)	8.1232(2)
<i>c</i> (Å)	28.3747(8)	8.5090(2)
<i>α</i> (°)	90	90

β (°)	90	91.957(7)
γ (°)	90	90
V (Å ³)	5743.3(3)	2194.96
Z	12	4
ρ_{calc} (g cm ⁻³)	1.812	1.786
μ (mm ⁻¹)	0.164	0.160
$F(000)$	3168	1192
Θ range (°)	2.315/26.372	4.267/28.282
Index range	$-10 \leq h \leq 10$	$-42 \leq h \leq 42$
	$-29 \leq k \leq 29$	$-10 \leq k \leq 10$
	$-35 \leq l \leq 35$	$-10 \leq l \leq 11$
Reflection collected	107924	20164
Reflection observed	11693	5344
Reflection unique	10875	4560
R_1, wR_2 (2 σ data)	0.0343/0.0768	0.0609/0.1435
R_1, wR_2 (all data)	0.0391/0.0790	0.0700/0.1492
Parameters	1072	389
GOOF an F ²	1.067	1.092
Larg. diff. peak/hole (e Å ⁻³)	-0.257/0.254	-0.299/0.300
CCDC entry	1587982	1587981

Energetic Properties

The calculated energetic parameters of **1–4** are listed in Table 2. The sensitivities were measured with respect to BAM standards. The sensitivities of compounds **1–4** are in the range of HNS. They are less sensitive towards friction (324–360 N) and only less or not sensitive towards impact (10–40 J) and electrical discharge (0.75–1.0 J). In terms of chemical properties the densities of **1–4** (1.81–1.84 g cm⁻³) are in the range of HNS (1.83 g cm⁻³), as well as the oxygen balance (**1–4**: –12 – –21%, HNS: –18 %) and nitrogen + oxygen content (**1–4**: 66%, HNS: 61%). Comparing the calculated energetic properties, compounds **1–4** also are similar to the values of HNS. The detonation velocities were calculated to be 7622–8015 m s⁻¹ for compound **1–4** and 8030 m s⁻¹ for HNS. Also the detonation pressures of compound **1–4** (234–274 kbar) are comparable to HNS (273 kbar).

Table 2. Physicochemical properties and calculated detonation, combustion parameters and sensitivity data of **1–4**.

	1	2	3	4	HNS	RDX
FW ^{a)}	522.26	590.29	521.28	588.33	450.23	222.12
T_{melt}/T_{dec} ^{b)}	250	320	270	340	320	205/210
ρ [g cm ⁻³] ^{c)}	1.814 ^{p)}	1.786 ^{p)}	1.84 ^{q)}	1.83 ^{q)}	1.837	1.806
IS [J] ^{d)}	40	10	20	10	5	7.5
FS [N] ^{e)}	360	360	324	324	360	120
ESD [J] ^{f)}	1.0	0.75	1.0	0.75	1.0	0.20
N [%] ^{g)}	26.82	28.47	29.56	33.33	18.67	37.84
O [%] ^{h)}	39.82	37.94	36.83	32.63	42.64	43.22
N+O [%] ⁱ⁾	66.64	66.41	66.39	65.96	61.31	81.06
Ω_{CO} [%] ^{j)}	–12.3	–13.5	–16.9	–21.8	–17.8	0
$\Delta_f H^\circ$ [kJ mol ⁻¹] ^{k)}	290.4	506.5	205.2	387.4	197.6	86.3
$-\Delta_{ex} U^\circ$	624.9	925.1	393.7	658.6	496.1	619.0

$[\text{kJ kg}^{-1}]$ ^{l)}						
$T_{\text{ex}} [\text{K}]$ ^{m)}	3582	3661	3287	3147	3681	4232
$P_{\text{CJ}} [\text{kbar}]$ ⁿ⁾	274	248	247	234	273	380
$V_{\text{det}} [\text{m s}^{-1}]$ ^{o)}	8015	7719	7748	7622	8030	8983

a) Formula. b) Decomposition temperature. c) Density at room temperature. d) Impact sensitivity. e). Friction sensitivity f) Sensitivity to electrostatic discharge g) Nitrogen content h) Oxygen content. i) Oxygen and nitrogen content j) Oxygen balance Ω assuming the formation of CO during the combustion. Detonation energy. k) Standard formation enthalpy calculated by the atomization method and CBS-4M electronic enthalpies from Gaussian 09 ^[25], ^[26] l) Energy of formation. m) Detonation temperature. n) Detonation pressure. o) Detonation velocity.^[19] p) X-ray. q) gas-pycnometry.

The compatibilities of compound **2** and **4** with different materials were measured by differential thermal analysis. For these measurements compounds **2** and **4** were mixed with equivalent weight percent of Cu, CuO, Al, RDX, TNT, DNAN and HTPB, respectively. The results of these tests are illustrated in Figure 5. By mixing compound **2** and **4** with different metals like Cu, CuO and Al the decomposition point is not influenced at all. Hence, both compounds are compatible with different types of metals. Also a mixture with RDX, TNT and DNAN as well as the binder HTPB does not influence the decomposition point of compound **2** and **4** either. Therefore both compounds also are compatible with different types energetic materials according to literature.^[27]

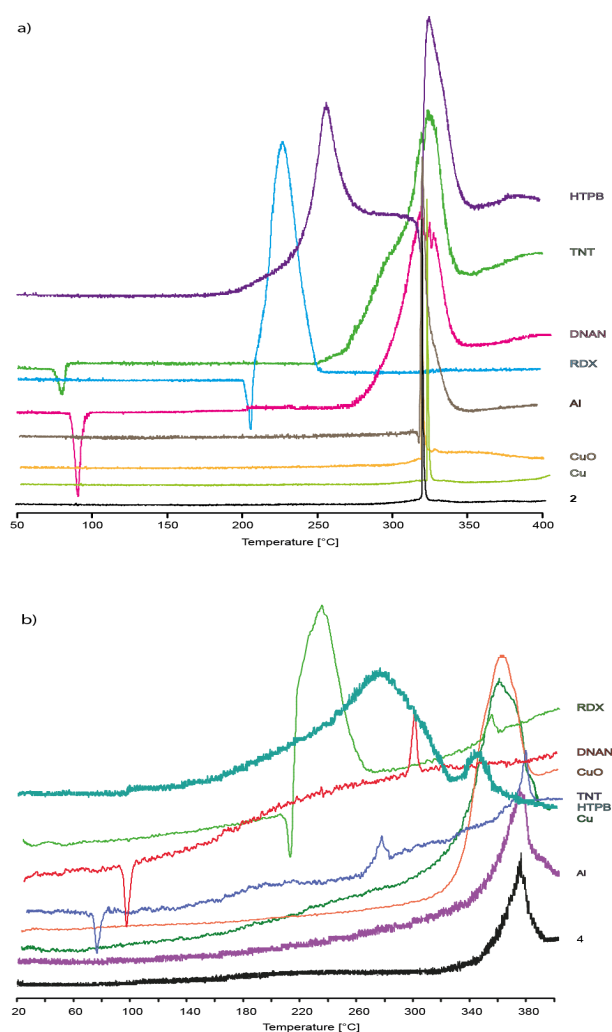


Figure 6: Compatibility test of compound a) 2 and b) 4 with different metals, energetic compounds and binder.

The vacuum stability also was tested on a Delti-Vac device.^[28] Each measurement contained 0.2 g of the sample, which was heated for 40 h at 120 °C. Here, compounds 1–4 are in the same range (1.1–1.2 mL/g). Using a higher amount of tested substance could decrease this value. Compared to this, the VST value of HNS (0.3 mL/g) is better, because a higher amount was tested for 30 min at 260°C.^[29]

Table 3. Vacuum stability test of compounds 1–4.

m=0.3g	1	2	3	4	HNS
mL/g (40h, 120 °C)	1.2	1.2	1.1	1.1	0.3

3. Conclusions

In this work, the physicochemical properties of picryl furazanes and triazoles were tested. The compounds were fully characterized by differential thermal analysis, vibrational spectroscopy, NMR and X-ray. Furthermore, the sensitivities were measured according to BAM standards, the vacuum stability and compatibility, with different metals and energetic compounds of the two most thermal stable compounds, were tested. All compounds are high thermal stable (240–340 °C), also in vacuum for at least 40 h. The compatibility test also shows a positive result, were compound **2** and **4** show good compatibility with the most common explosives and metals. The results of this work show, that simple synthesis and good physicochemical properties of the four compounds makes them a possible replacement for high thermal stable explosives.

4. Experimental Section

General Methods:

The low-temperature single-crystal X-ray diffraction measurements were performed on an Oxford XCalibur3 diffractometer equipped with a Spellman generator (voltage 50 kV, current 40 mA) and a KappaCCD detector operating with Mo α radiation ($\lambda = 0.7107$ Å). Data collection was performed using the CRYSLIS CCD software.^[12] The data reduction was carried out using the CRYSLIS RED software.^[13] The solution of the structure was performed by direct methods (SIR97)^[14] and refined by full-matrix least-squares on F2 (SHELXL)^[15] implemented in the WINGX software package^[16] and finally checked with the PLATON software.^[17] All non-hydrogen atoms were refined anisotropically. The hydrogen atom positions were located in a difference Fourier map. DIAMOND plots are shown with thermal ellipsoids at the 50 % probability level. These data can be obtained free of charge from The Cambridge Crystallographic Data Centre. All chemicals were used as supplied. Raman spectra were recorded in a glass tube with a Bruker MultiRAM FT-Raman spectrometer with Nd:YAG laser excitation up to 1000 mW (at 1064 nm). Infrared spectra were measured with a PerkinElmer Spectrum BX-FTIR spectrometer equipped with a Smiths Dura/SamplIR II ATRdevice. All spectra were recorded at ambient (25 °C) temperature. NMR spectra were recorded with a JEOL/Bruker instrument and chemical shifts were determined with respect to external Me $_4$ Si (^1H , 399.8 MHz; ^{13}C , 100.5 MHz) and MeNO $_2$ (^{14}N , 28.9 MHz). Analyses of C/H/N were performed with an Elemental Vario EL Analyzer. Melting and decomposition points were measured using differential scanning calorimetry (DSC) at a heating rate of 5° C min $^{-1}$ with an OZM Research DTA 552-Ex

instrument and are given as extrapolated onset temperatures. The sensitivity data were explored using a BAM drophammer and a BAM friction tester.^[3] The energetic properties were calculated using the computer code EXPLO6.03. It is based on the chemical equilibrium, a steady state model of detonation. It uses Becker–Kistiakowsky–Wilson’s equation of state (BKW EOS) for gaseous detonation products and Cowan–Fickett’s equation of state for solid carbon. The input is based on the sum formula, calculated heats of formation and the maximum densities according to their crystal structures (Table 1). All calculations were carried out using the Gaussian G09W (revision A.02) program package. The heats of formations were calculated by the atomization method based on CBS-4M electronic enthalpies.^[18] All calculations affecting the detonation parameters were carried out using the program package EXPLO5 6.03.^{[19], [20]}

3,4-Bis(picrylamino)furazan (1)

DTA (5 °C min⁻¹): 250 °C (dec.); **IR** (ATR): $\tilde{\nu}$ = 3361 (w), 3340 (w), 3117 (w), 1697 (m), 1644 (w), 1595 (m), 1500 (s), 1437 (m), 1411 (m), 1332 (s), 1284 (m), 1206 (m), 1188 (w), 1154 (w), 1113 (w), 1081 (w), 909 (w), 854 (m), 761 (m), 736 (m), 690 (m); **Raman** (1064 nm, 500 mW, 25 °C, cm⁻¹): $\tilde{\nu}$ = 3089 (2), 1621 (40), 1550 (14), 1457 (2), 1346 (100), 1303 (13), 1270 (12), 1177 (12), 1113 (3), 1090 (4), 1003 (2), 943 (4), 870 (2), 828 (9), 731 (4), 371 (5), 329 (7), 202 (12), 85 (46); **¹H NMR** (DMSO-D₆): δ = 10.6 (NH), 9.20 (CH₂); **¹³C{¹H} NMR** (DMSO-D₆): δ = 147.6 (C-furazan), 141.6 (C-Pyc), 140.7 (C-Pyc), 135.7 (C-furazan), 128.9 (C-Pyc), 126.3 (C-Pyc); **¹⁴N NMR** (DMSO-D₆): δ = -17 (NO₂); **EA** (C₁₄H₆N₁₀O₁₃, 522.26 g mol⁻¹): Calc.: C 32.20, H 1.16, N: 26.82%; found: C 32.31, H 1.35, N 26.59%. **Sensitivity** (100 μ m \geq g.s. \geq 50 μ m): **IS**: 40 J; **FS**: 360 N; **ESD**: 1.0 J.

4,4'-Bis(Picrylamino)-3,3'-bisfurazanyl (2)

DTA (5 °C min⁻¹): 320 °C (dec.); **IR** (ATR): $\tilde{\nu}$ = 3252 (w), 3083 (w), 1620 (m), 1604 (m), 1574 (m), 1557 (m), 1512 (s), 1441 (m), 1406 (w), 1345 (s), 1322 (s), 1181 (w), 1098 (m), 992 (w), 933 (m), 914 (m), 884 (w), 844 (w), 722 (m), 707 (m); **Raman** (1064 nm, 500 mW, 25 °C, cm⁻¹): $\tilde{\nu}$ = 3247 (2), 3085 (3), 1634 (24), 1622 (46), 1584 (8), 1550 (41), 1539 (25), 1504 (6), 1456 (9), 1436 (7), 1398 (6), 1355 (100), 1346 (62), 1306 (38), 1263 (23), 1183 (18), 1091 (4), 1048 (3), 942 (8), 829 (22), 740 (7), 586 (4), 454 (17), 334 (10), 202 (22), 87 (53); **¹H NMR** (DMSO-D₆): δ = 10.5 (NH), 9.17 (CH₂); **¹³C{¹H} NMR** (DMSO-D₆): δ = 151.7 (C-furazan), 141.8 (C-Pyc), 141.5 (C-Pyc), 138.2 (C-furazan), 134.7 (C-Pyc), 126.5 (C-Pyc); **¹⁴N NMR** (DMSO-D₆): δ = -

19 (NO₂); **EA** (C₁₆H₆N₁₂O₁₄, 590.29 g mol⁻¹): Calc.: C 32.56, H 1.02, N: 28.47%; found: C 32.48, H 1.15, N 28.27%. **Sensitivity** (100 μm ≥ g.s. ≥ 50 μm): **IS**: 10 J; **FS**: 360 N; **ESD**: 0.75 J.

3,5-Bis(picrylamino)-1,2,4-triazole (3)

DTA (5 °C min⁻¹): 270 °C (dec.); **IR** (ATR): $\tilde{\nu}$ = 3468 (w), 3388 (w), 3089 (w), 1673 (w), 1609 (m), 1573 (m), 1529 (s), 1342 (s), 1297 (m), 1174 (w), 1095 (w), 927 (w), 734 (w), 718 (w); **Raman** (1064 nm, 500 mW, 25 °C, cm⁻¹): $\tilde{\nu}$ = 1624 (38), 1590 (12), 1577 (14), 1556 (27), 1541 (39), 1407 (8), 1350 (100), 1299 (29), 1283 (18), 1175 (19), 1083 (6), 946 (10), 829 (16), 383 (6), 337 (9), 207 (13), 116 (35), 92 (39); **¹H NMR** (DMSO-D₆): δ = 11.8 (NH-ring), 10.3 (NH), 8.93 (CH₂); **¹³C{¹H} NMR** (DMSO-D₆): δ = 153.9 (C-triazole), 143.1 (C-triazole), 141.3 (C-Pyc), 140.9 (C-Pyc), 134.2 (C-Pyc), 126.2 (C-Pyc); **¹⁴N NMR** (DMSO-D₆): δ = -17 (NO₂); **EA** (C₁₄H₇N₁₁O₁₂, 521.28 g mol⁻¹): Calc.: C 32.26, H 1.35, N 29.56%; found: C 32.57, H 1.61, N 29.07%. **Sensitivity** (100 μm ≥ g.s. ≥ 50 μm): **IS**: 20 J; **FS**: 324 N; **ESD**: 1.0 J.

5,5'-Bis(picrylamino)-3,3'-bi-1,2,4-triazole (4)

DTA (5 °C min⁻¹): 340 °C (dec.); **IR** (ATR): $\tilde{\nu}$ = 3592 (w), 3287 (w), 3072 (w), 2806 (w), 2693 (w), 1696 (w), 1618 (m), 1597 (m), 1526 (s), 1474 (m), 1427 (m), 1340 (s), 1294 (s), 1176 (m), 1160 (m), 1099 (m), 965 (w), 932 (m), 859 (w), 771 (w), 737 (m), 722 (m); **Raman** (1064 nm, 500 mW, 25 °C, cm⁻¹): $\tilde{\nu}$ = 3073 (6), 1640 (35), 1623 (29), 1564 (26), 1534 (36), 1479 (9), 1455 (6), 1426 (10), 1400 (13), 1345 (100), 1297 (57), 1180 (14), 1170 (19), 1032 (9), 940 (13), 825 (19), 737 (7), 590 (5), 505 (9), 442 (13), 383 (16), 338 (18), 271 (16), 210 (28), 183 (23), 129 (38), 105 (47), 89 (45); **¹H NMR** (DMSO-D₆): δ = 12.5 (NH-ring), 10.5 (NH), 8.92 (CH₂); **¹³C{¹H} NMR** (DMSO-D₆): δ = 154.4 (C-triazole), 143.6 (C-triazole), 141.5 (C-Pyc), 141.1 (C-Pyc), 134.2 (C-Pyc), 126.1 (C-Pyc); **¹⁴N NMR** (DMSO-D₆): δ = -19 (NO₂); **EA** (C₁₆H₈N₁₄O₁₂, 588.33 g mol⁻¹): Calc.: C 32.66, H 1.37, N 33.33%; found: C 32.65, H 1.75, N 32.95%. **Sensitivity** (100 μm ≥ g.s. ≥ 50 μm): **IS**: 10 J; **FS**: 324 N; **ESD**: 1.0 J.

5. References

- [1] a) J. P. Agrawal, Mehilal, U. S. Prasad, R. N. Surve, *New J. Chem.*, **2000**, *24*, 583-585; b) H. S. Jadhav, M. B. Talawar, R. Sivabalan, D. D. Dhavale, S. N. Asthana, V. N. Krishnamurthy, *Indian J. Heterocycl.*

- Chem.*, **2006**, *15*, 383-386; c) A. E. C. M. D. Coburn, US3678061A, **1972**; d) W. P. R. Kuboszek, Warsaw, University of Technology, PL186580B1, **1997**.
- [2] a) K. G. Shipp, *J. Org. Chem.*, **1964**, *29*, 2620-2623; b) F. Gerard, A. Hardy, *Acta Crystallogr., Sect. C: Cryst. Struct. Commun.*, **1988**, *C44*, 1283-1287; c) J.-S. Lee, C.-K. Hsu, C.-L. Chang, *Thermochim. Acta*, **2002**, *392-393*, 173-176; d) R. M. Josef Köhler, *Explosives*, **2008**, Wiley-VCH, Weinheim, 5th edn.
- [3] T. M. Klapötke, *Chemistry of High-Energy Materials, 4th Edition*, Walter de Gruyter GmbH & Ko KG, Berlin, **2017**.
- [4] T. M. Klapötke, T. G. Witkowski, *ChemPlusChem*, **2016**, *81*, 357-360.
- [5] H. Gao, J. M. Shreeve, *Chem. Rev.*, **2011**, *111*, 7377-7436.
- [6] V. Thottempudi, H. Gao, J. M. Shreeve, *J. Am. Chem. Soc.*, **2011**, *133*, 6464-6471.
- [7] T. P. Kofman, G. Y. Kartseva, E. Y. Glazkova, K. N. Krasnov, *Russ. J. Org. Chem.*, **2005**, *41*, 753-757.
- [8] R. Haiges, K. O. Christe, *Inorg. Chem.*, **2013**, *52*, 7249-7260.
- [9] M. A. Kettner, K. Karaghiosoff, T. M. Klapötke, M. Suceśka, S. Wunder, *Chem. Eur. J.*, **2014**, *20*, 7622-7631.
- [10] M. A. Kettner, T. M. Klapötke, *Chem. Commun.*, **2014**, *50*, 2268-2270.
- [11] T. M. Klapötke, N. Mayr, J. Stierstorfer, M. Weyrauther, *Chem. - Eur. J.*, **2014**, *20*, 1410-1417.
- [12] *CrysAlis CCD, Version 1.171.35.11(release 16-05-2011CrysAlis 171.Net)*, Oxford Diffraction Ltd., Abingdon, Oxford (U.K.), **2011**.
- [13] *CrysAlis RED, Version 1.171.35.11(release 16-05-2011CrysAlis 171.Net)*, Oxford Diffraction Ltd., Abingdon, Oxford (U.K.), **2011**.
- [14] A. Altomare, M. C. Burla, M. Camalli, G. L. Cascarano, C. Giacovazzo, A. Guagliardi, A. G. G. Moliterni, G. Polidori, R. Spagna, *J. Appl. Crystallogr.*, **1999**, *32*, 115-119.
- [15] G. M. Sheldrick, *SHELX-97*, **1997**, Programs for Crystal Structure Determination.
- [16] L. J. Farrugia, *J. Appl. Crystallogr.*, **1999**, *32*, 837-838.
- [17] A. L. Spek, *Acta Crystallogr.*, **2009**, *65 D*, 148-155.
- [18] T. Altenburg, T. M. Klapötke, A. Penger, J. Stierstorfer, *Z. Anorg. Allg. Chem.*, **2010**, *636*, 463-471.
- [19] M. Suceśka, *Propellants, Explos., Pyrotech.*, **1991**, *16*, 197-202.
- [20] M. Suceśka, *EXPLO5 V.6.03*, **2014**, Zagreb (Croatia).
- [21] M. D. Coburn, *J. Heterocycl. Chem.*, **1968**, *5*, 83-87.
- [22] M. D. Coburn, T. E. Jackson, *J. Heterocycl. Chem.*, **1968**, *5*, 199-203.
- [23] M. D. Coburn, *J. Labelled Compd. Radiopharm.*, **1985**, *22*, 183-187.
- [24] N. Sugiyama, J.-i. Hayami, *Chem. Lett.*, **1999**, 691-692.

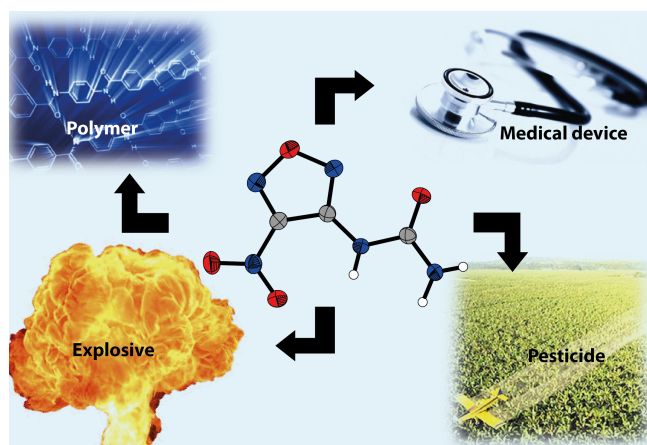
- [25] M. J. Frisch, G. W. Trucks, H. B. Schlegel, G. E. Scuseria, M. A. Robb, J. R. Cheeseman, G. Scalmani, V. Barone, B. Mennucci, G. A. Petersson, H. Nakatsuji, M. Caricato, X. Li, H. P. Hratchian, A. F. Izmaylov, J. Bloino, G. Zheng, J. L. Sonnenberg, M. Hada, M. Ehara, K. Toyota, J. H. R. Fukuda, M. Ishida, T. Nakajima, Y. Honda, O. Kitao, H. Nakai, M. T. Vreven, J. E. Peralta, F. Ogliaro, M. Bearpark, J. J. Heyd, E. Brothers, K. N. Kudin, V. N. Staroverov, R. Kobayashi, J. Normand, K. Raghavachari, A. Rendell, J. C. Burant, S. S. Iyengar, J. Tomasi, M. Cossi, N. Rega, J. M. Millam, M. Klene, J. E. Knox, J. B. Cross, V. Bakken, C. Adamo, J. Jaramillo, R. Gomperts, R. E. Stratmann, O. Yazyev, A. J. Austin, R. Cammi and C. Pomelli, J. W. Ochterski, R. L. Martin, K. Morokuma, V. G. Zakrzewski, G. A. Voth, P. Salvador, J. J. Dannenberg, S. Dapprich, A. D. Daniels, Ö. Farkas, J. B. Foresman, J. C. J. V. Ortiz, D. J. Fox, *Gaussian 09; Rev. C.01 ed., Gaussian, Inc., Wallingford CT (USA),*, **2010**.
- [26] R. D. Dennington II, T. A. Keith, J. M. Millam, *GaussView, Ver.5.08 ed., Semichem, Inc., Wallingford CT (USA),* **2009**.
- [27] NATO, Standardization Agreement (STANAG), *Chemical compatibility of ammunition components with explosives (non-nuclear application)*, **2006**, No. 4147, 2.ed.
- [28] <http://www.deltima.eu/en/>, **2017**.
- [29] R. Weinheimer, *Proc. Int. Pyrotech. Semin.*, **2000**, 27th, 649-661.

Synthesis, Characterization and Properties of Ureido-Furazan Derivatives

Tobias S. Hermann, Thomas M. Klapötke*, Burkhard Krumm and Jörg Stierstorfer

Dedicated to Professor Peter Politzer on the occasion of his 80th birthday

Journal of Heterocyclic Chemistry, **2018**, 55, 852–862.



Synthesis, Characterization and Properties of Ureido-Furazan Derivatives

Tobias S. Hermann, Thomas M. Klapötke*, Burkhard Krumm and Jörg Stierstorfer

Dedicated to Professor Peter Politzer on the occasion of his 80th birthday

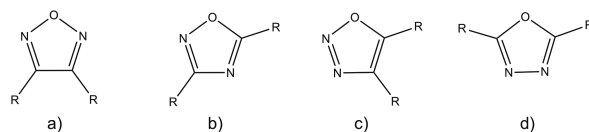
Journal of Heterocyclic Chemistry, **2018**, 55, 852–862.

Abstract:

The reaction of a variety of amino-furazans with chlorosulfonyl isocyanate (CSI) was carried out to synthesize ureido-furazans. The nitration to nitro-ureido-furazan was successful in the cases of 1-nitro-4-nitroureido-furazan and 1,4-dinitroureido-furazan. Furthermore; furazan derivatives linked to a second amino-oxadiazole were synthesized. All compounds were intensively characterized by X-ray diffraction measurements, NMR spectroscopy, vibrational spectroscopy (IR, Raman), BAM sensitivity tests and differential thermal analysis (DTA). The energetic properties were calculated using EXPLO5 6.03.

1. Introduction

Research toward new high-energy dense materials (HEDM) is still required for future applications in industrial, military and civil sectors.^{[1],[2]} Particularly, toxicity and safety problems that need to be solved to meet current regulations e.g. REACH.^[3] These new energetic materials must also be equal or better in performance compared to their traditional predecessors. Many nitrogen and oxygen containing heterocyclic compounds have been shown to have good energetic properties due to high densities and high positive heat of formations.^[4] Particularly, triazoles and oxadiazoles have been intensively investigated thus far.^{[5],[6],[7],[8],[9],[10]} They differ only by the replacement of a nitrogen atom with an oxygen atom. Different regioisomeric oxadiazole derivatives are depicted in Scheme 1. The great interest in these oxadiazoles can also be seen in the amount of patents in the last decade.^[11] The main use of oxadiazoles in the industrial sector is for medical devices, pesticides or polymers.^[12] Oxadiazole derivatives are also used as alternatives for carbonyl containing compounds, such as carbamates, amides, esters and hydroxamic esters.^{[13],[14]}



Scheme 1: Structures of oxadiazole derivatives: (a) 1,2,5-oxadiazole (furan), (b) 1,2,4-oxadiazole, (c) 1,2,3-oxadiazole (d) 1,3,4-oxadiazole

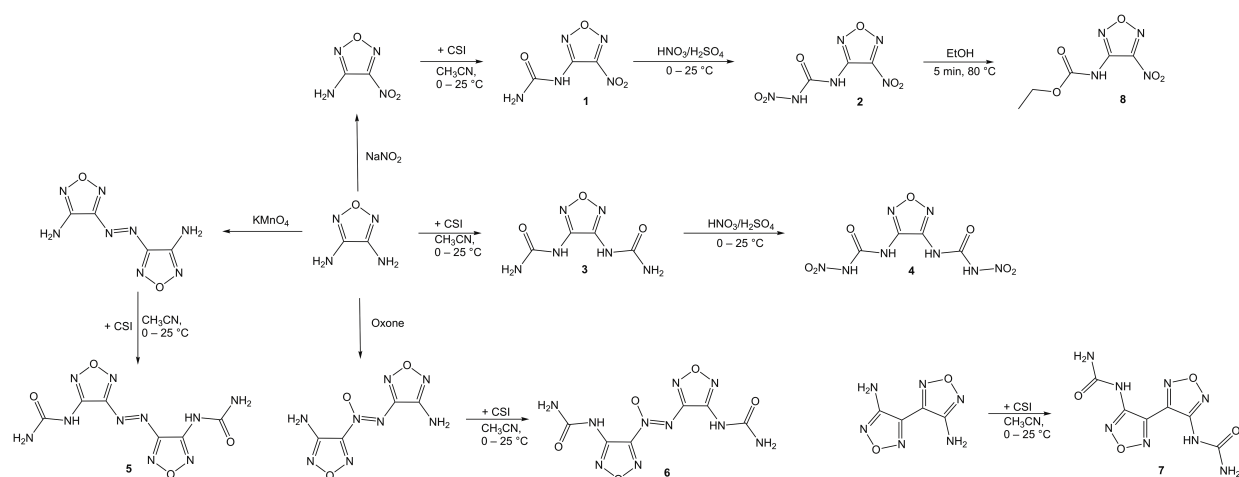
In the past decades, the furazan group has thoroughly been investigated and it was proven that the furazan ring and its energetic properties are perfect building blocks for energetic materials.^{[15],[16],[17],[18]} Amino furazans are not only known for their high heat of formation but also their thermal and chemical stability. Selected furazans such as potassium 4,5-bis(dinitromethyl)furoxanate have been described as green replacements for lead-based primary explosives, which require a high sensitivity toward impact, friction and electrostatic discharge.^[16] In terms of synthesizing oxygen-rich compounds (solid state oxidizers), furazans are useful backbones because of their ring oxygen atom. Oxidizers are compounds with a positive oxygen balance. The oxygen balance is defined as oxygen excess during combustion. This excess is used to oxidize the propellant's fuel. Oxidizers usually burn without residues, since all carbon atoms are converted into carbon mono- or dioxide, hydrogen atoms into water, and nitrogen into dinitrogen.^[19] Through the introduction of nitro groups the oxygen balance can be further tuned to positive values. In order to synthesize energetic compounds with outstanding performance, $N\text{-NO}_2$ groups play an important role. This functional group improves the oxygen and nitrogen balance and also yields to an improvement of the high heat of formation and density.^{[20], [21]} Nitro ureido compounds are known to have good explosive performances and high densities.^[22] In order to combine the benefits of oxadiazoles and nitro ureido, new energetic compounds were synthesized and described herein. According to our literature research, only carbon chains, phenyl and nitrated phenyl nitro ureidos were synthesized so far.^{[23],[24],[25]} Ureidos furazanes have not been synthesized so far. To the best of our knowledge, in this paper the first ureido 1,2,5-oxadiazolyl derivatives are described.

2. Results and Discussion

Synthesis and Characterization

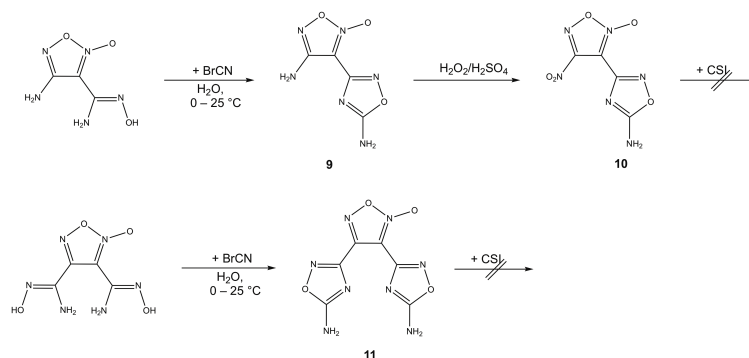
The synthesis of the starting materials, 3,4-diaminofurazan, 3-amino-4-nitrofurazan, 3,3'-diamino-4,4'-azofurazan, 3,3'-diamino-4,4'-azoxyfurazan and C-C coupled 3,3'-dinitro-4,4'-bifurazan, was performed according literature^{[26],[27],[28],[29],[30],[31]}. The starting materials were reacted with chlorosulfonyl isocyanate (CSI) under anhydrous conditions. The reaction of amines with CSI leads to ureido moieties (Scheme 2), which

further could be nitrated to a nitro ureido derivative. The CSI reaction conditions and mechanisms have been investigated in our research group to synthesize carbamates from alcohols.^{[32],[33]}



Scheme 2: Synthesis of ureido (**1**, **3**, **5**, **6** and **7**) and nitro ureido furazans (**2** and **4**).

Similar to literature known reactions using CSI, the yields of ureido derivatives reported in this investigation were about 90 %. In order to synthesize more energetic compounds, attempts were carried out to nitrate the ureido moieties. In this investigation different acids (fuming HNO₃, mixed acid, Ac₂O/HNO₃) and non-acidic conditions such as N₂O₅ were employed. The nitration was successful for 1-nitro-4-nitroureido-furazan (**2**) and 1,4-dinitroureido-furazan (**4**). In the case of 3,3'-diureido-4,4'-azoxyfurazan (**5**), 3,3'-diureido-4,4'-azofurazan (**6**) and 3,3'-diureido-4,4'-bifurazan (**7**), the nitration in acidic and non-acidic conditions led to the amines, with the loss of the CO-NH₂ moiety. The corresponding nitramine compounds have already been characterized by our research group.^[15] Upon heating of **2** in ethanol for the purpose of recrystallization, a replacement of the nitramino moiety to 1-nitro-4-ethoxycarbonyl furazan (**8**) occurred.



Scheme 3: Synthesis of amino-1,3,4-oxadiazol furazan derivatives.

Furthermore, two different attempts to synthesize more complex ureido derivatives with two different oxadiazols were investigated (Scheme 3). The reaction of 4-amino-3-amino(hydroxyimino)methyl-furoxan^[34] with cyanogen bromide in aqueous conditions led to 4-amino-3-(3-amino-1,2,4-oxadiazol) furoxan (**9**). In order to increase the energetic properties, further oxidation in peroxymonosulfuric acid (Caro's acid) yielded 4-nitro-3-(3-amino-1,2,4-oxadiazol) furoxan (**10**). Similar to the synthesis of **9**, 3,4-bis-amino(hydroxyimino)methyl furoxane^[35] was reacted with cyanogen bromide to 3,4-bis-(3-amino-1,2,4-oxadiazol) furoxan (**11**). Further reactions of **9**, **10** and **11** with CSI were unsuccessful. This result leads to the assumption that the reactivity of the amino group of the 1,3,4-oxadiazoles is not high enough for the reaction with CSI. Another important reason for their low reactivity is the very low solubility of the 1,3,4-oxadiazole derivatives in common organic solvents.

Spectroscopy

The vibrational analysis of **2** and **4** showed the characteristic antisymmetric $\nu_{as}(\text{NO}_2)$ and the symmetric $\nu_s(\text{NO}_2)$ stretching vibrations in the range of 1620–1506 cm^{-1} and 1385–1251 cm^{-1} , respectively. The C–N, C–O and C–C vibrations of **1–11** are observed in the typical ranges for heterocycles and CHNO based aliphatic compounds.

Comparing the ^1H NMR spectra, a trend for the ureido can be observed. All NH_2 resonances of the ureido moieties are found in the range between 7 and 5 ppm as broadened signals, because of the keto–enol tautomerism and restricted rotation.^{[36], [37]} Due to the higher acidity of the NHNO_2 hydrogen atom, the resonances of the nitro ureidos are shifted downfield below 10 ppm. This is shown in Figure 1, where the ^1H resonances of **1** and **2** are displayed. The carbonyl resonance, in the range of 140–150 ppm of the ureido and nitro ureido moiety, is the most significant resonance in the ^{13}C NMR spectra. The nitro groups of the

nitro ureidos (**2** and **4**) are observed at around -40 ppm and additionally the nitro moiety of **2** at -33 ppm in the ^{14}N NMR spectrum.

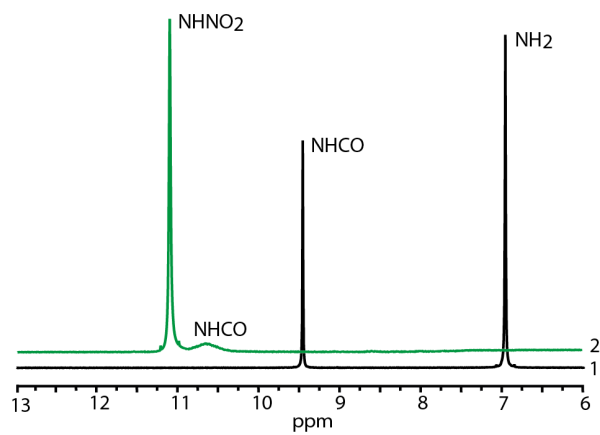


Figure 1: ^1H NMR spectra of 1-nitro-4-ureido-furazan (**1**) and 1-nitro-4-nitroureido-furazan (**2**) in $\text{DMSO}-\text{D}_6$.

Crystal Structures

The structures of **1**, **4**, **8** and **10** in the solid state were determined by low temperature X-ray diffraction.

The highest density at 173 K was measured for compound **4** in the triclinic space group $P\bar{1}$ (1.91 cm^{-3} , Figure 3) compared to **10** in the monoclinic space group $P2_1/c$ (1.87 cm^{-3} Figure 5), and the orthorhombic space groups, **1** $P2_12_12_1$ (1.72 cm^{-3} Figure 2) and **8** $Pbca$ (1.61 cm^{-3} , Figure 4).

The bond lengths and angles are in the range of literature reported N,O-heterocyclic compounds.^{[15], [38]} Selected bond lengths and angles are given in Figures 2–5. Details on the measurements and refinements are listed in Table 1.

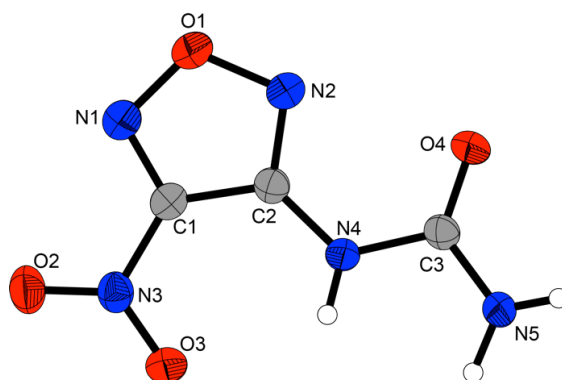


Figure 2: Molecular structure of 1-nitro-4-ureido-furazan (**1**). Selected bond lengths (Å) and angles (deg.): C3–N1 1.45(2), C2–N4 1.363(2), C3–N3 1.328(2), C2–C1–N3 129.04(14), C1–C2–N4 126.93(14), N4–C3–N5 113.80(14), N1–C1–C2–N4 179.67(14), N2–C2–C1–N3 0.49(18).

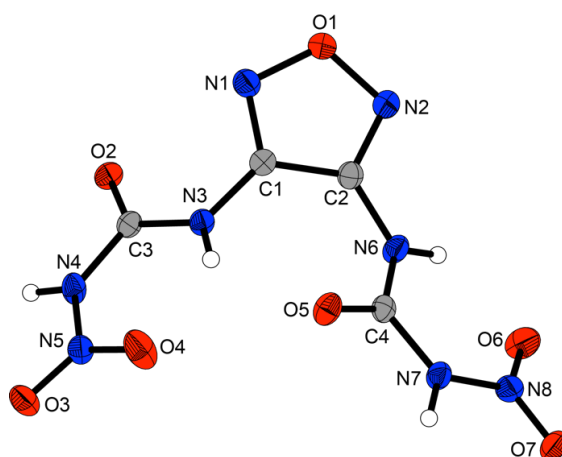


Figure 3: Molecular structure of 1,4-dinitroureido-furazan (**4**). Selected bond lengths (Å) and angles (deg.): C1–N3 1.388(2), C2–N6 1.391(2), C3–N4 1.395(2), C4–N7 1.390(2), N4–N5 1.369(2), N7–N8 1.370(2), C2–C1–N3 127.47(17), C1–C2–N6 129.81(17), N2–C2–C1–N3 177.44(17), N1–C1–C2–N6 176.56(18), N6–C4–N7–N8 4.4(3), N3–C3–N4–N5 3.1(3).

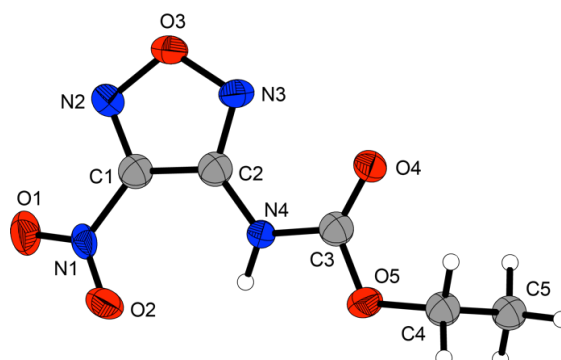


Figure 4: Molecular structure of 1-nitro-4-ethoxycarbonyl furazan (**8**). Selected bond lengths (Å) and angles (deg.): C1–N2 1.460(4), C2–N4 1.362(4), O5–C4 1.454(4), C2–C1–N1 107.6(3), C1–C2–N4 126.1(3), C3–O5–C4 117.1(3), N1–C2–C1–N3 176.9(3), N2–C1–C2–N4 178.7(3), O4–C3–O5–C4 2.8(5).

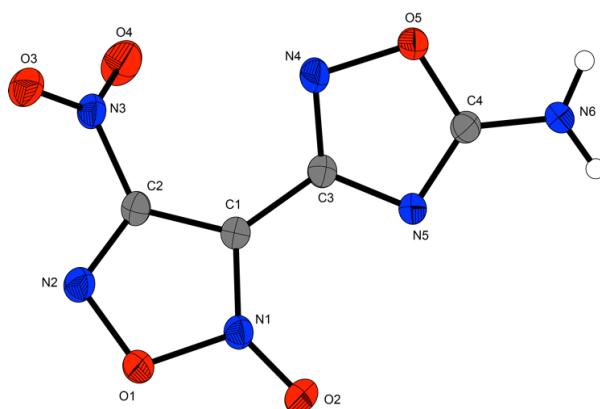


Figure 5: Molecular structure of 4-nitro-3-(3-amino-1,2,4-oxadiazolyl) furoxan (**10**). Selected bond lengths (Å) and angles (deg.): C2–N3 1.451(2), N1–O2 1.217(2), N4–O5 1.430(2), C4–N6 1.312(2); N2–C2–N3 117.8(1), C2–C1–C3 132.0(1), O5–C4–N6 118.1(1); O1–N2–C2–N3 173.9(1), C2–C1–C3–N5 170.9(2).

Table 1. X-ray parameters of **1**, **4**, **8** and **10**.

	1	4	8	10
Empirical formula	C ₃ H ₃ N ₅ O ₄	C ₄ H ₄ N ₈ O ₇	C ₅ H ₆ N ₄ O ₅	C ₄ H ₂ N ₆ O ₅
Formula mass (g mol ^{−1})	173.09	276.13	202.13	214.12
Temperature (K)	173(2)	173(2)	173(2)	173(2)
Crystal size (mm ³)	0.40x0.18x0.18	0.49x0.28x0.20	0.40x0.30x0.01	0.40x0.35x0.30
Crystal description	Colorless	Colorless	Colorless	Colorless

	block	block	block	block
Crystal system	Orthorhombic	Triclinic	Orthorhombic	Monoclinic
Space group	$P2_12_12_1$	P-1	Pbca	$P2_1/c$
a (Å)	5.4926(5)	7.8096(7)	10.9296(15)	6.0943(4)
b (Å)	8.6852(7)	8.0528(6)	8.1385(10)	8.2913(6)
c (Å)	14.0098(13)	8.1807(8)	18.7783(18)	15.1764(12)
α (°)	90	110.746(8)	90	90
β (°)	90	92.503 (8)	90	97.097(7)
γ (°)	90	93.290(7)	90	90
V (Å ³)	668.33 (10)	479.20(8)	1670.3(3)	760.98(10)
Z	4	2	8	4
ρ_{calc} (g cm ⁻³)	1.72	1.91	1.71	1.87
μ (mm ⁻¹)	0.158	0.181	0.145	0.172
$F(000)$	352	280	832	432
θ range (°)	4.39–27.86	4.437–25.996	4.72–21.32	4.255–26.495
Index range	$-7 \leq h \leq 7$	$-9 \leq h \leq 9$	$-13 \leq h \leq 13$	$-6 \leq h \leq 7$
	$-8 \leq k \leq 11$	$-9 \leq k \leq 9$	$-10 \leq k \leq 10$	$-10 \leq k \leq 8$
	$-18 \leq l \leq 17$	$-9 \leq l \leq 10$	$-23 \leq l \leq 12$	$-19 \leq l \leq 18$
Reflection collected	5706	3434	11251	6020
Reflection observed	1597	1871	1697	1569
Reflection unique	1415	1536	850	1241
R_1, wR_2 (2 σ data)	0.0328/0.0811	0.0385/0.0890	0.0655/0.0903	0.0322/0.0757
R_1, wR_2 (all data)	0.0392/0.0859	0.0495/0.0968	0.1547/0.1132	0.0456/0.0842
Parameters	121	172	133	144
GOOF an F ²	1.058	1.055	0.998	1.057

Larg. diff. peak/hole ($e \text{ \AA}^{-3}$)	-0.181/0.150	-0.252/0.251	-0.241/0.255	-0.204/0.244
CCDC entry	1533343	1533341	1533342	1566030

Energetic Properties

The calculated physicochemical and energetic properties of **1–4** are listed in Tables 2 and 3. In terms of energetic properties, the most interesting compounds are **2** and **4**, due to their functional nitro ureido groups and positive oxygen balance. The sensitivities were measured with respect to BAM standards. The sensitivities of compounds **5–11** were determined but not listed in Table 3, because of their expected complete insensitivity. Compounds **1–4** are not sensitive toward friction (360 N). Furthermore, compound **1** and **3** show no sensitivity toward impact or electrical discharge. Compared to this, **2** and **4** show higher sensitivities toward impact (4 and 7 J) and moderate sensitivity toward electrical discharge (0.75 and 1.5 J), respectively. The positive oxygen balances of **2** (+14.7) and **4** (+5.8) causes a residue-free burning. Additionally, the positive oxygen balance has a direct influence on the specific impulse. The specific impulse of **2** was calculated to be 260 s for the water-free compound. In mixtures with aluminum and binder the optimized specific impulse is 244 s. In comparison, **4** has a specific impulse of 239 s for the neat compound and 230 s for the optimized formulation. These values are slightly lower than that (264 s) for the widely used oxidizer ammonium perchlorate in mixtures.

The nitration of the ureido functional group leads to an improvement of about 70 kJ mol^{-1} (63 kJ mol^{-1} **1**, 136 kJ mol^{-1} **2**) according to the calculated enthalpies. The same trend is observed for compound **4**, where the increase in enthalpy is twice ($2 \times 70 \text{ kJ mol}^{-1}$) (-162 kJ mol^{-1} **3**, -22 kJ mol^{-1} **4**).

Compounds **2** and **4** also show interesting calculated detonation values. The values of **2** and **4** are comparable to RDX. Comparing the energetic properties of **2** and **4** with RDX and PETN the heat of detonation (-5692 (**2**), -4626 (**4**) and -5743 (**RDX**), -5995 kJ kg^{-1} (**PETN**)), detonation pressure (348 (**2**), 322 (**4**) and 380 (**RDX**), 316 kbar (**PETN**)), detonation velocity (8930, 8685 and 8983 (**RDX**), 8525 m s^{-1} (**PETN**)) and detonation temperature (4189 (**2**), 3405 (**4**) and 4232 (**RDX**), 3959 K (**PETN**)) are in a similar range or slightly better. Responsible for the good detonation values is the nitro ureido moiety and the energetic furazan backbone. This also is supported by the high nitrogen and oxygen content, such as for RDX. This is also displayed by comparing the detonation values of **1** and **3**, which are significantly lower.

The mentioned properties of **1–4**, make them not only green explosives, in a sense of being free of heavy metals, but also useful precursors for potential energetic polymers, for example if they would be reacted with dihalide compounds such as phosgene.

Table 2. Physicochemical properties of compounds 1–6.

	1	2	3	4	5	6
Formula	C ₃ H ₃ N ₅ O ₄	C ₃ H ₂ N ₆ O ₆	C ₄ H ₆ N ₆ O ₃	C ₄ H ₄ N ₈ O ₇	C ₆ H ₆ N ₁₀ O ₄	C ₆ H ₆ N ₁₀ O ₅
FW [g mol ⁻¹]	173.09	218.09	186.13	276.13	282.13	298.18
<i>T</i> _{dec} ^{a)}	182	122	239	140	250	260
<i>N</i> [%] ^{b)}	40.5	38.5	45.2	40.6	49.6	46.9
<i>O</i> [%] ^{c)}	36.9	44.0	25.8	40.6	22.7	26.8
<i>N</i> + <i>O</i> [%] ^{d)}	77.4	82.5	71.0	81.2	72.3	73.7
<i>Ω</i> _{CO} [%] ^{e)}	-4.6	+14.7	-25.8	+5.8	-28.3	-21.5
<i>IS</i> [J] ^{f)}	40	4	40	7	*	*
<i>FS</i> [N] ^{g)}	360	360	360	360	*	*
<i>ESD</i> [J] ^{h)}	1.5	0.75	1.5	1.5	*	*

a) Decomposition temperature from DSC measurements carried out at a heating rate of 5 °C min⁻¹. b) Nitrogen content. c) Oxygen content. d) Combined oxygen and nitrogen content. e) Oxygen balance *Ω* assuming the formation of CO at the combustion. f) Impact sensitivity. g) Friction sensitivity. h) Sensitivity toward electrostatic discharge. * Insensitive.

Table 2. Physicochemical properties of compounds 7–11.

	7	8	9	10	11
Formula	C ₆ H ₆ N ₈ O ₄	C ₅ H ₆ N ₄ O ₅	C ₄ H ₄ N ₆ O ₃	C ₄ H ₂ N ₆ O ₅	C ₄ H ₄ N ₈ O ₄
FW [g mol ⁻¹]	254.17	202.13	184.12	214.10	252.15
<i>T</i> _{dec} ^{a)}	240	153	188	198	273
<i>N</i> [%] ^{b)}	44.1	27.7	45.7	39.3	44.4
<i>O</i> [%] ^{c)}	25.2	39.6	26.1	37.4	25.4
<i>N</i> + <i>O</i> [%] ^{d)}	69.3	67.3	71.8	76.7	69.8
<i>Ω</i> _{CO} [%] ^{e)}	-31.5	-23.7	-26.0	0	-12.7
<i>IS</i> [J] ^{f)}	*	*	*	*	*
<i>FS</i> [N] ^{g)}	*	*	*	*	*

$ESD [J]^{h)}$ * * * * *

a) Decomposition temperature from DSC measurements carried out at a heating rate of 5 °C min⁻¹. b) Nitrogen content. c) Oxygen content. d) Combined oxygen and nitrogen content. e) Oxygen balance Ω assuming the formation of CO at the combustion. f) Impact sensitivity. g) Friction sensitivity. h) Sensitivity toward electrostatic discharge. * Insensitive.

Table 3. Calculated detonation, combustion parameters and sensitivity data of **1–4**.

	1	2	3	4	RDX	PETN
density (RT) ^{a)}	1.68	1.85 ⁿ⁾	1.95 ⁿ⁾	1.87	1.80 ^{[38], [39]}	1.75
$\Delta_f H^0$ [kJ mol ⁻¹] ^{b)}	63	136	-162	-22	86	480
$\Delta_f U^0$ [kJ kg ⁻¹] ^{c)}	41	420	-1196	-227	489	1423
$\Delta_{ex} U^0$ [kJ kg ⁻¹] ^{d)}	-4323	-5692	-2037	-4626	-5743	-5995
P_{CJ} [kbar] ^{e)}	236	348	245	322	380	316
V_{Det} [m s ⁻¹] ^{f)}	7759	8930	8283	8685	8983	8525
T_{ex} [K] ^{g)}	3317	4189	1767	3405	4232	3959
I_s [s] ^{h)}	225	260	161	239	258	257
I_s [s] (15 % Al, binder) ⁱ⁾	225	241	201	229	249	257
I_s [s] (Al, binder) ^{j)}	225	244	203	230	249	251

a) Densities at room temperature. b) Enthalpy calculated by the atomization method and CBS-4M electronic enthalpies from Gaussian 09 ^[40]. ^[41]. c) Energy of formation. d) Heat of detonation. e) Detonation pressure. f) Detonation velocity.^[42] g) Detonation temperature. h) Specific impulse (EXPRO5 6.03: 70 bar chamber pressure, 10 bar expansion conditions equilibrium expansion). i) Specific impulse (15 % Al, 6 % polybutadiene acrylic acid, 6 % polybutadiene acrylonitrile and 2 % bisphenyl A ether, EXPRO5 6.03: 70 bar chamber pressure, 1 bar expansion conditions equilibrium expansion). j) Optimized specific impulse (Al [%]: **1**: 15, **2**: 11, **3**: 17, **4**: 13; 6 % polybutadiene acrylic acid, 6 % polybutadiene acrylonitrile and 2 % bisphenyl A ether) n) Density measured by pycnometry.

3. Conclusion

In this article various heterocyclic ureido derivatives were synthesized in order to meet current requirements for safer and more powerful energetic materials. The synthetic routes to the heterocyclic compounds **1–11** are relatively easy. IR and NMR spectroscopy are valuable methods for identification. Two ureido moieties were converted successfully (**2** and **4**) to the corresponding nitro ureido derivatives. Comparison of the

enthalpy calculations showed, that nitration of an ureido functional group leads to an improvement of the enthalpy ($\sim 70 \text{ kJ mol}^{-1}$ per ureido group) but also leads to a decrease in thermal stability. Except for **2** and **4**, all compounds are low sensitive toward impact and friction and have moderate thermal stabilities. As expected, the ureidos show higher thermal stabilities than the corresponding nitro ureido derivatives. Compound **2** is very sensitive toward impact. The physicochemical and explosive properties of **1–4** make them potential energetic materials and furthermore potential precursors for energetic polymers.

4. Experimental Section

General methods

The low-temperature single-crystal X-ray diffraction measurements were performed on an Oxford XCalibur3 diffractometer equipped with a Spellman generator (voltage 50 kV, current 40 mA) and a KappaCCD detector operating with $\text{Mo}_{K\alpha}$ radiation ($\lambda = 0.7107 \text{ \AA}$). Data collection was performed using the CRYSLIS CCD software.^[43] The data reduction was carried out using the CRYSLIS RED software.^[44] The solution of the structure was performed by direct methods (SIR97)^[45] and refined by full-matrix least-squares on F2 (SHELXL)^[46] implemented in the WINGX software package^[47] and finally checked with the PLATON software.^[48] All non-hydrogen atoms were refined anisotropically. The hydrogen atom positions were located in a difference Fourier map. DIAMOND plots are shown with thermal ellipsoids at the 50 % probability level. These data can be obtained free of charge from The Cambridge Crystallographic Data Centre. All chemicals were used as supplied. Raman spectra were recorded in a glass tube with a Bruker MultiRAM FT-Raman spectrometer with Nd:YAG laser excitation up to 1000 mW (at 1064 nm). Infrared spectra were measured with a PerkinElmer Spectrum BX-FTIR spectrometer equipped with a Smiths Dura/SamplIR II ATRdevice. All spectra were recorded at ambient (25 °C) temperature. NMR spectra were recorded with a JEOL/Bruker instrument and chemical shifts were determined with respect to external Me_4Si (^1H , 399.8 MHz; ^{13}C , 100.5 MHz) and MeNO_2 (^{14}N , 28.9 MHz). Analyses of C/H/N were performed with an Elemental Vario EL Analyzer. Melting and decomposition points were measured using differential scanning calorimetry (DSC) at a heating rate of $5^\circ \text{ C min}^{-1}$ with an OZM Research DTA 552-Ex instrument. The sensitivity data were explored using a BAM drop hammer and a BAM friction tester.^[49] The energetic properties were calculated using the computer code EXPLO6.03. It is based on the chemical equilibrium, a steady state model of detonation. It uses Becker–Kistiakowsky–Wilson’s equation of state (BKW EOS) for gaseous detonation products and Cowan–Fickett’s equation of state for solid carbon. The input is based on the sum formula, calculated heats of formation and the maximum densities according to their crystal structures (Table 1). All calculations were carried out using the Gaussian G09W (revision A.02) program package. The heats of formations were calculated by the atomization method based on CBS-4M

electronic enthalpies.^[50] All calculations affecting the detonation parameters were carried out using the program package EXPLO5 6.03.^{[42], [51]}

General synthesis of ureido derivatives (**1**, **3**, **5**, **6**, **7**)

0.50 g of the corresponding amino furazan was poured to 20 mL dry acetonitrile in a round bottom flask and placed in an ice bath. Chlorosulfonyl isocyanate (CSI) (1.10 molar equivalent for **1**, 2.10 molar equivalent for **3**, **5**, **6** and **7**) was added slowly at 0 °C. The mixture was stirred at ambient temperature for 30 min and then cooled again to 0 °C. 15 mL of water was added very slowly at this temperature. After warming the mixture to room temperature it was stirred for 1 h, while a precipitate was generated. The organic solvent was removed under vacuum. The precipitate formed was filtered off and washed with ice water.

1-Nitro-4-ureido-furazan (**1**)

After drying in vacuum 0.58 g (88 %) 1-nitro-4-ureido-furazan was obtained as a pale green powder. DSC (5 °C min⁻¹): 179° C (m.p.), 182° C (dec.); IR (ATR, cm⁻¹): $\tilde{\nu}$ = 3319 (w), 3124 (w), 1593 (s), 1558 (m), 1484 (w), 1439 (m), 1291 (s), 1262 (s), 1134 (m), 1092 (s), 1040 (s), 975 (m), 846 (m), 816 (m), 783 (m), 754 (m), 720 (m); Raman (1064 nm, 500 mW, 25 °C, cm⁻¹): $\tilde{\nu}$ = 3302 (2), 1693 (6), 1614 (3), 1583 (4), 1554 (7), 1469 (49), 1411 (6), 1365 (29), 1321 (7), 1122 (3), 1052 (2), 976 (6), 836 (20), 793 (3), 765 (3), 656 (5), 465 (2), 402 (5), 332 (6), 218 (6), 146 (16), 85 (100); ¹H NMR (CDCl₃) δ = 9.46 (NH), 6.9 (br, NH₂); ¹³C{¹H} NMR (CDCl₃) δ = 154.8 (CNO₂), 153.1 (CNH), 146.6 (CO); EA (C₃H₃N₃O₄, 173.09 g mol⁻¹) Calc.: C 20.82; H 1.75; N 40.46 %; Found: C 20.97; H 1.84; N 40.36 %; Sensitivity (100 μ m \geq g.s. \geq 50 μ m) IS: 40 J; FS: 360 N; ESD: 1.5 J.

1-Nitro-4-nitroureido-furazan (**2**)

A mixture of fuming nitric and sulfuric acid (each 2 mL) was cooled to 0 °C. **1** (0.25 g; 1.44 mmol) was added slowly to this mixture. The reaction was stirred at 0 °C for 30 min, then allowed to warm up to room temperature and stirred additionally for one hour. Afterwards the mixture was poured on 30 g of ice and extracted three times with 50 mL ethyl acetate. The organic phases were washed twice with water and one time with brine. Subsequently the organic phases were dried with magnesium sulfate and the solvent removed on the rotary evaporator to obtain a pale yellow powder. After recrystallization from acetonitrile, 0.28 g (90 %) of colorless pure **2** was obtained.

DSC (5 °C min⁻¹): 122 °C (dec.); IR (ATR, cm⁻¹): $\tilde{\nu}$ = 3469 (w), 3446 (m), 3336 (m), 1710 (w), 1633 (s), 1520 (s), 1498 (m), 1435 (m), 1368 (s), 1347 (m), 1209 (m), 1107 (w), 1040 (m), 870 (w), 763 (w), 726 (w); Raman (1064 nm, 500 mW, 25 °C, cm⁻¹): $\tilde{\nu}$ = 2247 (3), 1748 (16), 1722 (10), 1629 (9), 1611 (10), 1567 (10), 1532 (16), 1467 (73), 1415 (13), 1366 (76), 1051 (6), 973 (25), 894 (6), 843 (20), 765 (8), 597 (3), 567 (4), 458 (4), 372 (9), 328 (12), 239 (14), 96 (102); ¹H NMR (CDCl₃) δ = 11.08 (NHNO₂), 10.67 (br, NHCO) ; ¹³C{¹H} NMR (CDCl₃) δ = 154.2 (CNO₂), 145.0 (CNH), 144.8 (CO); ¹⁴N NMR (CDCl₃) δ = -33 (CNO₂), -42 (NHNO₂); EA (218.09 g mol⁻¹) Calc.: C 16.52, H 0.92, N 38.54 %; Found: C 16.73, H 1.04, N 38.31 %; Sensitivity (100 μ m \geq g.s. \geq 50 μ m) IS: 4 J; FS: 360 N; ESD: 0.75 J.

1,4-Diureido-furazan (3)

Drying in vacuum yielded 0.87 g (94 %) of **3** as a powder.

DSC (5 °C min⁻¹): 239 °C (dec.); IR (ATR, cm⁻¹): $\tilde{\nu}$ = 3418 (m), 3334 (m), 3129 (m), 1716 (s), 1694 (s), 1632 (w), 1576 (m), 1553 (s), 1477 (m), 1397 (m), 1360 (m), 1251 (m), 1131 (m), 1056 (m), 992 (w), 923 (w), 887 (w), 856 (m), 778 (m), 717 (m), 660 (w); Raman (1064 nm, 500 mW, 25 °C, cm⁻¹): $\tilde{\nu}$ = 3231 (4), 1699 (3), 1570 (3), 1342 (16), 1305 (4), 1279 (3), 1136 (4), 1057 (5), 1016 (100), 889 (4), 857 (3), 681 (9), 556 (7), 537 (13), 362 (16), 179 (10), 123 (17). ¹H NMR (DMSO-D₆) δ = 9.38 (NH), 6.8 (br, NH₂); ¹³C{¹H} NMR (DMSO-D₆) δ = 154.8 (CNH), 146.6 (CO); EA (C₄H₆N₆O₃, 186.13 g mol⁻¹) Calc.: C 25.81, H 3.25, N, 45.15 %; Found: C 25.72, H 3.32, N 44.74 %; Sensitivity (100 μ m \geq g.s. \geq 50 μ m) IS: 40 J; FS: 360 N; ESD: 1.5 J.

1,4-Dinitroureido-furazan (4)

Into a mixture of 2 mL of fuming nitric acid and 2 mL of sulfuric acid, **3** (0.25 g; 1.30 mmol) was added slowly at 0 °C. The mixture was stirred at this temperature for 30 min and an additional hour at room temperature. Then the reaction was poured on 20 g of ice and extracted three times with 30 mL of ethyl acetate. The combined organic layers were washed twice with water and once with brine. After drying the organic phases with magnesium sulfate the solvent was removed in vacuum to yield a colorless powder. After recrystallization from acetonitrile, 0.32 g (90 %) of colorless pure **4** was obtained.

DSC (5 °C min⁻¹): 140 °C (dec.); IR (ATR, cm⁻¹): $\tilde{\nu}$ = 3308(w), 2358 (w), 1746 (s), 1601 (s), 1432 (s), 1377 (m), 1311 (m), 1280 (m), 1234 (s), 1156 (m), 1085 (m), 982 (m), 932 (w), 871 (w), 839 (w), 771 (m), 744 (m), 704 (m); Raman (1064 nm, 500 mW, 25 °C, cm⁻¹): $\tilde{\nu}$ = 1739 (41), 1702 (37), 1618 (36), 1565 (84), 1523 (28), 1410 (50), 1339 (90), 1065 (6), 1036 (12), 986 (100), 938 (11), 884 (54), 850 (18), 771 (20), 724 (9), 600 (12),

502 (23), 470 (22), 456 (18), 418 (17), 381 (9), 308 (22), 229 (18), 204 (23); ^1H NMR (CDCl_3) δ = 10.93 (2H, CNH), 13.5 (br, NHNO_2); $^{13}\text{C}\{^1\text{H}\}$ NMR (CDCl_3) δ = 147.2 (CNH); 146.4 (CO), ^{14}N NMR (CDCl_3) δ = -42 (NHNO_2); EA ($\text{C}_4\text{H}_4\text{N}_8\text{O}_7$, 276.13 g mol $^{-1}$) Calc.: C 17.40, H 1.46, N 40.58 %, Found: C 17.98, H 1.81, N 40.48 %; Sensitivity (100 μm \geq g.s. \geq 50 μm) IS: 7 J; FS: 360 N; ESD: 0.7 J.

3,3'-Diureido-4,4'-azoxyfurazan (5)

Compound **5** (0.63 g) was obtained as yellow powder (88 %).

DSC (5 $^\circ\text{C}$ min $^{-1}$): 250 $^\circ\text{C}$ (dec.); IR (ATR): $\tilde{\nu}$ = 3367 (w), 3314 (w), 3208 (w), 2357 (w), 1737 (w), 1700 (s), 1637 (m), 1594 (w), 1533 (s), 1477 (w), 1695 (s), 1347 (m), 1260 (m), 1133 (w), 1051 (m), 993 (w), 942 (w), 886 (w), 819 (m), 776 (w), 749 (w), 701 (w), 660 (w); Raman (1064 nm, 500 mW, 25 $^\circ\text{C}$, cm $^{-1}$): $\tilde{\nu}$ = 2859 (16), 2083 (4), 2028 (3), 1485 (5), 1450 (100), 1427 (13), 1355 (18), 1296 (5), 1259 (7), 999 (4), 948 (3), 929 (7), 806 (4), 538 (3), 466 (2); ^1H NMR ($\text{DMSO}-d_6$) δ = 9.43 (s, NH), 6.9 (br, NH_2); $^{13}\text{C}\{^1\text{H}\}$ NMR ($\text{DMSO}-d_6$) δ = 156.8 (CNN), 153.0 (CNH), 146.4 (CO); EA ($\text{C}_6\text{H}_6\text{N}_{10}\text{O}_4$, 282.06 g mol $^{-1}$): Calc.: C 24.75, H 2.42, N: 48.10 %; found: C 24.94, H 2.25, N 47.37 %.

3,3'-Diureido-4,4'-azofurazan (6)

Compound **6** (0.37 g) was obtained as orange powder (89 %).

DSC (5 $^\circ\text{C}$ min $^{-1}$): 260 $^\circ\text{C}$ (dec.); IR (ATR): $\tilde{\nu}$ = 3432 (m), 3291 (m), 3220 (w), 1717 (m), 1690 (vs), 1614 (m), 1538 (s), 1468 (m), 1392 (s), 1342 (m), 1302 (w), 1251 (w), 1169 (w), 1112 (w), 1049 (w), 975 (w), 820 (m), 771 (w), 712 (m); Raman (1064 nm, 500 mW, 25 $^\circ\text{C}$, cm $^{-1}$): $\tilde{\nu}$ = 2859 (26), 2084 (6), 2028 (3), 1692 (5), 1616 (5), 1497 (100), 1448 (75), 1397 (28), 1354 (42), 1308 (9), 1108 (6), 1053 (6), 980 (7), 949 (5), 912 (9), 875 (13), 808 (7), 642 (4), 538 (4), 432 (4), 404 (4); ^1H NMR ($\text{DMSO}-d_6$) δ = 9.80 (s, NH), 9.60 (s, NH), 6.9 (br, NH_2), 6.8 (br, NH_2); $^{13}\text{C}\{^1\text{H}\}$ NMR ($\text{DMSO}-d_6$) δ = 154.2 (N(NO)C), 153.2 (ONNC), 152.9 (CNH), 149.2 (CNH), 148.4 (CO), 146.6 (CO); EA ($\text{C}_6\text{H}_6\text{N}_{10}\text{O}_5$, 298.05 g mol $^{-1}$): Calc.: C 22.79, H 2.55, N 44.30 %; found: C 23.10, H 2.45, N 43.75 %.

3,3'-Diureido-4,4'-bifurazan (7)

Compound **7** (1.39 g) was obtained as colorless powder (91 %).

DSC (5 $^\circ\text{C}$ min $^{-1}$): 240 $^\circ\text{C}$ (dec.); IR (ATR): $\tilde{\nu}$ = 3502 (w), 3283 (m), 3183 (w), 2360 (w), 1694 (s), 1599 (m), 1519 (s), 1455 (w), 1377 (m), 1289 (m), 1103 (m), 1038 (m), 990 (s), 921 (m), 871 (m), 795 (m), 716 (m);

Raman (1064 nm, 500 mW, 25 °C, cm^{-1}): $\tilde{\nu}$ = 3286 (10), 2858 (11), 2553 (6), 2407 (6), 1700 (28), 1632 (100), 1601 (31), 1548 (52), 1525 (74), 1427 (75), 1365 (8), 1251 (9), 1117 (40), 1051 (8), 1038 (8), 969 (13), 883 (17), 815 (55), 660 (24), 585 (6), 544 (10), 530 (9), 463 (21), 443 (5), 367 (20), 286 (17), 221 (11); ^1H NMR ($\text{DMSO}-d_6$) δ = 9.63 (s, NH), 6.5 (br, NH_2); $^{13}\text{C}\{^1\text{H}\}$ NMR ($\text{DMSO}-d_6$) δ = 154.3 (CNN), 151.9 (CNH), 140.3 (CO); EA ($\text{C}_6\text{H}_6\text{N}_8\text{O}_4$, 254.17 g mol^{-1}): Calc.: C 28.35, H 2.38, N 44.09 %; found: C 28.05, H 2.70, N 43.37 %.

1-Nitro-4-ethoxycarbamoyl furazan (8)

Compound **2** (0.50 g, 2.30 mmol) was dissolved in 10 mL ethanol. The mixture was heated 5 min to reflux and cooled to room temperature. The solvent was evaporated slowly yielding **8** (0.43 g) as colorless crystals (91%).

DSC (5 °C min^{-1}): 126 °C (melt), 153 °C (dec.); IR (ATR): $\tilde{\nu}$ = 3280 (w), 2984 (w), 1757 (m), 1728 (s), 1616 (m), 1565 (m), 1536 (s), 1466 (m), 1408 (m), 1371 (m), 1338 (s), 1303 (m), 1227 (s), 1197 (s), 1092 (m), 1058 (s), 1040 (m), 993 (m), 942 (m), 854 (m), 831 (s), 773 (m), 724 (w). Raman (1064 nm, 500 mW, 25 °C, cm^{-1}): $\tilde{\nu}$ = 3748 (6), 3008 (7), 2981 (23), 2964 (10), 2841 (23), 1753 (6), 1729 (14), 1580 (7), 1548 (7), 1538 (11), 1472 (100), 1409 (22), 1391 (17), 1372 (18), 1341 (36), 1306 (7), 1099 (10), 1067 (7), 1042 (12), 1010 (7), 995 (14), 947 (9), 899 (7), 854 (17), 832 (17), 763 (10), 594 (8), 558 (8), 465 (15), 450 (12), 440 (14), 425 (14), 414 (13), 309 (20), 287 (16), 177 (23), 84 (63). ^1H NMR ($\text{DMSO}-d_6$) δ = 9.73 (NH), 4.28 (q, 7.1 Hz, CH_2), 1.31 (t, 7.1 Hz, CH_3); $^{13}\text{C}\{^1\text{H}\}$ NMR ($\text{DMSO}-d_6$) δ = 154.8 (CNO_2), 151.9 (CNH), 145.7 (CO), 62.9 (CH_2), 13.6 (CH_3); ^{14}N NMR ($\text{DMSO}-d_6$) δ = -26 (CNO_2); EA ($\text{C}_5\text{H}_6\text{N}_4\text{O}_5$, 202.13 g mol^{-1}): Calc.: C 29.71, H 2.99, N 27.72 %, found: C 29.41, H 3.75, N 28.08 %.

4-Amino-3-(3-amino-1,2,4-oxadiazol) furoxan (9)

Potassium bicarbonate (2.07 g, 20.72 mmol) was dissolved in 40 mL water and 4-amino-3-aminooxim furoxan (1.00 g, 6.28 mmol) was added. The reaction mixture was heated until a clear solution is obtained. After cooling to room temperature Cyanogen bromide (0.73 g, 6.91 mmol) was added in portions. The reaction mixture was stirred over night and then acidified with 2M hydrochloric acid. The precipitate was filtered off and washed extensively with water and diethyl ether. 0.62 g (54%) of **15** was obtained as yellowish brown powder.

DSC (5 °C min^{-1}): 198 °C (dec.). IR (ATR): $\tilde{\nu}$ = 3436 (w), 3334 (w), 3168 (w), 1689 (m), 1635 (m), 1574 (w), 1537 (s), 1494 (m), 1422 (w), 1350 (w), 1236 (w), 1161 (m), 1078 (w), 1034 (m), 948 (m), 913 (w), 857 (m), 760 (m), 687 (m), 666 (m). Raman (1064 nm, 500 mV, 25 °C) $\tilde{\nu}$ = 1757 (6), 1609 (82), 1571 (46), 1558 (4),

1455 (12), 1254 (5), 1219 (16), 1069 (8), 1053 (3), 955 (36), 827 (6), 751 (16), 669 (6), 556 (4), 504 (5), 449 (19), 406 (4), 375 (26), 308 (3), 264 (10), 242 (2), 205 (16), 124 (3), 96 (100); ^1H NMR ($\text{DMSO}-d_6$) δ = 8.4 (br, NH_2), 6.5 (br, NH_2). $^{13}\text{C}\{^1\text{H}\}$ NMR ($\text{DMSO}-d_6$) δ = 172.3 (CNO), 157.6 (C_{ring}), 156.3 (CN(O)O), 101.7 (CNH_2). EA ($\text{C}_4\text{H}_4\text{N}_6\text{O}_3$, $184.12 \text{ g mol}^{-1}$): Calc.: C 26.09, H 2.19, N 45.65 %; found: C 25.84, H 2.38, N 43.93 %.

4-Nitro-3-(3-amino-1,2,4-oxadiazolyl) furoxan (10)

For the preparation of Caro's acid, 10 mL of conc. sulfuric acid was added slowly to 30% hydrogen peroxide at 0 °C. Compound **9** (0.5 g, 1.36 mmol) was dissolved in 5 mL conc. sulfuric acid and slowly added to Caro's acid, while keeping the temperature between 0-10 °C. The reaction mixture was heated slowly to 40 °C and stirred for 30 min. After cooling to ambient temperature the mixture was quenched with ice and water. After extracting with ethyl acetate (3 x 30 mL), the combined organic phases were washed with water (2 x 20 mL), brine (1 x 20 mL) and dried over magnesium sulfate. The solvent was removed under reduced pressure and recrystallized from acetone. 0.20 g (66%) of **10** was obtained as yellow crystals.

DSC (5 °C min^{-1}): 188 °C (dec.). IR (ATR): $\tilde{\nu}$ = 3443 (m), 3363 (m), 3268 (m), 3188 (m), 3143 (m), 2963 (w), 2927 (w), 2855 (w), 1678 (s), 1634 (s), 1572 (s), 1503 (s), 1386 (s), 1342 (s), 1314 (s), 1261 (m), 1229 (s), 1141 (m), 1097 (s), 1070 (s), 1049 (s), 991 (s), 960 (s), 908 (s), 847 (m), 790 (s), 760 (s), 730 (s), 692 (s), 663 (s). Raman (1064 nm, 500 mV, 25 °C) $\tilde{\nu}$ = 1682 (18), 1625 (16), 1556 (24), 1540 (100), 1508 (23), 1492 (59), 1358 (20), 1315 (13), 1231 (31), 1073 (12), 992 (14), 964 (24), 749 (27), 489 (12), 458 (37), 398 (25), 358 (12), 259 (11), 204 (10), 132 (13), 88 (83). ^1H NMR ($\text{DMSO}-d_6$) δ = 8.2 (br, NH_2). $^{13}\text{C}\{^1\text{H}\}$ NMR ($\text{DMSO}-d_6$) δ = 173.4 (CNO), 161.5 (C_{ring}), 155.9 (CN(O)O), 102.6 (CNH_2). ^{14}N NMR ($\text{DMSO}-d_6$) δ = -35 (NO_2) ppm. EA ($\text{C}_4\text{H}_2\text{N}_6\text{O}_5$, $214.10 \text{ g mol}^{-1}$): Calc.: C 22.44, H 0.94, N 39.25 %, found: C 23.32, H 1.19, N 37.98 %.

3,4-Bis-(3-amino-1,2,4-oxadiazolyl) furoxan (11)

Into an aqueous solution of sodium hydroxide (0.72 g, 17.9 mmol) 3,4-bis-aminooxime furoxan (1.44 g, 7.1 mmol) was added. The reaction mixture was heated under reflux for 10 min forming a clear solution. After cooling to 40 °C cyanogen bromide (1.89 g, 17.85 mmol) was added in portions. The reaction mixture was stirred over night at ambient temperature and subsequently acidified with 2 M hydrochloric acid to pH 2. The precipitate was filtered off and washed extensively with water. 0.93 g (54%) of **11** was obtained as brownish powder.

DSC (5 °C min⁻¹): 273 °C (dec.). IR (ATR): $\tilde{\nu}$ = 3472 (w), 3340 (w), 3249 (w), 3177 (w), 1662 (s), 1608 (s), 1566 (m), 1529 (m), 1449 (m), 1416 (m), 1359 (w), 1259 (w), 1220 (w), 1112 (m), 1073 (w), 1050 (m), 1008 (w), 976 (w), 946 (m), 910 (w), 824 (s), 761 (m), 724 (m), 683 (m). Raman (1064 nm, 500 mV, 25 °C) $\tilde{\nu}$ = 2859 (20), 1661 (19), 1606 (7), 1569 (77), 1530 (24), 1509 (42), 1455 (8), 1425 (25), 1378 (22), 1220 (58), 1108 (16), 1099 (3), 1010 (8), 977 (59), 911 (11), 827 (13), 757 (42), 546 (6), 498 (12), 464 (11), 421 (18), 362 (28), 314 (3), 304 (4), 283 (9), 272 (3), 244 (2), 214 (21), 126 (100), 95 (8). ¹H NMR (DMSO-D₆) δ = 8.4 (br, NH₂), 8.3 (br, NH₂). ¹³C{¹H} NMR (DMSO-D₆) δ = 173.0 (CNH₂), 159.6 (CNH₂), 156.9 (C_{ring}), 155.9 (C_{ring}), 144.7 (CNO), 106.7(CN(O)O). EA (C₆H₄N₈O₄, 252.15 g mol⁻¹) Calc.: C 28.58, H 1.60, N 44.44 %, found: C 27.73, H 2.03, N 42.28 %.

5. Reverences

- [1] P. Srivastava, H. J. Singh, *J. Energ. Mater.*, 2010, *28*, 202–218.
- [2] M. J. Lipp, W. J. Evans, B. J. Baer, C.-S. Yoo, *Nat. Mater.*, 2005, *4*, 211–215.
- [3] J. J. Sabatini, K. D. Oyler, *Crystals*, 2016, *6*, 5/1-5/22.
- [4] H. Gao, J. M. Shreeve, *Chem. Rev.*, 2011, *111*, 7377–7436.
- [5] V. Thottempudi, H. Gao, J. M. Shreeve, *J. Am. Chem. Soc.*, 2011, *133*, 6464–6471.
- [6] T. P. Kofman, G. Y. Kartseva, E. Y. Glazkova, K. N. Krasnov, *Russ. J. Org. Chem.*, 2005, *41*, 753–757.
- [7] R. Haiges, K. O. Christe, *Inorg. Chem.*, 2013, *52*, 7249–7260.
- [8] M. A. Kettner, K. Karaghiosoff, T. M. Klapötke, M. Sucasca, S. Wunder, *Chem. - Eur. J.*, 2014, *20*, 7622–7631.
- [9] M. A. Kettner, T. M. Klapötke, *Chem. Commun.*, 2014, *50*, 2268–2270.
- [10] T. M. Klapötke, N. Mayr, J. Stierstorfer, M. Weyrauther, *Chem. - Eur. J.*, 2014, *20*, 1410–1417.
- [11] J. Bostroem, A. Hogner, A. Llinas, E. Wellner, A. T. Plowright, *J. Med. Chem.*, 2012, *55*, 1817–1830.
- [12] A. Pace, P. Pierro, *Org. Biomol. Chem.*, 2009, *7*, 4337–4348.
- [13] M. D. McBriar, J. W. Clader, I. Chu, R. A. Del Vecchio, L. Favreau, W. J. Greenlee, L. A. Hyde, A. A. Nomeir, E. M. Parker, D. A. Pissarnitski, L. Song, L. Zhang, Z. Zhao, *Bioorg. Med. Chem. Lett.*, 2008, *18*, 215–219.
- [14] G. A. Patani, E. J. LaVoie, *Chem. Rev.*, 1996, *96*, 3147–3176.

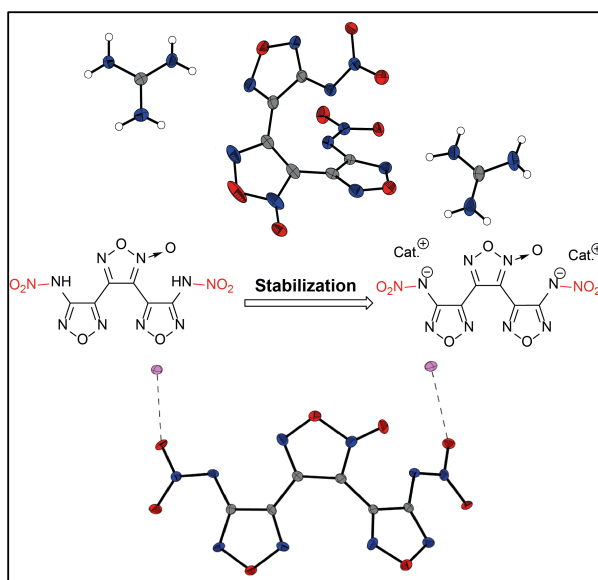
- [15] D. Fischer, T. M. Klapötke, M. Reymann, J. Stierstorfer, *Chem. - Eur. J.*, 2014, 20, 6401–6411.
- [16] C. He, J. M. Shreeve, *Angew. Chem., Int. Ed.*, 2016, 55, 772–775.
- [17] A. B. Sheremetev, *Russ. Khim. Zh.*, 1997, 41, 43–54.
- [18] A. B. Sheremetev, N. N. Makhova, W. Friedrichsen, *Adv. Heterocycl. Chem.*, 2001, 78, 65–188.
- [19] T. M. Klapötke, B. Krumm, S. F. Rest, M. Sucéska, *Z. Anorg. Allg. Chem.*, 2014, 640, 84–92.
- [20] N. Fischer, D. Izsak, T. M. Klapötke, S. Rappenglueck, J. Stierstorfer, *Chem. - Eur. J.*, 2012, 18, 4051–4062.
- [21] J. M. Veauthier, D. E. Chavez, B. C. Tappan, D. A. Parrish, *J. Energ. Mater.*, 2010, 28, 229–249.
- [22] K. Cui, G. Xu, Z. Xu, P. Wang, M. Xue, Z. Meng, J. Li, B. Wang, Z. Ge, G. Qin, *Propellants, Explos., Pyrotech.*, 2014, 39, 662–669.
- [23] Q. Liu, N. W. Luedtke, Y. Tor, *Tetrahedron Lett.*, 2001, 42, 1445–1447.
- [24] E. Artuso, I. Degani, R. Fochi, C. Magistris, *Synthesis*, 2007, 3497–3506.
- [25] R. Nec, *Chem. Prum.*, 1979, 29, 589–592.
- [26] A. Gunasekaran, M. L. Trudell, J. H. Boyer, *Heteroat. Chem.*, 1994, 5, 441–446.
- [27] A. Gunasekaran, T. Jayachandran, J. H. Boyer, M. L. Trudell, *J. Heterocycl. Chem.*, 1995, 32, 1405–1407.
- [28] T. S. Novikova, T. M. Mel'nikova, O. V. Kharitonova, V. O. Kulagina, N. S. Aleksandrova, A. B. Sheremetev, T. S. Pivina, L. I. Khmel'nitskii, S. S. Novikov, *Mendeleev Commun.*, 1994, 138–140.
- [29] E. G. Francois, D. E. Chavez, M. M. Sandstrom, *Propellants, Explos., Pyrotech.*, 2010, 35, 529–534.
- [30] D. E. Chavez, E. G. Francois, Process for Preparation of 3,3'-Diamino-4,4'-azoxyfurazan or 3,3'-diamino-4,4'-azofurazan from 3,4-Diaminofurazan, 2009, US20090306355A1.
- [31] D. E. Chavez, L. Hill, M. Hiskey, S. Kinkead, *J. Energ. Mater.*, 2000, 18, 219–236.
- [32] Q. J. Axthammer, B. Krumm, T. M. Klapötke, *J. Org. Chem.*, 2015, 80, 6329–6335.
- [33] Q. J. Axthammer, T. M. Klapötke, B. Krumm, *Chem. Asian J.*, 2016, 11, 568–575.
- [34] V. G. Andrianov, *Chem. Heterocycl. Compd.*, 1998, 33, 973–976.
- [35] D. Fischer, T. M. Klapötke, M. Reymann, J. Stierstorfer, M. B. R. Völkl, *New J. Chem.*, 2015, 39, 1619–1627.
- [36] Q. J. Axthammer, T. M. Klapötke, B. Krumm, R. Moll, S. F. Rest, *Z. Anorg. Allg. Chem.*, 2014, 640, 76–83.
- [37] C. R. Kemnitz, M. J. Loewen, *J. Am. Chem. Soc.*, 2007, 129, 2521–2528.

- [38] C. S. Choi, *Acta Crystallogr., Sect. B*, 1972, 28, 2857–2862.
- [39] R. Mayer, J. Köhler, and, A. Homburg, *Explosives*, 2002, Wiley-VCH, Weinheim, 5th edn.
- [40] M. J. Frisch, G. W. Trucks, H. B. Schlegel, G. E. Scuseria, M. A. Robb, J. R. Cheeseman, G. Scalmani, V. Barone, B. Mennucci, G. A. Petersson, H. Nakatsuji, M. Caricato, X. Li, H. P. Hratchian, A. F. Izmaylov, J. Bloino, G. Zheng, J. L. Sonnenberg, M. Hada, M. Ehara, K. Toyota, J. H. R. Fukuda, M. Ishida, T. Nakajima, Y. Honda, O. Kitao, H. Nakai, M. T. Vreven, J. E. Peralta, F. Ogliaro, M. Bearpark, J. J. Heyd, E. Brothers, K. N. Kudin, V. N. Staroverov, R. Kobayashi, J. Normand, K. Raghavachari, A. Rendell, J. C. Burant, S. S. Iyengar, J. Tomasi, M. Cossi, N. Rega, J. M. Millam, M. Klene, J. E. Knox, J. B. Cross, V. Bakken, C. Adamo, J. Jaramillo, R. Gomperts, R. E. Stratmann, O. Yazyev, A. J. Austin, R. Cammi and C. Pomelli, J. W. Ochterski, R. L. Martin, K. Morokuma, V. G. Zakrzewski, G. A. Voth, P. Salvador, J. J. Dannenberg, S. Dapprich, A. D. Daniels, Ö. Farkas, J. B. Foresman, J. C. J. V. Ortiz, D. J. Fox, *Gaussian 09; Rev. A.02 ed.*, Gaussian, Inc., Wallingford CT(USA), 2009.
- [41] R. D. Dennington II, T. A. Keith, J. M. Millam, GaussView, Ver.5.08 ed., Semichem, Inc., Wallingford CT (USA), 2009.
- [42] M. Sućeska, *Propellants, Explos., Pyrotech.*, 1991, 16, 197–202.
- [43] CrysAlis CCD, Version 1.171.35.11(release 16-05-2011CrysAlis 171.Net), Oxford Diffraction Ltd., Abingdon, Oxford (U.K.), 2011.
- [44] CrysAlis RED, Version 1.171.35.11(release 16-05-2011CrysAlis 171.Net), Oxford Diffraction Ltd., Abingdon, Oxford (U.K.), 2011.
- [45] A. Altomare, M. C. Burla, M. Camalli, G. L. Cascarano, C. Giacovazzo, A. Guagliardi, A. G. G. Moliterni, G. Polidori, R. Spagna, *J. Appl. Crystallogr.*, 1999, 32, 115–119.
- [46] G. M. Sheldrick, *SHELX-97*, 1997, Programs for Crystal Structure Determination.
- [47] L. J. Farrugia, *J. Appl. Crystallogr.*, 1999, 32, 837–838.
- [48] A. L. Spek, *Acta Crystallogr.*, 2009, 65 D, 148–155.
- [49] T. M. Klapötke, *Chemistry of High-Energy Materials, 4th Edition*, Walter de Gruyter GmbH & Ko KG, Berlin, 2017
- [50] T. Altenburg, T. M. Klapötke, A. Penger, J. Stierstorfer, *Z. Anorg. Allg. Chem.*, 2010, 636, 463–471.
- [51] M. Sućeska, *EXPLO5 V.6.03*, 2014, Zagreb (Croatia).

Energetic Compounds Based on 3,4-Bis(4-nitramino-1,2,5-oxadiazol-3-yl)-1,2,5-furoxan (BNAFF)

Ivan Gospodinov, Tobias S. Hermann, Thomas M. Klapötke* and Jörg Stierstorfer ^[a]

Propellants, Explosives, Pyrotechnics, **2018**, in press.



Energetic Compounds Based on 3,4-Bis(4-nitramino-1,2,5-oxadiazol-3-yl)-1,2,5-furoxan (BNAFF)

Ivan Gospodinov, Tobias S. Hermann, Thomas M. Klapötke* and Jörg Stierstorfer

Propellants, Explosives, Pyrotechnics, **2018**, in press.

Abstract:

3,4-Bis(4-amino-1,2,5-oxadiazol-3-yl)-1,2,5-furoxan (BAFF, **1**) was nitrated in 100% HNO₃ at –10 °C and then reacted with KOH to give the corresponding energetic dipotassium salt of 3,4-bis(4-nitramino-1,2,5-oxadiazol-3-yl)-1,2,5-furoxan (**2**, K₂BNAFF). The neutral nitramino-furoxan compound (**3**, H₂BNAFF) is unstable at room temperature and can be obtained from K₂BNAFF with 2 M HCl and ether as H₂BNAFF • 0.5 Et₂O. Several nitrogen-rich salts (*e.g.* ammonium, guanidinium, aminoguanidinium, hydrazinium and hydroxylammonium) were prepared from K₂BNAFF. The potassium, guanidinium, aminoguanidinium, hydroxylammonium and silver salts of BNAFF were characterized by low-temperature X-ray diffraction. In addition, all compounds were analyzed by vibrational spectroscopy (IR and Raman), multinuclear (¹H, ¹³C, ¹⁴N) NMR spectroscopy, differential thermal analysis (DTA) and elemental analysis. The heats of formation for the anhydrous compounds were calculated using the atomization method based on CBS-4M enthalpies. Several detonation parameters were predicted by using the EXPLO5 code (V6.03). In addition, the sensitivities of all BNAFF salts toward friction, impact and electrostatic discharge were determined.

1. Introduction

“High energy density materials” (HEDMs) have not only found use for military purposes but also for civilian applications *e.g.* mining and pyrotechnics.^[1] In the last century there have been a large number of publications that describe the chemistry, synthesis and properties of new explosive materials.^[2] Higher performance has always been a main requirement in the development of explosives. Hence explosives are

required for even more demanding applications (deep oil drilling or missiles for space missions); new advances in the technology of energetic materials have to be made.^[3] In addition, newly designed explosives should meet the future environmental requirements, exhibit lower sensitivities toward external stimuli (such as impact, friction and electrostatic discharge) and show high performance.^[4–8]

Five membered heterocycles containing nitrogen and oxygen have shown promising application as building blocks for energetic materials.^[9–11] Derivatives of nitro/nitramino substituted furazanes (1,2,5-oxadiazole) and furoxanes (1,2,5-oxadiazole-2-oxide) have been of particular interest in the development of new HEDMs since they usually possess good oxygen balance, high heat of formation and high density.^[12–15] Some well-known explosives based on furazanes and furoxanes are shown in Figure 1.

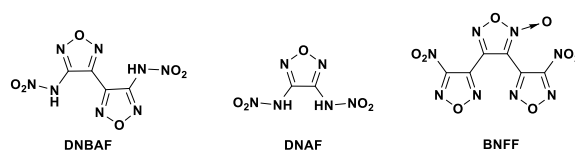


Figure 1. Literature known explosives based on furoxanes and furazanes: DNBAF (4,4'-dinitramino-3,3'-bifurazan),^[12] DNAF (3,4-dinitraminofurazan)^[16] and BNFF (3,4-bis(4-nitro-1,2,5-oxadiazol-3-yl)-1,2,5-furoxan).^[17]

Recently, the combination of both, the furazan and furoxan rings with nitro or nitramino groups in the molecule has proven to be a good strategy for the synthesis of new high-nitrogen containing explosives.^[17] A good example of a new high-density energetic material with good thermal stability and performance based on the furazan and furoxan rings is 3,4-bis(4-nitro-1,2,5-oxadiazol-3-yl)-1,2,5-furoxan (BNFF, also known as DNTF). BNFF can be synthesized by oxidizing 3,4-bis(4-amino-1,2,5-oxadiazol-3-yl)-1,2,5-furoxan (BAFF) with 50% hydrogen peroxide and trifluoroacetic acid.^[18] BNFF has a crystal density of 1.93 g cm^{-3} with a heat of formation of 657 kJ mol^{-1} and its energetic performance is 168% better than trinitrotoluene (TNT). It melts at 108–110 °C and decomposes at 292 °C, which makes the compound of special interest as a possible TNT replacement.^[17,19] All these physico-chemical properties make BNFF a promising candidate to use not only as a melt-castable ingredient in detonators but also as a high performing explosive.^[20,21] Replacement of the amino groups in BAFF with nitro groups to form BNFF improves the detonation parameters of the energetic material. Surprisingly, the nitration of 3,4-bis(4-amino-1,2,5-oxadiazol-3-yl)-1,2,5-furoxan (BAFF) has not been reported and the nitramino compound is unknown. In this contribution the nitration of BAFF to the nitramino compound (H_2BNAFF) is described as well as the formation and characterization of some nitrogen-rich salts.

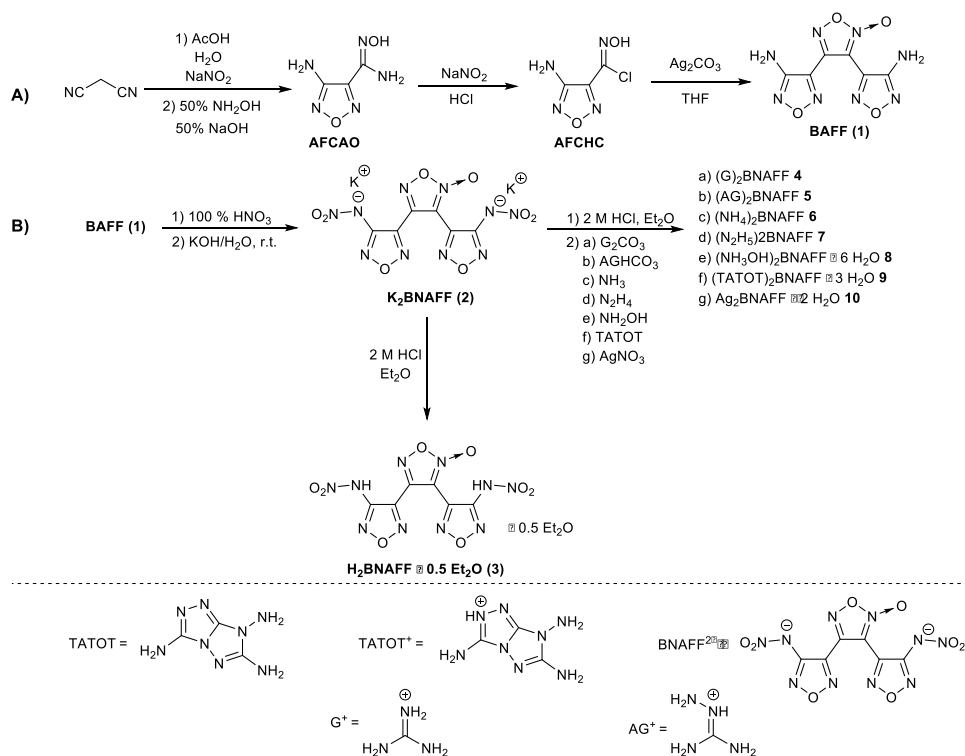
2. Results and Discussion

The synthesis of the starting material BAFF has been performed as reported previously in the literature. Initially 4-amino-1,2,5-oxadiazole-3-carboxamidoxime (AFCAO) was synthesized by reacting commercially

available malononitrile with aqueous nitrous acid and then with 50% aqueous hydroxylamine. AFCAO was treated with sodium nitrite in aqueous HCl to give 4-amino-1,2,5-oxadiazole-3-carbohydroximoyl chloride (AFCHC) which is then reacted with Ag_2CO_3 in THF to give BAFF.^[17,20,22]

The synthesis and nitration of BAFF are displayed in Scheme 1.

The amino groups of 3,4-bis(4-amino-1,2,5-oxadiazol-3-yl)-1,2,5-furoxan are nitrated with 100% HNO_3 at -10°C and the formed, unstable dinitramino derivative (H_2BNAFF) is converted with potassium hydroxide to the dipotassium salt (**2**, K_2BNAFF) in a good yield (90 %). The neutral compound **3** can be isolated by dissolving K_2BNAFF (**2**) in 2 M hydrochloric acid and then extracting with diethyl ether giving an oily liquid. H_2BNAFF is only stable at room temperature only with 0.5 equivalents ether as a solvate (BNAFF (**3**) \cdot 0.5 Et_2O).



Scheme 1. **A)** Literature known synthesis of 3,4-bis(4-amino-1,2,5-oxadiazol-3-yl)-1,2,5-furoxan (**1**, BAFF); **B)** Nitration of compound **1** and synthesis of new nitrogen-rich salts with BNAFF (**3**).

However, H_2BNAFF is unstable at room temperature without Et_2O and decomposes with the release of nitrous gases. Using other solvents as extraction medium resulted in decomposition of the neutral compound. Using K_2BNAFF (**2**) as the starting material nitrogen-rich salts of BNAFF can be synthesized.

For this purpose compound **2** is dissolved in a small amount of 2 M HCl and the *in situ* generated neutral compound (**3**) is reacted with the desired base giving compounds **4–10** (Scheme 1).

Crystal structures

During this work the crystal structures of compounds **2**, **4**, **5**, **8** and **10** were determined by low-temperature X-ray diffraction. Compounds **2**, **4** and **5** crystallize anhydrously whereas compound **8** crystallizes with six molecules of water. The crystal structure of **10** was determined of single crystals from conc. ammonia solution containing two molecules NH_3 . Selected data and parameters for the low-temperature X-ray data collection and refinements are given in the Supporting Information. A distortion of the N-oxide moiety in the furoxan ring of the BNAFF^{2-} anion can be observed in the obtained crystal structures for compounds **4**, **5**, **8** and **10**.

Dipotassium 3,4-bis(4-nitramino-1,2,5-oxadiazol-3-yl)-1,2,5-furoxane (**2**) crystallizes from water, without inclusion of solvent molecules, in the triclinic space group $P\bar{1}$ with two molecules per unit cell and a cell volume of $651.80 \cdot 10^6 \text{ pm}^3$. The density of **2** at a temperature of 103 K is 2.132 g cm^{-3} . Figure 2 illustrates the molecular unit of the potassium salt (**2**). The torsion angle of C1–C2–C3–N5 and N6–C4–C5–C6 in BNAFF^{2-} anion are $-63.0(5)$ and $18.1(6)^\circ$ respectively, showing that both furazan rings are not coplanar to the furoxan ring.

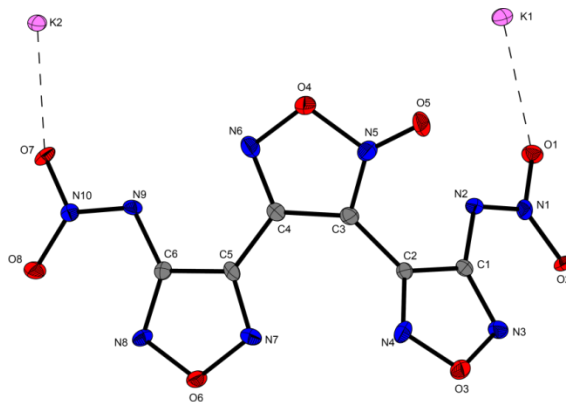


Figure 2. Molecular unit of **2**, showing the atom-labeling scheme and bond lengths (pm) with standard deviations. Thermal ellipsoids represent the 50 % probability level and hydrogen atoms are shown as small spheres of arbitrary radius.

Bis(guanidinium) 3,4-bis(4-nitramino-1,2,5-oxadiazol-3-yl)-1,2,5-furoxane (**4**) crystallizes in the monoclinic space group $P2_1/c$ with a cell volume of $1761.43 \cdot 10^6 \text{ pm}^3$ and four molecules per unit cell. The density at a temperature of 123 K is 1.736 g cm^{-3} . The furoxan and furazan rings in the BNAFF^{2-} anion have a planar structure (O4–N6–C4–C3 0.5° , N2–O1–N1–C1 -0.3° and O6–N7–C5–C6 0.2°). However, both furazan rings in the anion are not coplanar to the furoxan ring as indicated by the torsion angle of C2–C3–C4–C5 -14.6° . Both nitramino groups in BNAFF^{2-} are slightly tilted against the furazan rings as shown by the torsion angles of N10–N9–C6–N8 6.4° and N4–N3–C1–N1 -5.4° . The bond distances of the furoxan ring

(C3–C4 1.418 Å and N5–C3 132.0 pm), furazan rings (C1–C2 143.6 pm and N8–C6 131.1 pm) and the nitramino moiety (N3–N4 131.5 pm, N9–N10 132.2 pm, O2–N4 125.5 pm and O7–N10 125.7 pm) are in accordance with similar nitramino oxadiazoles reported in the literature.^[23]

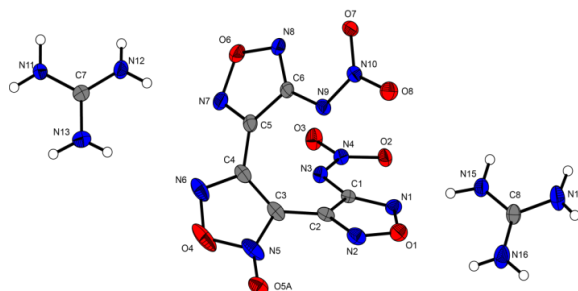


Figure 3. Representation of the molecular unit of **4**, showing the atom-labeling scheme. Thermal ellipsoids represent the 50 % probability level and hydrogen atoms are shown as small spheres of arbitrary radius. Selected bond distances (pm) and angles [°]: C3–C4 141.8(4), N5–C3 132.0(3), C1–C2 143.6(3), N8–C6 131.1(3), N3–N4 131.5(3), N9–N10 132.2(3), O7–N10 125.7(2), O4–N6–C4–C3 0.5(3), N2–O1–N1–C1 –0.3(2), O6–N7–C5–C6 0.2(2), C2–C3–C4–C5 –14.6(6), N10–N9–C6–N8 6.4(4), N4–N3–C1–N1 –5.4(4).

Bis(aminoguanidinium) 3,4-bis(4-nitramino-1,2,5-oxadiazol-3-yl)-1,2,5-furoxan (**5**) crystallizes from water, without inclusion of solvent molecules, in the monoclinic space group $P2_1/c$ with four molecules per unit cell and a cell volume of $1863.35 \cdot 10^6 \text{ pm}^3$. The density of **5** at a temperature of 123 K is 1.748 g cm^{-3} . Figure 4 illustrates the molecular unit of **5**. The torsion angle of C1–C2–C3–C3ⁱ in BNAFF²⁻ anion is -39.6° , showing that both furazan rings are not coplanar to the furoxan ring. The connecting C–C bond of the oxadiazoles (C2–C3) with a length of 145.9 pm is significantly shorter than a C–C single bond (154.0 pm). The nitramino moiety is slightly twisted from the furazan plane with torsion angle of -177.45° (C1–N3–N4–O3). The bond distances of the furoxan ring (O4–N5 139.8 pm and N5–C3 131.8 pm), furazan rings (O1–N2 136.5 pm and C1–C2 143.5 pm) and the nitramino moiety (N3–N4 131.42 pm, N3–C1 137.9 pm, O3–N4 126.68 pm) are in accordance with similar nitramino oxadiazoles reported in the literature.^[23]

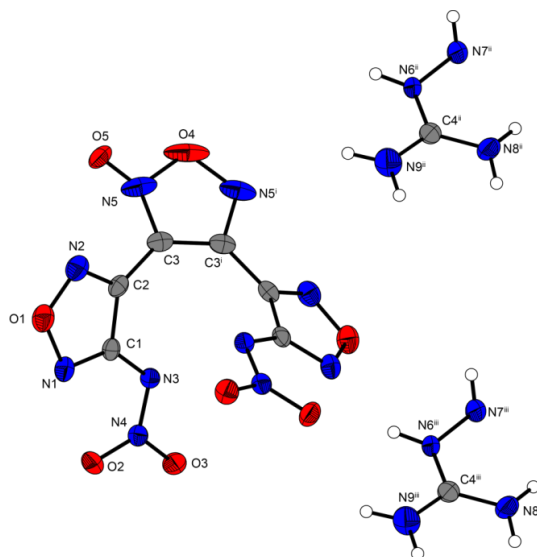


Figure 4. Molecular unit of **5**, showing the atom-labeling scheme and bond lengths (pm) with standard deviations. Thermal ellipsoids represent the 50 % probability level and hydrogen atoms are shown as small spheres of arbitrary radius. Symmetry codes: (i) x, y, z , (ii) $1-x, y, 0.5-z$, (iii) $1-x, 0.5+y, 1-z$. Selected bond distances (pm) and angles [°]: C2–C3 145.9(2), O4–N5 139.8(2), N5–C3 131.8(2), O1–N2 136.5(2), C1–C2 143.5(2), C1–C2–C3–C3 i –39.6(3), C1–N3–N4–O3 –177.45(13).

Disilver 3,4-bis(4-nitramino-1,2,5-oxadiazol-3-yl)-1,2,5-furoxan (**10**) is crystallized from hot water with conc. ammonia solution, with inclusion of two molecules ammonia, in the triclinic space group $P\bar{1}$ with two molecules per unit cell and a cell volume of $784.58(12) \cdot 10^6 \text{ pm}^3$. The density of **10** at a temperature of 173 K is 2.497 g cm^{-3} . Figure 5 illustrates the molecular unit of $\text{Ag}_2\text{BNAFF} \cdot 2 \text{ NH}_3$.

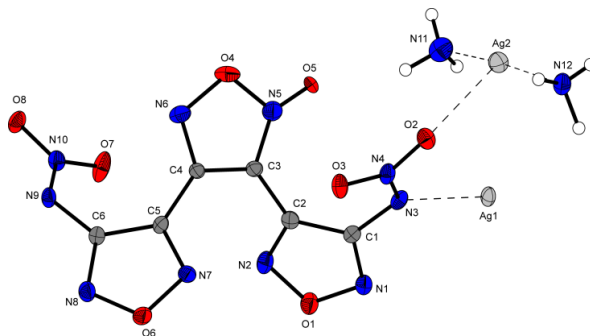


Figure 5. Molecular unit of **10**, showing the atom-labeling scheme and bond lengths (pm) with standard deviations. Thermal ellipsoids represent the 50 % probability level and hydrogen atoms are shown as small spheres of arbitrary radius.

NMR Spectroscopy

All synthesized compounds were characterized with multinuclear NMR (^1H , ^{13}C and ^{14}N) spectroscopy. In addition, ^{15}N NMR spectra of **2** and **3** $\cdot 0.5 \text{ Et}_2\text{O}$ were recorded. Compound **3** $\cdot 0.5 \text{ Et}_2\text{O}$ shows three different resonances in the ^1H NMR spectrum; one at 12.87 ppm for the acidic protons of the nitramine groups ($-\text{NHNO}_2$) and two at 3.34 ($-\text{OCH}_2\text{CH}_3$) and 1.04 ($-\text{OCH}_2\text{CH}_3$) ppm for the ether solvate (^1H , ^{13}C and ^{14}N NMR spectra of compound **3** $\cdot 0.5 \text{ Et}_2\text{O}$ are displayed in the Supporting Information). All six

observed resonances in ^{13}C spectrum of the neutral nitramine compound **3** • 0.5 Et₂O are high-field shifted in comparison to all observed resonances in the ^{13}C spectra of all energetic salts with the BNAFF²⁻ anion. The ^{14}N resonances for the nitro groups in compound **3** are detected at –26 ppm and the nitro groups of the energetic salts are observed in the range of –13 to –15 ppm. The values for all ^1H , ^{13}C and ^{14}N resonances of compounds **2** and **3** • 0.5 Et₂O are listed in Table 1.

Table 1. ^1H , ^{13}C and ^{14}N NMR shifts of compounds **2** and **3** • 0.5 Et₂O.

	^1H NMR δ [ppm]	^{13}C NMR δ [ppm]	^{14}N NMR δ [ppm]
2	–	158.6, 157.8, 146.6, 140.4, 137.4, 106.8.	–14
3	12.87, 3.34, 1.04	154.1, 152.8, 145.6, 141.1, 137.1, 106.2, 65.2, 15.4	–26

Figure 6 shows the comparison between both recorded ^{15}N NMR spectra for compounds **2** and **3**. In the spectrum of the neutral nitramine compound **3** the nitro groups are found at –28.3 and –29.0 ppm and the NH groups at –183.9 and –190.4 ppm (no coupling to hydrogen due to exchange with the solvent *d*₆-DMSO). Upon formation of the potassium salt (deprotonation) all resonances in ^{15}N NMR show strong low-field shift as observed in the case of the nitro (to –13.3 and –13.8 ppm) and NH groups (–151.7 and 152.8 ppm).

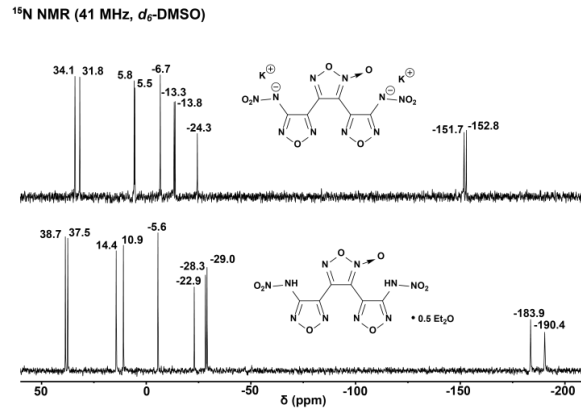


Figure 6. Recorded ^{15}N NMR spectra of K_2BNAFF (2) and BNAFF (3) • 0.5 Et_2O in d_6 -DMSO.

Table 2. Physico-chemical properties of 2, 4–7 in comparison to RDX.

	2	4	5	6	7	RDX
Formula	$\text{C}_6\text{K}_2\text{N}_{10}\text{O}_8$	$\text{C}_8\text{H}_{12}\text{N}_{16}\text{O}_8$	$\text{C}_8\text{H}_{14}\text{N}_{18}\text{O}_8$	$\text{C}_6\text{H}_8\text{N}_{12}\text{O}_8$	$\text{C}_6\text{H}_{10}\text{N}_{14}\text{O}_8$	$\text{C}_3\text{H}_6\text{N}_6\text{O}_6$
$IS^{[a]}$ [J]	3	15	8	7	8	7.5
$FS^{[b]}$ [N]	> 72	360	360	216	216	120
$ESD^{[c]}$ [J]	0.19	0.75	1.00	0.70	0.50	0.2
$\Omega^{[d]}$ [%]	−19.12	−48.66	−48.95	−34.02	−35.45	−21.6
$T_m^{[c]}$ [°C]	—	—	128	—	—	—
$T_{dev}^{[f]}$ [°C]	245	189	156	161	170	210
$\rho^{[g]}$ [g cm^{-3}]	2.07	1.692	1.703	1.735(pyc)	1.535(pyc)	1.806[24]
$\Delta H_f^{o[h]}$ [kJ kg^{-1}]	689	1275	1650	1635	2239	387
EXPLO5						
6.03 ^[25]						
$-\Delta_E U^{o[i]}$ [kJ kg^{-1}]	5483	4721	4981	5701	5953	5798
$T_{CJ}^{[j]}$ [K]	3772	3318	3389	3922	4169	3831

$P_{CJ}^{[k]}$ [GPa]	29.9	25.3	26.9	30.5	25.7	35.4
$V_{det}^{[l]}$ [m s ⁻¹]	8263	8099	8364	8579	8105	8834
$V_o^{[m]}$ [dm ³ kg ⁻¹]	470	796	819	779	846	792

[a] Impact sensitivity (BAM drophammer, method 1 of 6); [b] friction sensitivity (BAM drophammer, method 1 of 6); [c] electrostatic discharge device (OZM research); [d] oxygen balance; [e] melting point (DTA, $\beta = 5^{\circ}\text{C}\cdot\text{min}^{-1}$); [f] temperature of decomposition (DTA, $\beta = 5^{\circ}\text{C}\cdot\text{min}^{-1}$); [g] density at 298 K; [h] standard molar enthalpy of formation; [i] detonation energy; [j] detonation temperature; [k] detonation pressure; [l] detonation velocity; [m] volume of detonation gases at standard temperature and pressure conditions.

Physicochemical properties

Since all synthesized compounds can be considered as energetic materials, their energetic behaviors were investigated. However, only the physicochemical properties of compounds **2**, **4**, **5**, **6** and **7** are discussed because they were obtained as anhydrous compounds. All theoretical calculated and experimentally determined values for compounds **2**, **4–7** compared to the high explosive RDX are listed in Table 2.

Thermal Behavior

The thermal behavior of compounds **2**, **4–10** was investigated with an OZM Research DTA 552-Ex instrument at a heating rate of 5 °C min⁻¹. Critical temperatures are given as the onset temperature. The neutral compound **3** decomposes simultaneously as soon as the ether solvate is removed from the molecule. The neutral nitramine (**3**) exhibits only one sharp exothermal signal at 72 °C in the DTA plot. Additional data can be found in the Supporting Information. From all synthesized salts of BNAFF, compound **2** has the highest decomposition point at 245 °C. All formed nitrogen-rich salts with the BNAFF²⁻ anion decompose in the range of 150–200 °C, whereas the guanidinium salt (**4**) has the highest decomposition temperature of 189 °C.

Sensitivities

In addition, the sensitivities for all compounds toward friction, impact and electrostatic discharge were explored using the BAM standards.[26,27] The silver (**10**, IS = 1 J, FS = 60 N and ESD = 50 mJ) and potassium salts (**2**, IS = 3 J, FS = > 72 N and ESD = 0.19 J) are the most sensitive compounds from all synthesized energetic materials formed with the BNAFF²⁻ anion. From all nitrogen-rich compounds the ammonium salt (**6**) is the most sensitive compound (IS = 7 J and FS = 216 N) toward friction and impact. The impact and friction sensitivities for the others range from 7 J to 15 J and from 216 N to 360 N.

Detonation parameters

The detonation parameters for compounds **2**, **4**, **5**, **6** and **7** were calculated using the EXPLO5_V6.03 computer code.[25] The EXPLO5 detonation parameters of compounds **2**, **4–7** were calculated by using the room-temperature density values obtained from the X-ray structures (compounds **2**, **4** and **5**) as described in reference [28] or by using pycnometrical measured densities

of compounds **6** and **7**. The densities range from 1.535 g cm^{-3} (**7**, pyc) to 2.07 g cm^{-3} (**2**). All compounds reported in Table 2 exhibit a highly positive heat of formation from 689 kJ kg^{-1} (**2**) to 2239 kJ kg^{-1} (**7**), which exceed the value for the heat of formation of RDX (387 kJ kg^{-1}). Compounds **2**, **4–7** show good calculated detonation parameters with detonation velocities ($V_{det.}$) between $8000\text{--}8600 \text{ m s}^{-1}$ and detonation pressure (P_{CJ}) $25\text{--}31 \text{ GPa}$. Compound **6** shows the highest calculated detonation velocity (8579 m s^{-1}) and detonation pressure (30.5 GPa), whereas the guanidinium salt (**4**) exhibits the lowest values ($V_{det.} = 8099 \text{ m s}^{-1}$ and $P_{CJ} = 25.3 \text{ GPa}$).

3. Conclusion

In summary, 3,4-bis(4-nitramino-1,2,5-oxadiazol-3-yl)-1,2,5-furoxan (**3**) was synthesized for the first time by nitration of 3,4-bis(4-amino-1,2,5-oxadiazol-3-yl)-1,2,5-furoxan (**1**) with 100% nitric acid. Compound **3** is only stable at room temperature with 0.5 equivalents ether as a solvate. The stability of the BNAFF^{2-} anion can be tamed by forming alkali metal salts or by reacting it with nitrogen-rich bases. Starting from the potassium salt (**2**, K_2BNAFF), different metal and nitrogen-rich salts with the BNAFF^{2-} anion were synthesized and characterized using multinuclear NMR spectroscopy, vibrational spectroscopy (IR and Raman), X-ray single-crystal diffraction, DTA, BAM sensitivity methods and elemental analysis. In addition, the heats of formation and detonation properties of all anhydrous energetic compounds were calculated. Salt formation leads to the stabilization of the BNAFF^{2-} anion and increase of the thermal stability up to $245 \text{ }^\circ\text{C}$. High detonation velocities ($8000\text{--}8600 \text{ m s}^{-1}$) were calculated for the anhydrous compounds **2**, **4–7**.

4. Experimental Section

General procedures

^1H , ^{13}C , ^{14}N and ^{15}N NMR spectra were recorded on JEOL 270 and BRUKER AMX 400 instruments. The samples were measured at room temperature in standard NMR tubes (\varnothing 5 mm). Chemical shifts are reported as δ values in ppm relative to the residual solvent peaks of d_6 -DMSO (δ_{H} : 2.50, δ_{C} : 39.5). Solvent residual signals and chemical shifts for NMR solvents were referenced against tetramethylsilane (TMS, δ = 0 ppm) and nitromethane. Unless stated otherwise, coupling constants were reported in hertz (Hz) and for the characterization of the observed signal multiplicities the following abbreviations were used: s (singlet), d (doublet), t (triplet), q (quartet), quint (quintet), sept (septet), m (multiplet) and br (broad). Low resolution mass spectra were recorded on a JEOL JMS-700 MStation mass spectrometer (FAB+/-). Infrared spectra (IR) were recorded from 4500 cm^{-1} to 650 cm^{-1} on a PERKIN ELMER Spectrum BX-59343 instrument with a SMITHS DETECTION DuraSamplIR II Diamond ATR sensor. The absorption bands are reported in wavenumbers (cm^{-1}). Raman spectra were recorded using a Bruker MultiRAM FT-Raman instrument fitted with a liquid-nitrogen cooled germanium detector and a Nd:YAG laser (λ = 1064 nm). Elemental analysis was carried on a Elementar Vario el by pyrolysis of the sample and subsequent analysis of the formed gases. Decomposition temperatures were measured *via* differential thermal analysis (DTA) with an OZM Research DTA 552-Ex instrument at a heating rate of $5\text{ }^{\circ}\text{C min}^{-1}$ and in a range of room temperature to $400\text{ }^{\circ}\text{C}$. Melting points were determined in capillaries with a Büchi Melting Point B-540 instrument and are uncorrected. All sensitivities toward impact (IS) and friction (FS) were determined according to BAM (German: Bundesanstalt für Materialforschung und Prüfung) standards using a BAM drop hammer and a BAM friction apparatus. All energetic compounds were tested for sensitivity towards electrical discharge using an Electric Spark Tester ESD 2010 EN from OZM.

CAUTION! All investigated compounds are potentially explosive materials, although no hazards were observed during preparation and handling these compounds. Nevertheless, safety precautions (such as wearing leather coat, face shield, Kevlar sleeves, Kevlar gloves, earthed equipment and ear plugs) should be drawn.

3,4-Bis(4-amino-1,2,5-oxadiazol-3-yl)-1,2,5-furoxan (BAFF)

BAFF was synthesized according to the known literature.[17,18,20]

Dipotassium 3,4-bis(4-nitramino-1,2,5-oxadiazol-3-yl)-1,2,5-furoxan (2)

100% HNO₃ (9.0 mL) was placed in a round bottom flask and 3,4-bis(4-amino-1,2,5-oxadiazol-3-yl)-1,2,5-furoxane (BAFF, 4.0 g, 15.9 mmol) was added in small portions at -10 °C. The reaction was stirred for 1.5 h at the same temperature and then for 1.5 h at -5 °C. The reaction mixture was poured into ice and stirred at room temperature for 2 h. The solution was basified with potassium hydroxide to pH 11. The formed solid material was filtered, washed with small amount of cold water and dried on air to give K₂BNAFF (6.0 g, 90 %).

DTA (5 °C min⁻¹): 245 °C (dec.); **BAM: drop hammer**: 3 J (100–500 μm); friction tester: >72 N (100–500 μm); ESD: 0.19 J (100–500 μm); **IR** (ATR), $\tilde{\nu}$ (cm⁻¹) = 2323 (vw), 1630 (s), 1587 (m), 1518 (m), 1492 (w), 1453 (m), 1436 (m), 1397 (s), 1336 (s), 1290 (ws), 1159 (m), 1049 (w), 990 (m), 963 (m), 928 (m), 910 (m), 872 (w), 864 (w), 829 (w), 813 (s), 796 (s), 777 (s), 754 (m), 741 (m), 713 (m), 696 (w), 602 (vw). **Raman** (1064 nm, 200 mW, 25 °C): $\tilde{\nu}$ (cm⁻¹) = 1633 (11), 1590 (82), 1519 (59), 1492 (38), 1455 (50), 1437 (100), 1413 (13), 1404 (11), 1385 (29), 1214 (12), 1063 (24), 1049 (30), 1013 (61), 816 (19), 519 (22), 503 (17), 326 (17), 239 (12), 196 (24), 131 (93), 90 (52), 78 (26). **¹³C NMR** (*d*₆-DMSO, 101 MHz, ppm) δ = 158.6, 157.8, 146.6, 140.4, 137.4, 106.8. **¹⁴N NMR** (*d*₆-DMSO, 29 MHz, ppm) δ = -14. **¹⁵N NMR** (*d*₆-DMSO, 41 MHz, ppm) δ = 34.1, 31.8, 5.8, 5.5, -6.7, -13.3, -13.8, -24.3, -151.7, -152.8. **Elem. Anal.** (C₆K₂N₁₀O₈, 418.32 g mol⁻¹) calcd.: C 17.23, N 33.48, H 0.00 %. Found: C 17.50, N 33.36, H 0.00 %. *m/z* (FAB⁺): 39 (cation) *m/z* (FAB⁻): 341 (anion + H⁺);

3,4-Bis(4-nitramino-1,2,5-oxadiazol-3-yl)-1,2,5-furoxan (3) • 0.5 Et₂O

K₂BNAFF (277 mg, 0.65 mmol) was dissolved in 2 M hydrochloric acid (5 mL) at 50 °C. The water phase was extracted with Et₂O (4 x 50 mL) and after drying over MgSO₄ the solvent was removed under reduced pressure. 3,4-Bis(4-nitramino-1,2,5-oxadiazol-3-yl)-1,2,5-furoxan (**3**) was obtained with 0.5 Et₂O solvent as an oily liquid (247 mg, 100 %).

DTA (5 °C min⁻¹): 72 °C (dec.); **IR** (ATR), $\tilde{\nu}$ (cm⁻¹) = 2981 (w), 2883 (br), 2733 (br), 2002 (vw), 1612 (s), 1552 (m), 1536 (m), 1467 (m), 1449 (m), 1385 (w), 1298 (vs), 1212 (w), 1184 (vw), 1153 (m), 1094 (m), 1067 (m), 990 (s), 968 (m), 905 (m), 863 (w), 811 (s), 760 (m), 679 (w), 610 (vw), 488 (vw), 462 (vw). **¹H NMR** (*d*₆-DMSO, 400 MHz, ppm) δ = 12.87 (s, 2H, -NHNO₂), 3.34 (q, 4H, -CH₂CH₃), 1.04 (t, 6H, -CH₂CH₃). **¹³C NMR** (*d*₆-DMSO, 101 MHz, ppm) δ = 154.1, 152.8, 145.6, 141.1, 137.1, 106.2, 65.2, 15.4. **¹⁴N NMR** (*d*₆-DMSO, 29 MHz, ppm) δ = -26. **¹⁵N NMR** (*d*₆-DMSO, 41 MHz, ppm) δ = 38.7, 37.5, 14.4, 10.9, -5.6, -22.9, -28.3, -29.1, -183.6, -190.4.

Bis(guanidinium) 3,4-bis(4-nitramino-1,2,5-oxadiazol-3-yl)-1,2,5-furoxan (4)

K₂BNAFF (2.00 g, 4.80 mmol) was dissolved in 2 M hydrochloric acid (16 mL) at 50 °C. The water phase was extracted with Et₂O (4 x 60 mL) and after drying over MgSO₄ the solvent was removed under reduced pressure. The residue was suspended in H₂O (8 mL) and guanidinium carbonate (0.85 g, 4.70 mmol) was added in small portions. The reaction mixture was heated until all solid material was dissolved. After cooling to room temperature the separated solid material was filtered, washed with water and dried on air to give **4** (1.76 g, 80 %).

DTA (5 °C min⁻¹): 189 °C (dec.); **BAM: drop hammer**: 15 J (100–500 μm); friction tester: 360 N (100–500 μm); ESD: 0.75 J (100–500 μm); **IR** (ATR), $\tilde{\nu}$ (cm⁻¹) = 3499 (m), 3447 (s), 3322 (m), 3269 (m), 3187 (m), 1651 (s), 1584 (m), 1517 (m), 1491 (w), 1455 (m), 1433 (w), 1396 (s), 1338 (m), 1290 (vs), 1157 (m), 1014 (w), 985 (m), 958 (m), 927 (m), 919 (m), 919 (m), 874 (w), 820 (m), 799 (s), 775 (m), 738 (w), 703 (w), 687 (w), 609 (w). **Raman** (1064 nm, 200 mW, 25 °C): $\tilde{\nu}$ (cm⁻¹) = 1627 (10), 1585 (100), 1520 (42), 1490 (29), 1456 (47), 1430 (64), 1404 (11), 1385 (16), 1207 (14), 1045 (25), 1016 (86), 821 (12), 516 (20), 493 (10), 462 (10), 338 (12), 312 (10), 254 (10), 243 (10), 170 (20), 96 (89), 71 (36). **¹H NMR** (*d*₆-DMSO, 400 MHz, ppm) δ = 6.90 (s, 6H,) **¹³C NMR** (*d*₆-DMSO, 101 MHz, ppm) δ = 158.6, 157.9, 157.8, 146.6, 140.5, 137.3, 106.8. **¹⁴N NMR** (*d*₆-DMSO, 29 MHz, ppm) δ = -14. **Elem. Anal.** (C₈H₁₂N₁₆O₈, 460.29 g mol⁻¹) calcd.: C 20.88, H 2.63, N 48.69 %. Found: C 20.28, H 2.74, N 48.93 %. *m/z* (FAB⁺): 60 (cation); *m/z* (FAB⁻): 341 (anion + H⁺);

Bis(aminoguanidinium) 3,4-bis(4-nitramino-1,2,5-oxadiazol-3-yl)-1,2,5-furoxan (5)

K₂BNAFF (1.50 g, 3.60 mmol) was dissolved in 2 M hydrochloric acid (12 mL) at 50 °C. The water phase was extracted with Et₂O (4 x 60 mL) and after drying over MgSO₄ the solvent was removed under reduced pressure. The residue was suspended in H₂O (10 mL) and aminoguanidinium carbonate (0.98 g, 7.20 mmol) was added in small portions. The reaction mixture was heated until all solid was dissolved. After cooling to room temperature the separated solid material was filtered, washed with water and dried on air to give **5** (1.50 g, 85 %).

DTA (5 °C min⁻¹): 128 (m.p.), 156 °C (dec.); **BAM: drop hammer**: 8 J (100–500 μm); friction tester: 360 N (100–500 μm); ESD: 1.00 J (100–500 μm); IR (ATR), $\tilde{\nu}$ (cm⁻¹) = 3426 (m), 3347 (m), 3188 (br), 1651 (s), 1607 (m), 1578 (s), 1519 (m), 1494 (m), 1449 (w), 1410 (w), 1389 (m), 1335 (m), 1298 (vs), 1208 (m), 1091 (m), 1012 (w), 989 (m), 961 (s), 929 (m), 835 (m), 819 (m), 804 (m), 769 (m), 736 (w), 696 (vw). **Raman** (1064 nm, 200 mW, 25 °C): $\tilde{\nu}$ (cm⁻¹) = 1610 (38), 1583 (29), 1561 (24), 1521 (32), 1496 (100), 1448 (45), 1411 (69), 1365 (15), 1215 (10), 1163 (14), 1072 (13), 1041 (40), 1014 (95), 993 (18), 971 (32), 818 (14), 523 (10), 499 (18), 487 (18), 340 (22), 250 (28), 200 (10), 121 (80), 72 (78). **¹H NMR** (*d*₆-DMSO, 400 MHz, ppm) δ = 7.00 (br, 4H), 4.67 (s, 2H). **¹³C NMR** (*d*₆-DMSO, 101 MHz, ppm) δ = 158.8, 158.6, 157.9, 146.6, 140.5, 137.4, 106.8. **¹⁴N NMR** (*d*₆-DMSO, 29 MHz, ppm) δ = -13. **Elem. Anal.** (C₈H₁₄N₁₈O₈, 490.32 g mol⁻¹) calcd.: C 19.60, H 2.88, N 51.42 %. Found: C 20.08, H 2.86, N 51.05 %. ***m/z*** (FAB⁺): 75 (cation); ***m/z*** (FAB⁻): 341 (anion + H⁺);

Bis(ammonium) 3,4-bis(4-nitramino-1,2,5-oxadiazol-3-yl)-1,2,5-furoxan (6)

K₂BNAFF (1.67 g, 4.00 mmol) was dissolved in 2 M hydrochloric acid (20 mL) at 50 °C. The water phase was extracted with Et₂O (4 x 50 mL) and after drying over MgSO₄ the solvent was removed under reduced pressure. The residue was dissolved in methanol (10 mL) and aqueous ammonia (25 %, 0.64 mL) with methanol (3 mL) was added. The solution was stirred for 1 h at room temperature and the solvent was removed under reduced pressure. Compound **6** was obtained as white powder (1.41 g, 94 %).

DTA (5 °C min⁻¹): 161 °C (dec.); **BAM: drop hammer**: 7 J (100–500 μm); friction tester: 216 N (100–500 μm); ESD: 0.70 J (100–500 μm); **IR** (ATR), $\tilde{\nu}$ (cm⁻¹) = 3194 (br), 1624 (m), 1580 (m), 1519 (m), 1492 (w), 1402 (s), 1283 (vs), 1157 (m), 1047 (vw), 1007 (m), 989 (m), 962 (m), 927 (m), 911 (m), 875 (w), 865 (w), 832 (w), 814 (s), 795 (s), 772 (s), 753 (m), 741 (m), 712 (m), 694 (w). **Raman** (1064 nm, 200 mW, 25 °C): $\tilde{\nu}$ (cm⁻¹) = 1627 (11), 1590 (100), 1520 (57), 1494 (42), 1455 (45), 1439 (37), 1427 (37), 1401 (25), 1213 (14), 1064 (31), 1048 (28), 1011 (79), 817 (20), 518 (26), 501 (19), 330 (17), 185 (26), 126 (68). **¹H NMR** (*d*₆-DMSO, 400 MHz, ppm) δ = 7.10 (s, 4H, NH₄⁺). **¹³C NMR** (*d*₆-DMSO, 101 MHz, ppm) δ = 158.6, 157.8, 146.6, 140.5, 137.4, 106.8. **¹⁴N NMR** (*d*₆-DMSO, 29 MHz, ppm) δ = -13. **Elem. Anal.** (C₆H₈N₁₂O₈, 376.21 g mol⁻¹) calcd.: C 19.16, H 2.14, N 44.68 %. Found: C 19.36, H 2.12, N 44.48 %. ***m/z*** (FAB⁺): 18 (cation); ***m/z*** (FAB⁻): 341 (anion + H⁺);

Bis(hydrazinium) 3,4-bis(4-nitramino-1,2,5-oxadiazol-3-yl)-1,2,5-furoxan (7)

K₂BNAFF (1.67 g, 4.00 mmol) was dissolved in 2 M hydrochloric acid (20 mL) at 50 °C. The water phase was extracted with Et₂O (4 x 60 mL) and after drying over MgSO₄ the solvent was removed under reduced pressure. The residue was dissolved in methanol (10 mL) and hydrazinium hydroxide (0.40 mL) was added dropwise. The solution was stirred at room temperature for 1 h. The solvent was removed in vacuo and the yellowish solid was dried on air to give **7** (1.52 g, 93 %).

DTA (5 °C min⁻¹): 170 °C (dec.); **BAM: drop hammer**: 8 J (100–500 μm); friction tester: 216 N (100–500 μm); ESD: 0.50 J (100–500 μm); **IR** (ATR), $\tilde{\nu}$ (cm⁻¹) = 3352 (m), 3186 (m), 3042 (br), 2639 (br), 2048 (vw), 1644 (m), 1608 (m), 1582 (m), 15163 (m), 1492 (m), 1449 (m), 1435 (w), 1401 (m), 1357 (m), 1288 (vs), 1155 (m), 1089 (s), 1009 (w), 992 (m), 962 (s), 925 (m), 873 (w), 821 (m), 795 (s), 770 (s), 755 (m), 738 (m), 708 (w), 697 (m). **Raman** (1064 nm, 200 mW, 25 °C): $\tilde{\nu}$ (cm⁻¹) = 1591 (28), 1579 (42), 1569 (24), 1561 (23), 1518 (71), 1491 (27), 1450 (43), 1437 (93), 1402 (12), 1374 (11), 1336 (10), 1209 (18), 1060 (33), 1045 (16), 1011 (100), 969 (11), 821 (23), 596 (10), 515 (19), 480 (10), 408 (11), 287 (12), 243 (22), 85 (99). **¹H NMR** (*d*₆-DMSO, 400 MHz, ppm) δ = 6.24 (s, 5H, N₂H₅⁺). **¹³C NMR** (*d*₆-DMSO, 101 MHz, ppm) δ = 158.6, 157.9, 146.6, 140.5, 137.4, 106.8. **¹⁴N NMR** (*d*₆-DMSO, 29 MHz, ppm) δ = -13. **Elem. Anal.** (C₆H₁₀N₁₄O₈, 406.24 g mol⁻¹) calcd.: C

17.74, H 2.48, N 48.27 %. Found: C 18.20, H 2.78, N 47.70 %. m/z (FAB⁺): 33 (cation); m/z (FAB⁻): 341 (anion + H⁺);

Bis(hydroxylammonium) 3,4-bis(4-nitramino-1,2,5-oxadiazol-3-yl)-1,2,5-furoxan hexahydrate (8)

K₂BNAFF (1.50 g, 3.60 mmol) was dissolved in 2 M hydrochloric acid (16 mL) at 50 °C. The water phase was extracted with Et₂O (4 x 60 mL) and after drying over MgSO₄ the solvent was removed under reduced pressure. The residue was suspended in H₂O (8 mL) and hydroxylamine solution (50 wt % in H₂O, 0.45 mL) was added dropwise. The reaction was cooled down to 0 °C and the separated crystalline powder was filtered and dried on air to give compound 8 as hexahydrate (1.16 g, 63 %).

DTA (5 °C min⁻¹): 134 °C (dec.); **BAM: drop hammer**: 25 J (100–500 μm); friction tester: 360 N (100–500 μm); ESD: 1.00 J (100–500 μm); **IR** (ATR), $\tilde{\nu}$ (cm⁻¹) = 3577 (m), 3252 (br), 3014 (br), 2743 (s), 1634 (s), 1611 (m), 1527 (s), 1503 (s), 1463 (m), 1421 (w), 1402 (m), 1333 (vs), 1305 (vs), 1224 (m), 1168 (m), 1075 (vw), 1041 (vw), 1007 (m), 989 (m), 962 (m), 916 (vw), 878 (vw), 827 (w), 800 (m), 768 (m), 696 (w). **Raman** (1064 nm, 200 mW, 25 °C): $\tilde{\nu}$ (cm⁻¹) = 1630 (36), 1612 (36), 1597 (24), 1583 (39), 1527 (28), 1502 (100), 1464 (55), 1440 (16), 1420 (54), 1404 (23), 1169 (14), 1076 (13), 1042 (36), 1014 (78), 990 (23), 880 (12), 825 (10), 599 (12), 517 (10), 498 (18), 492 (20), 448 (11), 346 (22), 119 (15), 160 (32), 121 (91), 93 (91). **¹H NMR** (*d*₆-DMSO, 400 MHz, ppm) δ = 10.02 (s, H, NH₃OH⁺) **¹³C NMR** (*d*₆-DMSO, 101 MHz, ppm) δ = 158.7, 157.9, 146.6, 140.5, 137.5, 106.9. **¹⁴N NMR** (*d*₆-DMSO, 29 MHz, ppm) δ = -14. **Elem. Anal.** (C₆H₂₀N₁₂O₁₆, 516.29 g mol⁻¹) calcd.: C 13.96, H 3.90, N 32.56 %. Found: C 14.64, H 3.86, N 32.61 %. m/z (FAB⁺): 34 (cation); m/z (FAB⁻): 341 (anion + H⁺);

Bis(3,6,7-triamino-[1,2,4]triazolo[4,3-*b*][1,2,4]triazolium) 3,4-bis(4-nitramino-1,2,5-oxadiazol-3-yl)-1,2,5-furoxan trihydrate (9)

K₂BNAFF (428 mg, 1.02 mmol) was dissolved in 2 M hydrochloric acid (5 mL) at 50 °C. The water phase was extracted with Et₂O (4 x 30 mL) and after drying over MgSO₄ the solvent was removed under reduced pressure. The residue was dissolved in MeOH/H₂O (5:5 mL) and TATOT (316 mg, 2.05 mmol) was added. The reaction mixture was heated until the solid material was dissolved. The reaction mixture was stirred for an additional 1 h and then cooled down to room temperature. The separated solid was filtered and dried on air to yield 9 as trihydrate (482 mg, 68 %).

DTA (5 °C min⁻¹): 190 °C (dec.); **BAM: drop hammer**: 40 J (100–500 µm); friction tester: 360 N (100–500 µm); ESD: 0.70 J (100–500 µm); **IR** (ATR), $\tilde{\nu}$ (cm⁻¹) = 3643 (vw), 3457 (w), 3303 (m), 3124 (br), 1691 (m), 1652 (s), 1513 (m), 1425 (m), 1395 (m), 1288 (vs), 1164 (w), 1042 (m), 1014 (w), 959 (m), 933 (m), 881 (w), 848 (w), 823 (m), 772 (m), 753 (w), 724 (w), 708 (m), 684 (m), 619 (w). **Raman** (1064 nm, 200 mW, 25 °C): $\tilde{\nu}$ (cm⁻¹) = 1591 (35), 1584 (37), 1515 (41), 1456 (18), 1433 (56), 1263 (20), 1042 (17), 1016 (40), 852 (24), 620 (12), 602 (15), 400 (14), 236 (11), 108 (100), 85 (80). **¹H NMR** (*d*₆-DMSO, 400 MHz, ppm) δ = 8.12 (2, 2H, NH₂), 7.20 (2, 2H, NH₂), 5.76 (2, 2H, NH₂). **¹³C NMR** (*d*₆-DMSO, 101 MHz, ppm) δ = 160.1, 158.7, 157.9, 147.4, 146.6, 141.1, 140.4, 137.3, 106.8. **¹⁴N NMR** (*d*₆-DMSO, 29 MHz, ppm) δ = -13. **Elem. Anal.** (C₁₂H₂₀N₂₆O₁₁, 704.46 g mol⁻¹) calcd.: C 20.46, H 2.86, N 51.70 %. Found: C 20.80, H 2.81, N 51.36 %. ***m/z*** (FAB⁺): 155 (cation); ***m/z*** (FAB⁻): 341 (anion + H⁺);

Disilver 3,4-bis(4-nitramino-1,2,5-oxadiazol-3-yl)-1,2,5-furoxan dihydrate (10)

K₂BNAFF (420 mg, 1.00 mmol) was dissolved in 2 M hydrochloric acid (5 mL) at 50 °C. The water phase was extracted with Et₂O (4 x 30 mL) and after drying over MgSO₄ the solvent was removed under reduced pressure. The residue was dissolved in MeOH/H₂O (6:3 mL) and AgNO₃ (340 mg, 2.00 mmol) was added. The reaction mixture was stirred for 30 min at room temperature. The solid material was then filtered and dried on air to give 10 as a dihydrate (395 mg, 67 %) as white solid.

DTA (5 °C min⁻¹): 82 °C (dec.); **BAM: drop hammer**: 1 J (100–500 µm); friction tester: 60 N (100–500 µm); ESD: 50 mJ (100–500 µm); **IR** (ATR), $\tilde{\nu}$ (cm⁻¹) = 3562 (br), 3242 (br), 1636 (m), 1595 (w), 1563 (m), 1516 (m), 1501 (m), 1432 (s), 1364 (m), 1324 (s), 1290 (vs), 1170 (m), 1072 (w), 1009 (m), 995 (s), 974 (m), 941 (m), 911 (w), 871 (m), 817 (s), 768 (m), 748 (w), 693 (m), 598 (vw), 582 (vw),

521 (w). **Raman** (1064 nm, 200 mW, 25 °C): $\tilde{\nu}$ (cm⁻¹) = 1646 (15), 1599 (65), 1576 (22), 1531 (70), 1506 (37), 1439 (56), 1372 (20), 1171 (11), 1067 (65), 1014 (32), 926 (12), 815 (16), 773 (11), 762 (15), 753 (25), 598 (15), 552 (11), 505 (44), 460 (17), 434 (11), 321 (20), 308 (15), 248 (19), 98 (100). **¹³C NMR** (*d*₆-DMSO, 101 MHz, ppm) δ = 157.9, 156.9, 145.9, 140.1, 137.1, 106.6. **¹⁴N NMR** (*d*₆-DMSO, 29 MHz, ppm) δ = -15. **Elem. Anal.** (C₆H₄Ag₂N₁₀O₁₀, 591.89g mol⁻¹) calcd.: C 12.18, H 0.68, N 23.66 %. Found: C 12.11, H 0.51, N 23.69 %.

5. Reference

- [1] a) P. Yin, J. M. Shreeve, From *N*-Nitro to *N*-Nitroamino: Preparation of High-Performance Energetic Materials by Introducing Nitrogen-Containing Ions, *Angew. Chem. Int. Ed.* **2015**, *54*, 1–6. b) D. Fischer, J. L. Gottfried, T. M. Klapötke, K. Karaghiosoff, J. Stierstorfer and T. G. Witkowski, Synthesis and Investigation of Advanced Energetic Materials Based on Bispyrazolylmethanes, *Angew. Chem., Int. Ed.*, **2016**, *55*, 16132–16135.
- [2] J. P. Agrawal, Recent trends in high-energy materials, *Prog. Energy Combust. Sci.* **1998**, *24*, 1–30.
- [3] T. M. Klapötke, *Chemistry of High-Energy Materials*, 3rd Edition, Walter de Gruyter GmbH & Co KG, Berlin, **2015**.
- [4] J. J. Sabatini, K. D. Oyler, Recent Advances in the Synthesis of High Explosive Materials, *Crystals* **2016**, *6*, 5–22.
- [5] R. J. Spear, W. S. Wilson, Recent Approaches to the Synthesis of High Explosives and Energetic Materials: A Review, *J. Energ. Mater.* **1984**, *2*, 61–149.
- [6] B. T. Federoff, H. A. Aaronson, E. F. Reese, O. E. Sheffield, G. D. Clift, *Encyclopedia of Explosives and Related Items*, Picatinny Arsenal: Dover, USA, **1960**.
- [7] J. P. Agrawal, R. Hodgson, *Organic Chemistry of Explosives*, 2nd Edition, John Wiley & Sons: Chichester, England, **2007**.
- [8] P. F. Pagoria, G. S. Lee, A. R. Mitchell, R. D. Schmidt, A Review of Energetic Materials Synthesis, *Thermochim. Acta* **2002**, *384*, 187–204.
- [9] a) A. B. Sheremetev, E. A. Ivanova, N. P. Spiridonova, S. F. Melnikova, I. V. Tselinsky, K. Y. Suponitsky, M. Y. Antipin, Desilylative, Desilylative Nitration of *C,N*-Disilylated 3-Amino-4-methylfurazan, *J. Heterocycl. Chem.* **2007**, *42*, 1237–1242. b) Z. Feng-qi, C. Pei, H. Rong-zu, L. Yang, Z. Zhi-zhong, Z. Yan-shui, Y. Xu-wu, G. Yin, G. Sheng-li, S. Qi-zhen, Thermochemical

- properties and non-isothermal decomposition reaction kinetics of 3,4-dinitrofurazanfuroxan (DNTF), *J. Hazard. Mater.* **2004**, *113*, 67–71
- [10] A. I. Stepanov, D. V. Dashko, A. A. Astrat'ev, 1,2-Di(4-R-furazan-3-yl)glyoximes: Synthesis by the reduction of 3,4-bis(4-R-furazan-3-yl)furoxans and study of the reactivity of these compounds, *Chem. Heterocycl. Comp.* **2013**, *49*, 776–790.
- [11] D. E. Chavez, D. A. Parrish, P. Leonard, The Synthesis and Characterization of a New Furazan Heterocyclic System, *Synlett* **2012**, *23*, 2126–2128.
- [12] D. Fischer, T. M. Klapötke, M. Reymann, J. Stierstorfer, Dense Energetic Nitraminofurazanes, *Chem. Eur. J.* **2014**, *20*, 6401–6411.
- [13] a) Y. Tang, C. He, L. A. Mitchell, D. A. Parrish, J. M. Shreeve, Potassium 4,4'-Bis(dinitromethyl)-3,3'-azofurazanate: A Highly Energetic 3D Metal-Organic Framework as a Promising Primary Explosive, *Angew. Chem.* **2016**, *128*, 1–4. b) X. Wang, K. Xu, Q. Sun, B. Wang, C. Zhou, F. Zhao, The Insensitive Energetic Material Trifurazanooxacycloheptatriene (TFO): Synthesis and Detonation Properties, *Propellants Explos. Pyrotech.* **2015**, *40*, 9–12.
- [14] D. E. Chavez, *Energetic Heterocyclic N-Oxides*. In: Larionov O. (eds) *Heterocyclic N-Oxides. Topics in Heterocyclic Chemistry*, *53*, Springer, **2017**, 1–27.
- [15] P. W. Leonard, C. J. Pollard, D. E. Chavez, B. M. Rice, D. A. Parrish, 3,6-Bis(4-nitro-1,2,5-oxadiazol-3-yl)-1,4,2,5-dioxadiazene (BNDD): A Powerful Sensitive Explosive, *Synlett* **2011**, *14*, 2097–2099.
- [16] Y. Tang, J. Zhang, L. A. Mitchell, D. A. Parrish, J. M. Shreeve, Taming of 3,4-Di(nitramino)furazan, *J. Am. Chem. Soc.* **2015**, *123*, 15984–15987.
- [17] R. Tsyshevsky, P. Pagoria, M. Zhang, A. Racoveanu, A. DeHope, D. Parrish, M. Kuklja, Searching for Low-Sensitivity Cast-Melt High-Energy-Density Materials: Synthesis, Characterization, and Decomposition Kinetics of 3,4-Bis(4-nitro-1,2,5-oxadiazol-3-yl)-1,2,5-oxadiazole-2-oxide, *J. Phys. Chem. C* **2015**, *119*, 3509–3521.
- [18] S. Loebbecke, H. Schuppler, W. Schweikert, Thermal Properties of Different Substituted Energetic Furoxans. *Proceedings of the 33rd International Annual Conference of ICT (Energetic Materials)*, Karlsruhe, Germany, June 25–28, **2002**.
- [19] F.-Q. Zhao, P. Chen, R.-Z. Hu, Y. Luo, Z.-Z. Zhang, Y.-S. Zhou, X.-W. Yang, Y. Gao, S.-L. Gao, Q.-Z. Shi, Thermochemical properties and non-isothermal decomposition reaction kinetics of 3,4-dinitro-furazanfuroxan (DNTF), *J. Hazard. Mater.* **2004**, *113*, 67–71.

- [20] R. Tsyshkevsky, P. Pagoria, M. Zhang, A. Racoveany, D. A. Parrish, A. S. Smirnov, M. M. Kuklja, Comprehensive End-to-End Design of Novel High Energy Density Materials: I. Synthesis and Characterization of Oxadiazole Based Heterocycles, *J. Phys. Chem. C* **2017**, *121*, 23853–23864.
- [21] a) W. Zheng, J.-N. Wang, Review on 3,4-Bisnitrofurazanfuroxan (DNTF), *Chin. J. Energ. Mater.* **2006**, *14*, 463–466. b) C.-H. Lim, T.-K. Kim, K.-H. Kim, K.-H. Chung, J.-S. Kim, Synthesis and Characterization of Bisnitrofurazanofuroxan, *Bull. Korean Chem. Soc.* **2010**, *31*, 1400–1402. c) A. A. Kotomin, A. S. Kozlov, S. A. Dushenok, Detonability of High-Energy-Density Heterocyclic Compounds, *Russ. J. Phys. Chem. B* **2007**, *1*, 573–575.
- [22] I. V. Tselinski, S. F. Mel'nikova, T. V. Romanova, N. P. Spiridonova, E. A. Dundukova, Dimerization of Nitrile Oxides of the 1,2,5-Oxadiazole Series, *Russ. J. Org. Chem.* **2001**, *37*, 1335–1356.
- [23] T. M. Klapötke, P. Schmid, J. Stierstorfer, Crystal Structures of Furazanes, *Crystals* **2015**, *5*, 518–432.
- [24] C. S. Choi, E. Prince, The crystal structure of cyclotrimethylene-trinitramine, *Acta Crystallographica Section B* **1972**, *28*, 2857–2862.
- [25] M. Sućeska, EXPLO5 Version 6.03 User's Guide. Zagreb, Croatia: OZM; 2015.
- [26] Reichel & Partner GmbH, <http://www.reichelt-partner.de>.
- [27] *Test Methods According to the UN Recommendations on the Transport of Dangerous Goods, Manual of Test and Criteria, Fourth Revised Edition, United Nations Publication, New York and Geneva*, **2003**, ISBN 92-1-139087-7, Sales No. E.03.VIII. 2; 13.4.2 Test 3a (ii) BAM Fallhammer.
- [28] J. S. Murray, P. Politzer, Impact sensitivity and crystal lattice compressibility/free space. *J. Mol. Model* **2014**, *20*, 2223–2227.

6. Supporting Information

6.1 X-ray Diffraction

The low-temperature single-crystal X-ray diffraction measurements were performed on an Oxford XCalibur3 diffractometer equipped with a Spellman generator (voltage 50 kV, current 40 mA) and a KappaCCD detector operating with MoK α radiation ($\lambda = 0.7107$ Å). Data collection was performed using the CRYSLIS CCD software.^[S1] The data reduction was carried out using the CRYSLIS RED software.^[S2] The solution of the structure was performed by direct methods (SIR97)^[S3] and refined by full-matrix least-squares on F² (SHELXL)^[S4] implemented in the WINGX software package^[S5] and finally checked with the PLATON software.^[S6] All DIAMOND2 plots are shown with thermal ellipsoids at the 50% probability level and hydrogen atoms are shown as small spheres of arbitrary radius.

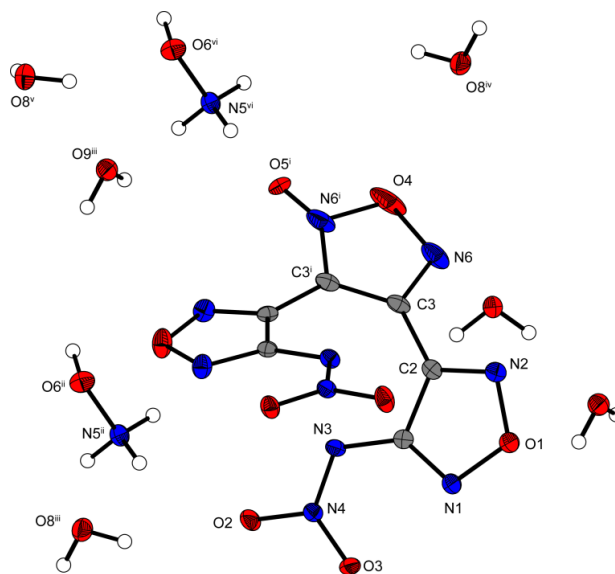


Figure S1. Representation of the molecular unit of **8**, showing the atom-labeling scheme. Thermal ellipsoids represent the 50 % probability level and hydrogen atoms are shown as small spheres of arbitrary radius. Symmetry code: (i) 1-x, y, 0.5-z; (ii) 1-x, 1-y, 1-z; (iii) -0.5+x, -0.5+y, z; (iv) 1.5-x, 1.5-y, 1-z; (v) -0.5+x, 1.5-y, 0.5+z; (vi) 1-x, 2-y, 1-z;

Bis(hydroxylammonium) 3,4-bis(4-nitramino-1,2,5-oxadiazol-3-yl)-1,2,5-furoxan (**8**) hexahydrate crystallizes with inclusion of six molecules of crystal water per molecular unit in the monoclinic

space group $C2/c$. The measured density at 123 K of 1.665 g cm^{-3} is rather low due to the six molecules water in the crystal structure.

Table S1. Crystallographic details of compounds **2**, **4** and **5**.

	2	4	5
Formula	$\text{C}_6\text{K}_2\text{N}_{10}\text{O}_8$	$\text{C}_8\text{H}_{12}\text{N}_{16}\text{O}_8$	$\text{C}_8\text{H}_{14}\text{N}_{18}\text{O}_8$
Form. Mass [g mol^{-1}]	418.36	460.29	490.32
Crystal system	triclinic	monoclinic	orthorhombic
Space Group	$P\bar{1}$ (No. 2)	$P2/c$ (No. 13)	$C2/c$ (No. 15)
Color / Habit	colorless block	colorless block	colorless block
Size [mm]	0.01 x 0.03 x 0.04	$0.26 \times 0.18 \times 0.12$	$0.20 \times 0.15 \times 0.10$
a [pm]	453.13(3)	1787.44(5)	1561.13(10)
b [pm]	693.55(5)	775.80(2)	826.35(4)
c [pm]	2156.75(16)	1356.32(4)	1480.72(8)
α [°]	91.561(3)	90	90
β [°]	91.303(3)	110.523(3)	102.714(7)
γ [°]	105.748(3)	90	90
V [pm^3]	$651.80(8) \cdot 10^6$	$1761.43(9) \cdot 10^6$	$1863.35(19) \cdot 10^6$
Z	2	4	4
$\rho_{\text{calc.}}$ [g cm^{-3}]	2.132	1.736	1.748
μ [mm^{-1}]	0.805	0.153	0.153
$F(000)$	416	944	1008
$\lambda_{\text{MoK}\alpha}$ [pm]	71.073	71.073	71.073
T [K]	103	123(2)	123(2)
ϑ min-max [°]	3.2, 26.3	4.1, 26.5	4.6, 30.5
Dataset h; k; l	-5:5; -8:8; 0:26	-22:22; -9:9; -17:17	-19:19; -10:9; -18:18
Reflect. coll.	2272	26218	7036
Independ. refl.	2272	3626	1928
R_{int}	0.079	0.029	0.028
Reflection obs.	2272	3150	1591

No. parameters	236	347	187
R_1 (obs)	0.0295	0.0484	0.0378
wR_2 (all data)	0.0716	0.0996	0.0872
S	1.20	1.22	1.08
Resd. Dens. [$e \text{ pm}^{-3}$]	$-0.33, 0.29 \cdot 10^{-6}$	$-0.35, 0.26 \cdot 10^{-6}$	$-0.32, 0.20 \cdot 10^{-6}$
Device type	Oxford Xcalibur3	Oxford Xcalibur3	Oxford Xcalibur3
	CCD	CCD	CCD
Solution	SIR-92	SIR-92	SIR-92
Refinement	SHELXL-97	SHELXL-97	SHELXL-97
Absorpt. corr.	multi-scan	multi-scan	multi-scan
CCDC	1589059	1589062	1589063

Table S2. Crystallographic details of compounds **8** and **10**.

Compound	8 · 6 H ₂ O	10 · 2 NH ₃
Formula	C ₆ H ₂₀ N ₁₂ O ₁₆	C ₈ H ₆ Ag ₂ N ₁₂ O ₈
Form. Mass [g mol^{-1}]	516.34	589.97
Crystal system	monoclinic	triclinic
Space Group	$C2/c$ (No. 15)	$P-1$ (No. 2)
Color / Habit	colorless block	colorless block
Size [mm]	$0.25 \times 0.15 \times 0.10$	$0.02 \times 0.08 \times 0.17$
a [pm]	2118.44(12)	706.07(6)
b [pm]	751.25(3)	1046.69(8)
c [pm]	1333.39(7)	1191.19(9)
α [°]	90	64.293(8)
β [°]	103.849(6)	81.963(7)
γ [°]	90	88.871(7)
V [pm ³]	$2060.37(19) \cdot 10^6$	$784.58(12) \cdot 10^6$
Z	4	2
$\rho_{\text{calc.}}$ [g cm^{-3}]	1.665	2.497

μ [mm ⁻¹]	0.162	2.572
$F(000)$	1072	568
$\lambda_{\text{MoK}\alpha}$ [pm]	71.073	71.073
T [K]	123(2)	173(2)
ϑ min-max [°]	4.4, 27.0	4.3, 26.0
Dataset h; k; l	-21:26;-9:9;-17:15	-8:8;-12:12;-14:12
Reflect. coll.	8343	5774
Independ. refl.	2247	3073
R_{int}	0.030	0.031
Reflection obs.	1898	2403
No. parameters	199	287
R_1 (obs)	0.0356	0.0322
w R_2 (all data)	0.0772	0.0710
S	1.08	1.01
Resd. Dens. [e pm ⁻³]	-0.38, 0.33 · 10 ⁻⁶	-0.67, 0.90 · 10 ⁻⁶
Device type	Oxford Xcalibur3 CCD	Oxford Xcalibur3 CCD
Solution	SIR-92	SIR-92
Refinement	SHELXL-97	SHELXL-97
Absorpt. corr.	multi-scan	multi-scan
CCDC	1589061	1589060

6.2 Computations

Quantum chemical calculations were carried out using the Gaussian G09 program package.[S7] The enthalpies (H) and free energies (G) were calculated using the complete basis set (CBS) method of Petersson and co-workers in order to obtain very accurate energies. The CBS models use the known asymptotic convergence of pair natural orbital expressions to extrapolate from calculations using a finite basis set to the estimated CBS limit. CBS-4 begins with an HF/3-21G(d) geometry optimization; the zero point energy is computed at the same level. It then uses a large basis set SCF calculation as a base energy, and an MP2/6-31+G calculation with a CBS extrapolation to correct

the energy through second order. An MP4(SDQ)/6-31+ (d,p) calculation is used to approximate higher order contributions. In this study, we applied the modified CBS.

Heats of formation of ionic compounds were calculated using the atomization method (equation 1) using room temperature CBS-4M enthalpies summarized in Table S3.[S8,S9]

$$\Delta_f H^\circ_{(g, M, 298)} = H_{(Molecule, 298)} - \sum H^\circ_{(Atoms, 298)} + \sum \Delta_f H^\circ_{(Atoms, 298)} \quad (1)$$

Table S3. CBS-4M electronic enthalpies for atoms C, H, N and O and their literature values for atomic $\Delta_f H^\circ_{298}$ / kJ mol⁻¹

	$-H^{298}$ / a.u.	NIST [S10]
H	0.500991	218.2
C	37.786156	717.2
N	54.522462	473.1
O	74.991202	249.5

In the case of the ionic compounds, the lattice energy (U_l) and lattice enthalpy (ΔH_l) were calculated from the corresponding X-ray molecular volumes according to the equations provided by *Jenkins and Glasser*. [S11] With the calculated lattice enthalpy the gas-phase enthalpy of formation was converted into the solid state (standard conditions) enthalpy of formation. These molar standard enthalpies of formation (ΔH_m) were used to calculate the molar solid state energies of formation (ΔU_m) according to equation 2.

$$\Delta U_m = \Delta H_m - \Delta n RT \quad (2)$$

(Δn being the change of moles of gaseous components)

The calculation results are summarized in Tables S4 and S5.

Table S4. CBS-4M results and calculated gas-phase enthalpies.

Ion	M [g mol ⁻¹] [a]	-H ²⁹⁸ [b] / a.u.	$\Delta_f H^\circ(\text{g,M})$ / kJ mol ⁻¹ [c]
BNAFF²⁻	340.1	1375.855059	563.9
K⁺	39.1	599.03597	487.7
G⁺	60.1	205.453192	571.2
AG⁺	75.1	260.701802	671.6
NH₄⁺	18.1	56.796608	635.8
N₂H₅⁺	66.1	112.030523	774.5

[a] Molecular weight; [b] CBS-4M electronic enthalpy; [c] gas phase enthalpy of formation;

Table S5. Calculation results.

Compound	$\Delta_f H^\circ(\text{g,M})$ / kJ mol ⁻¹ [a]	V _M / nm ³ [b]	ΔU_L kJ mol ⁻¹ [c]	ΔH_L kJ mol ⁻¹ [d]	$\Delta_f H^\circ(\text{s})$ kJ mol ⁻¹ [e]	Δn [f]	$\Delta_f U(\text{s})$ kJ kg ⁻¹ [g]
2	1539.3	0,3479348	1243.8	1251.2	288.1	9	742.4
4	1707.7	0.4641811	1113.4	1120.9	586.8	18	1371.8
5	1907.1	0.4894795	1090.8	1098.2	808.9	20	1750.9
6	1835.6	0.3714202	1213.1	1220.6	614.9	14	1726.9
7	2112.2	0.3861776	1195.2	1202.6	909.6	16	2336.7

[a] gas phase enthalpy of formation; [b] molecular volumes taken from X-ray structures and corrected to room temperature; [c] lattice energy (calculated using Jenkins and Glasser equations); [d] lattice enthalpy (calculated using Jenkins and Glasser equations); [e] standard solid state enthalpy of formation; [f] change of moles of gaseous components when formed; [g] solid state energy of formation.

6.3 Differential Thermal Analysis (DTA)

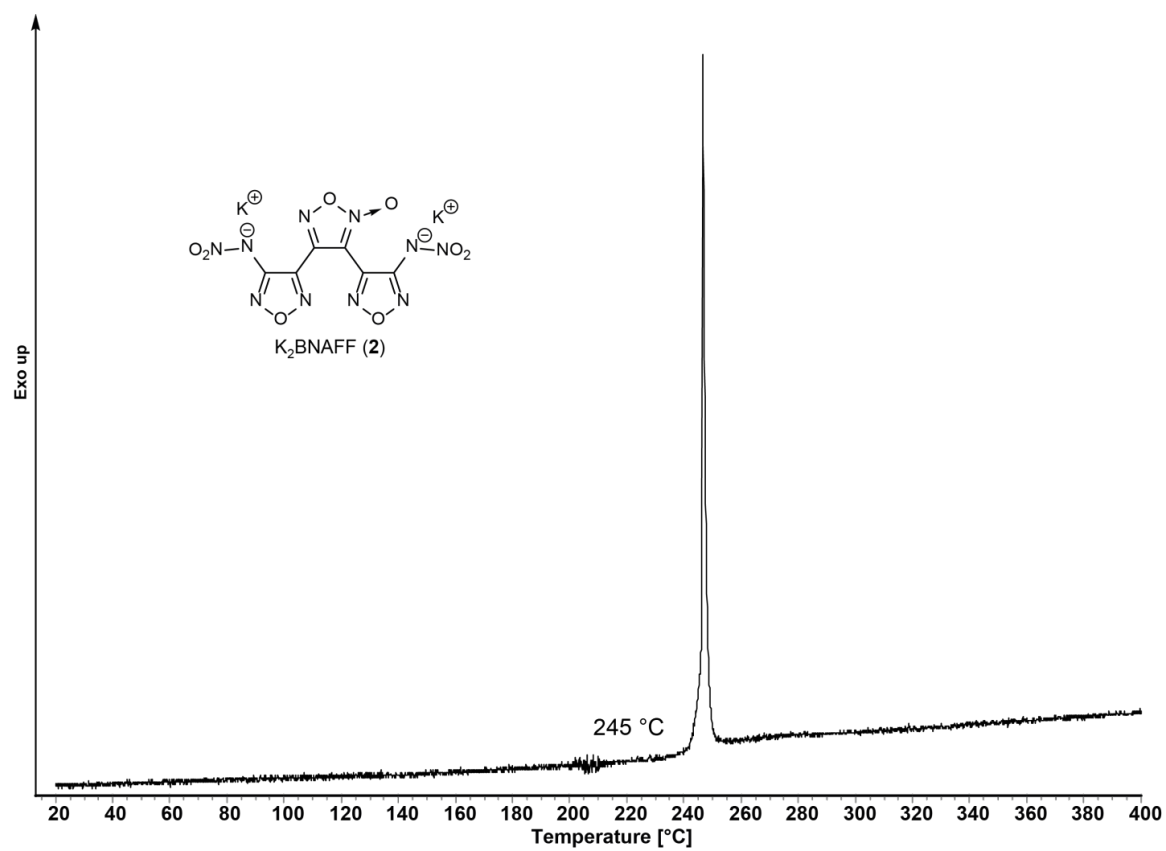


Figure S2. DTA plot of dipotassium 3,4-bis(4-nitramino-1,2,5-oxadiazol-3-yl)-1,2,5-furoxan K₂BNAFF (2)

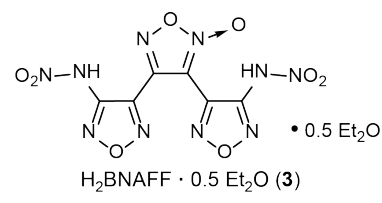


Figure S3. DTA plot of 3,4-bis(4-nitramino-1,2,5-oxadiazol-3-yl)-1,2,5-furoxan H₂BNAFF • 0.5 Et₂O.

6.4 NMR Spectra

^1H , ^{13}C and ^{14}N NMR data for H_2BNAFF (**3**) \cdot 0.5 Et_2O .

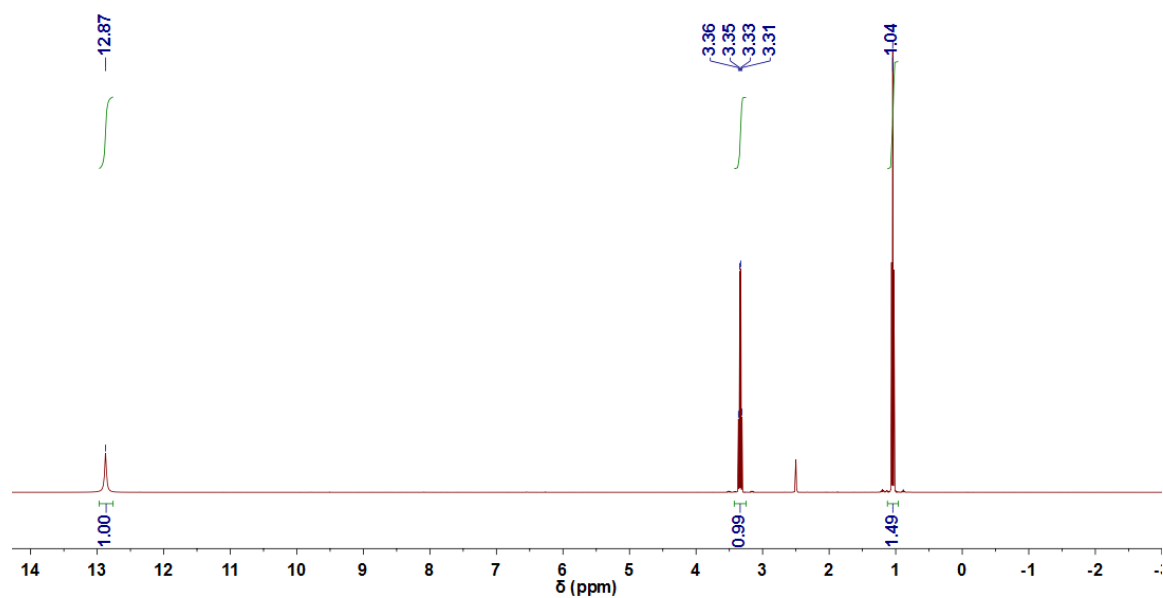


Figure S4. Recorded ^1H NMR spectrum of $\text{H}_2\text{BNAFF} \cdot 0.5 \text{Et}_2\text{O}$ (**3**) in d_6 -DMSO.

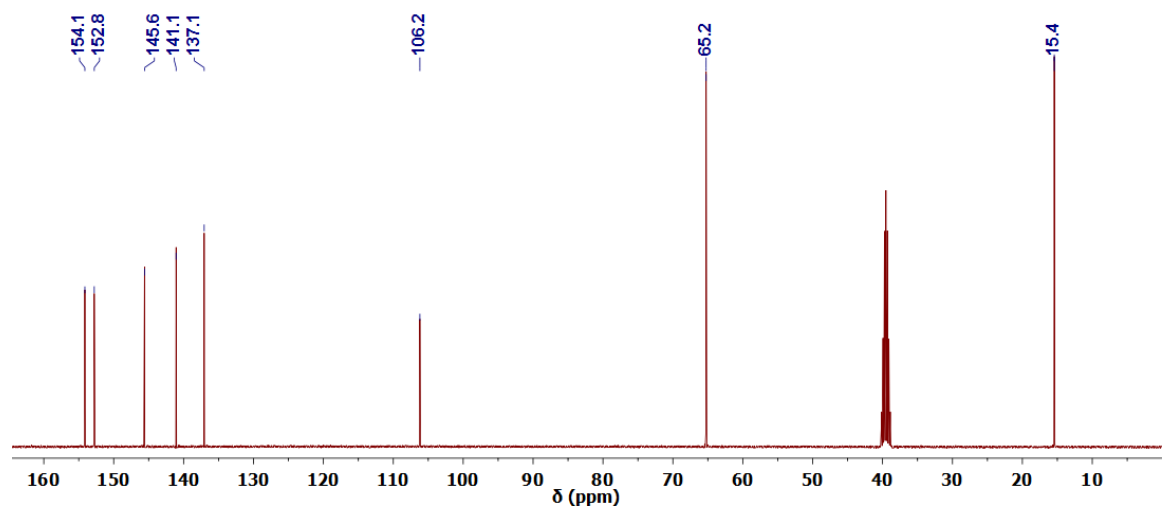


Figure S5. Recorded ^{13}C NMR spectrum of $\text{H}_2\text{BNAFF} \cdot 0.5 \text{Et}_2\text{O}$ (**3**) in d_6 -DMSO.

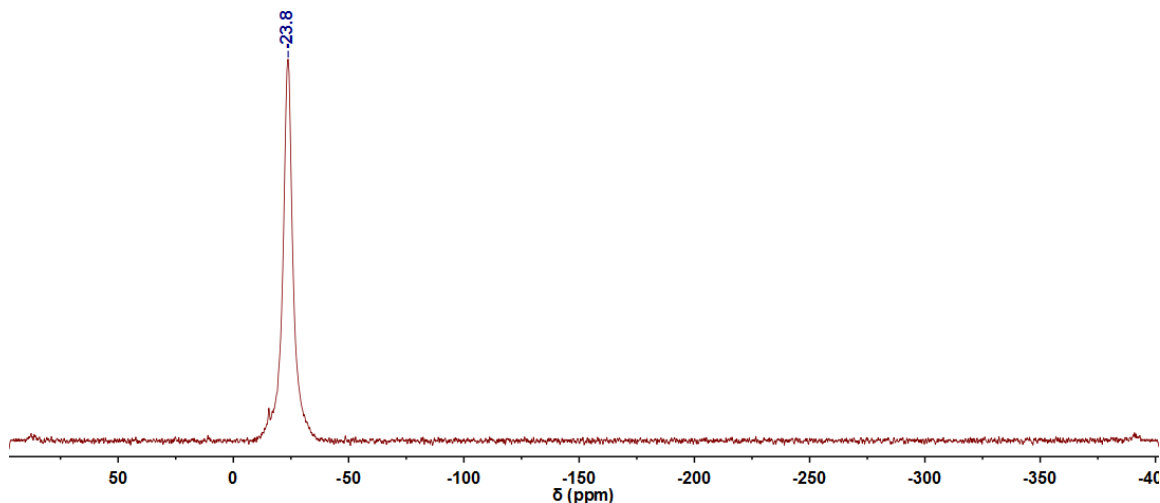


Figure S6. Recorded ^{14}N NMR spectrum of $\text{H}_2\text{BNAFF} \cdot 0.5 \text{Et}_2\text{O}$ (3) in d_6 -DMSO.

6.5 References

- [S1] CrysAlisPro, Oxford Diffraction Ltd. version 171.33.41, **2009**.
- [S2] CrysAlis RED, Version 1.171.35.11(release 16-05-2011CrysAlis 171.Net), Oxford Diffraction Ltd., Abingdon, Oxford (U.K.), **2011**.
- [S3] A. Altomare, M. C. Burla, M. Camalli, G. L. Cascarano, C. Giacovazzo, A. Guagliardi, A. G. G. Moliterni, G. Polidori and R. Spagna, SIR97: A New Tool for Crystal Structure Determination and Refinement, *J. Appl. Crystallogr.*, **1999**, 32, 115–119.
- [S4] G. M. Sheldrick, A Short History of SHELX, *Acta Crystallogr., Sect. A: Found. Crystallogr.*, **2008**, 64, 112–122.
- [S5] L. J. Farrugia, WinGX Suite for Small-Molecule Single-Crystal Crystallography, *J. Appl. Crystallogr.*, **1999**, 32, 837–838.
- [S6] A. L. Spek, PLATON, **1999**, A Multipurpose Crystallographic Tool, Utrecht University, The Diffraction Ltd.
- [S7] M. J. Frisch, G. W. Trucks, H. B. Schlegel, G. E. Scuseria, M. A. Robb, J. R. Cheeseman, G. Scalmani, V. Barone, B. Mennucci, G. A. Petersson, H. Nakatsuji, M. Caricato, X. Li, H.P. Hratchian, A. F. Izmaylov, J. Bloino, G. Zheng, J. L. Sonnenberg, M. Hada, M. Ehara, K. Toyota, R. Fukuda, J. Hasegawa, M. Ishida, T. Nakajima, Y. Honda, O. Kitao, H. Nakai, T. Vreven, J. A. Montgomery, Jr., J. E. Peralta, F. Ogliaro, M. Bearpark, J. J. Heyd, E. Brothers, K. N. Kudin, V. N. Staroverov, R. Kobayashi, J. Normand, K. Raghavachari, A. Rendell, J. C. Burant, S. S. Iyengar, J. Tomasi, M. Cossi, N. Rega, J. M. Millam, M. Klene, J. E. Knox, J. B. Cross, V. Bakken, C. Adamo, J. Jaramillo, R. Gomperts, R. E. Stratmann, O.

Yazyev, A. J. Austin, R. Cammi, C. Pomelli, J. W. Ochterski, R. L. Martin, K. Morokuma, V. G. Zakrzewski, G. A. Voth, P. Salvador, J. J. Dannenberg, S. Dapprich, A. D. Daniels, O. Farkas, J.B. Foresman, J. V. Ortiz, J. Cioslowski, D. J. Fox, Gaussian 09 A.02, Gaussian, Inc., Wallingford, CT, USA, **2009**.

[S8] (a) J. W. Ochterski, G. A. Petersson, and J. A. Montgomery Jr., A complete basis set model chemistry. V. Extensions of six or more heavy atoms, *J. Chem. Phys.* **1996**, *104*, 2598–2619; (b) J. A. Montgomery Jr., M. J. Frisch, J. W. Ochterski G. A. Petersson, A complete basis set model chemistry. VII. Use of the minimum population localization method, *J. Chem. Phys.* **2000**, *112*, 6532–6542.

[S9] (a) L. A. Curtiss, K. Raghavachari, P. C. Redfern, J. A. Pople, Assessment of Gaussian-2 and density functional theories for the computation of enthalpies of formation, *J. Chem. Phys.* **1997**, *106*, 1063–1079; (b) E. F. C. Byrd, B. M. Rice, Improved Prediction of Heats of Formation of Energetic Materials Using Quantum Mechanical Calculations, *J. Phys. Chem. A* **2006**, *110*, 1005–1013; (c) B. M. Rice, S. V. Pai, J. Hare, Predicting heats of formation of energetic materials using quantum mechanical calculations, *Comb. Flame* **1999**, *118*, 445–458.

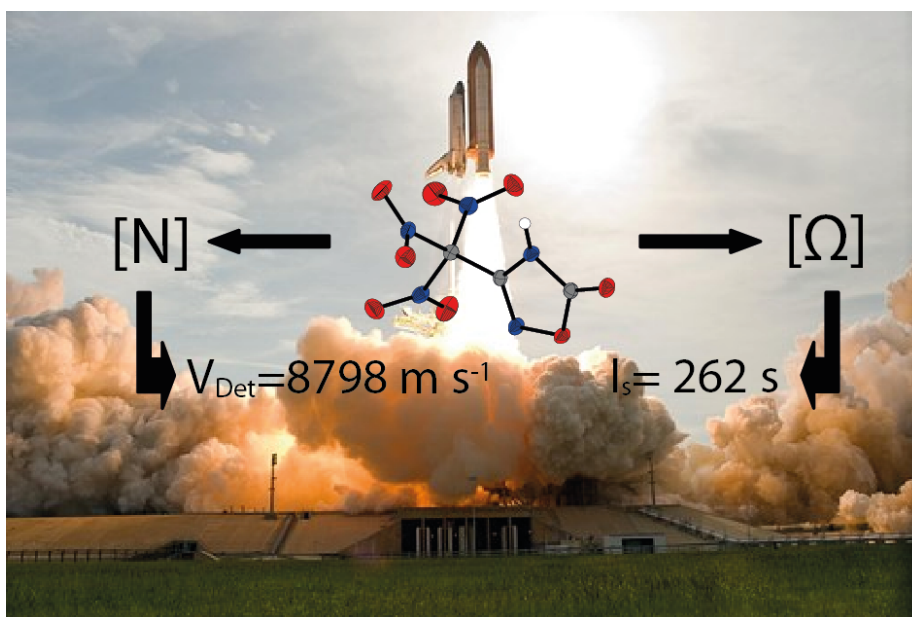
[S10] P. J. Lindstrom, W. G. Mallard (Editors), NIST Standard Reference Database Number 69, <http://webbook.nist.gov/chemistry/> (accessed November **2017**).

[S11] (a) H. D. B. Jenkins, H. K. Roobottom, J. Passmore, L. Glasser, Relationships among Ionic Lattice Energies, Molecular (Formula Unit) Volumes, and Thermochemical Radii, *Inorg. Chem.* **1999**, *38*, 3609–3620. (b) H. D. B. Jenkins, D. Tudela, L. Glasser, Lattice Potential Energy Estimation for Ionic Salts from Density Measurements, *Inorg. Chem.* **2002**, *41*, 2364–2367.

Synthesis, Characterization and Properties of Di- and Trinitromethyl-1,2,4-Oxadiazoles and Salts

Tobias S. Hermann, Thomas M. Klapötke*, Burkhard Krumm and Jörg Stierstorfer

Asian Journal of Organic Chemistry, **2018**, 7, 739–750.



Synthesis, Characterization and Properties of Di- and Trinitromethyl-1,2,4-Oxadiazoles and Salts

Tobias S. Hermann, Thomas M. Klapötke*, Burkhard Krumm and Jörg Stierstorfer

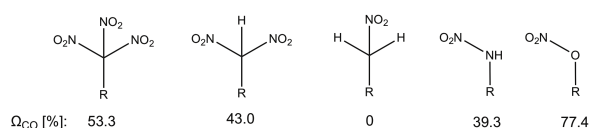
Asian Journal of Organic Chemistry, **2018**, 7, 739–750.

Abstract:

The syntheses of 3-trinitromethyl-(1,2,4-oxadiazol-5-one), its *N*-methyl derivative, and of 5-methyl-3-trinitromethyl-1,2,4-oxadiazole is described. The ring closure was carried out first yielding in oxadiazole acetic acid ethyl esters. Upon saponification the acetic acid derivatives were formed, which were nitrated in mixed acid to yield the trinitromethyl derivatives. The three energetic compounds show good detonation performance (V_{Det} : 8779–8804 m s⁻¹) but also good specific impulses (I_s : 244–262 s). Furthermore, starting from 1,2,4-oxadiazole ethyl ester derivatives the potassium, barium and ammonium salts of various dinitromethyl-1,2,4-oxadiazoles were prepared. All compounds were comprehensively characterized by vibrational spectroscopy (IR, Raman), NMR, DTA, elemental analysis and single crystal X-ray diffraction.

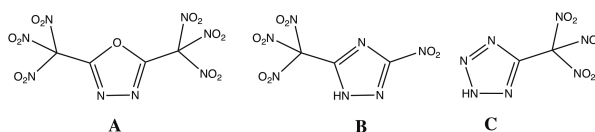
1. Introduction

There are several functional groups to increase the oxygen contents of organic molecules (Scheme 1). The use of di- and trinitromethyl groups for the design of new high-energy dense oxidizers (HEDOs) has been shown to be efficient.^{[1], [2], [3], [4], [5]}



Scheme 1: Overview over the oxygen balances (Ω_{CO}) of the trinitro-, dinitro-, nitromethyl, nitramine and nitrato functional group.

Trinitromethyl derivatives which mostly meet the requirements for an environmentally benign oxidizer, are potential substitutes for the widely used perchlorates.^[6] Several research groups have synthesized heterocyclic compounds with a trinitromethyl functional group and some examples are given in Scheme 2. Although the trinitromethyl moiety face some disadvantages, like almost every functional group, these problems could be overcome by hydrogen bond interactions of nitro groups and hydrogen atoms or oxygen-oxygen interactions between intermolecular layers. According to this assumption the molecule backbone should carry hydrogen atoms or oxygen functional groups like ketones.



Scheme 2: Examples of trinitromethyl heterocyclic compounds. A) 2,5-Bis(trinitromethyl)-1,3,4-oxadiazole^[7], B) 5-Nitro-3-trinitromethyl-1H-1,2,4-triazole^[1], C) 5-(Trinitromethyl)-2H-tetrazole^[8].

There are different methods that lead to trinitromethyl derivatives. The so-called Michael reaction works very well for the addition of trinitromethane (nitroform) with an electron deficient α,β -unsaturated reactant.^[4] Also the nitration of carbonyl activated methylene groups is a well-known synthesis strategy.^[9]

The oxygen balance is described as the excess of oxygen that is released during combustion to oxidize a fuel. Calculations of the oxygen balance Ω of a $C_aH_bN_cO_d$ based compound with the mass M are based on the assumption of a complete conversion into H_2O , N_2 and CO_2 during combustion (Equation 1).^[10]

$$\Omega_{CO_2} = \frac{d - 2a - b/2}{M} \cdot 1600 \quad (1)$$

Assuming that at higher temperatures the Boudouard reaction is preferred to form CO instead of CO_2 Equation 2 becomes more important.^[11]

$$\Omega_{CO} = \frac{d - a - b/2}{M} \cdot 1600 \quad (2)$$

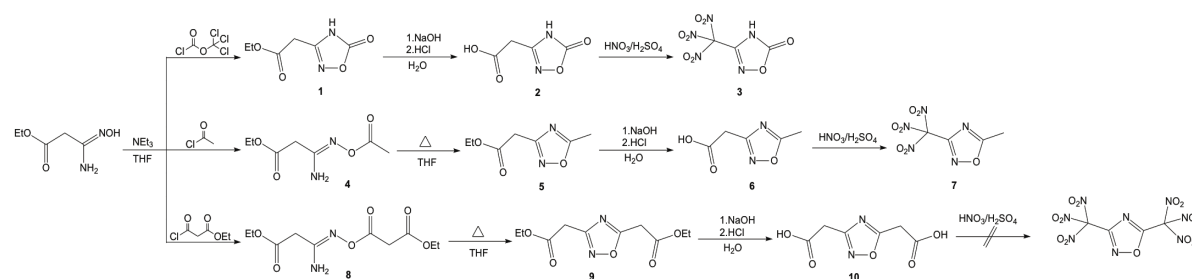
In order to boost the oxygen balance, oxygen and nitrogen containing molecule backbones like oxadiazoles, can be used.^[7] The heat of formation depends on the position of nitrogen and oxygen in the five-membered ring. The following trend has been observed: 1,2,5-oxadiazoles

(216 kJ mol⁻¹, furazan) > 1,2,3-oxadiazoles (158 kJ mol⁻¹) > 1,2,4-oxadiazoles (100 kJ mol⁻¹) to 1,3,4-oxadiazoles (72 kJ mol⁻¹).^[12] The research of 1,2,4-oxadiazoles as energetic materials has not extensively investigated so far; only a few polynitro compounds such as 5,5'-dinitromethyl-3,3'-1,2,4-oxadiazole or 5,5'-Bis(trinitromethyl)-3,3'-bi(1,2,4-oxadiazole) were synthesized.^{[12], [13], [14]} With the aim to develop environmentally friendly oxidizers with high oxygen content, several trinitromethyl 1,2,4-oxadiazoles were synthesized and described. Furthermore, dinitro ester 1,2,4-oxadiazoles derivatives and salts were prepared and all intermediates comprehensively characterized.

2. Results and Discussion

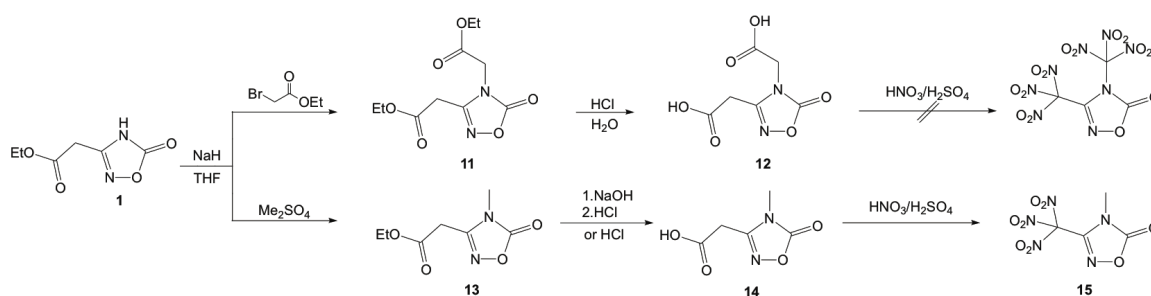
Synthesis

The functionalization of 1,2,4-oxadiazole was extensively studied for different functional groups like keto, methyl or second acetic acid functional group.^[15] Among the numerous possible synthesis routes of 1,2,4-oxadiazoles, in this investigation the synthetic route was chosen in which a hydroxylamine derivative is reacted with different carboxylic acid derivatives (Scheme 3). Ethyl (Z)-3-(hydroxylamino)-3-imino-propanoic acid ethyl ester was synthesized according to literature and served as starting material.^[16] Further reaction with different carboxylic acid derivatives (diphosgene, acetyl chloride and ethyl malonyl chloride) led to the open chain compound ethyl (Z)-3-(acetoxylimino)-3-aminopropanoate (**4**) and ethyl (Z)-3-amino-3-(((3-ethoxy-3-oxopropanoyl)oxy)imino)propanoate (**8**). The reaction with diphosgene yields in the already closed oxadiazolone 3-ethyl-(4,5-dihydro-1,2,4-oxadiazol-5-on-3-yl)-acetate (**1**). Upon heating a condensation reaction leads to the ring closure, forming oxadiazole acetic acid ester derivatives (**5** and **9**). The final precursor was synthesized by saponification under aqueous conditions yielding the oxadiazole acetic acid derivatives (2,5-dihydro-1,2,4-oxadiazol-5-on-3-yl) acetic acid (**2**), (5-methyl-1,2,4-oxadiazol-3-yl) acetic acid (**6**) and 1,2,4-oxadiazol-3,5-yl) diacetic acid (**10**). Finally the oxadiazole acetic acid derivatives were nitrated in mixed acid to yield trinitromethyl 1,2,4-oxadiazol derivatives 3,3,3-trinitromethyl-(4,5-dihydro-1,2,4-oxadiazol-5-one) (**3**) and 3,3,3-trinitromethyl-(5-methyl-1,2,4-oxadiazole) (**7**). The nitration of **10** yielded in an undefined mixture of decomposition products. Important to mention, the isolation of the intermediates **4** and **8** is not mandatory. The intermediates were isolated in order to be fully characterized. The trinitromethyl 1,2,4-oxadiazoles **3**, **7** and **15** also can be synthesized without further purification of the acetic acid derivatives.



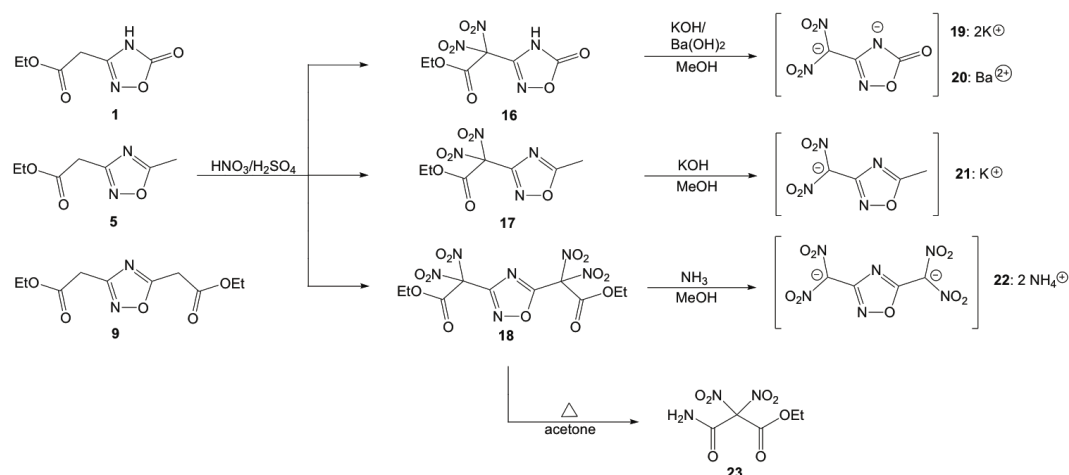
Scheme 3. Synthesis of 1,2,4-oxadiazole derivatives **1–10**.

Further reaction of **1** with dimethyl sulfate (Me_2SO_4) and ethyl bromoacetate under basic conditions led to 3-ethyl-4N-ethyl-(4,5-dihydro-1,2,4-oxadiazol-5-on-3-yl)-diacetate (**11**) and 3-ethyl-4-N-methyl-(4,5-dihydro-1,2,4-oxadiazol-5-on-3-yl)-acetate (**13**). The esters were hydrolyzed under basic conditions to yield the acetic acid derivatives (1,2,4-oxadiazol-5-on-3,4-yl)- diacetic acid (**12**) and 4-N-methyl-(1,2,4-oxadiazol-5-on-3-yl)-acetic acid (**14**). Further nitration to the trinitromethyl compound in mixed acid was successful in the case of compound **14** yielding 4-methyl-3-trinitromethyl-(1,2,4-oxadiazol-5-one) (**15**), while in the case of compound **12** again unidentified decomposition products were obtained (Scheme 4).



Scheme 4. Synthesis of 1,2,4-oxadiazole derivatives **11**–**15**.

Apart from the trinitromethyl 1,2,4-oxadiazoles, the ethyl dinitro ester derivatives ethyl 2,2-dinitro-(4*H*-1,2,4-oxadiazol-5-on-3-yl)acetate (**16**), ethyl 2,2-dinitro-(5-methyl-1,2,4-oxadiazol-3-yl)acetate (**17**) and diethyl bis-2,2-dinitro-(1,2,4-oxadiazol-3,5-diyl)diacetate (**18**) were synthesized (Scheme 4). Thus the ethyl esters (**1**, **5** and **9**) were nitrated in mixed acid. Compound **16** and **17** were obtained after extraction, while **19** precipitated during nitration and was isolated by filtration. Further substitution of the ethyl ester functional group to the dinitromethyl functional group was not performed, because of the low stability of the dinitromethyl unit. Generally it is possible to synthesize end on $-\text{CH}(\text{NO}_2)_2$ moieties in acidic conditions, however the high acidity of the proton makes them only short time stable and unsafe in handling. Therefore, the reaction of compound **16** and **17** with potassium and barium hydroxide yielded the more stable dipotassium (**19**) and barium (**20**) salt of **16** as well as the potassium (**21**) salt of **17**. Compound **18** was converted with concentrated ammonia into the diammonium salt **22** (Scheme 5). Recrystallization of **18** in hot acetone leads to an unexpected ring opening to give the malon amide ester **23**.



Scheme 5: Synthesis of 2,2-dinitromethyl ethyl ester 1,2,4-oxadiazole derivatives **16–18**, metal and ammonium salts **19–22** and malon amide ester **23**.

Analysis

The ethyl ester- and acetic acid intermediates, as well as the trinitromethyl compounds were thoroughly characterized by multinuclear NMR, vibrational spectroscopy (IR, Raman), differential thermal analysis and elemental analysis. The vibrational spectra of the intermediate compounds all show the expected signals. The ethyl ester intermediates (**1**, **5**, **9**, **11** and **13**) show the $\nu(\text{C}=\text{O})$ stretch vibration in the range of $1790\text{--}1730\text{ cm}^{-1}$, whereas the acetic acid derivatives (**2**, **6**, **10**, **12** and **14**) additionally show the broadened $\nu(\text{OH})$ vibrations in the region of $3200\text{--}3650\text{ cm}^{-1}$. In the vibrational spectra of the trinitromethyl compounds **3**, **7** and **15** the typical antisymmetric $\nu_{\text{as}}(\text{NO}_2)$ and symmetric $\nu_{\text{s}}(\text{NO}_2)$ stretching vibrations in the range of $1620\text{--}1506\text{ cm}^{-1}$ and $1385\text{--}1251\text{ cm}^{-1}$ were observed, respectively. The C–N, C–O and C–C vibrations observed are in the characteristic ranges for organic compounds.

In the ^1H and ^{13}C NMR spectra the resonances of the ester, carboxylic acid units ($168\text{--}177\text{ ppm}$) as well as the ring carbons ($155\text{--}173\text{ ppm}$) appear at the expected positions. The ^1H and ^{14}N NMR spectra of the trinitromethyl substituted 1,2,4-oxadiazol-5-ones (**3**, **15**) and 1,2,4-oxadiazole **7** are displayed in Figure 1. The ^1H NMR resonances are found in the expected regions, i.e. the NH resonance of **3** is detected at lower field showing a highly acidic character and the methyl hydrogen atoms of **7** and **15** at 2.72 (**7**) and 3.25 ppm (**15**). The resonance of **3** is typically broadened, not only because of the high acidity but also because of the keto-imine-tautomerism.

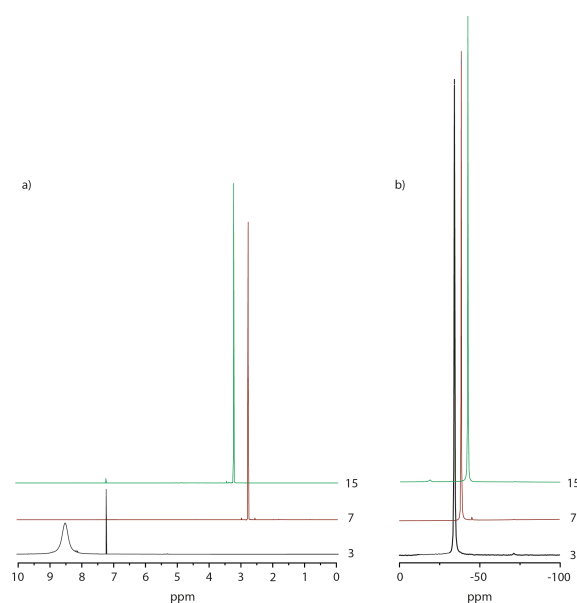


Figure 1: (a) ^1H and (b) ^{14}N NMR spectra of trinitromethyl-1,2,4-oxadiazole derivatives **3**, **7** and **15** in CDCl_3 at $25\text{ }^\circ\text{C}$.

A comparison of the ^{14}N NMR spectra of the trinitromethyl oxadiazoles **3**, **7** and **15** shows a trend of the resonances of trinitromethyl groups at the oxadiazole ring. The resonances of the nitro groups are shifted towards higher field in the order from **3** over **7** to **15** (Figure 1).

Suitable crystals of **3**, **4**, **15** and **16** for X-ray single diffraction were grown from chloroform. The structures are shown in Figures 2, 4, 7 and 9. The carboxylic acids **10** and **12** as well as the salts **19** and **20** of compound **16** were recrystallized from water, as well as **22** and **23** to obtain suitable single crystals (Figures 5, 6, 10–12). The X-ray data and parameter are listed in Table 1.

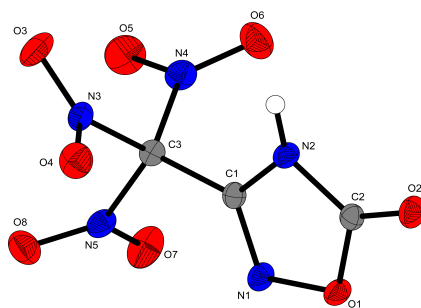
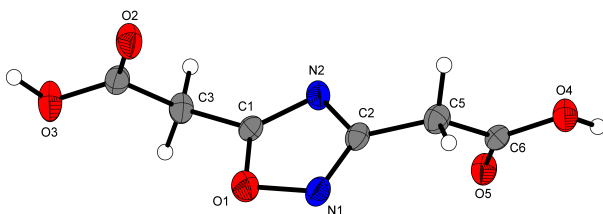
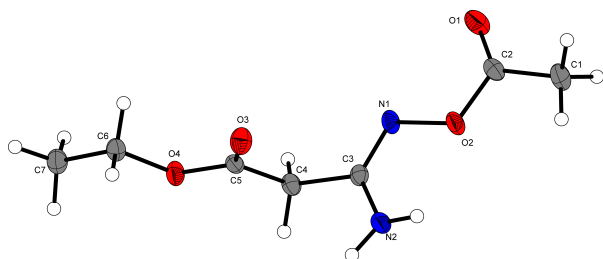
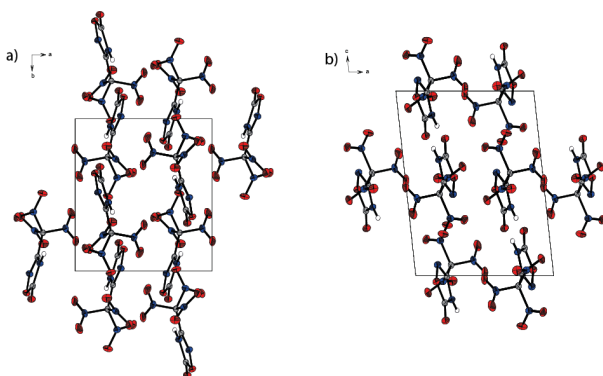


Figure 2: Molecular structure of 3-trinitromethyl-(1,2,4-oxadiazol-5-one) (**3**). Selected bond lengths (\AA) and angles ($^\circ$): C1–C3 1.4932(12), C2–O1 1.3669(11), C2–O2 1.2039(11); O1–C2–O2 123.69(9), N1–C1–C3 121.41(8), C1–N2–C2 106.72(8); C1–N1–O1–C2 0.40(10), C3–C1–N2–C2 $-178.18(8)$.



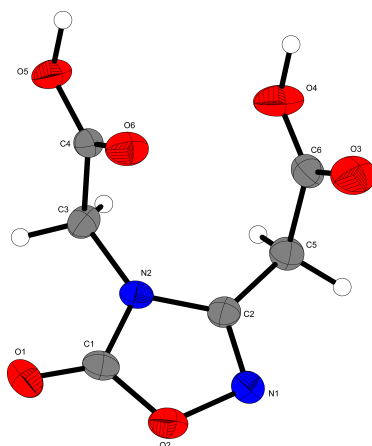


Figure 6: Molecular structure of 4,5-dicarboxymethyl-(1,2,4-oxadiazol-3-one) (**12**). Selected bond lengths (Å) and angles (deg.): O1–C1 1.213(3), O2–N1 1.440(3), C2–N2 1.368(3); O1–C1–O2 123.9(3), N1–C2–C5 122.2(3), C1–N2–C3 123.2(2); O1–C1–O2–N1 178.9(2), N1–C2–C5–C6 113.1(3), C1–N2–C3–C4 102.6(2).

To draw a comparison between the acetic acid derivatives compound **10**, which crystallizes in the orthorhombic space group *Pna2* has a lower density (1.67 g cm^{-3}), then compound **12**, which crystallizes in the monoclinic space group *P2₁/c* with a crystal density of 1.73 g cm^{-3} .

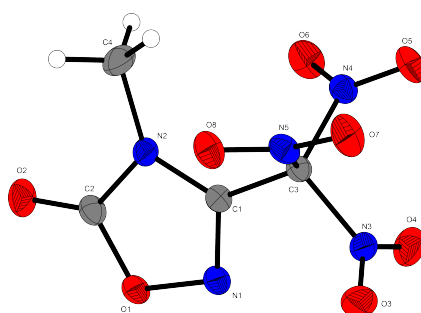


Figure 7: Molecular structure of 4-methyl-3-trinitromethyl-(1,2,4-oxadiazol-5-one) (**15**). Selected bond lengths (Å) and angles (deg.): C1–C3 1.497(2), C2–O2 1.199(2), C2–O1 1.367(2); O1–C2–O2 124.24(14), N1–C1–C3 116.66(14), C1–N2–C2 105.88(13); C1–N1–O1–C2 0.93(17), C3–C1–N2–C2 179.38(15).

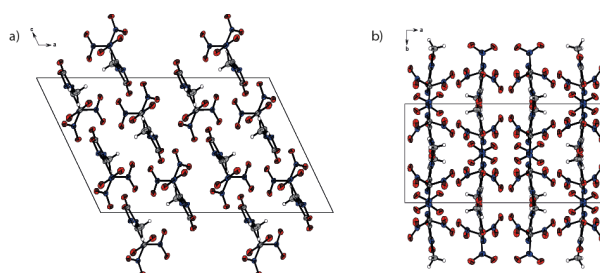


Figure 8: Molecule structure of **15** along a) *c*-axis and b) *b*-axis.

Compound **3**, which crystallizes in the monoclinic space group $P2_1/n$, has a higher density (1.99 g cm^{-3}) than **15** (1.80 g cm^{-3}), which crystallizes in the monoclinic space group $C2/n$. Both compounds show a propeller shape orientation for the trinitromethyl functional group. The ring of both compounds is only slightly twisted ($0.40^\circ / 0.93^\circ$) and therefore nearly perfectly flat. In both structures, each molecule is ordered antiparallel to its next partner molecule. For better describing of the orientation of both compounds, the molecule unit cells along the *b*- and *c*-axis are visualized in Figures 3 and 8

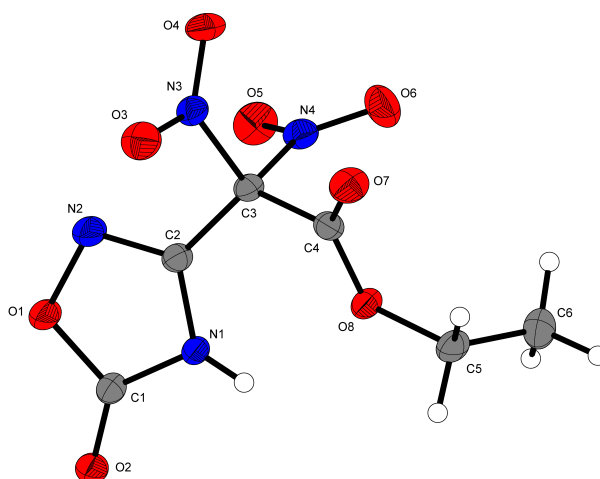


Figure 9: Molecular structure of ethyl 2,2-dinitro-(4*H*-1,2,4-oxadiazol-5-on-3-yl)acetate (**16**). Selected bond lengths (\AA) and angles (deg): C2–C3 1.4943(17), C3–C4 1.5504(18), C4–O7 1.1887(15), N1–H1 0.818(7); C2–C3–C4 118.19(10), C4–C3–N4 107.25(10), C2–C3–N3 108.33(10); N1–C2–C3–C4 34.46(18), N1–C2–C3–N3 155.68(12), C3–C4–O8–C5 173.05(10).

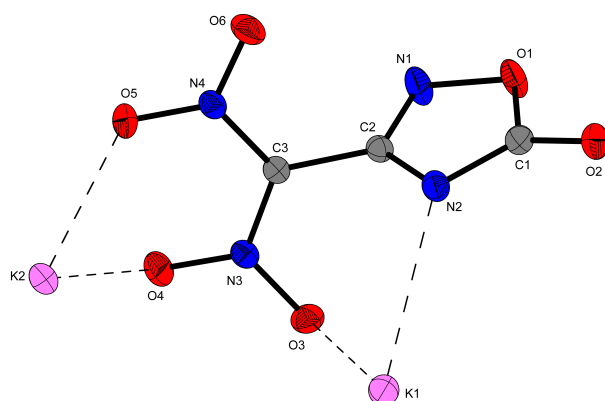


Figure 10: Molecular structure of dipotassium 3-dinitromethyl-(1,2,4-oxadiazol-5-one) (**19**). Selected bond lengths (Å) and angles (deg): C2–C3 1.4729(17), N1–O1 1.4292(14), C1–O2 1.2380(16); N2–C2–C3 123.00(11), N2–C1–O2 132.19(13), N3–C3–C2 121.13(11); N2–C2–C3–N4 94.40(15), C1–O1–N1–C2 0.13(13).

Compound **16** crystallizes in the monoclinic space group $P2_1/c$ with a density of 1.70 g cm^{-3} , while **19** crystallizes in the same space group with a density of 2.20 g cm^{-3} .

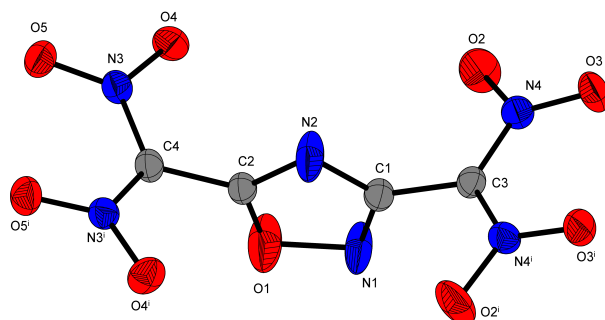


Figure 11: Molecular structure of the bis(2,2'-dinitromethyl)-(1,2,4-oxadiazol-3,5-diyl) dianion (**22**).

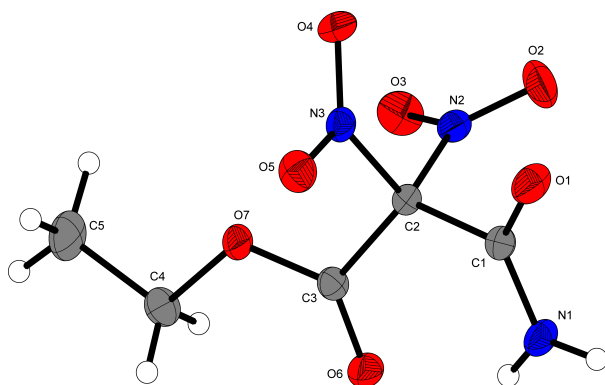


Figure 12: Molecular structure of ethyl 3-amino-2,2-dinitro-3-oxopropanoate (**23**). Selected bond lengths (Å) and angles (deg.): C3–C2 1.5548(16), C2–C1 1.5600(16), C1–N1 1.3111(16); C3–C2–N3 109.77(9), C3–C2–C1 119.16(10), C2–C1–N1 115.59(10); C1–C2–C3–O7 150.42(10), N3–C2–C3–O7 27.36(13).

Refinement of the crystal structure of **22** was not possible because of disordered ammonium and crystal water; therefore only the dianion of **22** is shown in Figure 11. Compound **23** crystallizes in the monoclinic space group $P2_1/c$ and a density of 1.67 g cm^{-3} . Details on the measurements and refinements of all compounds are listed in Table 1.

Table 1. X-ray parameters of **3**, **4**, **10**, **12**, **15**, **16**, **19** and **23**.

	3	4	10	12
Empirical formula	C ₃ HN ₅ O ₈	C ₇ H ₁₂ N ₂ O ₄	C ₆ H ₆ N ₂ O ₆	C ₆ H ₆ N ₂ O ₆
FW (g mol ⁻¹)	235.09	188.19	186.13	202.13
Temperature (K)	173	173	173	173
Crystal size (mm)	0.30x0.24x0.20	0.15x0.1x0.03	0.37x0.25x0.21	0.25x0.10x0.10
Crystal description	Colorless block	Colorless block	Colorless block	Colorless block
Crystal system	Monoclinic	Triclinic	Orthorhombic	Monoclinic
Space group	<i>P2₁/n</i>	<i>P</i> -1	<i>Pna2</i>	<i>P2₁/c</i>
<i>a</i> (Å)	9.1484(3)	7.6170(6)	5.0339(3)	11.2786(13)
<i>b</i> (Å)	8.4005(2)	8.0737(7)	14.6435(10)	6.5048(7)
<i>c</i> (Å)	10.2768(3)	8.9192(9)	9.9884(7)	10.7260(14)
α (°)	90	81.158(8)	90	90
β (°)	97.402(3)	65.733(9)	90	98.765(11)
γ (°)	90	62.926(9)	90	90
<i>V</i> (Å ³)	783.20(3)	444.87(8)	736.28(8)	777.72(16)
<i>Z</i>	4	2	4	4
ρ_{calc} (g cm ⁻³)	1.994	1.405	1.679	1.726
μ (mm ⁻¹)	0.201	0.166	0.149	0.158
<i>F</i> (000)	472	200	384	416
θ range (°)	4.493–26.500	4.936–32.188	4.281–26.982	4.234–26.490
Index range	$-11 \leq h \leq 11$	$-10 \leq h \leq 10$	$-6 \leq h \leq 6$	$-14 \leq h \leq 12$
	$-10 \leq k \leq 10$	$-11 \leq k \leq 11$	$-18 \leq k \leq 14$	$-8 \leq k \leq 7$
	$-12 \leq l \leq 12$	$-12 \leq l \leq 12$	$-12 \leq l \leq 12$	$-13 \leq l \leq 12$

Reflections collected	1475	2078	1496	1016
Reflections observed	1618	2705	1563	1607
Reflections unique	11420	4462	5697	5145
R1, wR2 (2 σ data)	0.0250/0.0617	0.0459/0.1002	0.0300/0.0787	0.0531/0.1041
R1, wR2 (all data)	0.0275/0.0633	0.0653/0.1132	0.0318/0.0804	0.0967/0.1287
Parameters	149	130	142	151
GOOF an F ²	1.062	1.038	1.060	1.048
Larg.diff.peak/ hole (e Å ⁻³)	-0.202/0.338	-0.338/0.344	-0.164/0.177	-0.278/0.261
CCDC entry	1584209	1585347	1584207	1584213

	15	16	19	23
Empirical formula	C ₄ H ₃ N ₅ O ₈	C ₆ H ₆ N ₄ O ₈	C ₃ K ₂ N ₄ O ₆	C ₅ H ₇ N ₃ O ₇
FW (g mol ⁻¹)	249.11	262.15	266.27	221.14
Temperature (K)	173	173	173	173
Crystal size (mm)	0.40x0.22x0.10	0.20x0.20x0.05	0.33x0.28x0.13	0.40x0.32x0.19
Crystal description	Colorless block	Colorless plate	Yellow block	Colorless block
Crystal system	Monoclinic	Monoclinic	Monoclinic	Monoclinic
Space group	<i>C2/n</i>	<i>P2₁/c</i>	<i>P2₁/c</i>	<i>P2₁/c</i>
<i>a</i> (Å)	22.1237(16)	12.6701(5)	7.1764(10)	8.4070(6)
<i>b</i> (Å)	7.8038(7)	7.8460(2)	13.9102(3)	10.2938(6)
<i>c</i> (Å)	12.2586(8)	11.2752(4)	8.0452(2)	10.3825(6)
α (°)	90	90	90	90

β (°)	119.830(6)	114.2752(4)	91.530(3)	102.036(5)
γ (°)	90	90	90	90
V (Å ³)	1836.0(3)	1022.68(7)	802.83(3)	878.75(5)
Z	8	4	4	4
ρ_{calc} (g cm ⁻³)	1.802	1.703	2.203	1.671
μ (mm ⁻¹)	0.177	0.161	1.200	0.158
$F(000)$	1008	536	528	456
Θ range (°)	4.247–26.492	4.441–30.422	4.751–32.166	4.255–25.492
Index range	$-27 \leq h \leq 27$	$-15 \leq h \leq 15$	$-8 \leq h \leq 8$	$-10 \leq h \leq 10$
	$-9 \leq k \leq 9$	$-9 \leq k \leq 9$	$-17 \leq k \leq 17$	$-12 \leq k \leq 12$
	$-15 \leq l \leq 16$	$-14 \leq l \leq 14$	$-9 \leq l \leq 9$	$-13 \leq l \leq 13$
Reflections collected	1511	1768	1477	1559
Reflections observed	1896	2108	1570	1812
Reflections unique	7020	14906	11584	6714
R1, wR2 (2 σ data)	0.0348/0.0811	0.0292/0.0655	0.0174/0.0455	0.0288/0.0695
R1, wR2 (all data)	0.0503/0.0881	0.0382/0.0697	0.0188/0.0462	0.0356/0.0738
Parameters	155	187	136	164
GOOF an F ²	1.047	1.043	1.069	1.040
Larg.diff.peak/ hole (e Å ⁻³)	−0.249/0.294	−0.220/0.258	−0.233/0.327	−0.242/0.344
CCDC entry	1584208	1584212	1584211	1584210

Energetic Properties

Assessing the energetic properties (Table 2) is important for the safe handling of energetic materials. For this purpose, vacuum dried trinitromethyl-1,2,4-oxadiazole derivatives were used. The sensitivity to impact (IS) is tested by the action of different weight falling from different heights using the BAM drophammer. The friction sensitivity (FS) is determined by rubbing a small amount of substance between a porcelain plate and a pin with different grater forces using the BAM friction tester.^[10a] According to the results of these measurements all three compounds are insensitive to impact, friction and electrostatic discharge. The thermal stabilities were determined by differential thermal analysis (DTA) at a heating rate of 5 °C min⁻¹. The decomposition temperature of compound **7** (148 °C) is in the range of similar trinitromethyl derivatives.^[4, 17] Compared to e.g. 2,2,2-trinitroethyl nitrocarbamate (T_{melt} : 109 °C, T_{dec} : 153 °C)^[18] the decomposition temperatures of **3** and **15** (112 °C and 119 °C) are low. This low thermal stability might not only be influenced by the trinitromethyl moiety but also by the acidic proton in the case of **3**. A deprotonation directly leads to decomposition of the compound.

Table 2. Physical properties and calculated detonation parameters (using EXPLO5 V6.03) of water-free compounds **3**, **7** and **15** in comparison to ammonium perchlorate.

	3	7	15	AP	PETN
ρ [g cm ⁻³] ^{a)}	1.95	1.84	1.80	1.95	1.75
Formula	C ₄ HN ₅ O ₈	C ₄ H ₃ N ₅ O ₇	C ₄ H ₃ N ₅ O ₈	NH ₄ ClO ₄	C ₅ H ₈ N ₄ O ₁₂
$\Delta_f H^\circ$ [kJ mol ⁻¹] ^{b)}	142	43	133	296	480
$\Delta_f U^\circ$ [kJ kg ⁻¹] ^{c)}	530	265	455	2623	1423
T_{dec} ^{d)}	112	148	119	240	202
IS [J] ^{e)}	25	30	30	20	3
FS [N] ^{f)}	324	324	324	360	60
ESD [J] ^{g)}	1.5	-	1.5	0.5	0.19
N [%] ^{h)}	29.8	30.1	28.1	11.9	17.7
Ω_{CO} [%] ⁱ⁾	+30.6	+10.3	+16.1	+34.0	+15.2

$\Delta_{\text{ex}} U^{\circ}$ [kJ kg ⁻¹] ^{j)}	-5301	1856	-5350	-1421	-5995
T_{ex} [K] ^{k)}	3862	4147	4072	1725	3959
P_{CJ} [kbar] ^{l)}	331	346	346	183	316
V_{det} [m s ⁻¹] ^{m)}	8798	8779	8804	1373	8525
I_{s} [s] ⁿ⁾	239	264	258	157	264
I_{s} (15% Al, 14% binder) [s] ^{o)}	262	244	244	264	257

a) Density at room temperature. b) Standard formation enthalpy calculated by the atomization method and CBS-4M electronic enthalpies from Gaussian 09 [19],[20]. c) Energy of formation. d) Decomposition temperature. Sensitivities (50 $\mu\text{m} \leq \text{grain size} \leq 100 \mu\text{m}$): e) Impact sensitivity. f) Friction sensitivity. g) Sensitivity to electrostatic discharge. h) Nitrogen content. i) Oxygen balance Ω assuming the formation of CO during the combustion. j) Detonation energy. k) Detonation temperature. l) Detonation pressure. m) Detonation velocity.[21] n) Specific impulse (EXPLO5 6.03: 70 bar chamber pressure, 1 bar expansion conditions equilibrium expansion). o) Specific impulse (15 % Al, 6 % polybutadiene acrylic acid, 6 % polybutadiene acrylonitrile and 2 % bisphenyl A ether; EXPLO5 6.03: 70 bar chamber pressure, 1 bar expansion conditions equilibrium expansion

One of the most important performance parameter of energetic materials is their detonation velocity (V_{det}), next to detonation pressure (P_{CJ}) and energy of explosion ($A_{\text{ex}}U^{\circ}$). The detonation velocities of the trinitromethyl-1,2,4-oxadiazoles were calculated using the program EXPLO5 6.03 and are shown in Table 3. The detonation velocities of all compounds are higher than for PETN ($> 8525 \text{ m s}^{-1}$) with the highest value for **3** (8798 m s^{-1}). The highest detonation temperatures and pressures were obtained for **7** (4147 K/346 kbar) and **15** (4072 K/346 kbar).

Table 3. Physical properties of water-free compounds **19**, **20**, **21** and **22**.

	19	20	21	22
$\rho [\text{g cm}^{-3}]^{\text{a)}$	2.16	2.07 ⁱ⁾	1.92 ⁱ⁾	1.75
Formula	$\text{C}_3\text{K}_2\text{N}_4\text{O}_6$	$\text{C}_2\text{BaN}_4\text{O}_6$	$\text{C}_4\text{H}_3\text{KN}_4\text{O}_6$	$\text{C}_4\text{H}_8\text{N}_8\text{O}_9$
$T_{\text{dec}}^{\text{b)}$	219	145	165	130
$IS [\text{J}]^{\text{c)}$	3	10	4	3
$FS [\text{N}]^{\text{d)}$	120	160	120	120
$ESD [\text{J}]^{\text{e)}$	0.1	0.1	0.75	0.75
$N [\%]^{\text{f)}$	21.04	17.22	17.29	35.90
$O [\%]^{\text{g)}$	36.05	29.50	35.37	46.13
$N + O [\%]^{\text{h)}$	57.09	46.72	52.66	82.03

a) Density at room temperature. b) Decomposition temperature. Sensitivities ($50 \mu\text{m} \leq \text{grain size} \leq 100 \mu\text{m}$): c) Impact sensitivity. d) Friction sensitivity. e) Sensitivity to electrostatic discharge. f) Nitrogen content. g) Oxygen content. h) Nitrogen and oxygen content i) Gas-pycnometry.

As usual for metal salts the densities ($1.92\text{--}2.20 \text{ g cm}^{-3}$) of **19–21** are higher than those for the neutral compounds **3**, **7** and **15** ($1.80\text{--}1.95 \text{ g cm}^{-3}$). Also the sensitivities of the dinitromethyl derivatives **19–22** are higher. As is visible from Table 3, it is obvious that these compounds (**19–22**) are more sensitive toward impact (3–10 J), than toward friction (120–160 N) and electrical discharge (0.1–0.75 J). Nevertheless, the sensitivity is lower than that of PETN. The decomposition temperatures for the potassium salts **19** and **21** (219/165 °C) are higher than those for the barium salt **20** (145 °C) and ammonium salt **22** (130 °C).

Heat of formation calculation

The enthalpies of the gas-phase species M were computed according to the atomization energy method (eq.1).

$$\Delta_f H^\circ_{(g, M, 298)} = H_{(Molecule, 298)} - \sum H^\circ_{(Atoms, 298)} + \sum \Delta_f H^\circ_{(Atoms, 298)} \quad (1)$$

Table 4. CBS-4M results and calculated gas-phase enthalpies.

	M	$-H^{298} / \text{a.u.}$	$\Delta_f H^\circ(g, M) / \text{kcal mol}^{-1}$	M / g mol ⁻¹	$\Delta_f U^\circ(s) / \text{kJ kg}^{-1}$
3	235.07	988.990052	-16.6	235.1	-530.0
7	233.10	935.071201	20.9	233.1	265.3
15	249.10	1028.22456	-21.2	249.1	-455.3

Table 5. CBS-4M values and literature values for atomic $\Delta_f H^\circ_{298} / \text{kcal mol}^{-1}$.

	$-H^{298} / \text{a.u.}$	NIST ^[22]
H	0.500991	52.1
C	37.786156	171.3
N	54.522462	113.0
O	74.991202	59.6

From the gas-phase enthalpies of formation $\Delta_f H^\circ(g)$, the enthalpies of the solid state can be calculated using the enthalpies of sublimation by the equation:

$$\Delta_f H^\circ(s) = \Delta_f H^\circ(g) - (\Delta_{\text{sub}} H) \quad (2)$$

For a solid compound the enthalpy of sublimation ($\Delta_{\text{sub}} H$) can be approximated on the basis of TROUTON's rule^[23] if the melting temperatures T_m are known:

$$\Delta_{\text{sub}} H. [\text{J mol}^{-1}] = 188 T_m [\text{K}] \quad (3)$$

3. Conclusions

In order to explore new energetic compounds with a high oxygen balance different trinitro-oxadiazole derivatives were prepared for the first time. The reaction of ethyl (Z)-3-amino-3-(hydroxylimino) propanoate with diphosgene, acetyl chloride and 3-chloro-3-oxopropanoate resulted in the formation of 3-trinitromethyl-(1,2,4-oxadiazol-5-one) (**3**), 5-methyl-3-trinitromethyl-(1,2,4-oxadiazole) (**7**) and 4-methyl-3-trinitromethyl-(1,2,4-oxadiazol-5-one) (**15**). All products and intermediates were characterized by multinuclear NMR, vibrational spectroscopy, DTA measurements and elemental analysis. Also the ethyl 2,2-dinitro esters (**16**, **17** and **18**) were synthesized, as well as the substitution of the ethyl ester and synthesis of the dipotassium- (**19**) and barium salt (**20**) of **16**. Additionally the potassium salt (**21**) of compound **17** and the ammonium salt (**22**) of compound **18** were prepared. Upon heating in acetone a ring opening was observed. The sensitivities of the energetic compounds **3**, **7** and **15** to various ignition stimuli according to BAM standard and the detonation properties calculated with EXPLO5 6.03 were also determined. The most promising energetic material is compound **3**. It has a high positive oxygen balance (+30.6) and a very good specific impulse in mixture with binder (262 s). Also energetic properties like the detonation pressure (331 kbar) or detonation velocity (8798 m s^{-1}) exceed those of PETN. Nevertheless, the other two trinitromethyl-1,2,4-oxadiazoles **7** and **15** also have good oxygen balances (+10 % and +16 %) and promising detonation values.

4. Experimental Section

General methods:

The low-temperature single-crystal X-ray diffraction measurements were performed on an Oxford XCalibur3 diffractometer equipped with a Spellman generator (voltage 50 kV, current 40 mA) and a KappaCCD detector operating with $\text{Mo}_{\text{K}\alpha}$ radiation ($\lambda = 0.7107 \text{ \AA}$). Data collection was performed using the CRYSLIS CCD software.^[24] The data reduction was carried out using the CRYSLIS RED software.^[25] The solution of the structure was performed by direct methods (SIR97)^[26] and refined by full-matrix least-squares on F2 (SHELXL)^[27] implemented in the WINGX software package^[28] and finally checked with the PLATON software.^[29] All non-hydrogen atoms were refined anisotropically. The hydrogen atom positions were located in a difference Fourier map. DIAMOND plots are shown with thermal ellipsoids at the 50 % probability level. These data

can be obtained free of charge from The Cambridge Crystallographic Data Centre. All calculations were carried out using the Gaussian G09W (revision A.02) program package. The enthalpies (H) and free energies (G) were calculated using the complete basis set (CBS) method of Petersson and coworkers in order to obtain very accurate energies. The CBS models use the known asymptotic convergence of pair natural orbital expressions to extrapolate from calculations using a finite basis set to the estimated complete basis set limit. CBS-4 begins with a HF/3-21G(d) geometry optimization; the zero point energy is computed at the same level. It then uses a large basis set SCF calculation as a base energy, and a MP2/6-31+G calculation with a CBS extrapolation to correct the energy through second order. A MP4(SDQ)/6-31+(d,p) calculation is used to approximate higher order contributions. In this study we applied the modified CBS-4M method (M referring to the use of Minimal Population localization), which is a re-parametrized version of the original CBS-4 method and also includes some additional empirical corrections.^{[30] [31]} All chemicals were used as supplied. Raman spectra were recorded in a glass tube with a Bruker MultiRAM FT-Raman spectrometer with Nd:YAG laser excitation up to 1000 mW (at 1064 nm). Infrared spectra were measured with a PerkinElmer Spectrum BX-FTIR spectrometer equipped with a Smiths Dura/SamplIR II ATRdevice. All spectra were recorded at ambient (25 °C) temperature. NMR spectra were recorded with a JEOL/Bruker instrument and chemical shifts were determined with respect to external Me₄Si (¹H, 399.8 MHz; ¹³C, 100.5 MHz) and MeNO₂ (¹⁴N, 28.9 MHz). Analyses of C/H/N were performed with an Elemental Vario EL Analyzer. Melting and decomposition points were measured using differential thermal analysis (DTA) at a heating rate of 5° C min⁻¹ with an OZM Research DTA 552-Ex instrument. The sensitivity data were explored using a BAM drop hammer and a BAM friction tester.^[10a] The heats of formations were calculated by the atomization method based on CBS-4M electronic enthalpies. All calculations affecting the detonation parameters were carried out using the program package EXPLO5 6.03.^{[21], [32]}

General method for the open chain compounds 4 and 8:

Ethyl (Z)-3-amino-3-(hydroxyimino)propanoate (5.0 g, 34 mmol) was dissolved in 80 mL THF. The solution was cooled to 0 °C and acetyl chloride (2.67 g, 34 mmol) or ethyl 3-chloro-3-oxopropanoate (5.13 g, 34 mmol) was added in portions. Triethylamine (3.22 g, 34 mmol) was added slowly and the resulting suspension was stirred at 0 °C for 3 h. The formed precipitate filtered and the remaining solution reduced in vacuum. For further purification 100 mL water was added and the solution was extracted with ethyl acetate (4 x 100 mL). The combined organic

phases were washed with brine and dried over MgSO_4 . The solvent was evaporated under reduced pressure.

General method for the ethyl esters 5 and 9:

Method 1: Compound **4** or **8** were dissolved in toluene and heated 4h at 140 °C. The solvent was removed under reduced pressure yielding the desired compound **5** and **9** as liquids.

Method 2: Compound **4** or **8** (4.7 mmol) were dissolved in 20 mL pyridine and heated to reflux. The reaction mixture was cooled to ambient temperatures and the solvent was evaporated under reduced pressure. Then 50 mL dichloromethane and 30 mL water were added and the phases were separated. The aqueous phase was extracted with dichloromethane (3 x 50 mL) and the combined organic phases were washed with brine and dried over MgSO_4 .

General method for the acetic acid derivatives 2, 6, 10 and 14:

The intermediate **1** (0.5 g, 3.5 mmol), **5** (0.41 g, 2.9 mmol), **9** (2.77 g, 12 mmol) or **13** (0.40 g, 2.1 mmol) was added to a 30mL aqueous solution of sodium hydroxide (4 eq). The solution was heated to 40 °C for 2 h. After cooling to room temperature, the mixture was acidified with conc. HCl to pH 1. The solution was extracted with ethyl acetate (3 x 100 mL), the combined organic phases were washed with brine and dried over MgSO_4 . The solvent was evaporated.

General method for the trinitromethyl compounds 3, 7 and 15:

A mixture of 6/20 mL sulfuric acid and 3/20 mL nitric acid were cooled to 0 °C and **2** (0.25 g, 1.7 mmol), **6** (3.08 g, 21.7 mmol) or **14** (0.92 g, 5.8 mmol) was added slowly. The reaction mixture was stirred over night allowing warming up to room temperature. Then the mixture was poured on ice, followed by extraction with ethyl acetate (3x) and twice with water and treatment with brine. The combined organic layers were dried with MgSO_4 and the solvent was removed in vacuum.

General method for the ethyl 2,2-dinitro esters 16, 17 and 18:

To a solution of mixed acid (each 20 mL) cooled to 0°C **1/5/9** (0.5 mg) was added slowly, holding the temperature below 10°C. The reaction mixture was stirred for 1 h at ambient temperatures, after which the solution was poured on ice. The solution was extracted with ethyl acetate (4 x 50 mL). The combined organic phases were washed with water (2 x 50 mL) and brine (50 mL) and dried over MgSO₄. The solvent was evaporated under reduced pressure, yielding the dinitro derivatives.

Ethyl-2-(4*H*-1,2,4-oxadiazol-5-on-3-yl)acetate (1)

Ethyl (*Z*)-3-amino-3-(hydroxyimino)propanoate (10.04 g, 68.7 mmol) was dissolved in 150 mL THF and diphosgene (7.63 g, 38.6 mmol) was added under ice-cooling. Triethylamine (13.00 g, 128.5 mmol), dissolved in 50 mL THF was added in portions. After stirring for 1 h at room temperature, the white precipitate was filtered off, giving a yellow filtrate. The solvent was removed under reduced pressure. N-pentane was added to the obtained oily liquid and the mixture was stored at -20 °C for 16 h, giving 3.97 g of **1** (60 %) as yellowish solid.

(2,5-Dihydro-1,2,4-oxadiazol-5-on-3-yl) acetic acid (2)

The obtained oil crystallized yielding 0.47 g of **2** (94 %).

DTA (5 °C min⁻¹): 177 °C (dec.); **IR** (cm⁻¹) $\tilde{\nu}$ = 3130 (m), 2982 (m), 2951 (w), 2723 (w), 2591 (w), 25170 (w), 2270 (w), 1958 (w), 1749 (m), 1716 (s), 1610 (m), 1538 (w), 1478 (m), 1403 (m), 1317 (w), 1280 (w), 1247 (m), 1178 (s), 1027 (w), 979 (m), 944 (m), 912 (m), 894 (w), 805 (m), 767 (w), 726 (w), 675 (w); **Raman** (1064 nm, 500 mW, 25 °C, cm⁻¹) $\tilde{\nu}$ = 2984 (24), 2951 (43), 2859 (12), 2267 (7), 2083 (4), 1773 (12), 1747 (9), 1719 (25), 1612 (34), 1485 (15), 1409 (25), 1285 (33), 1204 (7), 1185 (3), 1045 (6), 981 (56), 951 (17), 913 (58), 894 (12), 731 (12), 650 (30), 561 (9), 530 (17), 399 (20), 369 (7), 326 (7), 166 (39), 120 (50), 95 (91), 82 (100), **¹H NMR** (DMSO-D₆): δ : 12.33 (NH), 3.67 (CH₂); **¹³C{¹H} NMR** (DMSO-D₆): δ : 168.6 (COOH), 160.0 (C-ring), 155.4 (C-ring); **EA** (C₄H₃N₂O₄, 143.08 g mol⁻¹) calc: H 2.80, C 33.34, N 19.44 %; Found: H 3.03, C 33.33, N 19.22%.

3-Trinitromethyl-(1,2,4-oxadiazol-5-one) (3)

The obtained yellow oil was recrystallized with chloroform yielding 0.35 g of **3** as colorless crystals (88 %).

DTA (5 °C min⁻¹): 112 °C (dec.) **IR (ATR)**: $\tilde{\nu}$ = 3394 (w), 3165 (m), 2766 (w), 2503 (w), 1982 (w), 1905 (w), 1767 (s), 1703 (s), 1602 (s), 1584 (s), 1520 (w), 1501 (w), 1421 (m), 1277 (s), 1245 (s), 1194 (s), 1089 (m), 1026 (m), 1017 (m), 952 (m), 932 (s), 904 (m), 835 (m), 796 (m), 750 (m), 782 (w), 726 (s); **Raman** (1064 nm, 500 mW, 25 °C, cm⁻¹) $\tilde{\nu}$ = 2948 (9), 1815 (12), 1771 (25), 1694 (9), 1631 (27), 1623 (20), 1610 (35), 1575 (32), 1488 (22), 1414 (7), 1401 (7), 1339 (33), 1279 (23), 1204 (7), 988 (12), 974 (14), 964 (13), 941 (35), 914 (44), 838 (59), 799 (11), 764 (38), 648 (7), 636 (7), 620 (7), 559 (7), 499 (10), 423 (58), 377 (34), 358 (78), 346 (100), 301 (28), 219 (25), 205 (35), 150 (71), 128 (85), 91 (100); **¹H NMR** (DMSO-D₆): δ : 8.5 (br, NH); **¹³C{¹H} NMR** (DMSO-D₆): δ : 159.7 (C-ring), 156.9 (C-ring); 122.9 (C(NO₂)₃); **¹⁴N NMR** (DMSO-D₆): δ : -34.18 (NO₂); **EA** (C₃HN₅O₈, 235.07 g mol⁻¹) calc: H 0.43, C 15.33, N 29.79 %; Found: H 0.64, C 15.61, N 29.66 %. Sensitivity (50 μ m \leq grain size \leq 100 μ m): **IS**: 25 J; **FS**: 324 N; **ESD**: 1.5 J.

Ethyl (Z)-3-(acetoxymino)-3-aminopropanoate (4)

After the solvent was removed at high vacuum, the solid was washed with ethanol to give **4** (6.1 g, 95 %) as a colorless solid.

DTA (5 °C min⁻¹): 81.6 °C (melt). **IR** (cm⁻¹) $\tilde{\nu}$ = 3422 (w), 3334(w), 3222 (w), 2956 (w), 3002 (w), 2931 (m), 2360 (w), 1742 (m), 1723 (s), 1686 (w), 1650 (s), 1622 (m), 1482 (w), 1448 (w), 1429 (m), 1398 (w), 1366 (m), 1335 (m), 1230 (s), 1210, 1190, (s), 1115 (m), 1054 (m), 1025 (s), 1006 (m), 986 (s), 945 (m), 912 (m), 880 (s), 861 (m), 814 (w), 774 (w), 679 (w). **Raman** (1064 nm, 500 mW, 25 °C, cm⁻¹) $\tilde{\nu}$ = 3335 (6), 3224 (6), 2982 (38), 2954 (60), 2930 (100), 2878 (8), 1729 (28), 1647 (34), 1625 (36), 1481 (11), 1469 (10), 1446 (14), 1395 (10), 1267 (5), 1151 (7), 1116 (14), 1026 (6), 1009 (6), 991 (14), 954 (7), 914 (11), 882 (6), 862 (29), 644 (17), 623 (13), 588 (4), 414 (4), 366 (11), 338 (46), 306 (29), 196 (14), 154 (28), 128 (40), 113 (42), 88 (44); **¹H NMR** (DMSO-D₆) δ : 6.5 (br, NH₂), 4.11 (q, 7.0 Hz, OCH₂CH₃), 3.14 (s, CH₂), 2.05 (s, CH₃), 1.21 (t, 7.0 Hz, OCH₂CH₃). **¹³C{¹H} NMR** (DMSO-D₆) δ : 168.8 (COCH₂CNH₂), 168.1 (COON) 153.7 (CNONH₂), 61.0 (CH₂), 36.9 (OCH₂CH₃), 20.1 (CH₃), 14.5 (OCH₂CH₃); **EA** (C₇H₁₂N₂O₄, 188.18 g mol⁻¹) calc: H 6.43, C 44.68, N 14.89 %; Found: H 6.33, C 44.66, N 15.18 %.

Ethyl 2-(5-methyl-1,2,4-oxadiazol-3-yl)acetate (5)

Compound **5** (0.61 g, 77 %) was obtained as brown oil.

DTA (5 °C min⁻¹): 199.6 °C (dec.). **IR** (cm⁻¹) $\tilde{\nu}$ = 3479 (m), 3368 (m), 3186 (m), 2984 (m), 2937 (m), 2265 (w), 1727 (s), 662 (s), 1593 (m), 1467 (w), 1446 (w), 1391 (m), 1369 (m), 1326 (s), 1258 (m), 1183 (s), 1113 (w), 1096 (w), 1025 (s), 1023 (s), 971 (m), 8999 (m), 852 (m), 811 (w), 744 (w), 665 (w). **Raman** (1064 nm, 500 mW, 25 °C, cm⁻¹) $\tilde{\nu}$ = 3042 (2), 2976 (4), 2940 (100), 2877 (3), 2734 (6), 1738 (7), 1587 (7), 1531 (21), 1453 (8), 1413 (3), 11378 (4), 1012 (6), 883 (6), 656 (6), 410 (3), 384 (2), 342(6), 272 (2), 233 (2), 94 (30). **¹H NMR** (DMSO-D₆) δ : 4.13 (q, 7.1 Hz, OCH₂CH₃), 3.88 (s, CH₂), 2.59 (s, CH₃), 1.21 (t, 7.1 Hz, OCH₂CH₃). **¹³C{¹H} NMR** (DMSO-D₆) δ : 177.6 (C-ring), 168.2 (COO), 165.1 (C-ring), 61.5 (CH₂), 32.1 (OCH₂CH₃), 14.4 (OCH₂CH₃), 12.2 (CH₃). **EA** (C₇H₁₀N₂O₃, 170.17 g mol⁻¹) calc: H 5.92, C 49.42, N 16.46 %; Found: H 5.92, C 49.28, N 16.41 %.

2-(5-Methyl-1,2,4-oxadiazol-3-yl)acetic acid (6)

Compound **6** (0.1 g, 32 %) was obtained as a colorless solid.

DTA (5 °C min⁻¹): 206.8 °C (dec.). **IR** (cm⁻¹) $\tilde{\nu}$ = 2977 (w), 2823 (w), 2706 (w), 2587 (w), 2515 (w), 1719 (s), 1588 (s), 1535 (w), 1408 (s), 1383 (m), 1371 (s), 1338 (m), 1318 (m), 1279 (m), 1204 (s), 1043 (m), 1031 (m), 982 (m), 929 (m), 906 (s), 887 (w), 822 (w), 723 (w), 672 (w). **Raman** (1064 nm, 500 mW, 25 °C, cm⁻¹) $\tilde{\nu}$ = 2974 (24), 2959 (43), 2879 (12), 2227 (7), 2083(14) 1758 (100), 1587 (7), 1521 (21), 1473 (8), 1412 (3), 1137 (4), 1002 (6), 893 (6), 666 (6), 460 (3), 374 (2), 332(6), 282 (2), 243 (2); **¹H NMR** (DMSO-D₆) δ : 12.9 (br, COOH), 3.76 (CH₂), 2.58 (CH₃). **¹³C{¹H} NMR** (DMSO-D₆) δ : 177.4 (COOH), 169.7 (C-ring), 165.5 (C-ring), 32.3 (CH₂), 12.3 (CH₃). **EA** (C₅H₆N₂O₃, 142.11 g mol⁻¹): calc: H 4.26, C 42.26, N 19.71%; Found: H 4.51, C 41.97, N 19.51%.

5-Methyl-3-trinitromethyl-1,2,4-oxadiazole (7)

After filtration the solvent was evaporated under reduced pressure, yielding **7** as yellow liquid. For purification flash column chromatography was used (EtOAc/cyclohexane = 2/3) yielding **7** (1.34 g, 26%) as colorless liquid.

DTA (5 °C min⁻¹): 128°C (dec.). **IR** (cm⁻¹) $\tilde{\nu}$ = 2887 (w), 2362 (w), 1595 (s), 1576 (s), 1502 (w), 1436(w), 1383 (w), 1335 (w), 1284 (s), 1255 (m), 1107 (w), 1046 (w), 972 (w), 947 (w), 929 (w), 842 (m), 797 (s), 723 (w), 706 (w), 669 (w). **Raman** (1064 nm, 500 mW, 25 °C, cm⁻¹) $\tilde{\nu}$ = 3035 (4), 3020 (4), 3012 (2), 2989 (3), 2940 (68), 1636 (2), 1622 (13), 1579 (18), 1503 (60), 1373 (27), 1350 (5), 1337 (8), 1297 (12), 1283 (2), 1260 (5), 1108 (12), 1039 (8), 988 (3), 973 (4), 961 (2), 949 (46), 844 (77), 802 (8), 708 (15), 492 (5), 479 (3), 464 (4), 448 (3), 427 (2), 421 (15), 366 (4), 349 (100), 315 (4), 308 (2), 278 (9), 262 (3), 249 (5), 237 (4), 202 (16), 181 (3). **¹H NMR** (CDCl₃): δ : 2.72 (CH₃). **¹³C{¹H} NMR** (CDCl₃) δ : 180.4 (C-ring), 168.1 (C-ring), 120.0 (C(NO₂)₃), 12.5 (CH₃). **¹⁴N NMR** (CDCl₃): δ : -38 (NO₂), **EA** (C₄H₃N₅O₇, 233.10 g mol⁻¹): calc: H 1.30, C 20.61, N, 30.05 %. Found: H 1.44, C 20.38, N 29.94 %. Sensitivity (50 μ m \leq grain size \leq 100 μ m) **IS**: 30 J; **FS**: 324 N; **ESD**: 1.5 J.

Ethyl (Z)-3-amino-3-(((3-ethoxy-3-oxopropanoyl)oxy)imino)propanoate (8)

The solvent was evaporated under reduced pressure, resulting **8** as a yellowish liquid. For purification flash column chromatography (DCM/MeOH = 10/3) was used yielding **8** (7.72 g, 78%) as colorless liquid.

DTA (5 °C min⁻¹): 158.6 °C (dec). **IR** (cm⁻¹) $\tilde{\nu}$ = 3464 (w), 3355(w), 3204 (w), 2985 (w), 2942 (w), 3464 (m), 2360 (w), 1727 (s), 1644 (s), 1467 (w), 1446 (w), 1400 (m), 1370 (m), 1364 (m), 1326 (m), 1258 (m), 1180 (s), 1140 (s), 1026 (s), 960 (m), 919 (m), 881 (m), 856 (m), 813 (w), 785 (m), 679 (m). **Raman** (1064 nm, 500 mW, 25 °C, cm⁻¹) $\tilde{\nu}$ = 2983 (13), 2942 (100), 2883 (5), 1747 (17), 1735 (3), 1647 (22), 1605 (4), 1457 (24), 1410 (8), 1115 (18), 1097 (3), 1027 (8), 977 (4), 957 (9), 919 (4), 860 (17), 375 (3), 360 (3), 333 (12), 323 (12). **¹H NMR** (CDCl₃) δ : 5.6 (br, NH₂), 4.14 (q, 7.1 Hz, OCH₂CH₃), 4.06 (q, 7.1 Hz, OCH₂CH₃), 3.37 (CH₂COO), 3.16 (CH₂CNH₂), 1.21 (t, 7.1 Hz; OCH₂CH₃), 1.18 (t, 7.1Hz OCH₂CH₃). **¹³C{¹H} NMR** (CDCl₃) δ : 168.4 (COON), 166.7 (COCH₂CNH₂), 163.2 (COCH₂CO), 154.1 (CNH₂), 71.6 (CH₂CNH₂), 61.5 (CH₂COO), 40.4 (OCH₂CH₃), 35.8 (OCH₂CH₃), 13.9 (OCH₂CH₃), 13.8 (OCH₂CH₃). **EA** (C₁₀H₁₆N₂O₆, 142.11 g mol⁻¹) calc H 6.20, C 46.15, N, 10.76 %; Found: H 6.13, C 46.25, N 10.49 %.

Diethyl 2,2'-(1,2,4-oxadiazol-3,5-diyl)diacetate (9)

Distillation of compound **8** (7.7 g, 30 mmol) under reduced pressure ($T_{\text{in}} = 135\text{ }^{\circ}\text{C}$, $T_{\text{oil}} = 175\text{ }^{\circ}\text{C}$, $p = 1.8\text{ mbar}$) obtained **9** (6.1 g, 84 %) was as colorless liquid.

DTA ($5\text{ }^{\circ}\text{C min}^{-1}$): $204.1\text{ }^{\circ}\text{C}$ (dec.). **IR** (cm^{-1}) $\tilde{\nu} = 3467\text{ (w)}$, 2984 (w) , 2942 (w) , 2910 (w) , 2357 (w) , 1736 (s) , 1586 (m) , 1528 (w) , 1466 (w) , 1446 (w) , 1411 (m) , 1369 (m) , 1325 (m) , 1298 (m) , 1249 (m) , 1190 (s) , 1157 (s) , 1114 (m) , 1095 (m) , 1023 (s) , 939 (w) , 878 (w) , 813 (w) , 784 (w) , 736 (w) , 671 (w) . **Raman** (1064 nm , 500 mW , $25\text{ }^{\circ}\text{C}$, cm^{-1}) $\tilde{\nu} = 2978\text{ (7)}$, 2942 (100) , 2878 (6) , 1747 (12) , 1589 (8) , 1528 (24) , 1457 (14) , 1411 (5) , 1380 (3) , 1114 (9) , 1033 (3) , 1005 (9) , 938 (6) , 878 (14) , 685 (6) , 427 (2) , 337 (11) , 257 (2) , 221 (2) , 94 (43) . **$^1\text{H NMR}$** (CDCl_3) δ : $4.15\text{ (q, 7.1 Hz, OCH}_2\text{CH}_3)$, $4.13\text{ (q, 7.1 Hz, OCH}_2\text{CH}_3)$, $3.94\text{ (CH}_2)$, $3.76\text{ (CH}_2)$, $1.21\text{ (t, 7.1 Hz, OCH}_2\text{CH}_3)$, $1.20\text{ (t, 7.1 Hz, OCH}_2\text{CH}_3)$. **$^{13}\text{C}\{^1\text{H}\}$ NMR** (CDCl_3) δ : $173.2\text{ (COH}_2)$, $167.3\text{ (COCH}_2)$, 165.5 (C-ring) , 164.8 (C-ring) , $62.1\text{ (CH}_2\text{C-ring)}$, $61.6\text{ (CH}_2\text{C-ring)}$, $32.9\text{ (OCH}_2\text{CH}_3)$, $32.0\text{ (OCH}_2\text{CH}_3)$, $13.9\text{ (OCH}_2\text{CH}_3)$, $13.8\text{ (OCH}_2\text{CH}_3)$. **EA** ($\text{C}_{10}\text{H}_{14}\text{N}_2\text{O}_5$, 242.23 g mol^{-1}) calc: H 5.83, C 49.58, N 11.56 %; Found: H 5.88, C 49.31, N 11.51 %.

2,2'-(1,2,4-Oxadiazol-3,5-diyl)diacetic acid (10)

Compound **10** (0.8 g, 33%) was obtained as a colorless solid.

DTA ($5\text{ }^{\circ}\text{C min}^{-1}$): $117\text{ }^{\circ}\text{C}$ (melt), $251\text{ }^{\circ}\text{C}$ (dec.). **IR** (cm^{-1}) $\tilde{\nu} = 2991\text{ (w)}$, 2974 (w) , 2938 (w) , 2737 (w) , 2628 (w) , 2540 (w) , 1702 (s) , 1586 (m) , 1596 (m) , 1583 (w) , 1541 (w) , 1427 (m) , 1407 (m) , 1386 (w) , 1373 (m) , 1313 (m) , 1282 (m) , 1228 (s) , 1193 (m) , 1166 (m) , 1039 (w) , 1004 (w) , 940 (w) , 916 (m) , 891 (m) , 874 (m) , 843 (m) , 799 (m) , 728 (s) , 657 (s) . **Raman** (1064 nm , 500 mW , $25\text{ }^{\circ}\text{C}$, cm^{-1}) $\tilde{\nu} = 22975\text{ (18)}$, 2946 (100) , 1654 (5) , 1600 (13) , 1541 (46) , 1522 (10) , 1459 (10) , 1409 (24) , 1376 (15) , 1282 (9) , 1005 (20) , 934 (6) , 913 (56) , 668 (2) , 401 (9) , 375 (17) , 359 (7) , 191 (6) , 135 (15) , 97 (145) . **$^1\text{H NMR}$** (CDCl_3) δ : 10.73 (COOH) , 10.44 (COOH) , $8.90\text{ (CH}_2)$, $8.57\text{ (CH}_2)$. **$^{13}\text{C}\{^1\text{H}\}$ NMR** (CDCl_3) δ : 179.1 (COOH) , 174.3 (COOH) , 173.0 (C-ring) , 170.4 (C-ring) , $37.9\text{ (CH}_2\text{COOH)}$, $37.0\text{ (CH}_2\text{COOH)}$. **EA** ($\text{C}_6\text{H}_6\text{N}_2\text{O}_5$, 186.12 g mol^{-1}) calc: H 3.25, C 38.72, N 15.05 %; Found: H 3.72, C 39.04, N 15.15 %.

Diethyl-2,2'-(1,2,4-oxadiazol-5-on-3,4-yl)acetate (11)

After solving **1** (10.06 g, 58.4 mmol) in 200 mL THF, sodium hydride (2.53 g, 105.4 mmol) was added in portions. The reaction mixture was stirred at 60°C for 20 minutes, until gas development ceased. Ethyl bromoacetate (10.02 g, 60.0 mmol) was added and stirring at 60°C continued for another 3 hours. After cooling to room temperature, the brown precipitate was removed by filtration and the solvent was evaporated under reduced pressure. For purification flash column chromatography was used (EtOAc/cyclohexane = 2/3), yielding **11** (7.52 g, 50%) as yellowish liquid.

DTA (5 °C min⁻¹): 201 °C (dec.). **IR** (cm⁻¹) $\tilde{\nu}$ = 2986 (w), 1780 (s), 1736 (s), 1603 (w), 1471 (m), 1398 (w), 1372 (m), 1339 (m), 1260 (m), 1202 (s), 1097 (w), 1078 (w), 1020 (s), 948 (m), 870 (w), 785 (w), 756 (w), 705 (w), 661 (w). **Raman** (1064 nm, 500 mW, 25 °C, cm⁻¹) $\tilde{\nu}$ = 2974 (7), 2942 (100), 2878 (8), 2778 (3), 2732 (4), 2253 (6), 1785 (5), 1746 (12), 1604 (18), 1457 (20), 1425 (2), 1336 (6), 1303 (3), 1271 (3), 1115 (14), 1102 (2), 1078 (5), 1025 (7), 936 (5), 873 (31), 790 (12), 758 (3), 665 (6), 576 (5), 442 (4), 354 (15), 293 (3), 90 (67). **¹H NMR** (Acetone-D₆): δ : 4.43 (NCH₂), 4.11 (q, 7.1 Hz, OCH₂CH₃), 4.08 (q, 7.1 Hz, OCH₂CH₃), 3.76 (CCH₂), 1.21 (t, 7.0 Hz OCH₂CH₃), 1.11 (t, 7.0 Hz OCH₂CH₃). **¹³C{¹H} NMR** (Acetone-D₆): δ : 166.6 (COO), 166.0 (COO), 158.5 (C-ring), 154.8 (C-ring), 61.8 (NCH₂), 43.1 (CCH₂), 30.7 (OCH₂CH₃), 30.1 (OCH₂CH₃), 13.4 (OCH₂CH₃), 13.1 (OCH₂CH₃). **EA** (C₁₀H₁₄N₂O₆, 258.23 g mol⁻¹): calc: H 5.46, C 46.51, N 10.85 %; Found: H 5.54, C 47.40, N 10.52 %.

2,2'-(1,2,4-Oxadiazol-5-on-3,4-yl)diacetic acid (12)

To an aqueous solution of 4 mL hydrochloric acid in 100 mL water **11** (3.38 g, 13.1 mmol) was suspended. The reaction mixture was heated for 3 hours under reflux. The formed solution was extracted with ethyl acetate (4 x 50 mL). The combined organic phases were washed with 50 mL water, 50 mL brine and dried over MgSO₄. The solvent was evaporated under reduced pressure, yielding **12** as yellow powder. For purification the product was washed with 100 mL diethyl ether, giving **12** (1.05 g, 40%) as a white powder.

DTA (5 °C min⁻¹): 157 °C (melt), 225 °C (dec.). **IR** (cm⁻¹) $\tilde{\nu}$ = 2979 (w), 2945 (w), 2661 (w), 2574 (w), 1768 (s), 1706 (s), 1610 (m), 1465 (m), 1419 (m), 1400 (m), 1358 (w), 1342 (w), 1316 (w), 1243 (s), 1172 (s), 1146 (m), 1085 (w), 1019 (w), 953 (m), 894 (m), 834 (w), 810 (m), 767 (w), 745 (w), 676 (w). **Raman** (1064 nm, 500 mW, 25 °C, cm⁻¹) $\tilde{\nu}$ = 2979 (13), 2949 (84), 2877 (3), 2848

(2), 2264 (5), 1784 (3), 1761 (15), 1665 (6), 1611 (31), 1469 (10), 1419 (15), 1360 (3), 1344 (11), 1174 (6), 1147 (7), 1087 (10), 956 (3), 901 (16), 811 (33), 769 (10), 748 (6), 670 (17), 595 (11), 558 (9), 542 (3), 490 (4), 437 (3), 419 (9) 359 (5), 300 (6), 132 (9), 99 (100). **¹H NMR** (Acetone-D₆): δ : 9.2 (br, COOH), 4.43 (NCH₂), 3.76 (CCH₂). **¹³C{¹H} NMR** (Acetone-D₆): δ : 168.4 (COOH), 168.0 (COOH), 159.5 (C-ring), 155.9 (C-ring), 43.7 (NCH₂), 31.3 (CCH₂). **EA** (C₆H₆N₂O₆, 202.12 g mol⁻¹): calc: H 2.99, C 35.65, N 13.86 %; Found: H 3.15, C 36.08, N 13.64 %.

Ethyl-2-(4-methyl-1,2,4-oxadiazol-5-on-3-yl)acetate (**13**)

To a mixture of **1** (2.42 g, 14.1 mmol) was dissolved in 40 mL THF sodium hydride (0.60 g, 25.0 mmol) was added in portions. The reaction mixture was stirred at 60°C for 20 minutes, until gas development ceased. Dimethylsulfate (2.14 g, 17.0 mmol) was added and stirring at 60°C continued for another 3 hours. The brown precipitate was removed by filtration and the solvent was evaporated under reduced pressure, yielding **13** as a yellow liquid. For purification flash column chromatography was used (chloroform/EtOAc = 9/1), yielding **13** (2.09 g, 79%) as colorless liquid.

DTA (5 °C min⁻¹): 175 °C (dec.). **IR** (cm⁻¹) $\tilde{\nu}$ = 2985 (w), 1769 (s), 1732 (s), 1638 (w), 1604 (m), 1483 (m), 1418 (w), 1395 (w), 1371 (m), 1337 (m), 1297 (w), 1244 (m), 1220 (m), 1190 (s), 1115 (w), 1096 (w), 1023 (m), 992 (m), 951 (w), 888 (w), 870 (w), 803 (w), 751 (m), 715 (w), 646 (w), 623 (w). **Raman** (1064 nm, 500 mW, 25 °C, cm⁻¹) $\tilde{\nu}$ = 2941 (100), 2877 (4), 1779 (12), 1739 (7), 1606 (21), 1457 (19), 1320 (5), 1116 (10), 995 (5), 872 (15), 768 (8), 751 (15), 717 (21), 668 (13), 648 (7), 540 (5), 367 (18), 337 (7), 263 (11). **¹H NMR** (CDCl₃): δ : 4.19 (q, 7.0 Hz, OCH₂CH₃), 3.63 (CCH₂), 3.17 (NCH₃), 1.24 (t, 7.0 Hz, OCH₂CH₃). **¹³C{¹H} NMR** (CDCl₃): δ : 165.7 (COO), 159.3 (C-ring), 154.2 (OCH₂CH₃), 62.5 (OCH₂CH₃), 31.0 (CCH₂), 28.5 (NCH₃), 14.0 (OCH₂CH₃). **EA** (C₇H₁₀N₂O₄, 186.17 g mol⁻¹): calc: H 5.41, C 45.16, N 15.05 %; Found: H 5.24, C 45.10, N 15.16 %.

2-(4-Methyl-1,2,4-oxadiazol-5-on-3-yl)acetic acid (**14**)

Alternatively, **14** can also be prepared via acidic ester cleavage. Compound **13** (1.00 g, 6.3 mmol) was suspended to a solution of 1 mL conc. hydrochloric acid in 30 mL of water. The reaction mixture was heated for 2 hours under reflux. The formed solution was extracted with ethyl

acetate (4 x 10 mL), the combined organic phases were washed with brine and dried over MgSO_4 . The solvent was evaporated under reduced pressure, yielding **14** (0.30 g, 30%) as orange liquid.

The general synthesis method with basic conditions yielded **14** (0.30 g, 30%) as yellow liquid.

DTA (5 °C min⁻¹): 205 °C (dec.). **IR** (cm⁻¹) $\tilde{\nu}$ = 3102 (w), 2984 (w), 2608 (w), 2260 (w), 1729 (s), 1605 (m), 1485 (m), 1396 (m), 1376 (w), 1331 (w), 1221 (m), 1173 (s), 1044 (w), 995 (w), 951 (w), 937 (w), 895 (w), 849 (w), 814 (w), 753 (m), 696 (w). **Raman** (1064 nm, 500 mW, 25 °C, cm⁻¹) $\tilde{\nu}$ = 2942 (100), 2257 (12), 1780 (2), 1738 (11), 1607 (24), 1487 (3), 1458 (15), 1400 (5), 1334 (5), 1116 (7), 1003 (5), 900 (16), 850 (4), 769 (6), 754 (21), 699 (29), 637 (17), 536 (3), 392 (10), 320 (5), 94 (81). **¹H NMR** (Acetone-D₆): δ : 9.82 (s, 1H, COOH), 3.89 (CCH₂), 3.25 (NCH₃). **¹³C{¹H} NMR** (Acetone-D₆): δ : 172.1 (COOH), 168.2 (C-ring), 156.3 (C-ring), 31.1 (CCH₂), 28.7 (NCH₃). **EA** (C₅H₆N₂O₄, 158.11 g mol⁻¹): calc: H 3.83, C 37.98, N 17.72 %; Found: H 3.59, C 38.11, N 17.31 %.

4-Methyl-3-trinitromethyl-(1,2,4-oxadiazol-5-one) (**15**)

The solvent was evaporated under reduced pressure, yielding **15** as yellow liquid. For purification flash column chromatography was used (EtOAc/cyclohexane = 2/3), using *p*-anisaldehyde as colorant. **15** formed yellow crystals after purification (0.36 g, 25 %).

DTA (5 °C min⁻¹): 119 °C (dec.). **IR** (cm⁻¹) $\tilde{\nu}$ = 3584 (w), 2962 (w), 2920 (w), 2891 (w), 2866 (w), 2610 (w), 2218 (w), 2100 (w), 2028 (w), 1905 (w), 1808 (m), 1791 (s), 1758 (w), 1658 (w), 1618 (s), 1589 (s), 1562 (s), 1482 (w), 1418 (w), 1340 (w), 1302 (m), 1273 (s), 1185 (w), 1110 (w), 1035 (m), 992 (m), 955 (w), 925 (w), 919 (w), 838 (m), 804 (s), 795 (s), 747 (s), 693 (w), 672 (s). **Raman** (1064 nm, 500 mW, 25 °C, cm⁻¹) $\tilde{\nu}$ = 2962 (23), 2905 (5), 2822 (2), 1807 (10), 1796 (4), 1635 (2), 1623 (20), 1593 (4), 1563 (13), 1482 (9), 1420 (9), 1341 (12), 1304 (6), 1279 (9), 1221 (6), 1112 (3), 1036 (10), 995 (3), 972 (6), 937 (5), 919 (13), 839 (43), 805 (8), 797 (21), 673 (30), 601 (4), 556 (15), 438 (24), 393 (35), 347 (62), 262 (12), 205 (22), 114 (100), 97 (10). **¹H NMR** (CDCl₃): δ : 3.25 (NCH₃). **¹³C{¹H} NMR** (CDCl₃): δ : 156.3 (C(NO₂)₃), 145.5 (C-ring), 118.4 (C-ring), 29.7 (NCH₃). **¹⁴N NMR** (CDCl₃): δ : -42 (NO₂). **EA** (C₄H₃N₅O₈, 249.10 g mol⁻¹): calc: H 1.21, C 19.29, N 28.12 %; Found: H 1.32, C 19.23, N 28.21%. Sensitivity (50 μm \leq grain size \leq 100 μm) **IS**: 30 J; **FS**: 324 N; **ESD**: 1.5 J.

Ethyl-2,2 dinitro-(4H-1,2,4-oxadiazol-5-on-3-yl)acetate (16)

Compound **16** (0.57 g, 76 %) was obtained as a colorless solid

DTA (5 °C min⁻¹): 93 °C (melt), 197 °C (dec.). **IR** (cm⁻¹) $\tilde{\nu}$ = 3156 (m), 3038 (m), 2999 (m), 1797 (s), 1780 (s), 1601 (s), 1574 (s), 1467 (m), 1299 (s), 1274 (m), 1232 (s), 1092 (s), 1035 (m), 982 (m), 963 (m), 944 (m), 903 (s), 839 (s), 812 (m), 747 (s). **Raman** (1064 nm, 500 mW, 25 °C, cm⁻¹) $\tilde{\nu}$ = 3040 (39), 2994 (90), 2948 (100), 1792 (63), 1598 (43), 1572 (57), 1457 (42), 1353 (42), 1269 (52), 1234 (39), 949 (63), 846 (36), 816 (35), 747 (28), 542 (32), 394 (69), 371 (47), 333 (85), 237 (33). **¹H NMR** (CDCl₃): δ : 4.54 (q, ³J = 7.5 Hz), 1.29 (q, ³J = 7.4 Hz). **¹³C{¹H} NMR** (CDCl₃): δ : 13.4 (CH₃CH₂), 67.1 (CH₃CH₂), 109.4 (C(NO₂)₂), 152.9 (C-ring), 154.6 (COC(NO₂)₂), 163.6 (C-ring). **¹⁴N NMR** (CDCl₃): δ : -21 (NO₂). **EA** (C₆H₆N₄O₈, 262.13 g mol⁻¹): calc: H 2.31, C 27.49, N 21.38%; Found: H 2.37, C 27.53, N 20.99%. Sensitivity (50 μ m \leq grain size \leq 100 μ m) **IS**: >40 J; **FS**: 240 N; **ESD**: 1.5 J.

Ethyl 2,2 dinitro-(5-methyl-1,2,4-oxadiazol-3-yl)acetate (17)

Compound **17** (0.53 g, 69 %) was obtained as a yellowish liquid.

DTA (5 °C min⁻¹): 207 °C (dec.). **IR** (cm⁻¹) $\tilde{\nu}$ = 2988 (w), 1776 (m), 1740 (s), 1656 (w), 1580 (s), 1470 (w), 1412 (m), 1371 (m), 1334 (m), 1286 (m), 1238 (m), 1202 (m), 1096 (m), 1028 (m), 971 (w), 929 (w), 842 (m), 800 (s), 713 (w), 611 (w), 578 (w). **Raman** (1064 nm, 500 mW, 25 °C, cm⁻¹) $\tilde{\nu}$ = 2969 (22), 1746 (19), 1730 (17), 1581 (33), 1531 (50), 1505 (64), 1456 (40), 1423 (24), 1374 (40), 1298 (23), 1111 (20), 1031 (19), 1011 (18), 993 (17), 947 (57), 871 (21), 843 (53), 819 (18), 707 (20), 687 (17), 654 (27), 641 (22), 572 (23), 549 (18), 522 (20), 490 (22), 478 (21), 423 (49), 408 (42), 347 (100), 296 (32), 285 (34), 258 (37), 199 (43), 275 (41). **¹H NMR** (CDCl₃): δ : 4.49 (q, 7.1 Hz, OCH₂CH₃), 2.66 (s, CH₃), 1.35 (t, 7.1 Hz, OCH₂CH₃). **¹³C{¹H} NMR** (CDCl₃): δ : 170.1 (COO), 168.4 (C-ring), 165.8 (C-ring), 107.3 (CH₂), 33.1 (OCH₂CH₃), 16.6 (OCH₂CH₃), 12.7 (CH₃). **¹⁴N NMR** (CDCl₃): δ : -28 (NO₂). **EA** (C₇H₈N₄O₇, 260.16 g mol⁻¹): calc: H 3.10, C 32.32, N 21.54%; Found: H 3.25, C 32.59, N 21.15%. Sensitivity (50 μ m \leq grain size \leq 100 μ m) **IS**: >40 J; **FS**: >360 N; **ESD**: 1.5 J.

Diethyl bis 2,2'-dinitro -(1,2,4-oxadiazol-3,5-diyl)diacetate (18)

Compound **18** (0.53 g, 61 %) was obtained as a colorless solid

DTA (5 °C min⁻¹): 91 (melt), 129 °C (dec.). **IR** (cm⁻¹) $\tilde{\nu}$ = 3146 (w), 3000 (w), 2340 (w), 1792 (m), 1758 (s), 1725 (w), 1586 (s), 1480 (m), 1467 (s), 1374 (m), 1350 (m), 1332 (m), 1264 (s), 1152 (m), 1088 (s), 995 (m), 958 (w), 856 (m), 831 (m), 807 (s), 764 (m), 712 (m), 672 (m), 615 (m). **Raman** (1064 nm, 500 mW, 25 °C, cm⁻¹) $\tilde{\nu}$ = 3148 (61), 3098 (53), 2978 (100), 2926 (34), 1793 (21), 1755 (42), 1725 (12), 1608 (51), 1596 (16), 1485 (10), 1470 (12), 1456 (24), 1447 (20), 1399 (15), 1376 (19), 1356 (26), 1303 (24), 1265 (8), 1155 (11), 1093 (18), 995 (11), 982 (11), 963 (15), 942 (24), 856 (40), 828 (10), 809 (14), 800 (15), 670 (9), 617 (8), 599 (16), 576 (12), 539 (9), 526 (10), 433 (31), 413 (41), 398 (38), 377 (89), 342 (31), 323 (26), 289 (24), 272 (34), 237 (22). **¹H NMR** (CDCl₃): δ : 4.61 (CH₃CH₂, J = 7.1 Hz), 4.52 (CH₃CH₂, J = 7.1 Hz), 1.38 (CH₃CH₂, J = 7.1 Hz), 1.36 (CH₃CH₂, J = 7.1 Hz). **¹³C{¹H} NMR** (CDCl₃): δ : 12.6 (CH₃CH₂), 13.0 (CH₃CH₂), 65.6 (CH₃CH₂), 66.7 (CH₃CH₂), 124.9 (C(NO₂)₂), 153.8 (C-ring), 156.0 (C-ring), 156.3, 161.0 (CO), 166.7 (CO). **¹⁴N NMR** (CDCl₃): δ : -25 (br, NO₂). **EA** (C₁₀H₁₀N₆O₁₃, 422.22 g mol⁻¹): calc: H 2.39, C 28.45, N 19.90%; Found: H 2.46, C 28.62, N 19.65%. Sensitivity (50 μ m \leq grain size \leq 100 μ m) **IS**: >40 J; **FS**: 360 N; **ESD**: 1.5 J.

General synthesis of the alkali and ammonium salts:

Into a solution of compound **19/20/21/22** (2 mmol) in 15 mL methanol, potassium- or barium hydroxyde (5 mmol/2 mmol) or conc. ammonia (5 mmol) dissolved in 10 mL methanol were added in one portion. The formed yellow precipitate was filtered and washed with methanol.

Dipotassium 3-dinitromethyl-(1,2,4-oxadiazol-5-onate) (19)

Compound **19** (0.44 g, 86 %) was obtained as a yellow solid.

DTA (5 °C min⁻¹): 219 °C (dec.). **IR** (cm⁻¹) $\tilde{\nu}$ = 3604 (m), 3532 (m), 3349 (m), 1652 (s), 1626 (s), 1508 (s), 1458 (s), 1386 (m), 1315 (s), 1292 (s), 1240 (m), 1145 (s), 1123 (s), 992 (m), 957 (m), 911 (s), 829 (s), 780 (m), 763 (m), 735 (m), 709 (w), 611 (w).. **Raman** (1064 nm, 500 mW, 25 °C, cm⁻¹) $\tilde{\nu}$ = 1509 (73), 1452 (9), 1391 (17), 1328 (19), 1297 (100), 1246 (7), 1145 (9), 1123 (7), 995 (4), 912 (3), 830 (11), 766 (8), 736 (6), 712 (4), 692 (5), 503 (5), 449 (3), 410 (7), 341 (3), 272 (4),

214 (4). $^{13}\text{C}\{^1\text{H}\}$ NMR (CDCl_3): δ : 160.1 (C-ring), 153.0 (C-ring), 121.4 ($\text{C}(\text{NO}_2)_2$). ^{14}N NMR (CDCl_3): δ : -24 (NO_2). **EA** ($\text{C}_3\text{K}_2\text{N}_4\text{O}_6$, 266.25 g mol $^{-1}$): calc: C 13.53, N 21.04%; Found: C 13.78, N 20.88%. Sensitivity ($50\text{ }\mu\text{m} \leq \text{grain size} \leq 100\text{ }\mu\text{m}$) **IS**: 3 J; **FS**: 120 N; **ESD**: 0.1 J.

Barium 3-dinitromethyl-(1,2,4-oxadiazol-5- onate) (20)

Compound **20** (0.52 g, 84 %) was obtained as a yellow solid.

DTA (5 °C min $^{-1}$): 145 °C (dec.). **IR** (cm^{-1}) $\tilde{\nu}$ = 3604 (m), 3532 (m), 3349 (m), 1652 (s), 1626 (s), 1508 (s), 1458 (s), 1386 (m), 1315 (s), 1292 (s), 1240 (m), 1145 (s), 1123 (s), 992 (m), 957 (m), 911 (s), 829 (s), 780 (m), 763 (m), 735 (m), 709 (w), 611 (w). **Raman** (1064 nm, 500 mW, 25 °C, cm^{-1}) $\tilde{\nu}$ = 1509 (73), 1452 (9), 1391 (17), 1328 (19), 1297 (100), 1246 (7), 1145 (9), 1123 (7), 995 (4), 912 (3), 830 (11), 766 (8), 736 (6), 712 (4), 692 (5), 503 (5), 449 (3), 410 (7), 341 (3), 272 (4), 214 (4). $^{13}\text{C}\{^1\text{H}\}$ NMR (CDCl_3): δ : 121.7 ($\text{C}(\text{NO}_2)_2$), 153.4 (C-ring), 160.9 (C-ring). ^{14}N NMR (CDCl_3): δ : -24 (NO_2). **EA** ($\text{C}_2\text{BaN}_4\text{O}_6$, 325.38 g mol $^{-1}$): calc: C 11.07, N 17.22%; Found: C 11.31, N 17.01%. Sensitivity ($50\text{ }\mu\text{m} \leq \text{grain size} \leq 100\text{ }\mu\text{m}$) **IS**: 10 J; **FS**: 160 N; **ESD**: 0.1 J.

Potassium 2,2-dinitro-(5-methyl-1,2,4- oxadiazolate) (21)

Compound **21** (0.73 g, 81 %) was obtained as a colorless solid

DTA (5 °C min $^{-1}$): 165 °C (dec.). **IR** (cm^{-1}) $\tilde{\nu}$ = 3403 (w), 2942 (w), 2510 (w), 1627 (w), 1583 (w), 1540 (m), 1481 (m), 1464 (m), 1389 (m), 1357 (m), 1220 (s), 1137 (s), 1120 (s), 1110 (s), 1049 (w), 1037 (w), 979 (w), 960 (w), 905 (w), 894 (w), 825 (w), 784 (w), 754 (w), 693 (w). **Raman** (1064 nm, 500 mW, 25 °C, cm^{-1}) $\tilde{\nu}$ = 2986 (9), 2931 (12), 2858 (8), 1579 (13), 1512 (34), 1492 (13), 1479 (14), 1391 (49), 1373 (68), 1250 (21), 1236 (22), 1147 (30), 1114 (29), 1051 (11), 980 (17), 961 (33), 895 (7), 826 (100), 786 (8), 695 (7), 488 (10), 473 (29), 442 (9), 403 (21), 325 (7), 244 (12). ^1H NMR (CDCl_3): δ : 2.62 (CH_3). $^{13}\text{C}\{^1\text{H}\}$ NMR (CDCl_3): δ : 176.9 (C-ring), 163.4 (C-ring), 115.2 ($\text{C}(\text{NO}_2)$), 12.4 (CH_3). ^{14}N NMR (CDCl_3): δ : -22 (NO_2). **EA** ($\text{C}_4\text{H}_3\text{KN}_4\text{O}_5$, 226.19 g mol $^{-1}$): calc: H 1.34, C 21.24, N 24.77%; Found: H 1.39, C 21.59, N 24.39%. Sensitivity ($50\text{ }\mu\text{m} \leq \text{grain size} \leq 100\text{ }\mu\text{m}$) **IS**: 4 J; **FS**: 120 N; **ESD**: 0.75 J.

Diammonium bis-2,2'-dinitro-(1,2,4-oxadiazol-3,5-ate) (22)

Compound **22** (0.81 g, 65 %) was obtained as a colorless solid

DTA (5 °C min⁻¹): 130 °C (dec.). **IR** (cm⁻¹) $\tilde{\nu}$ = 3393 (m), 3205 (m), 3131 (m), 2985 (m), 2840 (w), 1731 (m), 1695 (s), 1591 (m), 1498 (m), 1477 (m), 1453 (m), 1406 (m), 1366 (w), 1305 (w), 1228 (s), 1113 (m), 1096 (m), 1020 (s), 967 (m), 867 (m), 829 (m), 776 (s), 757 (m). **Raman** (1064 nm, 500 mW, 25 °C, cm⁻¹) $\tilde{\nu}$ = 2985 (100), 2938 (93), 2900 (26), 1736 (50), 1503 (28), 1482 (42), 1461 (45), 1443 (27), 1278 (24), 1236 (19), 1118 (44), 1025 (21), 980 (100), 873 (31), 607 (23), 454 (58), 370 (50), 301 (25). **¹H NMR** (CDCl₃): δ : 7.4 (br, NH₄). **¹³C{¹H} NMR** (CDCl₃): δ : 154.5 (C-ring), 153.8 (C-ring), 113.8 (br, C(NO₂)₂). **¹⁴N NMR** (CDCl₃): δ : -24 (NO₂). **EA** (C₄H₈N₈O₉, 312.16 g mol⁻¹): calc: H 2.58, C 15.39, N 35.90%; Found: H 2.77, C 15.60, N 35.61%. Sensitivity (50 μ m \leq grain size \leq 100 μ m) **IS**: 3 J; **FS**: 120 N; **ESD**: 0.75 J.

Ethyl 3-amino-2,2-dinitro-3-oxopropanoate (23)

Heating of compound **18** in acetone for 4 hours yielded compound **23** (0.45 g, 52 %) as a colorless solid.

DTA (5 °C min⁻¹): 120 °C (dec.). **IR** (cm⁻¹) $\tilde{\nu}$ = 3386 (m), 3215 (w), 3003 (w), 2947 (w), 1753 (m), 1729 (s), 1580 (s), 1537 (m), 1469 (w), 1444 (w), 1365 (w), 1303 (s), 1279 (s), 1263 (s), 1115 (w), 1079 (m), 1023 (w), 998 (m), 918 (w), 859 (w), 839 (m), 811 (m), 778 (m), 724 (w), 693 (w). **Raman** (1064 nm, 500 mW, 25 °C, cm⁻¹) $\tilde{\nu}$ = 3003 (33), 2991 (34), 2977 (39), 2962 (17), 2947 (71), 2928 (24), 2904 (14), 1759 (34), 1714 (24), 1612 (16), 1595 (46), 1583 (25), 1457 (20), 1446 (14), 1393 (21), 1350 (35), 1266 (11), 1115 (17), 1027 (15), 861 (69), 840 (19), 815 (23), 604 (17), 432 (22), 401 (61), 378 (100), 369 (69), 339 (43). **¹H NMR** (CDCl₃): δ : 7.21 (NH₂), 4.16 (q, CH₂, J = 7.1 Hz), 1.21 (t, CH₃, J = 7.1 Hz). **¹³C{¹H} NMR** (CDCl₃): δ : 172.8 (CONH₂), 171.1 (CO), 117.3 (C(NO₂)₂), 58.4 (CH₂), 14.3 (CH₃). **¹⁴N NMR** (CDCl₃): δ : -23 (NO₂). **EA** (C₅H₇N₃O₇, 221.13 g mol⁻¹): calc: H 3.19, C 27.16, N 19.00%; Found: H 3.33, C 27.24, N 18.69%. Sensitivity (50 μ m \leq grain size \leq 100 μ m) **IS**: 4 J; **FS**: 160 N; **ESD**: 1.0 J.

5. References

- [1] X. Xiao, E. Yao, Q. Liu, K. Ding, H. Su, T. Li, M. Zhang, Z. Ge, *Huaxue Tuijinji Yu Gaofenzhi Cailiao*, **2015**, *13*, 63–68.
- [2] C. He, J. M. Shreeve, *Angew. Chem., Int. Ed.*, **2016**, *55*, 772–775.
- [3] A. G. Tyrkov, *Russ. J. Org. Chem.*, **2002**, *38*, 1218–1219.
- [4] Q. J. Axthammer, T. M. Klapötke, B. Krumm, R. Scharf, C. C. Unger, *Dalton Trans.*, **2016**, *45*, 18909–18920.
- [5] T. M. Klapötke, B. Krumm, R. Moll, S. F. Rest, Y. V. Vishnevskiy, C. Reuter, H.-G. Stammler, N. W. Mitzel, *Chem. - Eur. J.*, **2014**, *20*, 12962–12973.
- [6] M. Göbel, T. M. Klapötke, *Adv. Funct. Mater.*, **2009**, *19*, 347–365.
- [7] Q. Yu, P. Yin, J. Zhang, C. He, G. H. Imler, D. A. Parrish, J. M. Shreeve, *J. Am. Chem. Soc.*, **2017**, *139*, 8816–8819.
- [8] R. Haiges, K. O. Christe, *Inorg. Chem.*, **2013**, *52*, 7249–7260.
- [9] a) T. P. Kofman, G. Y. Kartseva, E. Y. Glazkova, K. N. Krasnov, *Russ. J. Org. Chem.*, **2005**, *41*, 753–757; b) A. L. Laikhter, V. P. Kislyi, V. V. Semenov, *Mendeleev Commun.*, **1993**, 20–21; c) O. V. Lukashevich, G. N. Novatskii, E. L. Golod, L. I. Bagal, *Zh. Org. Khim.*, **1972**, *8*, 908–913; d) O. P. Stepanova, M. A. Poryadkova, E. L. Golod, *Zh. Org. Khim.*, **1994**, *30*, 1458–1461.
- [10] a) T. M. Klapötke, *Chemistry of High-Energy Materials*, 4th Edition, Walter de Gruyter GmbH & Ko KG, Berlin, **2017**; b) T. M. Klapötke, B. Krumm, S. F. Rest, M. Suceśka, *Z. Anorg. Allg. Chem.*, **2014**, *640*, 84–92.
- [11] J. K. Guillory, *J. Med. Chem.*, **2009**, *52*, 5560.
- [12] T. M. Klapötke, N. Mayr, J. Stierstorfer, M. Weyrauther, *Chem. - Eur. J.*, **2014**, *20*, 1410–1417.
- [13] Y. Tang, C. He, G. H. Imler, D. A. Parrish, J. M. Shreeve, *Chem. - Eur. J.*, **2017**, *23*, 16401–16407.
- [14] M. A. Kettner, T. M. Klapötke, *Chem. Commun.*, **2014**, *50*, 2268–2270.
- [15] K. Hemming, *Sci. Synth.*, **2004**, *13*, 127–184.
- [16] a) L. Bauer, C. N. V. Nambury, C. L. Bell, *Tetrahedron*, **1964**, *20*, 165–171; b) Y. Oyola, S. Vukovic, S. Dai, *Dalton Trans.*, **2016**, *45*, 8532–8540; c) A. Kaplan, T. Keenan, M. Weinhouse, M. Wilson, A. Lindstrom, W. Ripka, M. Chen, Helicon Therapeutics, Inc., USA . **2012**, p. 285 pp.
- [17] Q. J. Axthammer, B. Krumm, T. M. Klapötke, *J. Org. Chem.*, **2015**, *80*, 6329–6335.
- [18] Q. J. Axthammer, T. M. Klapötke, B. Krumm, R. Moll, S. F. Rest, *Z. Anorg. Allg. Chem.*, **2014**, *640*, 76–83.

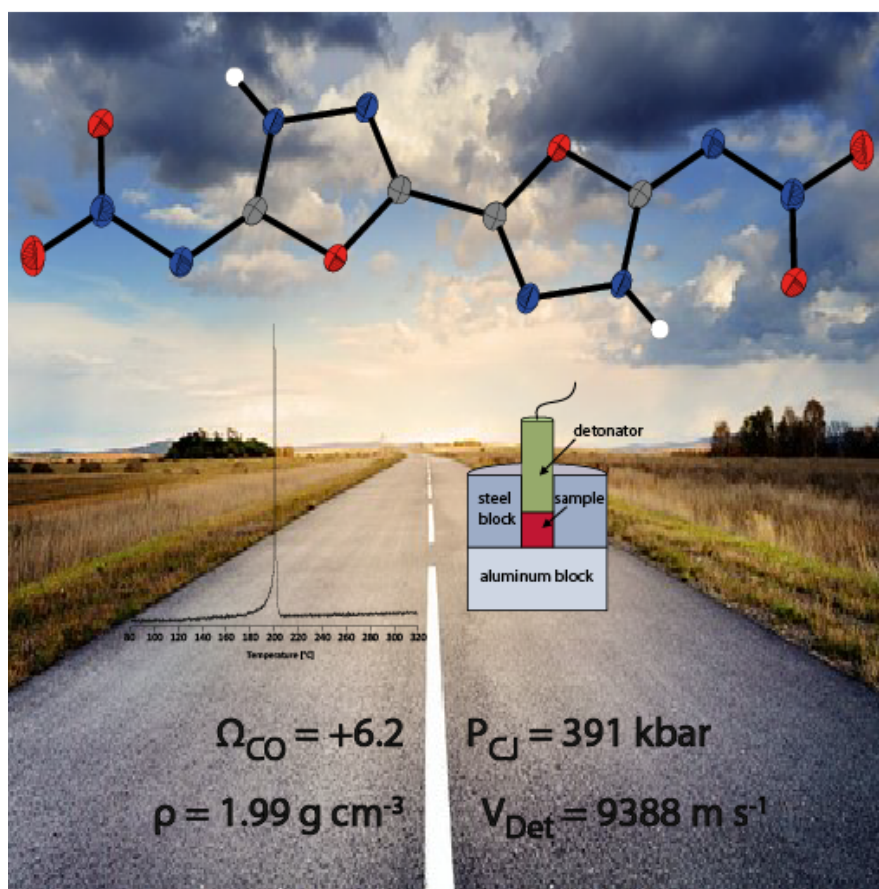
- [19] M. J. Frisch, G. W. Trucks, H. B. Schlegel, G. E. Scuseria, M. A. Robb, J. R. Cheeseman, G. Scalmani, V. Barone, B. Mennucci, G. A. Petersson, H. Nakatsuji, M. Caricato, X. Li, H. P. Hratchian, A. F. Izmaylov, J. Bloino, G. Zheng, J. L. Sonnenberg, M. Hada, M. Ehara, K. Toyota, J. H. R. Fukuda, M. Ishida, T. Nakajima, Y. Honda, O. Kitao, H. Nakai, M. T. Vreven, J. E. Peralta, F. Ogliaro, M. Bearpark, J. J. Heyd, E. Brothers, K. N. Kudin, V. N. Staroverov, R. Kobayashi, J. Normand, K. Raghavachari, A. Rendell, J. C. Burant, S. S. Iyengar, J. Tomasi, M. Cossi, N. Rega, J. M. Millam, M. Klene, J. E. Knox, J. B. Cross, V. Bakken, C. Adamo, J. Jaramillo, R. Gomperts, R. E. Stratmann, O. Yazyev, A. J. Austin, R. Cammi and C. Pomelli, J. W. Ochterski, R. L. Martin, K. Morokuma, V. G. Zakrzewski, G. A. Voth, P. Salvador, J. J. Dannenberg, S. Dapprich, A. D. Daniels, Ö. Farkas, J. B. Foresman, J. C. J. V. Ortiz, D. J. Fox, *Gaussian 09; Rev. C.01 ed., Gaussian, Inc., Wallingford CT (USA),*, **2010**.
- [20] R. D. Dennington II, T. A. Keith, J. M. Millam, *GaussView, Ver.5.08 ed., Semichem, Inc., Wallingford CT (USA),* **2009**.
- [21] M. Sućeska, *Propellants, Explos., Pyrotech.*, **1991**, *16*, 197–202.
- [22] P. J. Lindstrom, W. G. Mallard, **2011**, *NIST Standard Reference Database Number 69*.
- [23] M. S. Westwell, M. S. Searle, D. J. Wales, D. H. Williams, *J. Am. Chem. Soc.*, **1995**, *117*, 5013–5015.
- [24] *CrysAlis CCD, Version 1.171.35.11(release 16-05-2011CrysAlis 171.Net)*, Oxford Diffraction Ltd., Abingdon, Oxford (U.K.), **2011**.
- [25] *CrysAlis RED, Version 1.171.35.11(release 16-05-2011CrysAlis 171.Net)*, Oxford Diffraction Ltd., Abingdon, Oxford (U.K.), **2011**.
- [26] A. Altomare, M. C. Burla, M. Camalli, G. L. Cascarano, C. Giacovazzo, A. Guagliardi, A. G. G. Moliterni, G. Polidori, R. Spagna, *J. Appl. Crystallogr.*, **1999**, *32*, 115–119.
- [27] G. M. Sheldrick, *SHELX-97*, **1997**, Programs for Crystal Structure Determination.
- [28] L. J. Farrugia, *J. Appl. Crystallogr.*, **1999**, *32*, 837–838.
- [29] A. L. Spek, *Acta Crystallogr.*, **2009**, *65 D*, 148–155.
- [30] J. W. Ochterski, G. A. Petersson, J. A. Montgomery, Jr., *J. Chem. Phys.*, **1996**, *104*, 2598–2619.
- [31] J. A. Montgomery, Jr., M. J. Frisch, J. W. Ochterski, G. A. Petersson, *J. Chem. Phys.*, **2000**, *112*, 6532–6542.
- [32] M. Sućeska, *EXPLO5 V.6.03*, **2014**, Zagreb (Croatia).

Synthesis and Characterization of 2,2'-Dinitramino-5,5'-bi(1-oxa-3,4-diazole) and Derivatives as Economic and Highly Dense Energetic Materials

Tobias S. Hermann, K. Karaghiosoff, Thomas M. Klapötke* and Jörg Stierstorfer

Dedicated to John Fronabarger on the occasion of his 90th birthday.

Chemistry - A European Journal, **2017**, 23, 12087–12091.



Synthesis and Characterization of 2,2'-Dinitramino-5,5'-bi(1-oxa-3,4-diazole) and Derivatives as Economic and Highly Dense Energetic Materials

Tobias S. Hermann, K. Karaghiosoff, Thomas M. Klapötke* and Jörg Stierstorfer

Dedicated to John Fronabarger on the occasion of his 90th birthday.

Chemistry - A European Journal, **2017**, 23, 12087–12091.

Abstract:

2,2'-Dinitramino-5,5'-bi(1-oxa-3,4-diazole) (**2**) is a new highly energetic material with superior calculated detonation performance in comparison to cyclo-1,3,5-trimethylene-2,4,6-trinitramine (RDX) and penta erythritoltetranitrate (PETN) and can be prepared by an economical and practical two-step synthesis. The starting material 2,2'-diamino-5,5'-bi(1-oxa-3,4-diazole) (**1**) is synthesized by the reaction of oxalyl dihydrazide with cyanogen bromide. Nitration of **1** yields the title compound in perfect yield and purity. The combination of its high density of 1.986 g cm^{-3} , the positive heat of formation ($+190 \text{ kJ mol}^{-1}$), and a slightly positive oxygen balance ($+6.2\%$) results in ideal calculated detonation parameters (e.g. detonation velocity 9296 m s^{-1}). The sensitivities toward impact and friction can be adjusted by deprotonation and formation of corresponding nitrogen-rich salts, for example, ammonium (**3**), hydroxylammonium (**4**), and guanidinium (**5**) salts.

1. Introduction

Most high energy density materials (HEDMs) used in military and civilian applications (explosives, propellants, and pyrotechnics) have been invented more than 100 years ago. Prominent examples for the class of explosives are cyclo-1,3,5-trimethylene-2,4,6-trinitramine

(RDX), 1,3,5,7-tetranitrotetraaza-cyclooctane (HMX), 2,4,6-trinitrotoluene (TNT), and pentaerythritoltetranitrate (PETN). Although these compounds work excellent, further research is indispensable with the main focus on safety, toxicity, but also on performance reasons.^[1] Imposing examples with high predicted performances were described during the last years.^{[2] [3] [4]} Also the number of publications related to the misuse and detection of explosives is still increasing.^[5] Next to the upper mentioned main goals, the compounds have to meet numerous further demands for getting into industrial scales. This includes i) low sensitivities (impact, friction electrostatic discharge), ii) high thermal stability, iii) longevity, iv) compatibility (toward binders, antioxidants, shells, etc.), and many more. If all stability, performance, and safety aspects are complied, usually the synthetic costs prevent potential applications. Commonly used explosives can be prepared very cheap. For example one kg of hexogen (RDX) can be produced for less than 2\$, which is hard to keep with. In this contribution, we report on nitrated 2,2'-diamino-5,5'-bi-1-oxa-3,4-diazoles that interestingly have never been described yet. In contrast to 1,2,5-oxadiazoles (furazanes), 1,3,4-oxadiazoles are much less described as energetic materials. Some prominent energetic examples of C-C connected bi oxadiazoles are shown in Figure 1.

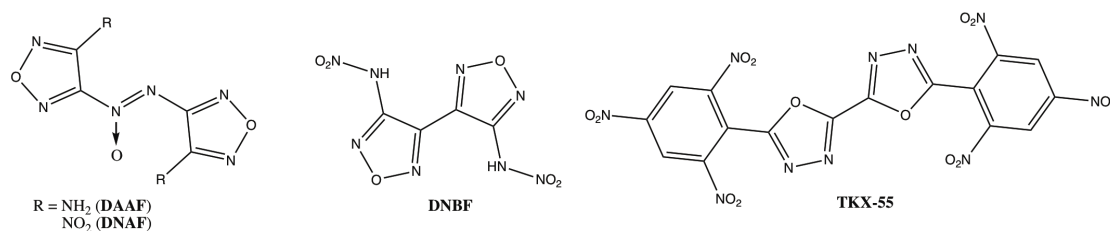
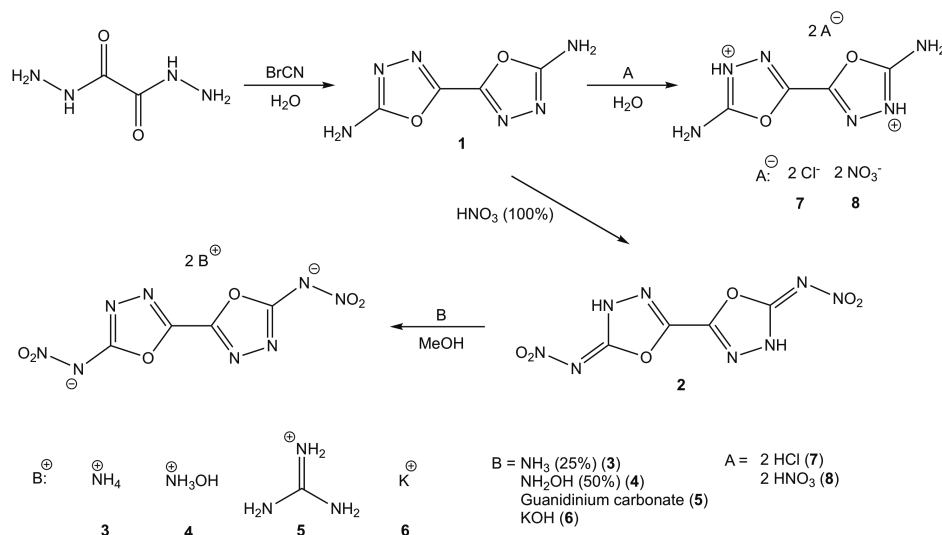


Figure 1: Chemical structures of selected prominent explosives oxadiazole based on bi-oxadiazoles: 3,3'-amino-4,4'-azoxyfurazan (**DAAF**)^[6], 3,3'-dinitro-4,4'-azoxyfurazan (**DNAF**)^[7], 3,3'-dinitramino-4,4'-bifurazane (**DNBF**)^[8] and 5,5'-bis(2,4,6-trinitrophenyl)-2,2'-bi(1,3,4-oxadiazole) (**TKX-55**)^[9].

2. Results and Discussion

Particularly, 1,3,4-oxadiazoles show a very good compromise of the above mentioned demands for new energetic materials. In contrast to previously described energetic materials based on five-membered heterocycles such as many tetrazole, triazole, pyrazole, and also furazanes derivatives, 1,3,4-oxadiazoles can be prepared very cost effective! The reaction of oxalyl dihydrazide with cyanogen bromide yields the precursor 2,2'-diamino-5,5'-bi(1-oxa-3,4-diazole) (**1**) in a yield larger than 85% (Scheme 1). Nitration of **1** in fuming nitric acid yields 2,2' dinitramino-5,5'-bi(1-oxa-3,4-diazole) (**2**) also in high yield (>80%) and purity. Compound **2** (which has a very low solubility in nearly all organic solvents) starts to precipitate free of solvent from the concentrated

nitration mixture after roughly 2 h. The precipitate could be characterized comprehensively after washing with ethanol and diethyl ether. Attempts to recrystallize low soluble **1** from concentrated mineral acids such as HCl or HNO₃ yielded the diprotonated chloride (**7**) and the dinitrate salt (**8**).



Scheme 1. Synthetic route toward explosive **2** and derivatives.

Up to now all attempts to recrystallize compound **2** from very polar solvents led to the formation of solvents. During this study we obtained single crystals of the monohydrate, dihydrate, di-DMSO and di-DMF adduct (shown in the SEI). Exemplarily the structure of the dihydrate^[10] which has an astonishing high density of 1.968 g cm⁻³ (at 173 K) is shown in Figure 2. In all structures, the remaining acid protons are located at the ring nitrogen N1 forming an intramolecular hydrogen bond, leading to a complete planar system. To tune the physico-chemical properties, additionally selected nitrogen-rich salts were prepared in methanol. These are the di-ammonium (**3**), di-hydroxylammonium (**4**), di-guanidinium (**5**) and di-potassium (**6**) salts. Except of compound **6**, which precipitates as dihydrate, all compounds precipitate from methanol free of solvent. Recrystallization of **3**, **4** and **6** from hot water yields the dihydrates (molecular structures of **3**·2H₂O and **4**·2H₂O are shown in Figure 3). Compound **5** does not form single crystals for XRD from any organic solvent at all.

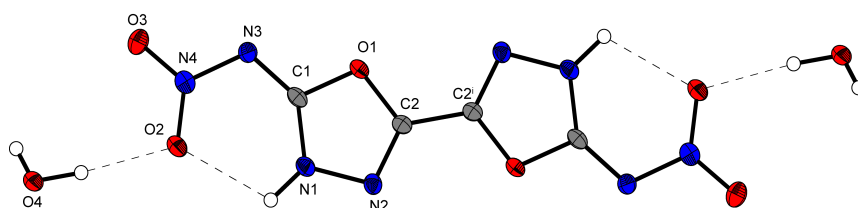


Figure 2. Molecular structure of **2**·2H₂O determined by XRD. Thermal ellipsoids show the 50% probability level. Symmetry code: (i) $-x, -y, -z$.

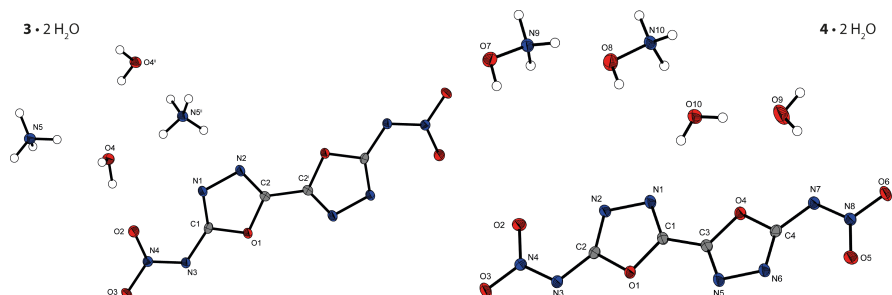


Figure 3. Molecular structure of the dihydrate of **3** and **4**. Thermal ellipsoids show the 50% probability level. Symmetry codes: **3**: (i) $2-x, 1-y, -z$; (ii) $0.5-x, 0.5+y, 0.5-z$.

The formation of compound **2** and its salts can easily be followed by NMR spectroscopy. In the ¹H NMR spectrum the amino groups of **1** are observed at 7.65 ppm, whereas for **2** the more acidic protons are shifted to 12.66 ppm. In ¹³C NMR spectroscopy **1** and **2** only slightly differ (**1**: 164.7 and 147.0 ppm; **2**: 163.5 and 145.8 ppm). Deprotonation causes only a small shift to lower fields (166.5 and 148.7 ppm for **3** and **4**).

The densities, which are strongly related to the energetic performance, of solvent free **2–4** were measured by Helium gas-pycnometry. The observed very high values are close to 2 g cm⁻³ (**1**: 1.99, **2**: 1.95, **3**: 1.92 g cm⁻³) which is impressively high for organic CHNO compounds. Heats of formation were calculated using the atomization method [11] based on CBS-4M electronic enthalpies. Compounds **2** and **4** are formed endothermic (**2**: 190 kJ mol⁻¹, **4**: 70 kJ mol⁻¹) while **3** is formed slightly exothermic (−72 kJ mol⁻¹). The calculated detonation parameters (calculated with EXPLO5 6.03 [12] of **2–4** are very promising and significantly better than those for hexogen (RDX). The sensitivities (impact, friction and electrostatic discharge) of **2–4** were also measured. Unfortunately **2** is very sensitive toward impact (1 J), in contrast **3** (10 J) and **4** (4 J) are less sensitive. The same trend is observed for friction and electrical discharge. Compound **2** (72 N, 0.15 J) is more sensitive than **3** (360 N, 1.0 J) and **4** (120 N, 0.5 J), respectively. The thermal behavior was studied by DTA and TGA measurements (5 K min⁻¹). Compound **2** decomposes at 200 °C. Water free ammonium salt **2** shows a loss of ammonia starting at already 40 °C and then decomposes also at 200 °C. In contrast the hydroxylammonium salt shows no loss of weight until its decomposition temperature of 160 °C. Compound **1** shows the highest temperature of decomposition (310 °C).

Table 1. Physical and chemical properties of **1–6** and **RDX**.

	1	2	3	4	5	6	RDX ^{[1c], [1a]}
$FW / g\ mol^{-1}$	168.12	258.11	292.17	324.17	376.25	370.32	222.12
$T_m / T_{dec} / ^\circ C$ ^{a)}	-/310	-/200	148/197	-/160	-/260	140/230	205/210
$\rho_{RT} / g\ cm^{-3}$ ^{b)}	1.93 ^{c)}	1.98 ^{c)}	1.95 ^{c)}	1.92 ^{c)}	1.79	2.04	1.806
IS / J ^{e)}	>40	1	10	4	40	5	7.5
FS / N ^{d)}	>360	72	360	120	360	288	120
ESD / J ^{e)}	>1.50	0.15	1.00	0.50	1	0.75	0.2
$N / \%$ ^{f)}	49.99	43.41	47.97	43.21	52.12	33.52	37.84
$O / \%$ ^{g)}	19.03	37.19	32.86	39.48	25.51	28.72	43.22
$N+O / \%$ ^{h)}	69.02	80.60	80.83	82.69	77.63	62.24	81.06
$\Omega_{CO} / \%$ ⁱ⁾	-38.1	+6.2	-11.0	0	-25.5	+9.5	0
$\Delta_f H^\circ / kJ\ mol^{-1}$ ^{j)}	77.4	278.6	-71.8	70.2	-59.9	-382.7	86.3
$-A_{ex} U^\circ / kJ\ kg^{-1}$ ^{k)}	-	5140	4035	4281	3561	3886	6190
T_{ex} / K ^{l)}	-	3920	2795	2899	2785	2941	4232
$P_{CJ} / kbar$ ^{m)}	-	391	349	341	248	233	380
$V_{det} / m\ s^{-1}$ ⁿ⁾	-	9388	9225	9186	8027	7567	8983

a) Onset melting point T_{mt} and decomposition point T_{dec} from DTA measurement carried out at a heating rate of 5 K min⁻¹. b) Density at room temperature from pycnometric measurements. c) Impact sensitivity (BAM drophammer, 1 out of 6). d) Friction sensitivity. e) Sensitivity towards electrostatic discharge. f) Nitrogen content. g) Oxygen content. h) Sum of nitrogen and oxygen content. i) Oxygen balance Ω assuming the formation of CO at the combustion. j) Calculated heat of formation. k) Detonation energy. l) Detonation temperature. m) Detonation pressure. n) Detonation velocity.

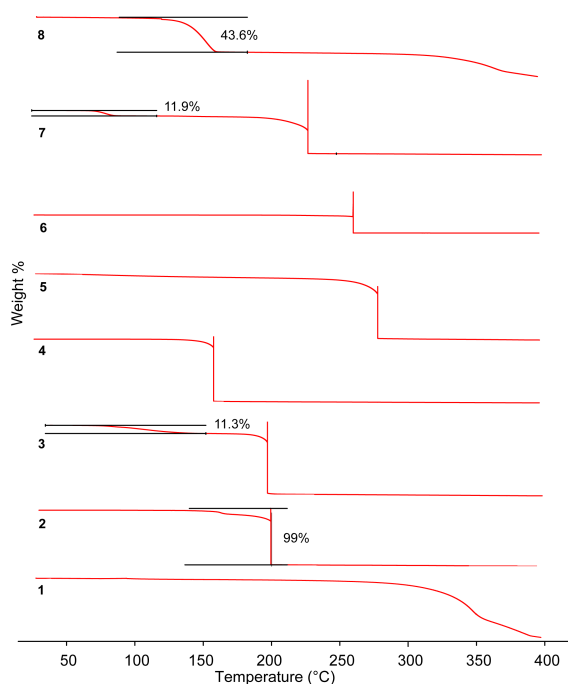


Figure 4. Thermoplots of **1–8** taken from TGA measurements (30–400°C, heating rate 5 deg min^{−1}).

3. Conclusion

In summary 2,2'-dinitramino-5,5'-bi(1-oxa-3,4-diazole) (**2**) is a high performing easy available explosive with a high impact sensitivity. Due to its high density of about 2 g cm^{−3}, its calculated detonation performance is significantly higher than that of hexogen. It could be successfully initiated by a standard detonator. Deprotonation with nitrogen bases such as ammonia or hydroxylamine yields the corresponding nitrogen-rich salts, which are also calculated to have high detonation performance. It is suggested to explore suitable composition of **2** in order to decrease its sensitivities or to synthesize further nitrogen-rich derivatives such as triazolium or tetrazolium salts. The salts should show better sensitivity values and similar stability and performance values.

Experimental Section

All experimental procedures and general methods are described in the Supporting Information.

4. Supporting Information

4.1 X-ray Diffraction

For XRD, an Oxford Xcalibur3 diffractometer with a CCD area detector was employed for data collection using Mo- $K\alpha$ radiation ($\lambda = 0.71073 \text{ \AA}$). By using the CRYSLISPRO software^[13] the data collection and reduction was performed. The structure was solved by direct methods (SIR-92^[14]^[15]) and refined by full-matrix least-squares on F^2 (SHELXL^[16]^[17]) and finally checked using the PLATON software^[18] integrated in the WinGX software suite. The non-hydrogen atoms were refined anisotropically and the hydrogen atoms were located and freely refined. The absorptions were corrected by a SCALE3 ABSPACK multiscan method.^[19] All DIAMOND2 plots are shown with thermal ellipsoids at the 50% probability level and hydrogen atoms are shown as small spheres of arbitrary radius.

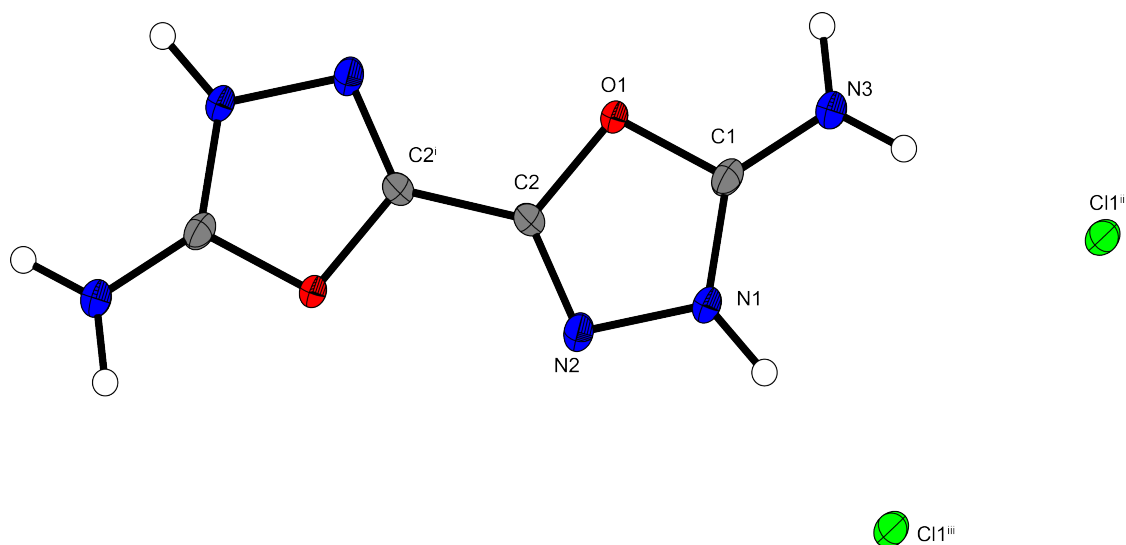


Figure S1: Molecular structure of 2,2'-diamino-5,5'-bi(1-oxa-3,4-diazolium) dihydrochloride (**7**). Selected Structural Information: monoclinic, $P2_1/c$, 1.743 g cm^{-3} . Selected bond lengths (\AA) and angles ($^\circ$): C2–C2' 1.434(4), N1–N2 1.384(3), C1–N3 1.290(3); C2–O1–C1 103.3(16), O1–C1–N3 120.6(2); C2i–C2–N2–N1 178.4(3), N2–N1–C1–N3 179.8(2). Symmetry codes: (i) $x, 1-y, -z$; (ii) $1-x, 0.5+y, 0.5-z$; (iii) $x, 0.5-y, 0.5+z$.

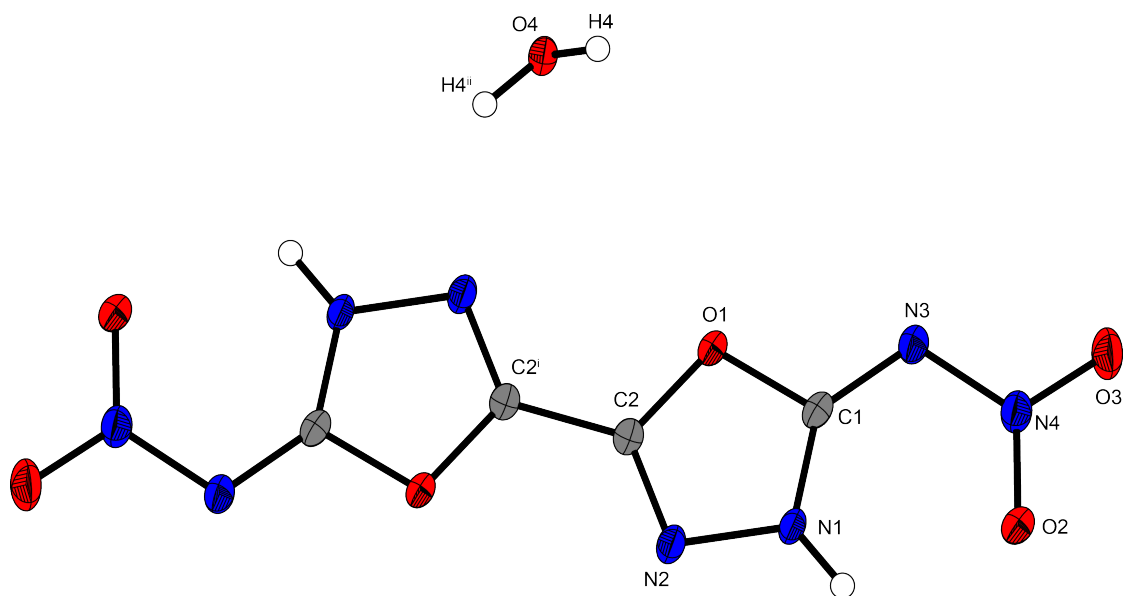


Figure S2: Molecular structure of 2,2'-dinitramino-5,5'-bi(1-oxa-3,4-diazolate) hydrate(2). Selected Structural Information: monoclinic, $C2/c$, 1.889 g cm⁻³. Selected bond lengths (Å) and angles (deg.): C2–C2ⁱ 1.441(2), N1–N2 1.3792(15), C1–N3 1.3179(16), N3–N4 1.3613(15); C2–O1–C1 104.25(9), O1–C1–N3 115.57(10), C1–N3–N4 114.37(10); C2ⁱ–C2–O1–C1 177.96(13), N2–N1–C1–N3 177.14(14); O1^c–C2^c–C2–O1 180.00(10), N1–C1–N3–N4 5.8(2). Symmetry codes: (i) 0.5–x, 0.5–y, 1–z; (ii) –x, y, 0.5–z.

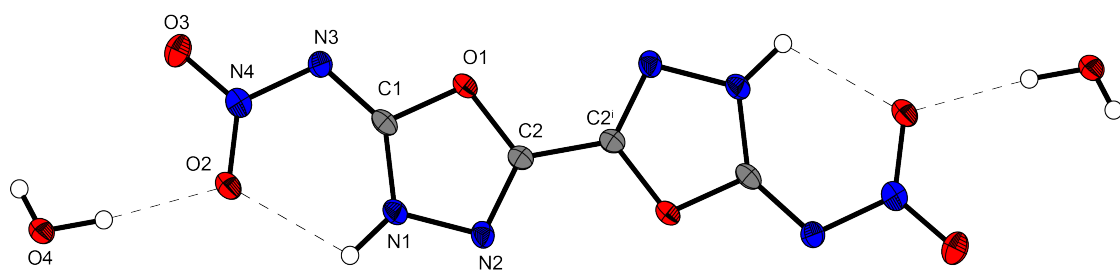


Figure S3: Molecular structure of 2,2'-dinitramino-5,5'-bi(1-oxa-3,4-diazolate) dihydrate (2). Selected Structural Information: monoclinic, $P2_1/n$, 1.968 g cm⁻³. Selected bond lengths (Å) and angles (deg.): C2–C2ⁱ 1.430(5), N2–N1 1.384(3), C1–N3 1.311(3), N3–N4 1.373(3); C1–O1–C2 104.92(19), O1–C1–N3 115.1(2), N1–C1–N3 138.1(3); C2ⁱ–C2–O1–C1 179.7(3), N2–N1–C1–N3 178.0(3), N1–C1–N3–N4 2.6(4). Symmetry codes: (i) –x, –y, –z.

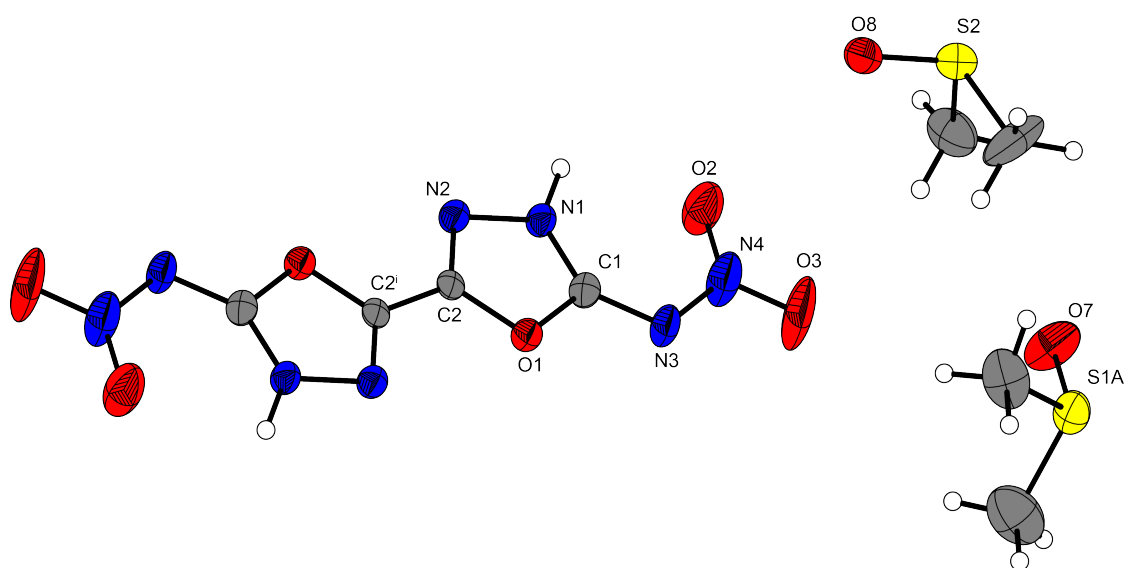


Figure S4: Molecular structure of 2,2'-dinitramino-5,5'-bi(1-oxa-3,4-diazolate) · 2DMSO (**2**). Selected Structural Information: monoclinic, $P2_1/c$, 1.537 g cm⁻³. Selected bond lengths (Å) and angles (deg.): C2–C2ⁱ 1.453(7), N2–N1 1.387(4), C1–N3 1.312(5), N3–N4 1.367(4); C2–O1–C1 103.9(3), O1–C1–N3 114.1(3), C1–N3–N4 114.0(3); N2–N1–C1–N3 177.3(5), N1–C1–N3–N4 0.7(7). Symmetry codes: (i) $-x, -y, -z$.

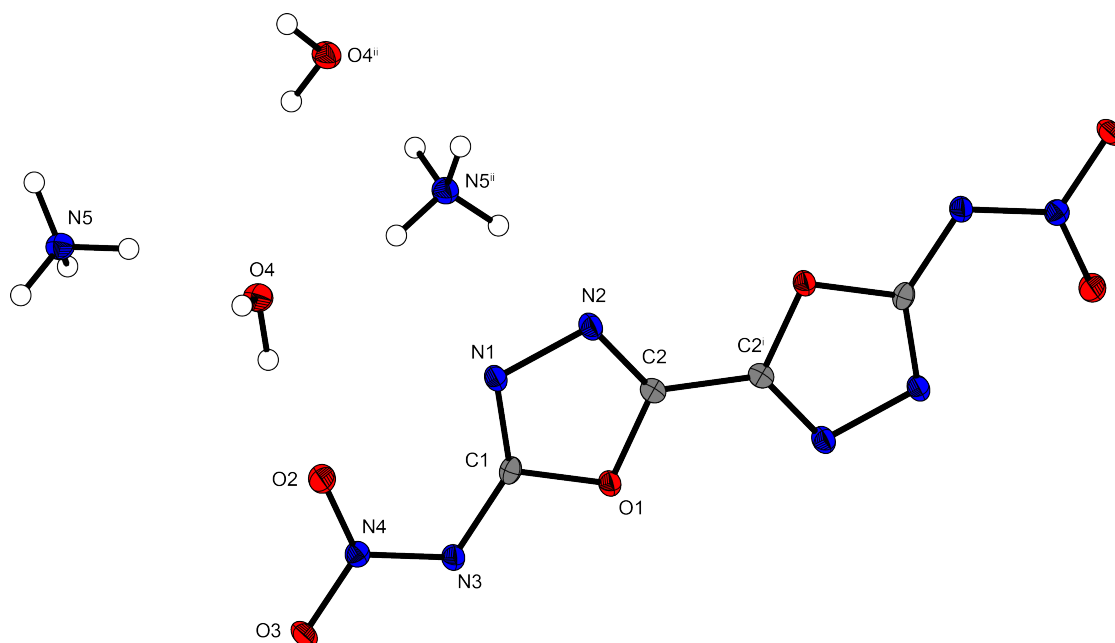


Figure S5: Molecular structure of di-ammonium 2,2'-dinitramino-5,5'-bi(1-oxa-3,4-diazolate) dihydrate (**3**). Selected Structural Information: monoclinic, $P2_1/n$, 1.742 g cm⁻³. Selected bond lengths (Å) and angles (deg.): C2–C2ⁱ 1.451(2), N2–N1 1.4067(14), C1–N3 1.3598(16), N3–N4 1.3374(15); C1–O1–C2 102.00(9), N1–C1–N3 136.36(11), C1–N3–N4 115.47(10); C2ⁱ–C2–O1–C1 178.66(13), O1–C1–N3–N4 175.77(9). Symmetry codes: (i) $2-x, 1-y, -z$; (ii) $0.5-x, 0.5+y, 0.5-z$.

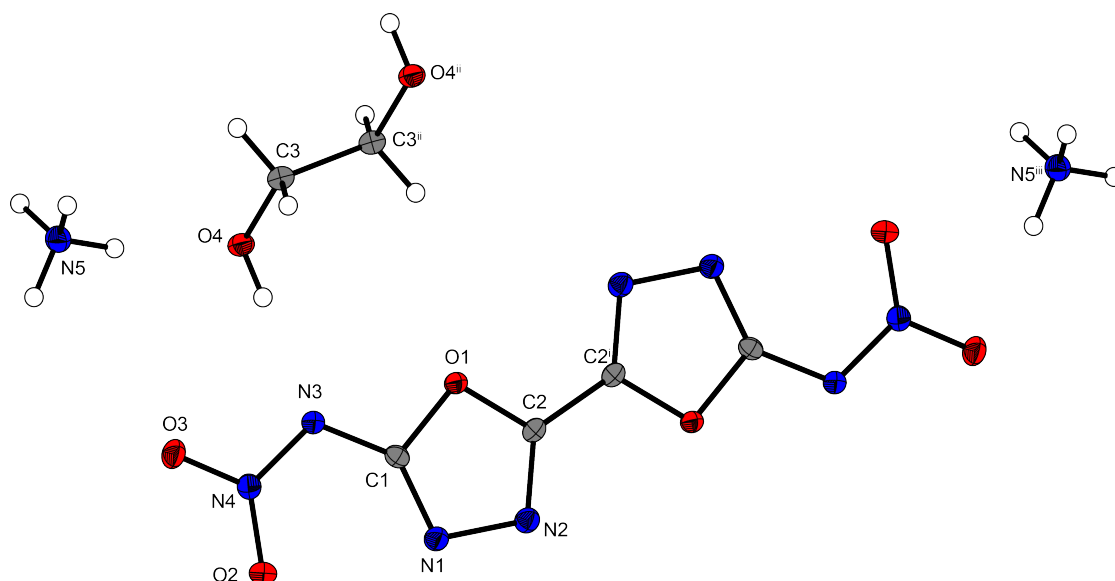


Figure S6: Molecular structure of di-ammonium 2,2'-dinitramino-5,5'-bi(1-oxa-3,4-diazolate) · ethylene glycol (**3**). Selected Structural Information: triclinic, $P\bar{1}$, 1.726 g cm⁻³. Selected bond lengths (Å) and angles (deg.): C2–C2ⁱ 1.447(2), N1–N2 1.4099(16), C1–N3 1.3624(17), N3–N4 1.3359(15); C1–O1–C2 101.74(9), N1–C1–N3 137.08(12), C1–N3–N4 116.58(10); C2ⁱ–C2–N2–N1 179.52(15), N2–N1–C1–N3 178.66(14). Symmetry codes: (i) 1–x, 1–y, –z; (ii) –x, –y, –z.

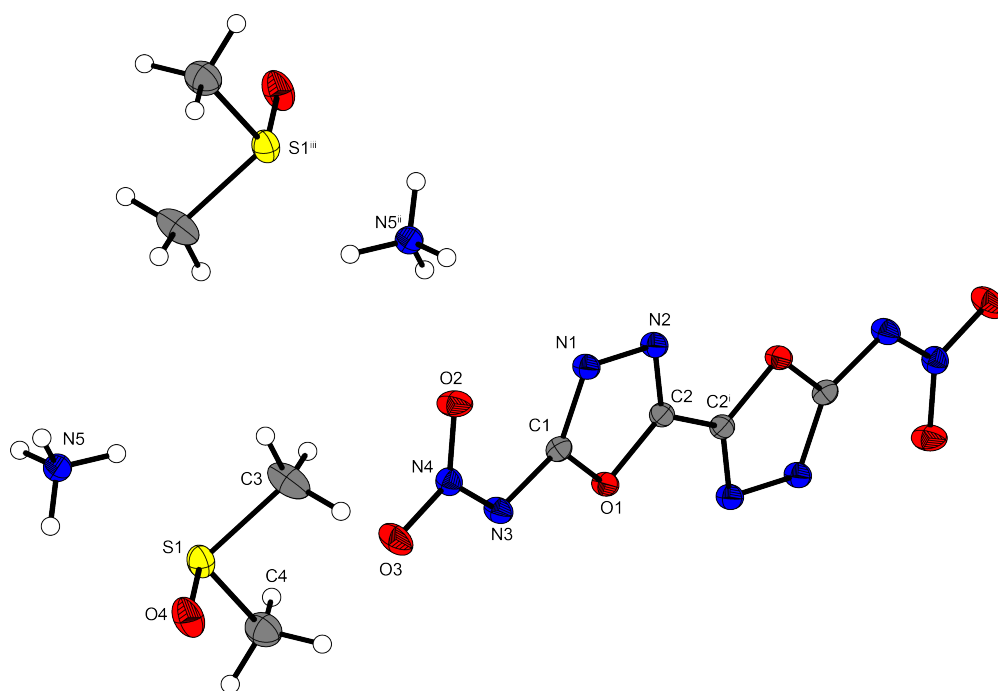


Figure S7: Molecular structure of di-ammonium 2,2'-dinitramino-5,5'-bi(1-oxa-3,4-diazolate) · 2DMSO (**3**). Selected Structural Information: triclinic, $P\bar{1}$, 1.569 g cm⁻³. Selected bond lengths (Å) and angles (deg.): C2ⁱ–C2 1.439(2), N1–N2 1.4070(14),

C1–N3 1.3544(16), N3–N4 1.3332(15); C1–O1–C2 102.17(9), N1–C1–N3 137.06(11), C1–N3–N4 115.28(11);
 C2i–C2–N2–N1 179.97(16), N1–C1–N3–N4 2.8(2). Symmetry codes: (i) 1–x, –y, 2–z; (ii) 1–x, 1–y, 1–z; (iii) 1–x, 1–y, 1–z.

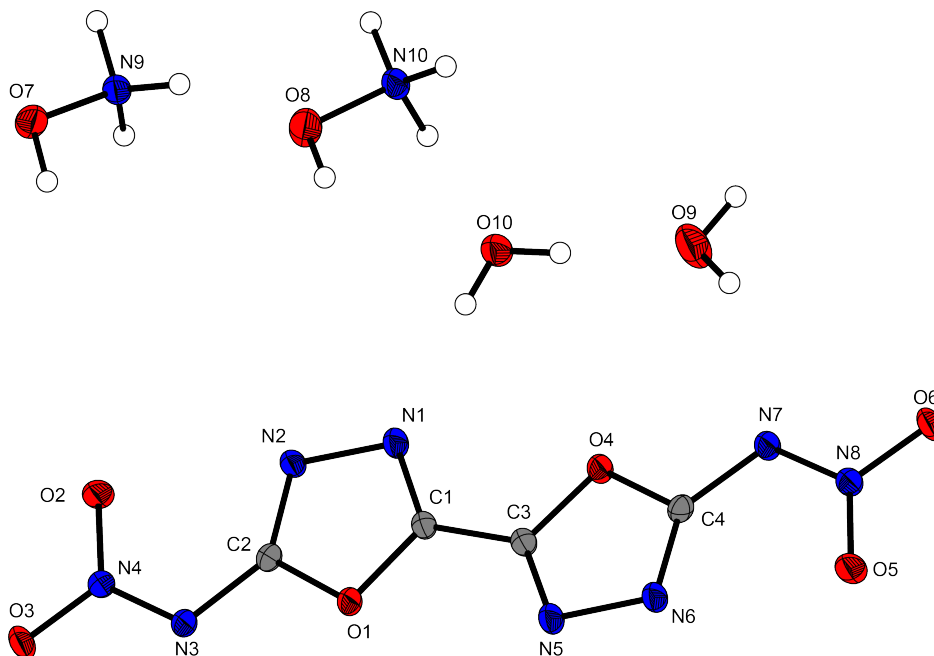


Figure S8: Molecular structure of di-hydroxylammonium 2,2'-dinitramino-5,5'-bi(1-oxa-3,4-diazolate) dihydrate (**4**). Selected Structural Information: triclinic, $P\bar{1}$, 1.789 g cm⁻³. Selected bond lengths (Å) and angles (deg.): C1–C3 1.4470(19), N1–N2 1.4018(15), C2–N3 1.3647(17), N3–N4 1.3228(15); C1–O1–C2 102.04(10), N2–C2–N3 135.96(12), C2–N3–N4 115.45(11); C3–C1–N1–N2 179.73(13), N2–C2–N3–N4 3.2(2).

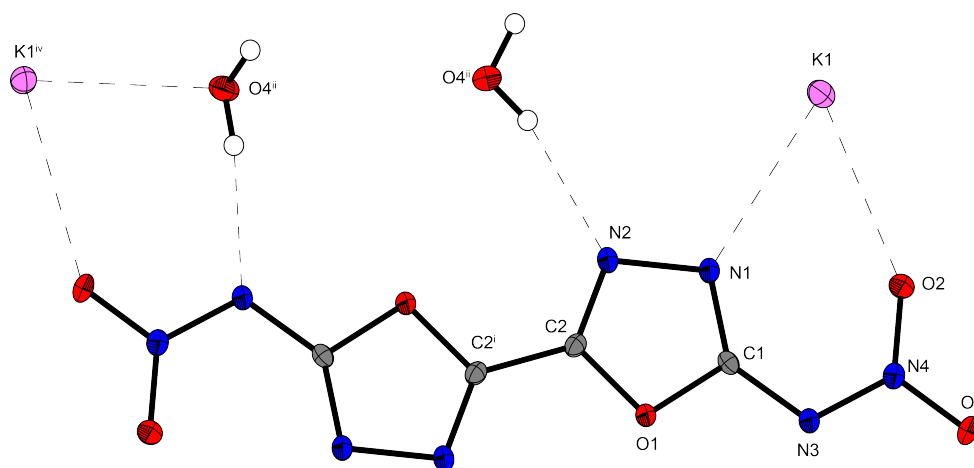


Figure S9: Molecular structure of di-potassium 2,2'-dinitramino-5,5'-bi(1-oxa-3,4-diazolate) dihydrate (**5**). Selected Structural Information: monoclinic, $P2_1/n$, 2.04 g cm⁻³. Selected bond lengths (Å) and angles (deg.): N1–N2 1.4072(18), C1–N3 1.3569(19),

N3–N4 1.3330(17); C1–O1–C2 101.99(11), N1–C1–N3 136.74(14), C1–N3–N4 115.99(11); C1–O1–C2–C2 179.13(16), N1–C1–N3–N4 1.7(3). Symmetry codes: (i) 1–x, –y, 1–z; (ii) 0.5–x, –0.5+y, 0.5–y; (iii) x, –1+y, z; (iv) 0.5–x, –1.5+y, 0.5–z.

Table S1: X-ray parameters of compound **1–3** recrystallized from different solvents.

	1 2HCl	2 H ₂ O	2 2H ₂ O	2 2DMSO
Empirical formula	C ₄ Cl ₂ H ₆ N ₆ O ₂	C ₄ H ₄ N ₈ O ₇	C ₄ H ₆ N ₈ O ₈	C ₈ H ₁₄ N ₈ O ₈ S ₂
FW (g mol ^{–1})	241.05	276.15	294.17	414.39
Temperature (K)	173	173	173	173
Crystal size (mm)	0.197x0.126x0.022	0.299x0.174x0.117	0.404x0.091x0.036	0.424x0.046x0.022
Crystal description	Colorless block	Colorless block	Colorless block	Colorless block
Crystal system	monoclinic	monoclinic	monoclinic	monoclinic
Space group	<i>P</i> 2 ₁ / <i>c</i>	<i>C</i> 2/ <i>c</i>	<i>P</i> 2 ₁ / <i>n</i>	<i>P</i> 2 ₁ / <i>c</i>
<i>a</i> (Å)	8.8134(9)	16.5972(8)	9.3932(11)	9.1708(10)
<i>b</i> (Å)	5.7001(3)	7.1863(4)	4.6744(5)	22.0442(15)
<i>c</i> (Å)	9.2328(6)	8.1556(4)	11.8477(16)	9.7667(13)
α (°)	90	90	90	90
β (°)	98.047(7)	93.608(4)	107.173(14)	114.949
γ (°)	90	90	90	90
<i>V</i> (Å ³)	459.26(6)	970.81(4)	496.48(11)	1790.2(4)
<i>Z</i>	2	4	2	4
ρ_{calc} (g cm ^{–3})	1.743	1.889	1.968	1.537
μ (mm ^{–1})	0.692	0.178	0.188	0.353
<i>F</i> (000)	244	560	300	856
θ range (°)	4.44–31.07	4.65–26.49	4.54–26.73	4.30–25.99

Bis-Nitramino-1,3,4-Oxadiazoles

Index range	$-11 \leq h \leq 8$	$-20 \leq h \leq 15$	$-11 \leq h \leq 8$	$-11 \leq h \leq 10$
	$-7 \leq k \leq 7$	$-8 \leq k \leq 9$	$-5 \leq k \leq 5$	$-27 \leq k \leq 27$
	$-11 \leq l \leq 11$	$-10 \leq l \leq 10$	$-14 \leq l \leq 14$	$-12 \leq l \leq 12$
Reflection collected	3315	3489	3089	12108
Reflection observed	950	1003	1036	3506
Reflection unique	734	897	691	1798
R1, wR2 (2 σ data)	0.0318, 0.0739	0.0282, 0.0696	0.0444, 0.0923	0.0648, 0.0961
R1, wR2 (all data)	0.0499, 0.0814	0.0323, 0.0727	0.0822, 0.1067	0.1477, 0.1258
Parameters	76	95	103	155
GOOF an F ²	1.040	1.085	0.979	1.016
Larg.diff.peak/hole (e Å ⁻³)	-0.234, 0.316	-0.243, 0.183	-0.257, 0.270	-0.349, 0.350
CCDC entry	1538692	1538695	1538691	1538699

Table S2: X-ray parameters of compound **3**, **4** and **6** recrystallized from different solvents.

	3 H ₂ O	3 DMSO	3 EG	4 2H ₂ O	6 2H ₂ O
Empirical formula	C ₄ H ₂₀ N ₁₀ O ₈	C ₈ H ₂₈ N ₁₀ O ₈	C ₆ H ₁₄ N ₁₀ O ₈	C ₄ H ₁₂ N ₁₀ O ₁₀	C ₄ K ₂ N ₈ O ₇
FW (g mol ⁻¹)	328.24	448.46	354.27	360.24	334.29
Temperature (K)	173	173	173	173	173
Crystal size (mm ³)	0.267x 0.197x 0.043	0.416x 0.199x 0.066	0.471x 0.231x 0.041	0.261x 0.269x 0.371	0.261x 0.269x 0.371
Crystal description	Colorless block	Colorless block	Colorless block	Colorless block	Colorless block
Crystal system	monoclinic	triclinic	triclinic	triclinic	monoclinic

Space group	$P2_1/n$	$P-1$	$P-1$	$P-1$	$P2_1/n$
a (Å)	6.7702(2)	5.1853(3)	4.5672(4)	8.1507(5)	6.7259(2)
b (Å)	6.9690(2)	8.5700(4)	8.1773(5)	8.4378(5)	6.7967(2)
c (Å)	13.3103(5)	10.8132(6)	9.9586(6)	11.5507(5)	13.2599(4)
α (°)	90	87.061 (4)	71.583(5)	71.186(5)	90
β (°)	94.649(3)	81.831(4)	89.403(6)	83.242(4)	95.426(3)
γ (°)	90	87.831(4)	75.535(6)	62.849(6)	90
V (Å ³)	625.93(3)	474.54(4)	340.74(4)	668.67(7)	603.45(3)
Z	2	1	1	2	2
ρ_{calc} (g cm ⁻³)	1.742	1.569	1.726	1.789	2.038
μ (mm ⁻¹)	0.163	0.342	0.157	0.172	0.850
$F(000)$	340	234	184	372	372
θ range (°)	4.20–26.49	4.16–30.50	4.30–26.49	4.59–26.49	4.27–26.49
Index range	$-8 \leq h \leq 8$	$-7 \leq b \leq 7$	$-5 \leq b \leq 5$	$-10 \leq b \leq 10$	$-8 \leq b \leq 8$
	$-8 \leq k \leq 8$	$-12 \leq k \leq 12$	$-10 \leq k \leq 10$	$-10 \leq k \leq 10$	$-8 \leq k \leq 8$
	$-16 \leq l \leq 16$	$-15 \leq l \leq 15$	$-12 \leq l \leq 12$	$-14 \leq l \leq 14$	$-16 \leq l \leq 12$
Reflection collected	8814	9295	4867	10005	4410
Reflection observed	1288	2894	1415	2763	1242
Reflection unique	1123	2337	1248	2157	1108
R1, wR2 (2 σ data)	0.0289, 0.0733	0.0355, 0.0796	0.0310, 0.0812	0.0323, 0.0816	0.0235, 0.0548
R1, wR2 (all data)	0.0344, 0.0761	0.0493, 0.0873	0.0363, 0.0849	0.0453, 0.0909	0.0281, 0.0574
Parameters	124	143	137	265	108
GOOF an F ²	1.027	1.047	1.066	1.021	1.075

Larg.diff/hole (e Å ⁻³)	-0.224, 0.279	-0.253, 0.320	-0.257, 0.287	-0.247, 0.319	-0.267, 0.350
CCDC entry	1538696	1538694	1538693	1538698	1538697

4.2 Analytical Data

DTA:

The DTA measurements of all compounds listed in Table 1 in the main journal are depicted in Figure S10 and S11. The thermal stabilities were investigated with an OZM Research DTA 552-Ex instrument and a heating rate of 5 °C/min. In Figure S10 the amines: 2,2'-diamino-5,5'-bi(1-oxa-3,4-diazole) (**1**), 2,2'-diamino-5,5'-bi(1-oxa-3,4-diazolium) dihydrochlorid (**7**) and 2,2'-diamino-5,5'-bi(1-oxa-3,4-diazolium) dinitrate (**8**) are shown. Here compound **8** shows an endothermic peak at around 150 °C. According to TGA this is the loss of two molecules of nitric acid.

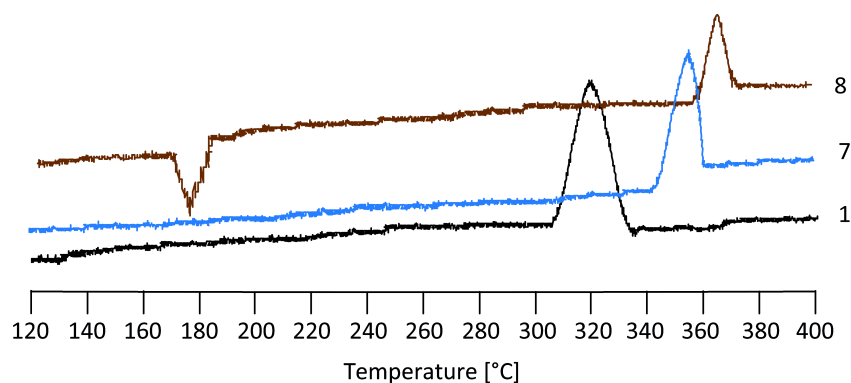


Figure S10: DTA measurements of **1**, **7** and **8**.

In Figure S11 the nitramines: 2,2'-dinitramino-5,5'-bi(1-oxa-3,4-diazole) (**2**), di-ammonium 2,2'-dinitramino-5,5'-bi(1-oxa-3,4-diazolate) (**3**), di-hydroxylammonium 2,2'-dinitramino-5,5'-bi(1-oxa-3,4-diazolate) (**4**), di-guanidinium 2,2'-dinitramino-5,5'-bi(1-oxa-3,4-diazolate) (**5**), di-potassium 2,2'-dinitramino-5,5'-bi(1-oxa-3,4-diazolate) (**6**) are displayed. Figure S11 clarifies that at around 140 °C compound **3** has an endothermic peak before it decomposes at around 200 °C. This is due to the loss of ammonium, which is also displayed in the TGA measurements.

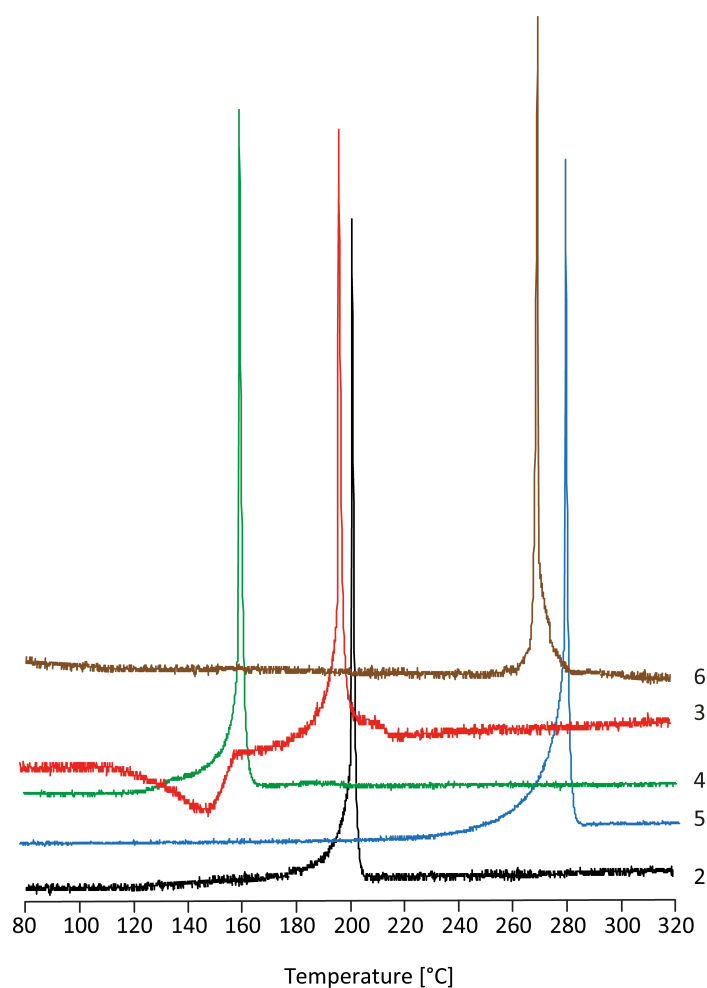


Figure S11: DTA measurements of 2–6.

NMR:

The compounds were characterized by ^1H , ^{13}C and ^{14}N NMR spectroscopy. The multinuclear NMR spectra were recorded in $\text{DMSO-}D_6$ at room temperature. The NMR shifts of **1–8** are in the typical range of CHNO based compounds. In the ^1H NMR spectrum the amino groups of **1** are observed at 7.65 ppm, were as for **2** the nitramine groups are shifted to 12.66 ppm. The ring proton of **7** and **8** are detected as broadened signals at 10.6 ppm, while the amino groups are shifted to 7.9 ppm. The ammonium resonance of compound **3** is observed at 7.17 ppm, while for compound **4** just one signal of the hydroxylammonium cation is visible at 10.1 ppm. For compound **5** one broadened signal at 6.9 ppm is displayed in the ^1H spectrum. In the ^{13}C NMR spectra, **1,7** and **8** shows two signals of the ring at 164.7 and 147.0 ppm, while for **2** these signals are observed at 163.5 and 145.8 ppm, respectively. For compound **3–6** the ring carbon signals are the same, however they are shifted to 166.5 and 148.7 ppm. In the ^{14}N NMR of **2** one signal for

the nitramine groups at -18 ppm are detected, while compared to this the nitro signals of **3–6** are shifted to -14 ppm. Additionally for **3** the ammonium cation is visible at -359 ppm.

Vibrational spectroscopy:

The infrared vibrational spectra of **1–8** show the typical antisymmetric $\nu_{\text{as}}(\text{NO}_2)$ and symmetric $\nu_{\text{sy}}(\text{NO}_2)$ stretching vibrations in the range of 1620–1506 cm^{-1} and 1385–1251 cm^{-1} , respectively. The C–N, C–O and C–C vibrations observed are in the characteristic ranges for CHNO compounds. Additionally the NH stretching vibration of **1–8** are detected in the range of 3250–3418 cm^{-1} , while the NH stretching vibration of **2** are a single broadened signal at 3168 cm^{-1} .

4.3 Heat of formation calculation

All calculations were carried out using the Gaussian G09W (revision A.02) program package. The enthalpies (H) and free energies (G) were calculated using the complete basis set (CBS) method of Petersson and coworkers in order to obtain very accurate energies. The CBS models use the known asymptotic convergence of pair natural orbital expressions to extrapolate from calculations using a finite basis set to the estimated complete basis set limit. CBS-4 begins with a HF/3-21G(d) geometry optimization; the zero point energy is computed at the same level. It then uses a large basis set SCF calculation as a base energy, and a MP2/6-31+G calculation with a CBS extrapolation to correct the energy through second order. A MP4(SDQ)/6-31+(d,p) calculation is used to approximate higher order contributions. In this study we applied the modified CBS-4M method (M referring to the use of Minimal Population localization), which is a re-parametrized version of the original CBS-4 method and also includes some additional empirical corrections.^{[20] [21]} The enthalpies of the gas-phase species M were computed according to the atomization energy method (eq.1).

$$\Delta_f H^\circ_{(\text{g}, \text{M}, 298)} = H_{(\text{Molecule}, 298)} - \sum H^\circ_{(\text{Atoms}, 298)} + \sum \Delta_f H^\circ_{(\text{Atoms}, 298)} \quad (1)$$

Table S3: CBS-4M results and calculated gas-phase enthalpies.

	M	$-H^{298} / \text{a.u.}$	$\Delta_f H^\circ(\text{g,M}) / \text{kcal mol}^{-1}$
2	258.11	1041.432975	66.5
dianion	256.10	1040.360805	32.4
NH₄⁺	36.08	56.796608	635.3
Hx⁺	68.07	131.863229	686.5
G⁺	118.14	205.453192	571.2
K⁺	78.18	599.035967	487.4

Table S4: CBS-4M values and literature values for atomic $\Delta_f H^\circ_{\text{f}}^{298} / \text{kcal mol}^{-1}$.

	$-H^{298} / \text{a.u.}$	NIST ^[S8]
H	0.500991	52.1
C	37.786156	171.3
N	54.522462	113.0
O	74.991202	59.6

In the case of the ionic compounds, the lattice energy (U_L) and lattice enthalpy (ΔH_L) were calculated from the corresponding X-ray molecular volumes according to the equations provided by Jenkins and Glasser. With the calculated lattice enthalpy (Table S5) the gas-phase enthalpy of formation (Table S3) was converted into the solid state (standard conditions) enthalpy of formation (Table S5). These molar standard enthalpies of formation (ΔH_m) were used to calculate the molar solid state energies of formation (ΔU_m) according to equation 2.

$$\Delta U_m = \Delta H_m - \Delta n RT \quad (2)$$

(Δn being the change of moles of gaseous components)

Table S5: Calculated gas phase heat of formation, molecular volumes, lattice energies and lattice enthalpies of **3** and **4**.

	$\Delta_f H^\circ(\text{g,M}) / \text{kcal mol}^{-1}$	V_M / nm^3	$U_L / \text{kJ mol}^{-1}$	$\Delta H_L / \text{kJ mol}^{-1}$
3	667.7	0.264	1367.3	1374.8
4	718.9	0.285	1327.7	1335.1
5	603.6	0.351	1227.2	1234.6

6	519.8	0.253	1389.9	1389.9
----------	-------	-------	--------	--------

The standard molar enthalpy of formation of solid **1** was calculated using $D_fH(g)$ subtracting the enthalpy of sublimation estimated by applying Trouton's rule.^{[22], [23]} ($\Delta H_{\text{sub}} = 188 \cdot T_m$). (**1**: T_m 125°C, $\Delta H_{\text{sub}} = 74.9 \text{ kJ mol}^{-1}$).

Table S6: Solid state energies of formation ($\Delta_f U^\circ$).

	$\Delta_f H^\circ(s) /$ kcal mol ⁻¹	$\Delta_f H^\circ(s) /$ kJ mol ⁻¹	Δn	$\Delta_f U^\circ(s) /$ kJ mol ⁻¹	M / g mol ⁻¹	$\Delta_f U^\circ(s) /$ kJ kg ⁻¹
2	45.3	189.6	8	209.4	258.11	811.6
3	-304.9	-71.8	12	-42	292.17	-143.8
4	294.1	70.2	13	102.4	324.17	315.9
5	-250.9	-59.9	16	-20.2	376.25	-53.8
6	-1603.1	-382.7	7	-365.4	334.29	1093.0

Notes: Δn being the change of moles of gaseous components when formed.

4.4 Experimental

General methods:

All chemicals were used as supplied. Raman spectra were recorded in a glass tube with a Bruker MultiRAM FT-Raman spectrometer with Nd:YAG laser excitation up to 1000 mW (at 1064 nm). Infrared spectra were measured with a PerkinElmer Spectrum BX-FTIR spectrometer equipped with a Smiths Dura/SamplIR II ATRdevice. All spectra were recorded at ambient (25 °C) temperature. NMR spectra were recorded with JEOL/Bruker instruments^{[24], [25]} and chemical shifts were determined with respect to external Me₄Si (¹H, 399.8 MHz; ¹³C, 100.5 MHz) and MeNO₂ (¹⁴N, 28.9 MHz; ¹⁵N, 40.6 MHz). Analyses of C/H/N were performed with an Elemental Vario EL Analyzer. Melting and decomposition points were measured using differential thermal analysis (DTA) at a heating rate of 5° C min⁻¹ with an OZM Research DTA 552-Ex instrument^[26] or by thermogravimetric analysis (TGA) with a PerkinElmer TGA4000 instrument. The sensitivity data were explored using a BAM drop hammer and a BAM friction tester.^{[27], [28], [29], [30], [31]} The heats of formations were calculated by the atomization method based on CBS-4M electronic enthalpies. All calculations affecting the detonation parameters were carried out using the program package EXPLO5 6.03.^{[12b], [12a]}

Caution! All high nitrogen and oxygen containing compounds are potentially explosive energetic materials, although no hazards were observed during preparation and handling these compounds. Nevertheless, this necessitates additional safety precautions (earthed equipment, Kevlar gloves, Kevlar sleeves, face shield, leather coat and ear plugs).

2,2'-Diamino-5,5'-bi(1-oxa-3,4-diazole) (1)

A solution of oxalyl dihydrazide (2.00 g, 16.93 mmol) and potassium bicarbonate (3.74 g, 37.35 mmol) in 100 mL water was cooled to 0 °C. To this solution was added cyanogen bromide (3.58 g, 33.80 mmol) in one portion. The mixture was stirred at 0 °C for 1 h and additionally 5 h at ambient temperature. The formed precipitate was collected by filtration and washed with water, methanol and diethyl ether (each 20 mL). After drying in vacuum 2.47 g (87 %) **1** was obtained as yellowish powder.

DSC (5 °C min⁻¹): 310 °C (dec.); **IR** (ATR, cm⁻¹): $\tilde{\nu}$ = 3255 (m), 3101 (m), 2777 (w), 1656 (s), 1588 (s), 1499 (m), 1395 (w), 1136 (m), 1108 (m), 1051 (m), 955 (w), 820 (w), 759 (w), 737 (w), 690 (w); **Raman** (1064 nm, 500 mW, 25 °C, cm⁻¹): $\tilde{\nu}$ = 2924 (2), 1669 (36), 1633 (100), 1580 (6), 1341 (4), 1135 (12), 1066 (19), 1000 (13), 975 (7), 769 (3), 558 (5), 410 (3), 329 (5), 233 (4), 113 (20); **¹H NMR** (DMSO-D₆, 25 °C, ppm) δ : 7.65 (NH₂); **¹³C NMR** (DMSO-D₆, 25 °C, ppm) δ : 164.7 (CNH₂), 147.0 (OCN); **EA** (C₄H₄N₆O₂, 168.12 g mol⁻¹) Calc.: C 28.58, H 2.40, N 49.99 %; Found: C 28.09, H 2.78, N 49.48 %. Sensitivity (grain size < 100 μ m) **IS**: 40 J; **FS**: 360 N; **ESD**: 1.5 J.

2,2'-Dinitramino-5,5'-bi(1-oxa-3,4-diazole) (2)

Fuming nitric acid (8 mL) was cooled to 0 °C and **1** (1.00 g, 5.95 mmol) was added in portions keeping the temperature below 10 °C. The mixture was stirred at room temperature for 12 h forming a precipitate. The mixture was quenched with ice and the precipitate collected by filtration. After washing with water, methanol and diethyl ether (each 20 mL) the white powder was dried in vacuum affording 1.29 g (84 %) of **2**.

DSC (5 °C min⁻¹): 200 °C (dec.); **IR** (ATR, cm⁻¹): $\tilde{\nu}$ = 3168 (w), 1583 (s), 1565 (m), 1520 (m), 1489 (s), 1385 (w), 1300 (s), 1235 (s), 1150 (s), 1073 (s), 957 (s), 943 (m), 841 (w), 777 (m), 721 (w), 658 (w); **Raman** (1064 nm, 500 mW, 25 °C, cm⁻¹): $\tilde{\nu}$ = 1693 (100), 1594 (10), 1443 (4), 1280 (15), 1103 (5), 1076 (5), 987 (9), 969 (7), 843 (6), 774 (10), 514 (3), 425 (1), 226 (7), 116 (10), 99 (23), 84 (16); **¹H NMR** (DMSO-D₆, 25 °C, ppm) δ : 12.66 (NHNO₂); **¹³C NMR** (DMSO-D₆,

25 °C, ppm) δ : 163.5 (CNH), 145.8 (OCN); ^{14}N NMR (DMSO- D_6 , 25 °C, ppm) δ : -18 (NO_2); **EA** ($\text{C}_4\text{H}_2\text{N}_8\text{O}_6$, 258.11 g mol $^{-1}$) Calc.: C 18.61, H 0.78, N 43.41 %; Found: C 18.52, H 1.10, N 42.82 %; Sensitivity (grain size < 100 μm) **IS**: 1 J; **FS**: 72 N; **ESD**: 0.15 J.

Di-ammonium 2,2'-dinitramino-5,5'-bi(1-oxa-3,4-diazolate) (3)

To a suspension of **2** (0.50 g, 1.94 mmol) in 20 mL methanol conc. aqueous ammonium (0.35 g, 4.07 mmol) was added in one portion. The solution turned colorless for short time, followed by forming a white precipitate. Filtration and washing with methanol obtained **3** (0.40 g, 70 %) as white powder.

DSC (5 °C min $^{-1}$): 148 °C (melt), 197 °C (dec.); **IR** (ATR, cm $^{-1}$): $\tilde{\nu}$ = 3437 (w), 3365 (w), 3204 (w), 3037 (w), 1681 (w), 1626 (w), 1518 (s), 1487 (m), 1400 (m), 1307 (m), 1265 (s), 1149 (m), 1066 (s), 1020 (m), 962 (m), 857 (w), 774 (w), 756 (w), 727 (w), 667 (w); **Raman** (1064 nm, 500 mW, 25 °C, cm $^{-1}$): $\tilde{\nu}$ = 1631 (100), 1524 (40), 1079 (13), 1043 (41), 1001 (7), 971 (6), 865 (3), 765 (6), 411 (3), 129 (5), 81 (3); ^1H NMR (DMSO- D_6 , 25 °C, ppm) δ : 7.2 (br, NH_4); ^{13}C NMR (DMSO- D_6 , 25 °C, ppm) δ : 166.5 (CNH), 148.7 (OCN); ^{14}N NMR (DMSO- D_6 , 25 °C, ppm) δ : -14 (NO_2), -359 (NH_4); **EA** ($\text{C}_4\text{H}_8\text{N}_{10}\text{O}_6$, 292.17 g mol $^{-1}$) Calc.: C 14.82, H 2.49, N 43.21 %; Found: C 15.33, H 2.53, N 42.64 %; Sensitivity (grain size < 100 μm) **IS**: 10 J; **FS**: 360 N; **ESD**: 1.0 J.

Di-hydroxylammonium 2,2'-dinitramino-5,5'-bi(1-oxa-3,4-diazolate) (4)

To a suspension of **2** (0.50 g, 1.94 mmol) in 20 mL methanol aqueous hydroxylamine 50%w (0.27 g, 4.07 mmol) was added in one portion. The solution turned colorless for a short time, followed by forming a white precipitate. Filtration and washing with methanol obtained **4** (0.37 g, 59 %) as white powder.

DSC (5 °C min $^{-1}$): 160 °C (dec.); **IR** (ATR, cm $^{-1}$): $\tilde{\nu}$ = 3055 (w), 2933 (w), 2815 (w), 2735 (w), 2361 (w), 1985 (w), 1615 (w), 1604 (w), 1521 (s), 1488 (s), 1435 (m), 1266 (s), 1205 (m), 1172 (m), 1083 (m), 1018 (m), 1000 (m), 971 (m), 859 (w), 778 (w), 751 (w), 734 (w), 662 (w); **Raman** (1064 nm, 500 mW, 25 °C, cm $^{-1}$): $\tilde{\nu}$ = 1642 (100), 1525 (20), 1443 (2), 1094 (5), 1055 (38), 1014 (14), 979 (2), 864 (3), 759 (9), 420 (2), 235 (2), 92 (4), 67 (3); ^1H NMR (DMSO- D_6 , 25 °C, ppm) δ : 10.10 (NH_3); ^{13}C NMR (DMSO- D_6 , 25 °C, ppm) δ : 166.5 (CNH), 148.7 (OCN); ^{14}N NMR (DMSO- D_6 , 25 °C, ppm) δ : -14 (NO_2); **EA** ($\text{C}_6\text{H}_{12}\text{N}_{14}\text{O}_8$, 324.17 g mol $^{-1}$) Calc.: C 16.44, H 2.76, N 47.94 %; Found: C 16.12, H 2.58, N 47.47 %; Sensitivity (grain size < 100 μm) **IS**: 4 J; **FS**: 120 N; **ESD**: 0.5 J.

Di-guanidinium 2,2'-dinitramino-5,5'-bi(1-oxa-3,4-diazolate) (5)

To a suspension of **2** (0.50 g, 1.94 mmol) in 20 mL water guanidine carbonate (0.73 g, 4.07 mmol) was added in one portion. The solution was stirred until no further gas discharge was observed. Filtration and washing with methanol obtained **5** (0.54 g, 75 %) as white powder.

DSC (5 °C min⁻¹): 260 °C (dec.); **IR** (ATR, cm⁻¹): $\tilde{\nu}$ = 3378 (m), 3270 (w), 3204 (m), 3168 (m), 2805 (w), 1680 (m), 1655 (s), 1573 (w), 1524 (s), 1494 (m), 1405 (m), 1285 (s), 1155 (m), 1072 (s), 1022 (m), 967 (w), 959 (w), 858 (w), 750 (w), 730 (w); **Raman** (1064 nm, 500 mW, 25 °C, cm⁻¹): $\tilde{\nu}$ = 1640 (100), 1586 (2), 1530 (34), 1414 (2), 1083 (6), 1049 (50), 1011 (4), 1001 (10), 973 (9), 862 (4), 759 (9), 706 (2), 418 (4), 232 (3), 131 (6); **¹H NMR** (DMSO-D₆, 25 °C, ppm) δ : 6.9 (br, NH₂); **¹³C NMR** (DMSO-D₆, 25 °C, ppm) δ : 166.5 (CNH), 158.3 (C(NH₂)₃), 148.8 (OCN); **¹⁴N NMR** (DMSO-D₆, 25 °C, ppm) δ : - 14 (NO₂); **EA** (C₆H₁₂N₁₄O₆, 376.25 g mol⁻¹) Calc.: C 19.15, H 3.21, N 52.12 %; Found: C 19.38, H 3.28, N 51.88 %; Sensitivity (grain size < 100 μ m) **IS**: 40 J; **FS**: 360 N; **ESD**: 1.0 J.

Dipotassium 2,2'-dinitramino-5,5'-bi(1-oxa-3,4-diazolate) (6)

To a suspension of **2** (0.50 g, 1.94 mmol) in 20 mL methanol potassium hydroxide (0.27 g, 4.07 mmol) dissolved in 5 mL methanol was added in one portion. For a short time a clear solution was formed, followed by forming a colorless precipitate. After filtration and washing with methanol, **4** (0.37 g, 59 %) was obtained as white powder.

DSC (5 °C min⁻¹): 230 °C (dec.); **IR** (ATR, cm⁻¹): $\tilde{\nu}$ = 3477 (w), 3419 (w), 1634 (w), 1592 (w), 1558 (w), 1516 (s), 1491 (m), 1421 (m), 1309 (s), 1283 (s), 1245 (s), 1166 (m), 1153 (m), 1068 (s), 1020 (m), 959 (m), 857 (w), 776 (w), 757 (w), 728 (w), 667 (w); **Raman** (1064 nm, 500 mW, 25 °C, cm⁻¹): $\tilde{\nu}$ = 1634 (100), 1524 (57), 1448 (2), 1079 (8), 1044 (40), 1002 (8), 967 (5), 862 (3), 767 (7), 720 (1), 410 (3), 232 (2), 132 (6); **¹³C NMR** (DMSO-D₆, 25 °C, ppm) δ : 166.5 (CNH), 158.3 (C(NH₂)₃), 148.8 (OCN); **¹⁴N NMR** (DMSO-D₆, 25 °C, ppm) δ : - 14 (NO₂); **EA** (C₄K₂N₈O₆, 334.29 g mol⁻¹) Calc.: C 14.37, N 33.52 %; Found: C 13.45, N 33.22 %; Sensitivity (grain size < 100 μ m) **IS**: 5 J; **FS**: 288 N; **ESD**: 0.75 J.

2,2'-Diamino-5,5'-bi(1-oxa-3,4-diazolium) dihydrochlorid (7)

To 10 mL of concentrated hydrochloric acid **1** (0.50 g, 2.97 mmol) is added in one portion. The mixture is heated to reflux for 5 minutes and subsequently cooled to room temperature

precipitating a white solid. After further cooling with an ice bath the precipitate was isolated by filtration. Washing with water, methanol and ether yielded 0.68 of **7** (95 %) as a white powder.

DSC (5 °C min⁻¹): 345 °C (dec.); **IR** (ATR, cm⁻¹): $\tilde{\nu}$ = 3251 (m), 3085 (m), 2776 (w), 1733 (w), 1654 (s), 1587 (s), 1498 (m), 1395 (m), 1395 (w), 1243 (w), 1135 (s), 1108 (m), 1049 (s), 954 (w), 758 (w), 738 (m), 689 (m); **Raman** (1064 nm, 500 mW, 25 °C, cm⁻¹): $\tilde{\nu}$ = 1669 (39), 1633 (100), 1342 (3), 1136 (11), 1066 (18), 1001 (15), 975 (7), 769 (2), 559 (6), 410 (2), 328 (5), 233 (3), 182 (2), 128 (9), 113 (8); **¹H NMR** (DMSO-D₆, 25 °C, ppm) δ : 10.6 (br, NH), 7.8 (br, NH₂); **¹³C NMR** (DMSO-D₆, 25 °C, ppm) δ : 164.3 (CNH), 146.8 (OCN); **EA** (C₄H₆Cl₂N₆O₂, 241.93 g mol⁻¹) Calc.: C 19.93, H 2.51, N 34.87 %; Found: C 19.71, H 2.82, N 34.45 %; Sensitivity (grain size < 100 μ m) **IS**: 40 J; **FS**: 360 N; **ESD**: 1.5 J.

2,2'-Diamino-5,5'-bi(1-oxa-3,4-diazolium) dinitrate (**8**)

To 10 mL of concentrated nitric acid **1** (0.50 g, 2.97 mmol) is added in one portion. The mixture is heated to reflux for 5 minutes and subsequently cooled to room temperature precipitating a white solid. After further cooling with an ice bath the precipitate was isolated by filtration. Washing with water, methanol and ether yielded 0.78 of **8** (90 %) as white powder.

DSC (5 °C min⁻¹): 360 °C (dec.); **IR** (ATR, cm⁻¹): $\tilde{\nu}$ = 3305 (w), 3195 (w), 2419 (w), 2320 (w), 1711 (s), 1478 (w), 1369 (m), 1299 (s), 1148 (m), 1086 (w), 1048 (w), 1015 (w), 968 (m), 918 (m), 819 (m), 745 (w), 721 (m), 695 (w), 656 (w); **Raman** (1064 nm, 500 mW, 25 °C, cm⁻¹): $\tilde{\nu}$ = 1735 (20), 1677 (100), 1514 (4), 1463 (5), 1364 (3), 1117 (43), 1053 (50), 979 (15), 751 (13), 729 (6), 689 (4), 543 (5), 392 (3), 309 (10), 238 (14), 192 (4), 137 (21), 113 (4); **¹H NMR** (DMSO-D₆, 25 °C, ppm) δ : 10.6 (br, NH), 7.9 (br, NH₂); **¹³C NMR** (DMSO-D₆, 25 °C, ppm) δ : 164.3 (CNH), 146.8 (OCN); **EA** (C₄H₆N₈O₈, 294.14 g mol⁻¹) Calc.: C 16.33, H 2.06, N 38.10 %; Found: C 16.60, H 2.01, N 37.67 %; Sensitivity (grain size < 100 μ m) **IS**: 15J; **FS**: 324N; **ESD**: 0.75 J.

5 References

- [1] a) J. P. Agrawal, *High Energy Materials*, **2010**, Wiley-VCH, Weinheim, 1st edn, 189; b) T. M. Klapötke, *Chemistry of High-Energy Materials, 3rd Edition*, Walter de Gruyter GmbH & Ko KG, Berlin, **2015**; c) R. M. Josef Köhler, *Explosives*, **2008**, Wiley-VCH, Weinheim, 5th edn.
- [2] a) D. E. Chavez, D. A. Parrish, L. Mitchell, *Angew. Chem., Int. Ed.*, **2016**, *55*, 8666–8669; b) D. G. Piercey, D. E. Chavez, B. L. Scott, G. H. Imler, D. A. Parrish, *Angew. Chem., Int.*

- Ed.*, **2016**, *55*, 15315–15318; c) T. W. Myers, C. J. Snyder, D. E. Chavez, R. J. Scharff, J. M. Veauthier, *Chem. - Eur. J.*, **2016**, *22*, 10590–10596; d) D. E. Chavez, J. C. Bottaro, M. Petrie, D. A. Parrish, *Angew. Chem., Int. Ed.*, **2015**, *54*, 12973–12975.
- [3] a) Y. Liu, J. Zhang, K. Wang, J. Li, Q. Zhang, J. M. Shreeve, *Angew. Chem., Int. Ed.*, **2016**, *55*, 11548–11551; b) P. Yin, J. Zhang, L. A. Mitchell, D. A. Parrish, J. n. M. Shreeve, *Angew. Chem., Int. Ed.*, **2016**, *55*, 12895–12897.
- [4] a) M. S. Klenov, A. A. Guskov, O. V. Anikin, A. M. Churakov, Y. A. Strelenko, I. V. Fedyanin, K. A. Lyssenko, V. A. Tartakovsky, *Angew. Chem., Int. Ed.*, **2016**, *55*, 11472–11475; b) D. Fischer, J. L. Gottfried, T. M. Klapötke, K. Karaghiosoff, J. Stierstorfer, T. G. Witkowski, *Angew. Chem., Int. Ed.*, **2016**, *55*, 16132–16135; c) D. Fischer, T. M. Klapötke, J. Stierstorfer, *Angew. Chem., Int. Ed.*, **2014**, *53*, 8172–8175.
- [5] a) X. Sun, Y. Wang, Y. Lei, *Chem. Soc. Rev.*, **2015**, *44*, 8019–8061; b) M. Marshall, J. Oxley, *Aspects of Explosives Detection 1st Edition*, **2008**; c) H. Östmark, S. Wallin, H. G. Ang, *Propellants, Explos., Pyrotech.*, **2012**, *37*, 12–23.
- [6] E.-C. Koch, *Propellants, Explos., Pyrotech.*, **2016**, *41*, 526–538.
- [7] A. K. Zelenin, M. L. Trudell, R. D. Gilardi, *J. Heterocycl. Chem.*, **1998**, *35*, 151–155.
- [8] D. Fischer, T. M. Klapötke, M. Reymann, J. Stierstorfer, *Chem. Eur. J.*, **2014**, *20*, 6401–6411.
- [9] T. M. Klapötke, T. G. Witkowski, *ChemPlusChem*, **2016**, *81*, 357–360.
- [10] Crystal metrics at 173K: 2·2H₂O: P21/n, 4.6744(5), 11.8477(16), 107.173(14), 496.48(11), 2, 1.968 g cm⁻³, 173K; 3·2H₂O: P21/n, 6.7702(2), 6.9690(2), 13.3103(5), 94.649(3), 625.93(3), 2, 1.742 g cm⁻³; 4·2H₂O: P-1, 8.1507(5), 8.4378(5), 11.5507(5), 71.186(5), 83.242(4), 62.849(6), 668.68(8), 2, 1.789 g cm⁻³.
- [11] CBS-4M.
- [12] a) M. Sućeska, *EXPLO5 V.6.03*, **2014**, Zagreb (Croatia); b) M. Sućeska, *Propellants, Explos., Pyrotech.*, **1991**, *16*, 197–202.
- [13] CrysAlisPro, *Oxford Diffraction Ltd. version 171.33.41*, **2009**.
- [14] SIR-92 A Program for Crystal Structure Solution: A. Altomare, G. Cascarano, C. Giacovazzo, A. Guagliardi, *J. Appl. Crystallogr.*, **1993**, *26*, 343–350.
- [15] A. Altomare, G. Cascarano, C. Giacovazzo, A. Guagliardi, A. G. G. Moliterni, M. C. Burla, G. Polidori, M. Camalli, R. Spagna, *SIR97*, **1997**.
- [16] G. M. Sheldrick, *SHELX-97*, **1997**, University of Göttingen, Göttingen, Germany.
- [17] G. M. Sheldrick, *Acta Crystallogr., Sect. A: Found. Crystallogr.*, **2008**, *64*, 112–122.

- [18] A. L. Spek, *PLATON*, **1999**, A Multipurpose Crystallographic Tool, Utrecht University, The Diffraction Ltd.
- [19] *SCALE3 - An Oxford Diffraction Program (1.0.4, gui: 1.0.3)*, **2005**, Oxford Ltd.
- [20] J. W. Ochterski, G. A. Petersson, J. A. Montgomery, Jr., *J. Chem. Phys.*, **1996**, *104*, 2598–2619.
- [21] J. A. Montgomery, Jr., M. J. Frisch, J. W. Ochterski, G. A. Petersson, *J. Chem. Phys.*, **2000**, *112*, 6532–6542.
- [22] F. Trouton, *Philos. Mag.*, **1884**, *18*, 54–57.
- [23] M. S. Westwell, M. S. Searle, D. J. Wales, D. H. Williams, *J. Am. Chem. Soc.*, **1995**, *117*, 5013–5015.
- [24] Bruker, <https://www.bruker.com>.
- [25] JEOL, <http://www.jeolusa.com>.
- [26] Bundesanstalt für Materialforschung und -prüfung, <http://www.bam.de>.
- [27] Reichel & Partner GmbH, <http://www.reichelt-partner.de>.
- [28] *Test Methods According to the UN Recommendations on The Transport of Dangerous Goods, Manual of Test and Criteria, Fourth Revised Edition, United Nations Publication, New York and Geneva*, **2003**, ISBN 92–1–139087–7, Sales No. E.03.VIII. 2; 13.4.2 Test 3a (ii) BAM Fallhammer.
- [29] *WIWEB-Standardarbeitsanweisung 4-5.1.03, Ermittlung der Explosionsgefährlichkeit oder der Reibeempfindlichkeit mit dem Reibeapparat*, **2002**.
- [30] *WIWEB-Standardarbeitsanweisung 4-5.1.02, Ermittlung der Explosionsgefährlichkeit, hier der Schlagempfindlichkeit mit dem Fallhammer*, **2002**.
- [31] *Impact: Insensitive > 40 J, less sensitive 35 J, sensitive 4 J, very sensitive 3 J; friction: Insensitive > 360 N, less sensitive = 360 N, sensitive < 360 N a. > 80 N, very sensitive 80 N, extreme sensitive 10 N; according to the UN recommendations on the transport of dangerous goods. (+) Indicates: not safe for transport.*

III Summary and Conclusion

In the course of this work, new nitrogen and oxygen-rich energetic materials with different energetic functional groups and a mainly heterocyclic backbone were synthesized and comprehensively investigated. Compounds containing high oxygen contents and therefore have a positive oxygen balance are categorized in the field of high-energy dense oxidizers (HEDO). The main application of these compounds may be in solid rocket composite propellants. Compounds with high nitrogen content mainly are categorized in the field of secondary (high) explosives. Their application is mainly in the military sector but also in the civil sector as gun propellants or mining agents.

The main part of this thesis is section *II Results and Discussion* that contains eight chapters. Each chapter is an enclosed research project including its own abstract, introduction, results and discussion, experimental section and conclusion. The main part of this thesis is about energetic materials based on heterocyclic compounds, based on different types of oxadiazoles and triazoles. The first chapter deals with high-energy dense oxidizers based on nitrate esters and oxygen containing backbone. For the synthesis, the dihydroxyacetone dimer was nitrated with different types of nitrating agents. This project emphasizes the different consequences of mixed acid and dinitrogenpentoxide. The result ends in two compounds, an open chain compound of the monomer and the dimer a heterocyclic compound.

Based on a triazole backbone, in chapter 2, another high-energy dense oxidizers were synthesized. In order to increase the oxygen content a trinitromethyl functional group was introduced by the nitration of an acetic acid. Also, a nitramine functional group included in the compound increases the oxygen content. Furthermore, the triazole backbone in addition to the polynitro groups leads to good detonation properties. The sensitivities as well as the detonation parameters were diversify by the formation of nitrogen-rich salts.

In chapter 3–6, 1,2,5-oxadiazoles (furazan) were used to synthesize energetic compounds. Depending on their behavior, these compounds are categorized as primary explosives, (high thermal-) secondary explosives or oxidizers. In chapter 3, the nitration of a furazan leads to an unusual ring closure and a furazan fused pyrazole *N*-oxide. The use of different functional groups brings advantages in the application. The advantage of *N*-oxides is higher density, better enthalpy of formation and better detonation properties. Salt formation of the compound makes it useful either as pyrotechnics, if metal cation or as secondary explosive, if nitrogen-rich cations are used. The high sensitivity to outer stimuli defines the heavy metal free compound as a primary explosive.

The advantage of heterocyclic compounds linked to a picrylamine is shown in chapter 4. The physiochemical properties of 5,5'-bis(2,4,6-trinitrophenyl)-2,2'-bi(1,3,4-oxadiazole) (TKX-55) and 2,6-bis(picrylamino)-3,5-dinitropyridine (PYX) served as a role model for this research topic. Here, two different furazans and 1,3,4-triazoles were used. The conjugated electron system as well as the steric ring systems leads to high thermal explosives with good detonation properties. Furthermore, the applicability of these compounds was tested with different methods.

Chapter 5 deals with the synthesis of furazan ureido and nitroureido compounds. The combination of the before mentioned benefits of heterocyclic backbones and the detonation properties and high densities of ureido groups should end in energetic compounds with good explosive properties. Furthermore, the oxygen content of the compounds are increased by the oxygen in the furazan ring and the introduction of $N-NO_2$ group, which leads to an increase of the heat of formation and density. The assumptions of synthesizing interesting energetic compounds with good performances by combination of heterocycles and ureido groups were confirmed by characterization and calculation of the detonation values.

The research in chapter 6 belongs to the synthesis, characterization and adjustment of new secondary explosives. The nitration of 3,4-bis(4-amino-1,2,5-oxadiazol-3-yl)-1,2,5-furoxan leads to the nitramine derivative. The conjugated electron system of the tricyclic heterocyclic compound leads to thermal stability. The introduction of nitramine functional compounds increases the energetic properties in accordance to the advantages and energetic properties of the heterocyclic backbone. Further, the formation of nitrogen-rich salts adjusts the physiochemical properties as well as the detonation parameters. Although the neutral compound is barely stable, the nitrogen-rich salts with the $BNAFF^-$ anion decompose in the range of 150–200 °C. The impact and friction sensitivities for the nitrogen-rich compounds are in the range from 7 J to 15 J and from 216 N to 360 N.

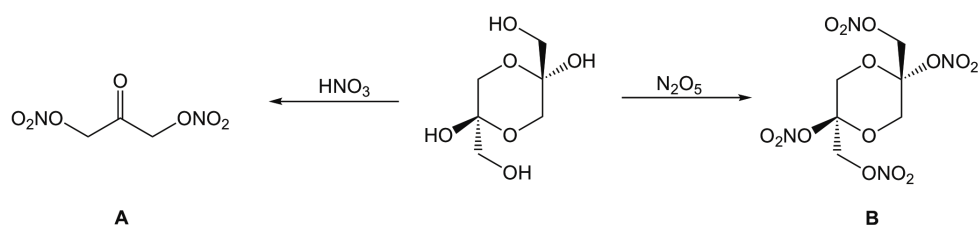
The synthesis of high energy dense oxidizers based on dinitromethyl- and trinitromethyl-1,2,4-oxadiazoles has been investigated in chapter 7. In this study, the advantage of high oxygen content through the dinitromethyl- and trinitromethyl functional group and the advantage of high heat of formation, high density and high thermal stability of 1,2,4-oxadiazoles were combined. At the beginning the precursors were synthesized and extensively characterized, as they are also new compound. Nitration of the last precursor, the acetic acids, leads to the trinitromethyl derivatives. Nitration of the dinitro ethyl ester yielded the dinitromethyl derivatives, which were further modified to salts. The formation of salts increases the physiochemical properties

According to the investigation of new secondary explosives, easy and cheap synthesis is indispensable. Nevertheless the detonation properties should be higher or at least equal to

common secondaries. The study of dinitramino-bis-1,3,4-oxadiazole should include all of these requirements through easy synthesis and good detonation properties. Furthermore, salt formation adjusted the physiochemical properties in sense of thermals stability and increased detonation values.

1 Nitration of Dihydroxyacetone

In the first chapter, two different nitrating agents nitrated 1,3-dihydroxyacetone dimer. Nitration with fuming nitric acid yielded 1,3-dinitratoacetone (**A**), while nitration with N_2O_5 yielded 2,5-bis(nitratomethyl-2,5-nitrato)-1,4-dioxane (**B**) as shown in Scheme S.1.



Scheme S. 1: Synthesis of 1,3-dinitratoacetone (**A**) and 2,5-bis(nitratomethyl-2,5-nitrato)-1,4-dioxane (**B**).

Both compounds show high oxygen balance $\Omega_{CO}(A,B) = +17.8 \%$, which is higher than the oxygen balance of PETN ($\Omega_{CO} = +15.2 \%$). According to the positive oxygen balance, the specific impulse for neat product was calculated to **A** = 258 s and **B** = 259 s and an optimized specific impulse, with the addition of aluminum and binder, to **A** = 271 s and **B** = 277 s. These properties as well as the moderate sensitivities and the easy and cheap synthesis make them promising candidates as high energy dense oxidizer replacements.

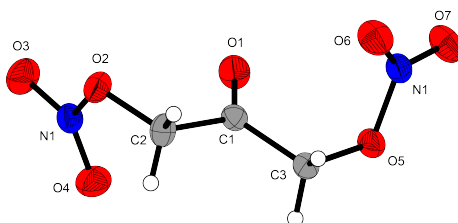
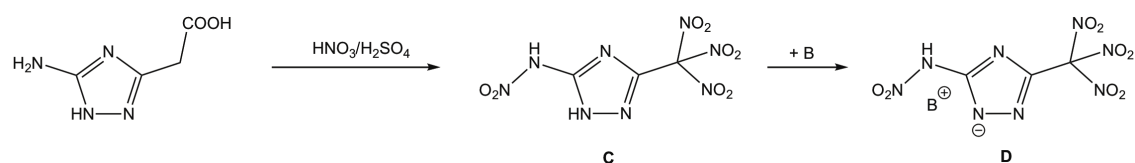


Figure S. 1: X-ray molecular structure of 1,3-dinitratoacetone (**A**).

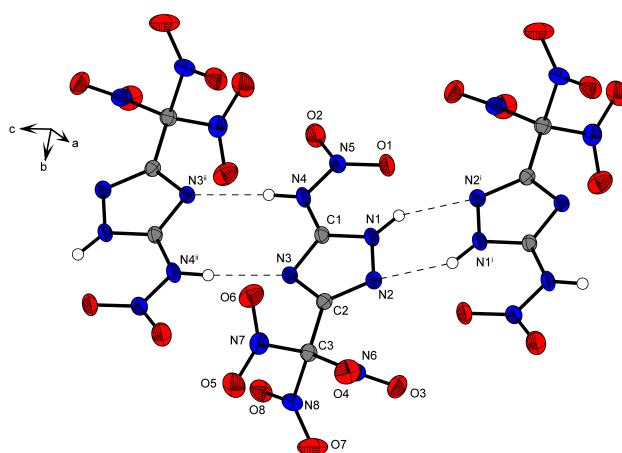
2 Trinitromethyl-1,2,4-triazoles

In chapter 2, a high-energy dense oxidizer (**C**) was synthesized. Based on a triazoles backbone, a trinitromethyl- and a nitramine functional group were introduced (Figure S.2) in order to reach a high oxygen balance combined with good detonation values (Scheme S.2). Salt formation (**D**) with nitrogen-rich cations was included in this study in order to adjust the detonation properties, as well as the sensitivity.



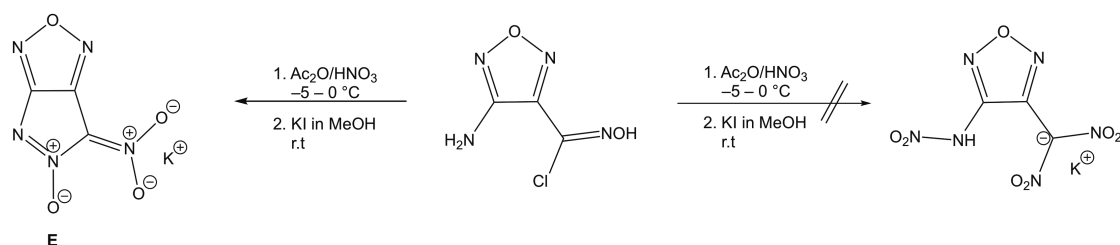
Scheme S. 2: Synthesis of 3-trinitromethyl-5-nitramino-1H-1,2,4-triazole (**C**) starting from 5-amino-1H-1,2,4-triazol-3-acetic acid and salts (**D**).

The neutral compound (**C**) show good oxygen balance (+23.0 %) and a good optimized specific impulse (264 s), which is the same as for AP. The nitrogen-rich salts show better detonation properties but are more likely secondary explosives than oxidizers. All compounds have been comprehensively characterized. Furthermore, the CHNO based molecules burn residue-free and, compared to AP, have no corrosive gases are released.



3 Pyrazole Fused Furazanes

The unusual reaction and consequent unusual ring formation of a furazan to a pyrazole fused furazan (**E**) was investigated in chapter 3. According to literature, the hydroxyl chloride functional group should react to a potassium dinitromethyl group upon nitration and subsequent reaction with potassium iodide. However, the potassium salt of 5-nitro-pyrazolo-(3,4,c)-furazan-5-*N*-oxide (**E**) was yielded. Further salt exchange with heavy alkali metals and silver were possible. The compounds have been characterized fully and the physiochemical properties were calculated.



Scheme S. 3: Attempt synthesis and unusual reaction to potassium 5-nitro-pyrazolo-(3,4,c)-furazan-5-*N*-oxide (**E**).

The potassium salt (**E**) was yielded in two different space groups upon recrystallization from different solvents (Figure S.3). All compounds have good thermal stabilities (>200 °C), high sensitivities towards impact (1–2 J) and moderate sensitivities toward friction (30–72 N). According to their physiochemical properties these compounds can be classified as primary explosives. The potassium salt is a potential candidate as replacement for common primary explosives.

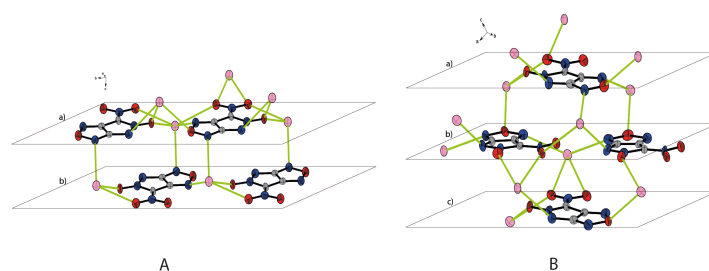


Figure S. 3: Comparison of the two space groups of the different X-ray crystal structures of potassium 5-nitro-pyrazolo-(3,4,c)-furazan-5-*N*-oxide (**E**).

4 Picrylamine-1,2,4-Oxadiazoles and 1,3,4-Triazoles

The invention of new thermally stable explosives is very challenging. The characterization and usability of potential replacements of common used high thermal explosives like for example PYX was investigated in chapter 4. The easy synthesis of heterocyclic compounds, like furazanes and triazoles, with amine functional groups and picryl fluoride was performed in DMSO yielding heterocyclic compounds with picryl groups linked over an amine (**F**) (Scheme S.4).



Scheme S. 4: General synthesis of picryl amine furazanes and triazoles (**F**).

The synthesized compounds (3,4-bis(Picrylamino)furazan, 4,4'-bis(picrylamino)-3,3'-bifurazane, 3,5-bis(picrylamino)-1,2,4-triazole and 5,5'-bis(picrylamino)-3,3'-bi-1,2,4-triazole) all show good thermal behavior (250 °C – 340 °C). Furthermore, their vacuum stability and compatibility to the most used metals and explosives was tested. All tests results were positive, which makes these compounds, because of their easy synthesis and good detonation properties potential replacements for other high thermal explosive.

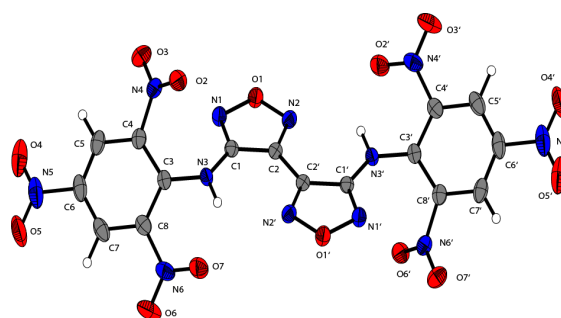
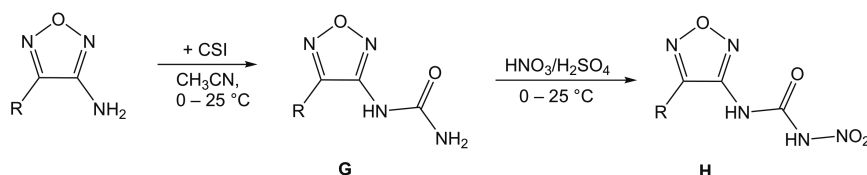


Figure S. 4: X-ray molecular structure of 4,4'-bis(picrylamino)-3,3'-bifurazane.

5. Nitroureido-1,2,3-Oxadiazoles

In chapter 5, different amino furazan derivatives were reacted with chlorosulfonylisocyanat (CSI) to yield furazanes with an ureido group (**G**). These ureido furazanes were further nitrated in order to yield the nitro ureido derivatives (**H**) as shown in Scheme S.5.



Scheme S. 5: General synthesis of ureido furazanes (**G**) and nitro ureido furazanes (**H**).

The synthesis of these nitro ureido furazanes meet several requirements for new energetic materials, like easy and safe synthesis, as well as good detonation properties. The nitration of the ureido functional group was shown to increase the enthalpy by 70 kJ mol^{−1} per ureido group. At the end the physicochemical and explosive properties ($V_{\text{Det}} = 8685\text{--}8930 \text{ m s}^{-1}$, $P_{\text{Cj}} = 322\text{--}348 \text{ kbar}$) make the nitro ureido furazanes (**H**) potential energetic materials but also potential precursors for energetic polymers in the case of the ureido derivatives (**G**).

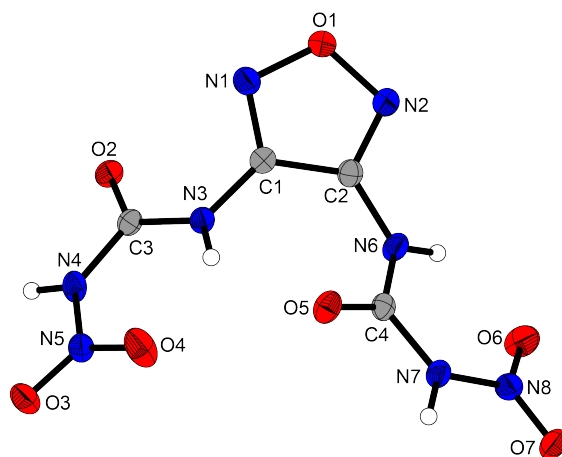
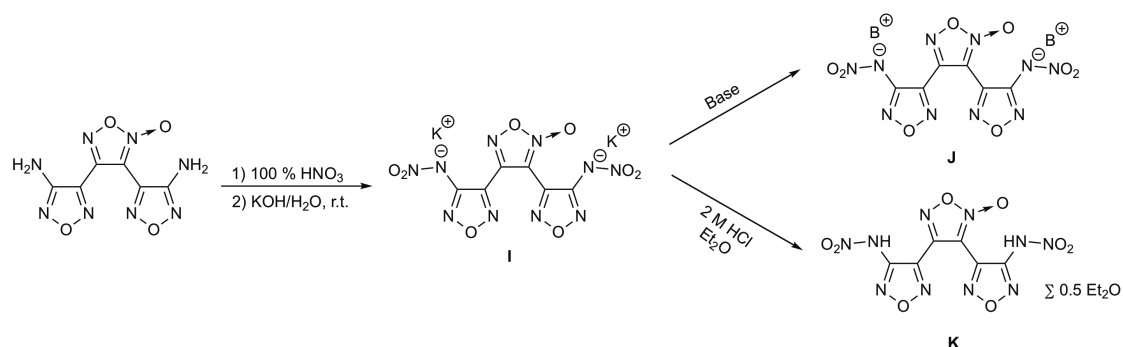


Figure S. 5: X-ray molecular structure of 3,4-dinitroureido-furazan.

6. Bis-(Nitramino-1,2,5-oxadiazol)-furoxanes

The synthesis of bis-(4''-nitramino [3,3'-4',3'']-tertfurazan-4-yl)-diazene was investigated in chapter 6. The bis potassium-bis-(4''-nitramino [3,3'-4',3'']-tertfurazan-4-yl)-diazene was synthesized (**I**) by nitration of bis-(4''-amino [3,3'-4',3'']-tertfurazan-4-yl)-diazene. Further reaction with nitrogen-rich bases yielded salt formation (**J**). Furthermore, the neutral bis-(4''-nitramino [3,3'-4',3'']-tertfurazan-4-yl)-diazene (**K**) was obtained in acidic conditions.



Scheme S. 6: Synthesis of bis potassium-bis-(4''-nitramino [3,3'-4',3'']-tertfurazan-4-yl)-diazene (**I**), nitrogen-rich salts of bis-(4''-nitramino [3,3'-4',3'']-tertfurazan-4-yl)-diazene (**J**) and neutral bis-(4''-nitramino [3,3'-4',3'']-tertfurazan-4-yl)-diazene (**K**).

The Synthesis of nitrogen-rich salts of bis-(4''-nitramino [3,3'-4',3'']-tertfurazan-4-yl)-diazene reveal the possibility to increase the physicochemical properties of neutral compounds. While the neutral compound has no long-term stability the nitrogen-rich compounds have thermal decompositions of 150–190 °C and sensitivities of 3–15 J and 72–360 N. The decomposition velocities and pressures are near to RDX with 8099–8579 m s⁻¹ and 253–305 kbar.

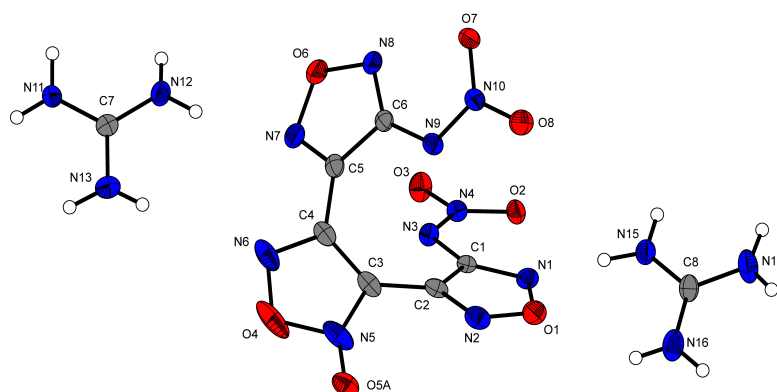
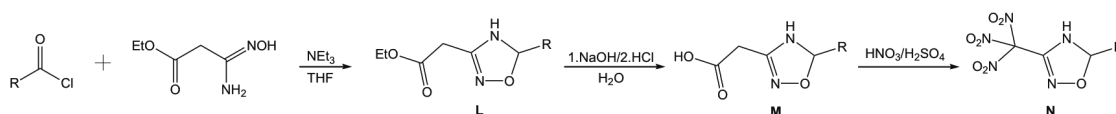


Figure S. 6: X-ray molecular structure of di-guanidinium bis-(4''-nitramino [3,3'-4',3'']-tertfurazan-4-yl)-diazene.

7. Trinitomethyl-1,2,4-oxadiazoles

Chapter 7 is about the synthesis of different 1,2,4-oxadiazoles as HEDOs. The ethyl (*Z*)-3-(hydroxylamino)-3-imino-propanoic acid ethyl ester was reacted with different acid chlorides to yield ethyl ester 1,2,4-oxadiazoles (**L**). Further saponification leads to acetic acid 1,2,4-oxadiazoles (**M**), which were subsequently nitrated to yield the trinitromethyl-1,2,4-oxadiazoles (**N**) (Scheme S.7). Nitration of the ethyl ester 1,2,4-oxadiazoles (**L**) and basic following the reaction of bases lead to dinitromethyl-1,2,4-oxadiazole salts.



Scheme S. 7: Synthesis of different 1,2,4-oxadiazoles (**L**), acetic acid 1,2,4-oxadiazoles (**M**) and trinitromethyl 1,2,4-oxadiazoles (**N**).

The trinitromethyl compounds show high densities 1.80 – 1.95 g cm⁻³. The oxygen balances are very promising (+10.3 – 30.6 %) with the highest density for 3-trinitromethyl-(1,2,4-oxadiazol-5-one) of +30.6 % (Figure S.7), which is comparable with AP (+34.0 %). The specific impulse, which is one of the most important properties of HEDOs, was calculated to be 244–262 s, which also is in the range of AP (264 s). In course of this study, all compounds, including the precursor, were new compounds and therefore fully characterized.

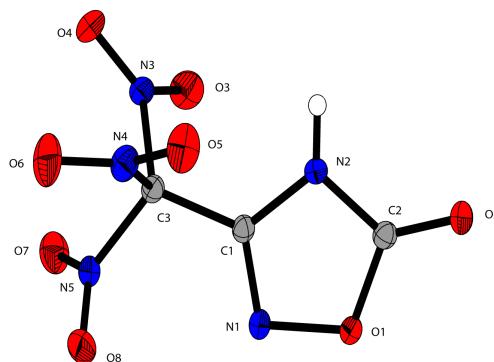
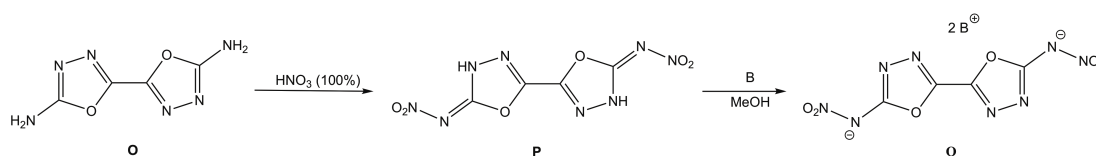


Figure S. 7: X-ray molecular structure of 3-trinitromethyl-(1,2,4-oxadiazol-5-one).

8. Bis-Nitramine-1,3,4-Oxadiazole

To find a promising RDX replacement, a 1,3,4-oxadiazole was synthesized in chapter 8. Here, over a fast, easy and cheap synthesis a diamino-bi-1,3,4-oxadiazole (**O**) was synthesized, which was further nitrated to dinitramino-bi-1,3,4-oxadiazole (**P**). Basic reaction with nitrogen-rich cation yielded the salts of di-nitramino-bi-1,3,4-oxadiazole (**Q**) (Scheme S.8)



Scheme S. 8: Synthesis of diamino-1,3,4-oxadiazole (**O**), dinitramino-1,3,4-oxadiazole (**P**) and nitrogen-rich salts of di-nitramino-1,3,4-oxadiazoles (**Q**).

Apart from a fast and cheap synthesis, the detonation properties of di-nitramino-1,3,4-oxadiazole (**P**) (Figure S.8) are equal or even better than RDX. The density at room temperature was measured to be 1.98 g cm⁻³, detonation velocity 9388 m s⁻¹ (RDX: 8983 m s⁻¹) and detonation pressure 391 kbar (RDX: 380 kbar). The detonation values are convincing that this compound is a potential replacement of RDX.

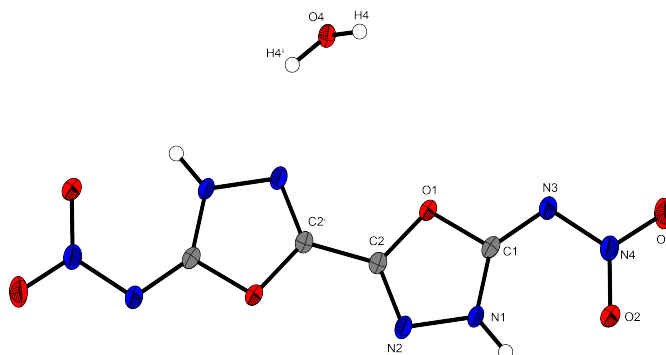


Figure S. 8: X-ray molecular structure of bis-nitramino-bi-1,3,4-oxadiazole.

IV Appendix

Abbreviations

BAM	<i>Bundesanstalt für Materialforschung und -prüfung</i>
br	broad (IR and NMR)
CJ	Chapman-Jouguet point
d	doublet (NMR)
DDT	detonation-to-deflagration transition
DMSO	dimethylsulfoxide
DSC	differential scanning calorimetry
DTA	differential thermal analysis
EA	elemental analysis
ESD	electrostatic discharge
FS	friction sensitivity
GOF	goodness of fit
HE	high (secondary) explosive
HEDM	high energy-dense material
HEDO	high energy-dense oxidizer
HMX	high melting explosive (1,3,5,7-tetranitro-1,3,5,7-tetrazocane)
IR	infrared spectroscopy
IS	impact sensitivity
LA	lead azide

LS	lead styphnate
M	molar (mol L^{-1})
m	medium (IR), multiplet (NMR)
MF	mercury fulminate
NMR	nuclear magnetic resonance
PETN	pentaerythritol tetranitrate
ppm	parts per million
RDX	royal demolitions explosive (1,3,5-trinitro-1,3,5-triazinane)
s	strong (IR), singlet (NMR)
SII	simple initiating impulse
TAG	bistriaminoguanidinium
TATB	2,4,6-triamino-1,3,5-trinitrobenzene
TNT	2,4,6-trinitrotoluene
t	triplet (NMR)
w	weak (IR)

Formula Symbols

δ	isotropic chemical shift
D	detonation velocity
nJ	coupling constant over n nuclei
M	molar mass
N	nitrogen content

n	amount of substance
$\tilde{\nu}$	wave number
Ω	oxygen balance
p_{CJ}	detonation pressure
Q_V	heat of explosion
ρ	density
T_{dec}	decomposition temperature
T_{det}	detonation temperature
T_{melt}	melting temperature
V_0	volume of detonation gases

Curriculum Vitae

Tobias Sebastian Hermann

Munich, Germany

EDUCATION

Ludwig-Maximilians University

Munich, Germany

PhD in Chemistry;

January 2015 – April 2018

- Thesis: Investigation of oxygen- and nitrogen-rich heterocyclic compounds as potential high-energy dense oxidizers or secondary explosives.
- Relevant subjects: Organic and inorganic chemical laboratory working by designing, synthesis and characterization of new high-energy dense materials and oxidizers.

University of Maryland

College Park, USA

Master Thesis in Inorganic Chemistry;

February 2014 – October 2014

- Thesis: Electro spray into liquids as a direct route to nanoparticle synthesis.
- Relevant subjects: Chemical working by set-up designing, synthesis and characterization of nano particles.

Ludwig-Maximilians University

Munich, Germany

Master of Science in Chemistry;

November 2012 – July 2014

- Relevant subjects: Theoretical background and chemical laboratory working in the fields of organic, inorganic, physical chemistry and material science.

Ludwig-Maximilians University

Munich, Germany

Bachelor of Science in Chemistry and Biochemistry;

October 2009 – October 2012

Final Grade Bachelor thesis

- Topic: Polynitro compounds, their salts and kindred nitroalcohols.
- Relevant subjects: Theoretical background and chemical laboratory working in the fields of organic, inorganic, physical chemistry and biochemistry

Bibliography

1. T.S. Hermann, T.M. Klapötke, B. Krumm, J. Stierstorfer, The Reagent-depending Nitration of 1,3-Dihydroxyacetone Dimer, *Z. Anorg. Allg. Chem.* **2017**, *643*, 149–151.
2. T.S. Hermann, T.M. Klapötke, B. Krumm, J. Stierstorfer, The Energetic 3-Trinitromethyl-5-nitramino-1*H*-1,2,4-triazole and Nitrogen-rich Salts, *New J. Chem.* **2017**, *41*, 3068–3072.
3. T.S. Hermann, T.M. Klapötke, B. Krumm, Formation and Characterization of Heavy Alkali and Silver Salts of the 4-Nitro-pyrazolo-(3,4-*c*)-furazan-5-*N*-oxide Anion, *Propellants Explos. Pyrotech.* **2017**, *42*, 1–9
4. T.S. Hermann, T.M. Klapötke, K. Karagiosoff, J. Stierstorfer, Synthesis and Characterization of 2,2'-Dinitramino-5,5'-bi(1-oxa-3,4-diazole) and Derivatives as Economic and Highly Dense Energetic Materials, *Chem. Eur. J.* **2017**, *23*, 12087–12091.
5. T.S. Hermann, T.M. Klapötke, B. Krumm, J. Stierstorfer, Synthesis, Characterization and Properties of Ureido-Furazan Derivatives, *J. Heterocyc. Chem.* **2018**, *55*, 852–862.
6. T.S. Hermann, T.M. Klapötke, B. Krumm, J. Stierstorfer, Synthesis, Characterization and Properties of Di- and Trinitromethyl-1,2,4-Oxadiazoles and Salts, *Asian J. Org. Chem.* **2018**, *7*, 739–750.

7. I. Gospodinov, T.S. Hermann, T.M. Klapötke, B. Krumm, J. Stierstorfer, Energetic Compounds Based on 3,4-Bis(4-nitramino-1,2,5-oxadiazol-3-yl)-1,2,5-furoxan, *Propellants, Explos. Pyrotech.* **2018**, in press.
8. T.S. Hermann, T.M. Klapötke, J. Stierstorfer, I. Gospodinov, High Temperature Explosives Based on Furazanes and Triazoles, *Propellants, Explos. Pyrotech.* **2018**, in press.